Waveform Analysis of Intracranial Pressure and Craniospinal Compliance: Clinical and Experimental Studies

A thesis submitted for the degree of Doctor of Philosophy
in the Faculty of Medicine, University of Edinburgh
by

Ian Ross Piper, B.Sc.

Department of Clinical Neurosciences
University of Edinburgh
Scotland

May, 1990.

To the Memory of
John Douglas Piper

TABLE OF CONTENTS

SUMMARY

Raised intracranial pressure (ICP > 20 mm Hg) occurs in at least thirty percent of severely head injured patients and is associated with a significant increase in the number of deaths and severely disabled survivors. A study of the ICP waveform may yield information of relevance to the management of raised ICP either as a predictor of raised ICP or of its underlying cause.

The first section of this thesis describes pilot clinical studies, aimed at determining the practicality of applying waveform analysis techniques to the ICP waveform in head injured patients. Following on from the pilot studies, an observational study in thirty severely head injured patients was designed and carried out, where fifteen hundred ICP and blood pressure (BP) waveform samples were collected under microcomputer control. The waveform samples were analysed through the use of spectral methods in a systems analysis approach to quantifying pressure transmission across the cerebrovascular bed. The amplitude transfer functions, as a measure of cerebrovascular pressure transmission, were calculated for the first 6 cardiac harmonics from the ICP and BP spectra and were found to cluster into four classes: those with an overall flat amplitude transfer function (curve type 1), those with an elevated low frequency response (curve type 2), those with an elevated high frequency response (curve type 3) and those exhibiting both an elevated low and an elevated high frequency response (curve type 4). Curve types 2 and 4 (elevated low frequency, elevated low frequency in combination with elevated high frequency) were most often associated with raised ICP (ICP > 20 mm Hg) whereas curve types 1 and 3 (flat, elevated high frequency) were most often associated with ICP less than 15 mm Hg.

The interpretation of the data from this study was restricted as concurrent measurements of craniospinal compliance and cerebral blood flow (CBF), as a measure of cerebrovascular resistance, were not performed. To aid in the interpretation of these clinically observed forms of cerebrovascular pressure transmission, an experimental investigation into the relationship between cerebrovascular resistance, craniospinal compliance and cerebrovascular pressure transmission was undertaken.

Before such an experimental study could be carried out an improved method of measuring craniospinal compliance was needed. Existing

measures of lumped craniospinal compliance such as the volume pressure response method (VPR) were considered too variable chiefly as a result of the manual injection method. The VPR technique was modified from a manual to an automatic injection sequence using an electronic square wave pressure generator to produce a small (0.05 ml), exact and reproducible transient volume increase into the CSF space. Compliance was calculated from the amplitude of the intracranial pressure response to this volume increment. The ICP response was time-averaged using a biological signal averager which facilitates separation of the pressure response from background noise. The new method was validated against the VPR method in physical and animal models, where it accurately followed compliance changes and demonstrated significantly less variation between measurements then the VPR method.

The experimental studies were then performed in animal models of raised ICP, arterial hypercarbia and arterial hypertension, using the improved compliance technique. The data obtained from those studies were an aid to the interpretation of the four forms of cerebrovascular pressure transmission that were observed in the clinical studies.

A flat amplitude transfer function (curve type 1) indicates equal transmission of all harmonics of the arterial pressure waveform through to the CSF space and was found in the experimental studies associated with ICP less than 15 mm Hg and with normal craniospinal compliance, normal cerebrovascular resistance and a negative fundamental phase shift. This form of cerebrovascular pressure transmission may characterize a functionally normal cerebrovascular bed.

An elevated low frequency pressure transmission (curve type 2) either solely or in combination with an elevated high frequency pressure transmission (curve type 4) was associated with raised ICP above 20 mm Hg. Experimentally, this form of pressure transmission was found whether ICP increased through intraventricular infusion of fluid or through inhalation of 5% CO2. Associated with these changes, both craniospinal compliance and cerebrovascular resistance were usually decreased in conjunction with a more negative fundamental phase shift when compared to curve type 1. The curve type 2 form of cerebrovascular pressure transmission seen in patients is indicative of raised ICP, reduced craniospinal compliance, reduced arteriolar vasomotor tone and increased vasomotor compliance.

In the clinical study, the amplitude transfer function curve type 3 (elevated high frequency) was associated with a positive fundamental phase shift and ICP below 15 mm Hg. From the experimental data a positive phase was exclusively associated with the post arterial hypertension stage of the arterial hypertension group of animals where ICP had decreased to below 10 mm Hg in conjunction with an abnormally high craniospinal compliance. This combination of factors may indicate a generalized cerebral vasodilation.

This work should be extended by a further clinical study using on-line minute by minute analysis of the ICP and BP waveforms in order to study cerebrovascular pressure transmission with regard to the development of raised ICP in head injured patients.

DECLARATION

I declare that this thesis is of my own composition, comprises my own original work and has not been presented previously as a thesis in any form.

Ian Piper
May 1990

ACKNOWLEDGEMENTS

This research was carried out under the supervision of Professor J. Douglas Miller and Dr Jim Neilson. Their helpful guidance, advice, patience and enthusiasm made possible the successful development of this project. This work was funded by project grants from Action Research for the Crippled Child (A/8/1671) and the Medical Research Council (G8804953N).

I would like especially to thank Dr Mark Dearden for many hours of helpful discussion and for freely giving his time, unflagging enthusiasm and support for this project.

Particular thanks to Mr Ian Whittle, Mr Alistair Lawson, Dr Kwan Hon Chan and Miss Janis Tocher for their advice, assistance and especially their companionship over the last three years.

I would also like to thank: Mr Jim Slattery for advice and support with statistical analysis, Dr Alex Gordon for preparing brain specimens for light microscopical analysis, Mr Jim Leggate for thirty late night phone calls and Dr Paul Kelly for his moral support and for finding me a desk.

Only two people know how hard a person works: the person who puts in the hours and the one who waits for you to come home. My final thanks must go to my wife Kate for her love and support over the last three years.

LIST OF FIGURES

LIST OF TABLES

LIST OF APPENDICES

LIST OF ABBREVIATIONS

ICP	Intracranial Pressure
ICP_{plse}	Intracranial Pressure Pulse Amplitude
BP	Blood Pressure
CPP	Cerebral Perfusion Pressure
CVP	Central Venous Pressure
SSP	Sagittal Sinus Pressure
HRT	Heart Rate
Tc	Core Body Temperature
PaCO2	Arterial Blood Partial Pressure of Carbon Dioxide
PACO2	Alveolar Partial Pressure of Carbon Dioxide
PaO2	Arterial Blood Partial Pressure of Oxygen
pH	Arterial Blood PH
SaO2	Percentage Arterial Blood Oxygen Saturation
ETCO2	End Tidal Concentration of Carbon Dioxide
CSF	Cerebrospinal Fluid
EEG	Electroencephalogram
CBF	Cerebral Blood Flow
PVI	Pressure Volume Index
VPR	Volume Pressure Response
dP/dV	Elastance (where d = difference)
dV/dP	Compliance (where d = difference)
FFT	Fast Fourier Transform
SPR	Short Pulse Response (compliance method)
RC	System Time Constant (product of resistance and capacitance)

PREFACE

In Britain, severe head injury occurs in 150 per million people per year, with the majority being under 25 years old. Raised intracranial pressure (ICP > 20 mm Hg) occurs in at least 30 percent of these patients and is associated with a significant increase in the number of deaths and severely disabled survivors. The higher the level of ICP, the greater is the morbidity and mortality with virtually no survivors when ICP exceeds 50 mmHg. Elevations in ICP can rapidly cause cerebral ischaemia and irreversible brain damage. The prediction of imminent rises in ICP coupled with determination of the probable underlying cause is of primary importance if the rapid matching of appropriate treatment with cause of raised ICP is to be successful.

A study of the ICP waveform may yield information of relevance to the management of raised ICP either as a predictor of raised ICP or of its underlying cause. Towards this end, the first section of this thesis describes pilot clinical studies, aimed at determining the practicality of applying waveform analysis techniques to the ICP waveform in head injured patients and other patients at risk of developing raised ICP. This section also describes the basic methods and technical development required to carry out these studies. The results obtained from these clinical investigations posed questions that required testing in experimental waveform analysis studies. These were aimed at developing an improved understanding of the physiological relationship between cerebrovascular resistance, craniospinal compliance and pressure transmission across the cerebrovascular bed. The middle section of this thesis describes the technical development and experimental validation of an improved method of measuring craniospinal compliance, a development required by the design of the proposed experimental work. The design and results of these experimental waveform analysis studies are described in the final section of this thesis.

CHAPTER I. INTRODUCTION

The field of intracranial pressure (ICP) research is a wide ranging one, and, to date, has been the subject of seven international symposia embracing such diverse disciplines as neurosurgery, anaesthesia, radiology, biophysics, electronic and mechanical engineering, mathematics and computer science. There is an extensive literature on ICP. Consequently this introductory chapter contains only a limited review of the historical and current concepts behind analysis of intracranial pressure and craniospinal compliance that are of direct relevance to this thesis.

A. Relevant Anatomy of the Craniospinal System

The craniospinal system (Figure 1) comprises brain, spinal cord, cerebrospinal fluid (CSF), blood and its containing vasculature, and is enclosed within a rigid skull and vertebral column. Neural tissue accounts for 70% of the total volume; CSF, blood and extracellular fluid make up the remaining 30% in approximately equal portions of 10% each. Under normal conditions, three quarters of the vascular blood volume is contained within the venous system (1). The CSF is contained within the ventricles and subarachnoid space.

There are three membranous coverings of the brain and spinal cord: the dura, arachnoid and pia. The dura is a fibrous tissue containing the craniospinal constituents and in the cranial vault is immediately adjacent to the inner table of the skull, whereas in the spinal canal it is separated from the vertebral column by fatty tissue and a venous vascular plexus. The arachnoid membrane is an avascular layer of connective tissue bridging the sulci of the brain and spinal cord, thus forming the major cisterns, the two largest of which are the cisterna magna and lumbar cistern. The pia is a thin vascular layer accurately following the contour of the nervous tissue. The subarachnoid space is the region contained between the arachnoid and Pia.

There are four interconnecting ventricles. Two lateral ventricles within the cerebral hemispheres are linked through the inter-ventricular foramina of Monro into the single mid-line third ventricle, and the aqueduct of Sylvius connects the third and fourth ventricles. Entry into the subarachnoid space is made through three openings within the fourth

ventricle: a medial foramen of Magendie opening posteriorly into the cisterna magna and the paired foramina of Luschka opening laterally into the cerebromedullary cistern. Once outside the ventricular system, the CSF enters the subarachnoid space, circulates through it and exits into the superior sagittal sinus through the specialized structures in the sinus wall, the arachnoid villi.

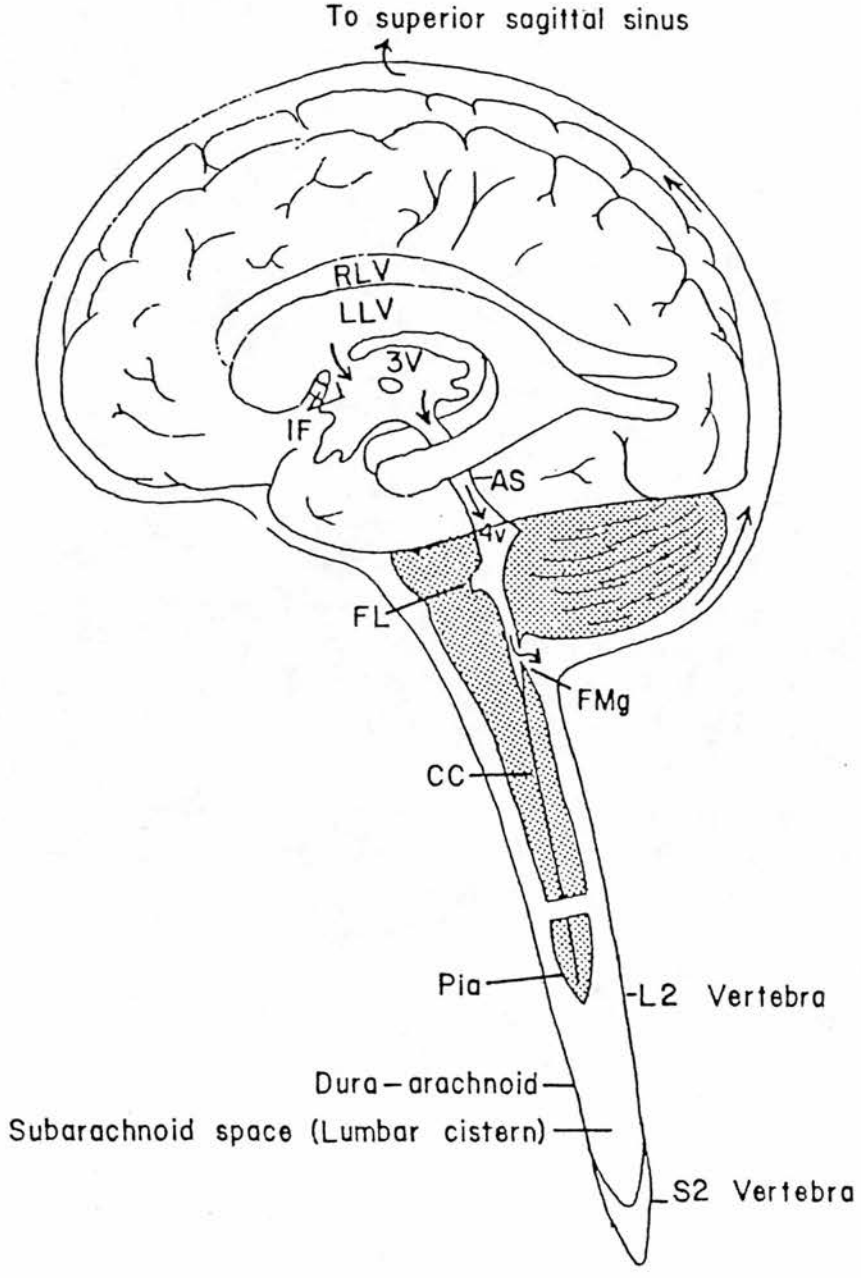

Figure 1: The Craniospinal System. (not drawn to scale) Arrows indicate the direction of flow of CSF. RLV, right lateral ventricle, LLV, left lateral ventricle; 3V, third ventricle; IF, interventricular foramina; AS, aqueduct of Sylvius; 4V, fourth ventricle; FL, foramen of Luschka, FMg, foramen of Magendie, CC, central canal.

B. Literature Review of Intracranial Pressure and Craniospinal Compliance

1. History

The history of this subject (2,3,4) starts from the doctrine named after Monro (5) and Kellie (6), which proposed that the brain and its contained blood were incompressible, enclosed in a rigid and inextensible skull, of which the total volume remained constant. In its original form the Monro-Kellie doctrine did not take into account the CSF as a component of the cranial compartment. The concept of reciprocal volume changes between blood and CSF was introduced in 1846 by Burrows (7) and later extended in the early twentieth century by Weed et al (8,9) to allow for reciprocal changes in all the craniospinal constituents.

Kocher (10) in 1901 translated into clinical terms the four stages of cerebral compression proposed almost 25 years earlier by the experimental studies of Duret (11). Kocher described four stages of cerebral compression related to the expansion of intracranial brain tumours. In stage 1, the initial increase in tumour volume is compensated by a reduction in volume of the other intracranial components, chiefly CSF and venous blood. This spatial compensation results in no net increase in intracranial volume or pressure and hence no clinical symptoms. In stage 2 the compensatory mechanisms are exhausted, ICP increases and the patient becomes drowsy with headache. Stage 3 is characterized by a considerable increase in ICP, an associated deterioration in conscious level with intermittent elevations of blood pressure (BP) accompanied by bradycardia. In the fourth and final stage, the patient is unconscious, with bilateral fixed dilated pupils and falling BP usually leading to death.

Cushing (12,13,14), then a research worker for Kocher, described in both experimental and clinical studies the close relationship between increases in ICP and BP and proposed that the BP rose in order to maintain adequate blood supply to the hind brain, the stimulus to this vasopressor response believed to be medullary ischaemia (15,16).

At about this time a false confidence developed in the lumbar CSF pressure technique (lumbar puncture) which caused Cushing's findings to be challenged. Reports emerged (17,18,19) that some patients showing clinical signs of brain compression had normal lumbar CSF pressures and that in other patients elevations in BP were found at times when ICP was well below the level of BP.

Partly because of this apparent dissociation between ICP and clinical symptoms, emphasis switched away from ICP measurement towards the relationship between craniospinal volume and pressure, particularly the importance of the elastic properties of the craniospinal system. Ayala (20,21) studied the fall in lumbar pressure which occurred when CSF was removed from patients, describing the degree of decline in terms of the volume of CSF removed and the "elasticity" of the meninges. "Ayala's index" developed from this work and is defined as the fall in pressure divided by the volume of fluid removed. This index was found to be low in patients diagnosed with benign intracranial hypertension and high in patients with cerebral tumours.

Weed, Flexner and Clark (22,23,24,25) systematically studied the effect of hydrostatic columns on the elastic properties of the craniospinal system by observing the pressure and volume changes during up/down head tilting experiments in animals. They defined a coefficient of elasticity based on Hook's law (Eo = stress/strain) which failed to show any change under a variety of experimental conditions. Their work was critically reviewed by Massermann who carried out similar studies in patients (26,27). Ryder (28) was the first to characterize the craniospinal volume-pressure relationship as a non-linear quantity describing it as a hyperbolic function which implies an increase in elastance as pressure increases. This was in conflict with the work by Weed and co-workers although the latter group only studied the elastic properties over a limited physiological pressure range. Furthermore, it was also partly the work of Ryder (29) which restored confidence in intracranial pressure measurement by demonstrating a differential pressure between intraventricular and lumbar CSF pressure recording. This phenomenon was reported as early as 1895 by Bayliss (30) who noted it was impossible to obtain valid ICP measurements below the tentorium during later stages of progressive supratentorial brain compression.

It was not until the 1960's when Lundberg (31) published his now classic monograph that interest in clinical ICP measurement was rekindled. Using ventricular fluid pressure recording in brain tumour patients, Lundberg was the first to delineate the frequency with which raised ICP occurs clinically, at times reaching pressures as high as 100 mm Hg. Lundberg also described three types of spontaneous pressure wave fluctuations: "A" waves or plateau waves of large amplitude (50 - 100 mm

Hg) with a variable duration (5 - 20 min.), "B" waves which are smaller (up to 50 mm Hg), sharper waves with a dominant frequency of 0.5 - 2 per minute, and finally "C" waves which are small (up to 20 mm Hg) rhythmic oscillations with a frequency of 4 - 8 per minute.

This work was then extended to include head injuries (32,33), intracranial haemorrhage (34), post-hypoxic brain damage (35) and benign intracranial hypertension (36). ICP can therefore increase under an assortment of experimental and clinical circumstances, the frequency often being underestimated by the lumbar pressure recording technique. This phenomenon of pressure underestimation was fully defined by Langfitt and co-workers (37,38) in experimental studies of extradural brain compression where progressive loss of transmission of ICP across the tentorial hiatus occurred, with the pressure in the posterior fossa and lumbar subarachnoid space progressively under-reading the ventricular pressure and eventually returning to normal pressure.

Some of the most important work at this time was also carried out by Langfitt's group (39) who redefined Kocher's four stages of cerebral compression under controlled experimental conditions in Rhesus monkeys with simultaneous measurement of arterial and intracranial pressure, jugular or sagittal sinus pressure, cerebral blood flow (CBF) and measures of brain metabolism. They defined stage 1 as the period of spatial compensation, with very little increase in ICP despite slow inflation of an extradural balloon. Electroencephalogram (EEG), CBF and brain oxygenation were normal and stable at this time. Stage 2 occurred at the end of spatial compensation and was characterized by an exponential increase in ICP with a steady extradural balloon inflation rate. Towards the end of this stage, ICP increased by more than 15 mm Hg with 0.1ml injections into the extradural balloon, and spontaneous increases in BP occurred which initiated further increases in ICP. Further waves of increased ICP could be triggered at this time by hypercapnia and hypoxia. In stage 3, ICP was approaching the level of BP with the vasomotor reflexes becoming less effective in driving BP up above the ICP. EEG slowed and became flat as ICP reached the level of BP. At this stage, altering the arterial concentration of carbon dioxide (PaCO2) had no response, an effect which Langfitt termed vasomotor paralysis. Also at this stage induced changes in BP produced almost identical changes in ICP. Deflation of the balloon at this stage could cause a return of ICP to

normal levels, with a partial return of EEG. If balloon inflation continued, stage 4 was entered where decompensation was irreversible, BP dropped and death followed. Deflation of the balloon at this time resulted in only a temporary fall in ICP.

2. Current Concepts

Following on from this earlier work, the research carried out in the 1970's and early 80's provides much of the basis for our current concepts of intracranial pressure and craniospinal compliance.

Marmarou, interested in CSF dynamics in relation to the pathological state of hydrocephalus, was the first to provide a full mathematical description of the craniospinal volume-pressure relationship. Marmarou (40) developed a mathematical model of the CSF system which produced a general solution for the CSF pressure. The model parameters were subsequently verified experimentally in an animal model of hydrocephalus. As a corollary from this study, Marmarou demonstrated that the non-linear craniospinal volume-pressure relationship could be described as a straight line segment relating the logarithm of pressure to volume, which implies a monoexponential relationship between volume and pressure (Figure 2). The slope of this relationship Marmarou termed the pressure-volume index (PVI) which is the notional volume required to raise ICP tenfold. Unlike elastance (change in pressure per unit change in volume dP/dV), or its inverse, compliance (change in volume per unit change in pressure dV/dP), the PVI characterizes the craniospinal volume-pressure relationship over the whole physiological range of ICP.

The PVI is calculated from the pressure change resulting from a rapid injection or withdrawal of fluid from the CSF space (Figure 3), and has found widespread use both clinically and experimentally as a measure of lumped craniospinal compliance (41,42,43,44,45,46). Any factor increasing in volume within the craniospinal axis will deplete available compensatory exchange space (decompensation), reduce compliance and eventually lead to increased intracranial pressure. Shapiro (47) has found that a PVI reduced by 80% of control values to be predictive of raised ICP in paediatric head injury. Tans and Poortvliet (48), also using the PVI in patients, state that the values of 10 and 13 ml to be key values, with lower values indicating that active ICP reduction and improvement in compliance are required.

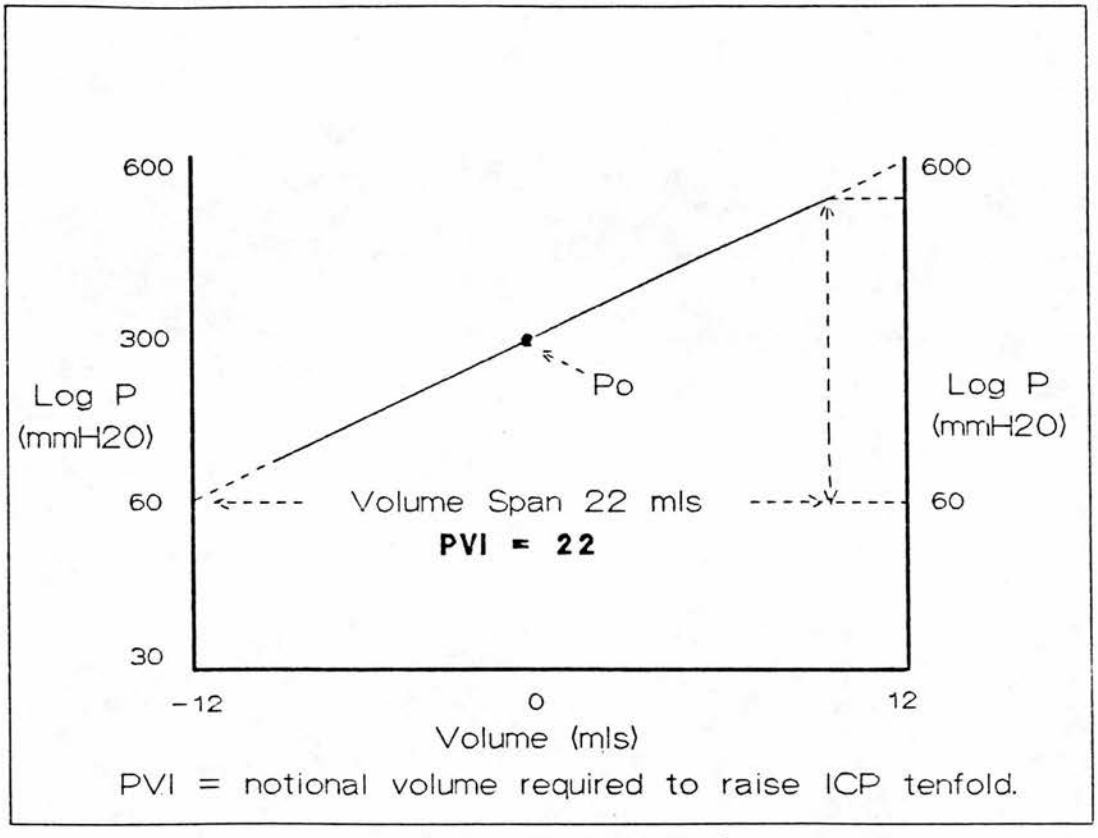

Figure 2: Log ICP vs Volume Relationship (Adapted from Marmarou, reference 40).

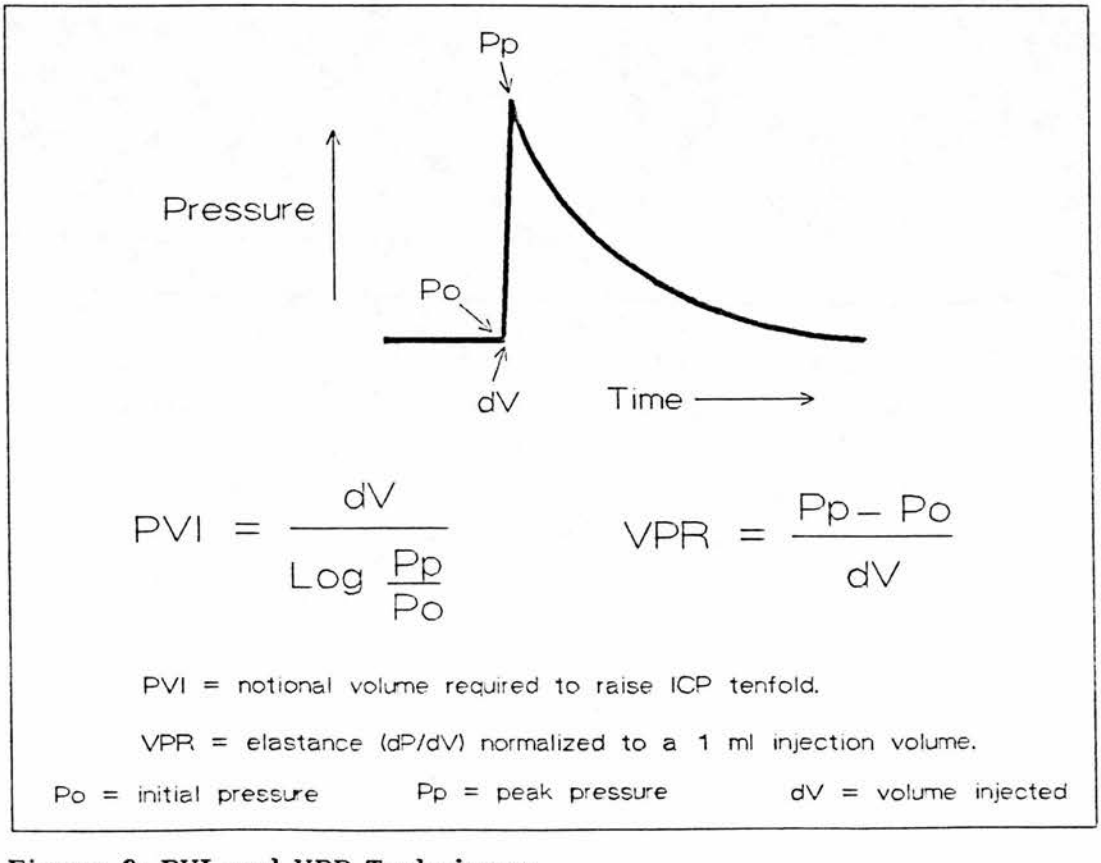

Figure 3: PVI and VPR Techniques.

At about the same time that Marmarou introduced the PVI technique, Miller and co-workers (49,50) defined a further measure of the craniospinal volume-pressure relationship, the volume pressure response (VPR). The VPR, calculated from the intracranial pressure response resulting from a rapid bolus injection of saline into the CSF space, was a direct measure not of compliance but of its inverse: elastance. The VPR technique was in several ways preferable to the PVI technique in that it was a simpler measure of craniospinal volume depletion, involving none of the assumptions about the monoexponential nature of the pressure versus volume relationship inherent in Marmarou's technique. Furthermore, the VPR increases in value as the patient's condition worsens, which makes it easier to understand clinically.

Miller pointed out that if there were only a single volume-pressure curve then no new information would be gained by measuring compliance or elastance, and a knowledge of absolute ICP alone would suffice in determining the state of a patient's craniospinal volume decompensation. However, Miller and co-workers (51,52,53) have shown that the shape of the volume-pressure relationship changes under a variety of conditions between patients and within patients at different times and under different circumstances. In head injured patients, the VPR correlated better to the degree of brain mid-line shift, as imaged on C-T scan, than it did to absolute ICP alone. The VPR served as an indicator for surgical decompression, critical levels being between 3-5 mm Hg/ml (50,54).

Löfgren (55,56,57,58) extended the ICP range over which the volume-pressure relationship was studied, including a negative pressure range (relative to atmospheric pressure). In experimental studies in dogs using spinal block techniques, he showed the volume-pressure curve to be the sum of two separate curves representing high compliance related to the spinal portion of the dural sac and a low compliance curve, at elevated ICP, related mostly to the cranial portion (Figure 4). At the most elevated ICP, there was a sudden decrease in elastance as ICP approached diastolic pressure, possibly due to shifting of blood from the vascular bed when CBF ceased (56).

The importance of vascular factors as a determinant of lumped craniospinal compliance was shown clearly by the work of Gray and Rosner (59,60) who showed that, when CBF autoregulation was intact with cerebral perfusion pressure (CPP) levels greater than 50 mm Hg, there

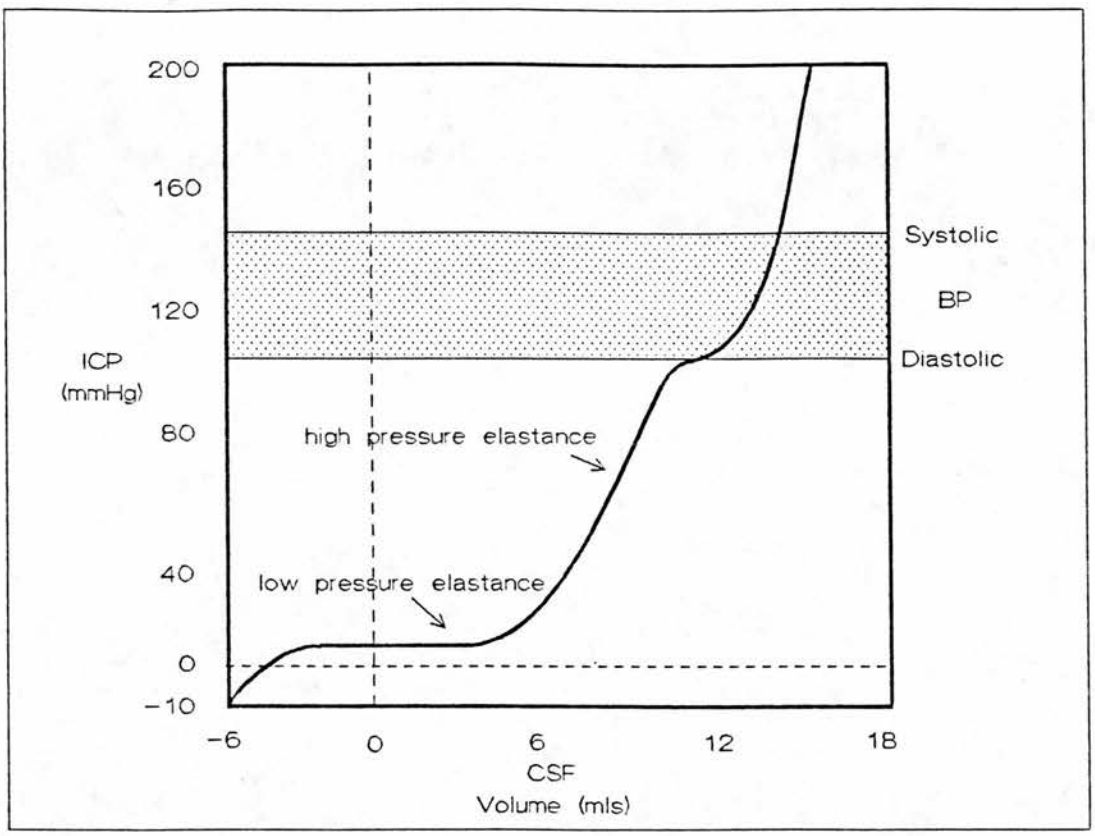

Figure 4: Extended Volume-Pressure Relationship (Adapted from Löfgren, reference 55).

was a linear increase in PVI with increasing CPP. However, with CPP's below the autoregulatory range, CBF fell progressively followed this time by increases in the PVI again. This work demonstrates that the PVI is a complex function of CPP, the direction of the CPP-PVI relationship dependent on whether CPP is above or below the autoregulatory range for CBF. Similarly the role of vascular factors in the pathogenesis of raised ICP was demonstrated by Marmarou (61) who studied the relative contributions of CSF and vascular factors to raised ICP in head injured patients, concluding that CSF parameters accounted for only one-third of the ICP rise after severe head injury, and that vascular mechanisms may be the predominant factor in elevation of ICP.

Anile and co-workers (62) have demonstrated that compliance is time dependent showing that the VPR calculated from slow, medium and rapid bolus injections yields different values. They conclude that lumped craniospinal compliance can be divided into two components based on the rate of injection of the volume bolus: physical compliance and physiological compliance. Physical compliance is a measure of such factors

as expansion of spinal dura matter and of any minute amount of brain compression and skull expansion that may occur (63). Physiological compliance of the intracranial system is related to cerebrovascular alterations, particularly venous outflow resistance (64).

This data shows that to understand craniospinal pressure-volume relationships, the dynamic and the viscoelastic properties of CSF, nervous tissue and vascular factors must be considered. Zee and Shapiro (65), using a gas bearing electrodynamometer and a linear variable displacement transducer, measured the relationship between brain compression force and displacement to study the viscoelastic properties of the brain. They demonstrated that dogs, made hydrocephalic with intracisternal injection of kaolin, developed brains which became less stiff (more compliant) and more viscous than normal brain. They propose that this weakening of brain tissue may account for the increase in brain compliance associated with hydrocephalus, although the time course of these changes is still unknown.

Walsh and Schettini (66) have shown that brain tissue elasticity bears no relation to lumped craniospinal elastance as measured by the VPR. The brain elastic response was measured extradurally with a coplanar transducer recording the brain displacement simultaneous to the pressure required to cause that brain displacement. The resulting pressure versus brain displacement relationship is similar to the pressure versus injection volume relationship previously described. The tangent of this brain elastic response curve is a parameter G_0 which is a measure of brain tissue elasticity. They have shown in ten dogs in an extradural balloon inflation model of raised ICP, that the VPR increases with increasing ICP but G_0 remains unchanged. Upon cardiac arrest, however, the VPR decreases and G_0 increases. They propose that G_0 increases due to an ion shift from the extracellular to the intracellular compartment, leading to increased intracellular water and hence increased cellular tension (67).

From this work it is clear that a knowledge of a patient's craniospinal volume-pressure relationship is an adjunct to ICP measurement for predicting states of raised ICP. However, the use of the PVI or VPR methods is not without disadvantages. With these techniques there is an increased risk of infection, usually due to staphylococcus epidermis, with reported infection rates ranging from 0.5% up to 9% (31,68,69). Other disadvantages include a risk of provoking secondary pressure rises with

rapid volume injection through activation of secondary vasodilation (70,71). Furthermore, variability between measurements is high as it is difficult to manually inject consistent volumes of fluid rapidly at a constant rate of injection. As a result an average of repeated measures is usually required.

As a consequence of these limitations the PVI or VPR tests are not routinely used in neurosurgical practice. In an effort to find a less invasive means to obtain this data Avezaat and Van Eijndhoven (70,73) systematically studied the ICP waveform pulse amplitude (ICP_{plse}) as a measure of craniospinal elastance. The rationale behind this concept is that with each heartbeat there is a pulsatile increase in cerebral blood volume, the equivalent of a small intracranial volume injection, and the ICP_{plse} is the intracranial pressure response to that volume increment and should therefore be directly related to the craniospinal elastance (dP/dV). That is, as craniospinal elastance increases (compliance decreases) the ICP_{plse} should increase. The observation that as ICP increases so does the amplitude of the intracranial pressure pulsations is not a new one, having been first described in 1866 by Leyden (72).

Avezaat and Van Eijndhoven first extended the mathematical description of the exponential craniospinal volume-pressure relationship by introducing a constant term Po into the pressure-volume equation (Figure 5). Primarily for mathematical convenience this term shifts the volume-pressure curve as a whole up or down its axis which allows correction for pressure transducer reference position and postural changes. Mathematically, Po is the pressure at zero elastance (see eqtn. 1 in Figure 5) and must therefore have physiological significance as a determinant of the normal intracranial equilibrium pressure (Peq). Löfgren (56) showed that alterations in CVP can shift the pressure-volume curve up or down its axis which would suggest CVP may be a factor determining Po.

Avezaat and Van Eijndhoven described the mathematical relationship between ICP_{plse} and ICP by substituting the ICP_{plse} for the elastance (dP/dV) and pulsatile blood volume for the volume injection (Appendix A). This relationship was verified in both clinical and experimental studies.

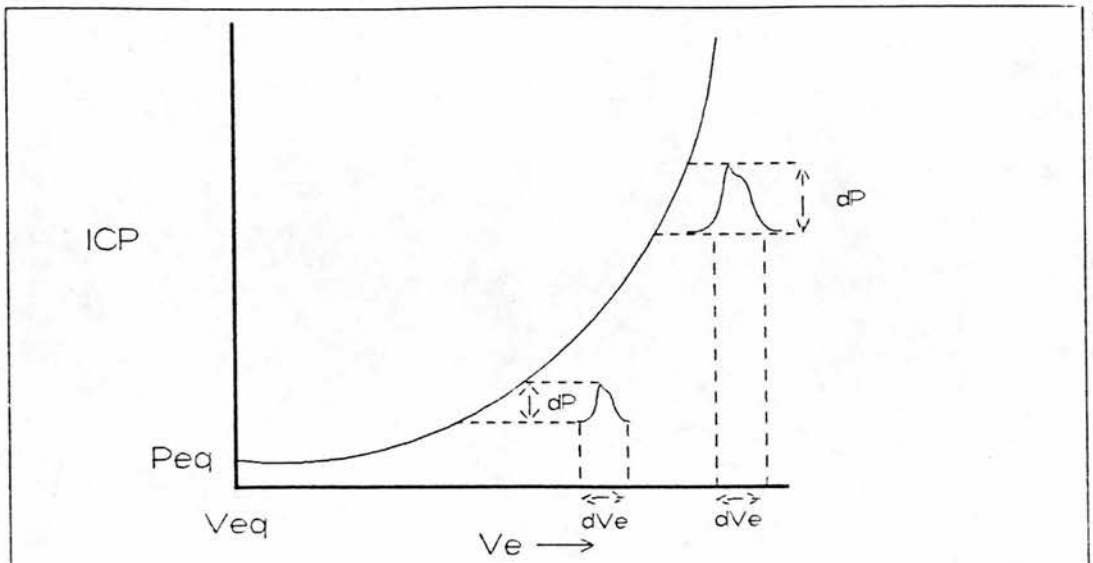

The exponential volume-pressure relationship is described mathematically:

$$\text{equation 1)} \quad P = Peq\ e^{E1\ dVe} + Po$$

where: P = ICP; Peq = equilibrium ICP; E1 = Elastic coefficient; Ve = elastic volume (addition to total volume); Po = constant term

Figure 5: Exponential Volume-Pressure Relationship (Adapted from Avezaat and Van Eijndhoven, reference 70).

They found the ICP_{plse} increased linearly with ICP up until a pressure of 60 mm Hg whereupon a breakpoint occurred (Figure 6). Above 60 mm Hg the ICP_{plse} increased more rapidly with increasing ICP. They argue that the breakpoint is a marker for loss of CBF autoregulation, postulating that onset of vasomotor paralysis causes a decreased arteriolar inflow resistance which results in an increased phase shift between the inflow and outflow pulsatile blood volume. This translates to an overall increased intracranial pulsatile blood volume and will tend to increase the slope of the ICP_{plse} versus ICP relationship.

It is assumed the pulsatile blood volume (dV), the input function to the elastance calculation (dP/dV), is unchanging. This is a tenuous assumption in severely injured patients some of whom may have compromised or fluctuating cardiovascular function. As a consequence of the dependence of the ICP_{plse} versus ICP relationship on the pulsatile blood volume, the clinical utility of this technique as a measure of lumped craniospinal elastance is limited unless a measure of the pulsatile blood volume can be monitored simultaneously and controlled for in patients. Despite this limitation, this method is being used clinically by several investigators (74,75,76,77).

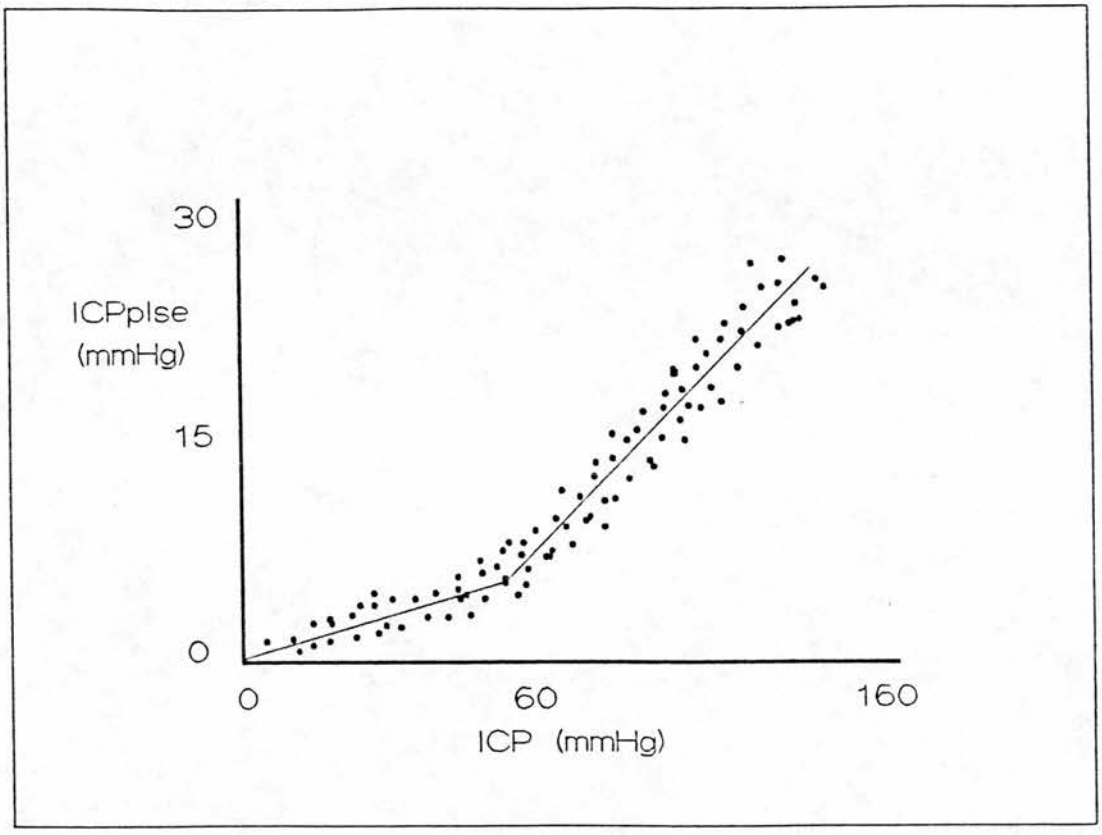

Figure 6: ICP_{plse} vs ICP Relationship (Adapted from Avezaat and Van Eijndhoven, reference 70).

Portnoy and Chopp recognized the importance of measurement of the input function in an analysis of the ICP_{plse} and were the first to apply a systems analysis approach to the ICP waveform (78). Systems analysis is a technique whereby an attempt is made to define the physical characteristics of a system using only the system input and output signals (79). Portnoy's and Chopp's method assumes the BP waveform is the chief input signal to the cerebrovascular system and the ICP waveform is the output response to that stimulus. Both BP and ICP waveforms are converted into the frequency domain by Fourier analysis, and the resulting frequency spectra are used in the calculation of the system transfer function. The system transfer function consists of amplitude and phase components. The amplitude transfer function is a measure of how much pressure is transmitted through the cerebrovascular bed at a given frequency. The phase transfer function is a measure of how much a pressure signal is phase shifted as it is transmitted through the cerebrovascular bed at a given frequency.

Using these methods, Portnoy and Chopp (81) found, in an experimental model of raised ICP in cats, that arterial hypercarbia and hypoxia

produced an increase in ICP_{plse} and an increase mainly in the fundamental of the amplitude transfer function. The changes induced were greater than those caused by intraventricular infusion of saline to the same ICP level. The VPR was less during hypercapnia than during intraventricular infusion at the same ICP level, which suggests that the increase in ICP_{plse} is related to arteriolar vasodilation and not to steepening of the craniospinal volume-pressure relationship.

Extending their model by including analysis of the sagittal sinus pressure (SSP) waveform in dogs (82), Portnoy et al found that the ICP waveform and SSP waveform were almost identical, indicating that the ICP_{plse} is derived from the cerebral venous bed. With the animals breathing pure oxygen it was observed that an attenuation of the amplitude transfer function fundamental occurred in the transmission of the arterial pulse through to the CSF space under conditions of low ICP (ICP < 7 mm Hg). They attributed this attenuation to functional autoregulatory tone of the precapillary cerebral resistance vessels, and further demonstrated that a flat amplitude transfer function (equal transmission of all harmonics) can be experimentally induced by intraventricular infusion of mock CSF or arterial hypercarbia. They propose that the conversion from an attenuated low frequency transmission to a flat amplitude transfer function is evidence for reduced arteriolar vasomotor tone.

Applying these techniques to hydrocephalic dogs, Portnoy et al (83) found that when ICP was less than 9 mm Hg, there was an attenuated low frequency transmission from BP to ICP; however, when ICP was greater than 12 mm Hg a flat amplitude transfer function was present. These findings in hydrocephalic dogs were identical to non-hydrocephalic controls, and they concluded that pressure transmission from BP to ICP in hydrocephalic dogs was determined by the cerebrovascular bed and not the hydrocephalic process.

Branch (84), also from Portnoy's group, recording the pressure waveform from a small cortical vein, provided further evidence that the ICP waveform was derived from the cerebral venous bed by demonstrating that the ICP and cortical venous amplitude spectra were identical across a variety of experimental conditions.

Using similar techniques to Portnoy and Chopp, Takizawa et al (85) have shown that the first four harmonics of the ICP waveform and the

amplitude transfer function all show a positive correlation to raised ICP and an inverse correlation to CPP. A distortion factor "k" was used to show that as ICP increased towards 50 mm Hg the ICP waveform became more like a sine wave, changing less as ICP continued to increase. Takizawa (86) also found that cerebrovascular pressure transmission increased to saline infusion and arterial hypercarbia equally when ICP was recorded either in the lateral ventricle or in the cisterna magna, but transmission was attenuated to the lumbar space. This attenuation to the lumbar space was decreased by saline loading the craniospinal axis. They propose that the spinal sac functions as a low pass filter to the conduction of the $ICP_{pl\text{s}e}$

Also using a systems analysis approach to studying cerebrovascular pressure transmission, but using different methods, Kasuga et al (87) have demonstrated resonance within the intracranial cavity in dogs. They randomized pressure pulse transmission into the cranial cavity through the control of an implanted cardiac pacemaker. Using the carotid pulse waveform as an input function and the extradural pressure waveform as the output function, they calculated the transfer function from the autocorrelation of the input function and the cross correlation of the input and output functions by means of a least squares method. They showed that the amplitude transfer function decreased between the frequencies of 1 and 7 Hz, then suddenly increased to form a marked peak at about 10 - 15 Hz, whereupon the phase transfer function also changed from positive to negative. This showed that the lower frequencies of the pulse wave were suppressed during transmission through the intracranial cavity and that resonance was present under normal intracranial conditions. Kasuga et al (88) subsequently showed that with both extradural balloon inflation and intraventricular infusion models of raised ICP in dogs, the resonant frequency increased above the control value. Associated with this increase in resonant frequency, there was an increased transfer of the low frequency components. However, with arterial hypercarbia, ICP increased but with no significant change in the resonant frequency, although low frequency pressure transmission increased in a similar fashion to both groups.

Finally, Bray and Robertson (89) using Fourier analysis of the ICP waveform in patients, identified two main frequency bands in the ICP waveform power spectrum. The centroid (power weighted average

frequency) of the low frequency band (0.2 - 2.6 Hz) they correlated to cerebral blood flow using the nitrous oxide method, while the high frequency band centroid (4 - 15 Hz) they found inversely correlated to the PVI as a measure of craniospinal compliance. Further clinical experience (90) with the high frequency centroid showed that the percentage of time spent with a high frequency centroid greater than 9 Hz bore no relation to ICP but that the centroid frequency correlated exponentially to increased mortality. Case reports showed that the high frequency centroid was a better measure of the clinical state of the patient than was the absolute ICP alone.

C. Aims

It would appear from this review of the literature that the systems analysis approach to studying cerebrovascular pressure transmission may prove to be a powerful aid to the investigation of the pathophysiology and, of more immediate clinical importance, the prediction of raised ICP. To date, these reported studies have been performed in experimental models of raised ICP, but this approach has yet to be applied to patients in a systematic fashion.

Of the two systems analysis methods reported, the method used by Kasuga et al (87) is clinically impractical, while the method of Portnoy and Chopp (78) is unproven in a clinical setting. The primary purpose of the work described in this thesis is to determine the feasibility of applying this approach to patients, and in doing so to define the inherent variability of the pressure transmission characteristics of the cerebrovascular bed in patients at risk of raised ICP. A secondary aim of this work, not yet addressed in the current experimental literature, is to define better the relationship between cerebrovascular pressure transmission, cerebrovascular resistance and craniospinal compliance, a knowledge of which may prove of value in the interpretation of the clinical data.

CHAPTER II. CLINICAL STUDIES

The aim of this work was to make a series of analytical measurements of intracranial pressure in head injured patients applying the principles of systems analysis. To do this required a number of methodological studies which are also described in this section.

A. General Methods

1. Systems Analysis

Systems analysis is a technique whereby an attempt is made to define the physical characteristics of a system using only the system input and output signals (79) (Figure 7). In the present studies, the assumption is made with this analysis that the cardiac based pulsations of the BP waveform are the chief input signal (f(t)) to the cerebrovascular system and, similarly, the same pulsations in the ICP waveform are the output response (g(t)) to that stimulus. Both BP and ICP waveforms are transformed from the time domain into the frequency domain by Fourier analysis (80) which permits any complex waveform to be described as a series of simpler component harmonics, consisting of a fundamental or first harmonic (related to the heart rate frequency) and a series of higher harmonics at multiples of the fundamental frequency. The Fourier analysis technique, as applied to systems analysis of cerebrovascular pressure transmission, will be only summarized in this section. A fuller description of the analytical method is given in Appendix B. The system transfer function (H(w)) is defined as the relationship that describes how the stimulus signals are transformed by the system into response signals. The transfer function consists of amplitude and phase components. As an example (Figure 7), the first component of the amplitude transfer function is calculated as the ratio of the first cardiac component harmonic in the ICP spectrum (G(w)) to the amplitude of the first cardiac component harmonic in the BP spectrum (F(w)). This process is repeated for each of the significant ICP and BP cardiac component harmonics present in the ICP and BP amplitude spectra. By similar means, the difference between the ICP and BP phase values (phase shift) for each of the measured cardiac component harmonics yields the phase transfer function. The amplitude transfer function is a measure of how much pressure is transmitted through the cerebrovascular bed at a

given frequency. The phase transfer function is a measure of how much a sinusoidal pressure signal is shifted in phase as it is transmitted through the cerebrovascular bed at a given frequency.

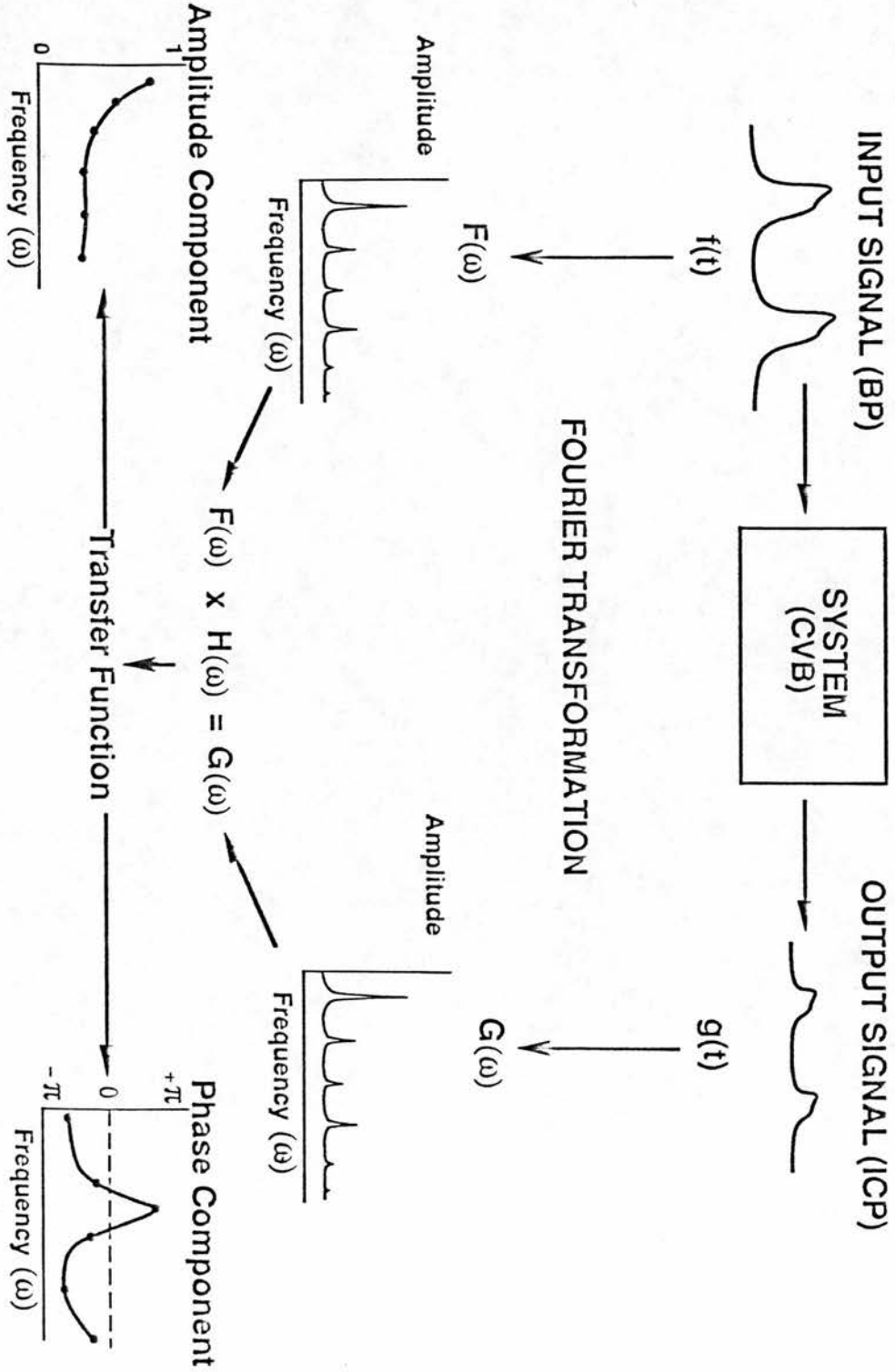

Figure 7: Systems Analysis.

2. Pressure Measurement

The general criteria of pressure recording accuracy have been well reviewed by Fry (91), Geddes (92) and Gabe (93). The weakest link in the pressure recording system is often the catheter-transducer system used for monitoring pressure. The catheter-transducer system consists of a pressure transducer and any fluid-filled linkages (needles, tubing, 3-way taps) that may separate the pressure source from the pressure sensor. A catheter-transducer system can be described as a second order mechanical system consisting of a mass of fluid which acts against the viscous (damping) and elastic properties of the walls of both the catheter and the pressure transducer dome (94,95).

Hanson and Warburg (95) demonstrated that a fluid-filled catheter-transducer system, if underdamped, will oscillate at its own natural frequency and can produce significant pressure waveform amplitude and phase distortion. The degree of distortion will depend on the damping factor (ß) of the system. The natural frequency and damping properties of a system can be tested by applying a step or transient pressure to the input of the system and recording the output pressure response (Appendix C). This transient response or "pop" test technique can show that for most purposes a damping factor of 0.64 (optimal damping) is desirable as the amplitude error will be less than 2% for up to two-thirds of the natural frequency of the system and the phase lag will be approximately linear over this range.

Transient response analysis of the fluid-filled catheter-transducer system used in these studies has shown, from a series of 10 sequential pop tests[1], that it is underdamped (ß = 0.310 +- 0.021[2]) with a resonant frequency of 21 Hz. Figure 8 shows the configuration of the catheter-transducer system used for pressure measurement throughout these studies which consisted of a Medex[3] Novatrans strain gauge transducer, a 30 cm connecting line, two 3-way taps, an acudynamic[4] adjustable

---

[1]For each of the 10 sequential pop tests a new Medex transducer dome, Cordis catheter, 3-way tap and Acudynamic adjustable damping device was fitted to the test apparatus.

[2]mean +- SD

[3]Medex Inc., Ohio, USA

[4]Abbott Critical Care Systems, Chicago, USA

damping device, and for ICP measurement a Cordis[5] subdural catheter or, for BP measurement, typically an 18 gauge 2.25 inch needle. The acudynamic adjustable damping unit is a device which, when placed in series with the catheter-transducer system tubing, can be adjusted to provide an optimally damped (ß = 0.622 +- 0.04[6]) flat frequency response with minimal amplitude distortion up to 14 Hz (96) (Appendix C). Bench testing determined the optimal setting of the acudynamic adjustable damping device for standard lengths and diameters of catheters and needles used for pressure monitoring throughout this study (Table 1).

Table 1: Settings of the Acudynamic Adjustable Damping Device Required to Correct Underdamping.

Catheter	Gauge	Resonant Frequency (fo)	Damping (ß) Pre Correction	Acudynamic Turns	Damping (ß) Post Correction
Vygon	18g	19.5 Hz	0.298	2 1/4	0.600
Vygon	20g	19.4 Hz	0.362	1 3/4	0.667
Cathlon	18g	19.5 Hz	0.286	2 1/2	0.608
Cathlon	20g	19.8 Hz	0.240	2	0.617
Cordis	Sub Dural	21 Hz	0.310	2 1/2	0.622

Test Conditions:
- Medex Novatrans transducer
- 30 cm extension tubing
- Acudynamic adjustable damping device
- 2 X 3-way taps

[5]Cordis (UK) Ltd., Brentford, UK

[6]mean +- SD

Pressure was also monitored in these studies by Camino[7] catheter-tip transducer systems (Figure 9). These fibre-optic devices have at the tip a semi-rigid membrane with a mirrored surface. This membrane deflects as pressure is applied to it. A source at the other end of the fibre sends light towards the tip, which is reflected back towards photosensitive cells, and the amount of light reflected is proportional to the deflection of the membrane tip and hence the applied pressure. Camino catheter-tip pressure transducers have a natural resonant frequency well outside our analysis frequency band and, when used with the appropriate high frequency research monitors (420 XP), have a flat amplitude frequency response up to 70 Hz. Table 2 summarizes the static and dynamic characteristics of the transducer systems used throughout this study.

Table 2: Static and Dynamic Characteristics of Pressure Transducer Systems.

Characteristic	Medex Novatrans	Camino	Bentley Trantec
Pressure Range	-50->400 mmHg	-10->250 mmHg	-100->300 mmHg
Linearity & Hysteresis	+- 2 percent	1%->50 mmHg 6% thereafter	+- 1 percent
Temperature Drift	0.3 mmHg/ Degree C	0.2 mmHg/ Degree C	0.2 mmHg/ Degree C
Frequency Response	DC->14 Hz	DC->70 Hz	DC->25 Hz

[7]Camino Laboratories, San Diego, USA

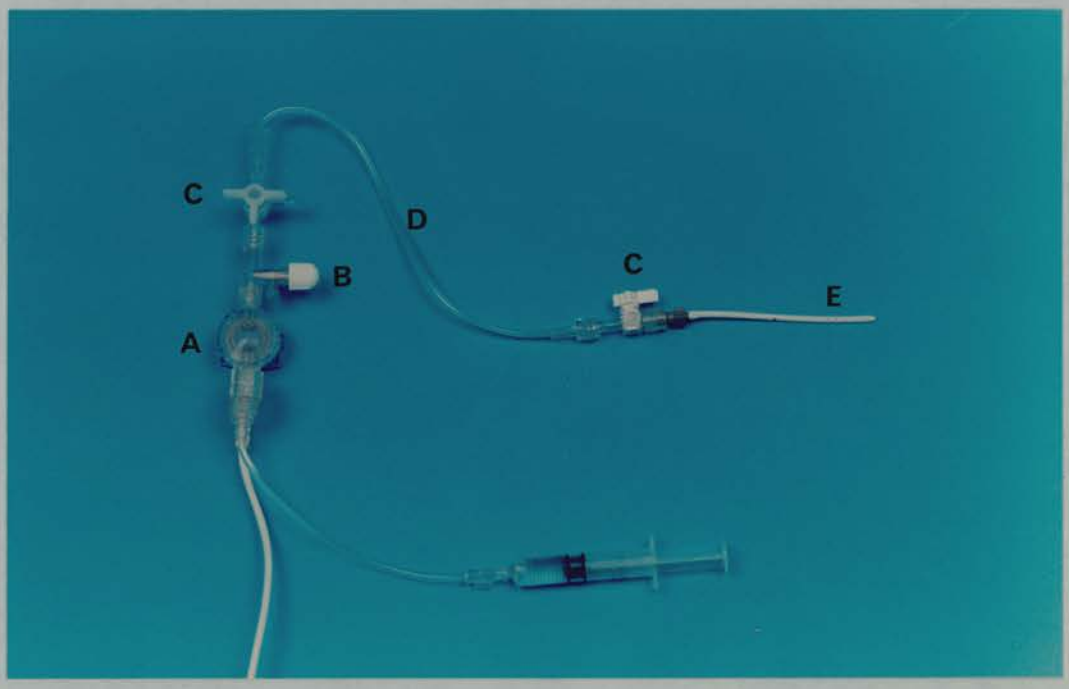

Figure 8: Clinical Catheter–Transducer System. A, Medex Novatrans transducer; B, Acudynamic adjustable damping device; C, 2 X 3 way taps; D, 30 cm low compliance extension tubing; E, Cordis subdural catheter.

Figure 9: Camino Catheter–Tip Transducer System. A, Camino 420XP high frequency research monitor; B, Camino catheter-tip ICP transducer.

3. Data Collection

ICP was monitored subdurally by Camino catheter-tip transducers using the Camino 420 XP research monitors. Over 80% of ICP recordings were obtained using the Camino system, whilst the remaining ICP recordings were obtained using optimally damped Medex fluid-filled systems connected to Kontron[8] Supermon patient monitors. BP was monitored through radial artery cannulation by optimally damped Medex fluid-filled catheter-transducer systems connected to Kontron Supermon patient monitors.

Samples of ICP and BP waveform data were stored to a magnetic tape by a TEAC[9] MR-10 FM cassette analogue data recorder. Data collection was under automatic microcomputer control using an IBM-XT[10] microcomputer configured with a general purpose interface bus adapter controlling the TEAC data recorder. Automatic and manual starting and stopping of the waveform data collection could be carried out at any time. With each waveform segment stored to tape, a computer file was created storing the starting tape count and the time and date of sample collection. Comments could be entered and stored to the current active computer file at any time, thus allowing precise annotation of significant events. A flow chart summarizing the data collection program is contained in Appendix D.

A two channel variable gain amplifier, incorporating a 5th order low pass filter with a corner frequency of 70 Hz, was designed and built to allow conditioning of the analogue waveform data prior to digitizing. The fast roll off filter characteristic (30 db per octave) of this amplifier limited frequencies higher than 70 Hz from aliasing with the sampling frequency. A schematic diagram for the amplifier design is contained in Appendix E. The entire waveform recording system, including pressure transducers, patient monitors, FM tape recorder and pre-aliasing low-pass filter, had a flat amplitude frequency response from DC to 70 Hz +- 1 db (DC to 14 Hz +- 1 db with the optimally damped fluid-filled catheter-transducer system) and a linear phase shift of 0.096 radians/Hz. Corrections were carried out in software for the linear phase shifts

---

[8]Kontron Ltd., Watford, U.K.

[9]Teac Corp., Tokyo, Japan

[10]IBM UK LTD., Portsmouth, U.K.

inherent in the waveform recording system. The frequency analysis of the waveform recording system is contained in Appendix F.

4. Data Analysis

Waveform data stored to tape was analysed off-line by a microcomputer based waveform analysis system developed for this project. An Apricot[11] XEN-i microcomputer running the 32-Bit 80386 microprocessor at 16 MHz forms the basis of the system. An enhanced graphics adapter displays 740 X 348 pixel graphics for display of raw and transformed waveform data. Twenty seconds of concurrent ICP and BP waveform data (8192 points) is digitized at a sampling rate of 400 Hz using a Data Translation[12] DT2818 analogue to digital converter (A/D). The DT2818 uses a 12-bit simultaneous sample and hold A/D converter, which allows 4 channels of analogue data to be sampled within 5 nanoseconds at a resolution of 1/4096 of the full scale pressure range. Aliasing artifacts are avoided by restricting the bandwidth of the waveform data using pre-alias filtering in combination with the technique of four times over sampling (97,100).

Once digitized, the sampled ICP and BP waveforms are displayed graphically so as to allow a waveform segment free of mechanical and other non-physiological artifacts to be selected for analysis. A graphics cursor permits measurement of ICP and BP waveform event amplitudes and periods prior to spectral analysis. The sampled ICP and BP waveform segments consist of three main terms: a slow sinusoidal term (0.2 - 0.3 Hz) linked to respiration rate, a higher frequency term (1 - 3 Hz) linked to heart rate, and a DC or static pressure term (Figure 10). The DC term, if not removed prior to spectral analysis, will cause a very large side lobe in the spectrum to obscure the lower frequency components (80). To prevent this, the arithmetic mean term of each waveform segment is calculated and subtracted from each waveform data point value. This mean rejection algorithm removes the DC term present in the ICP and BP waveforms while leaving the respiratory component and cardiac component frequencies unaffected.

---

[11]Apricot Computers Ltd., Birmingham, U.K.

[12]Data Translation Ltd., Marlboro, USA.

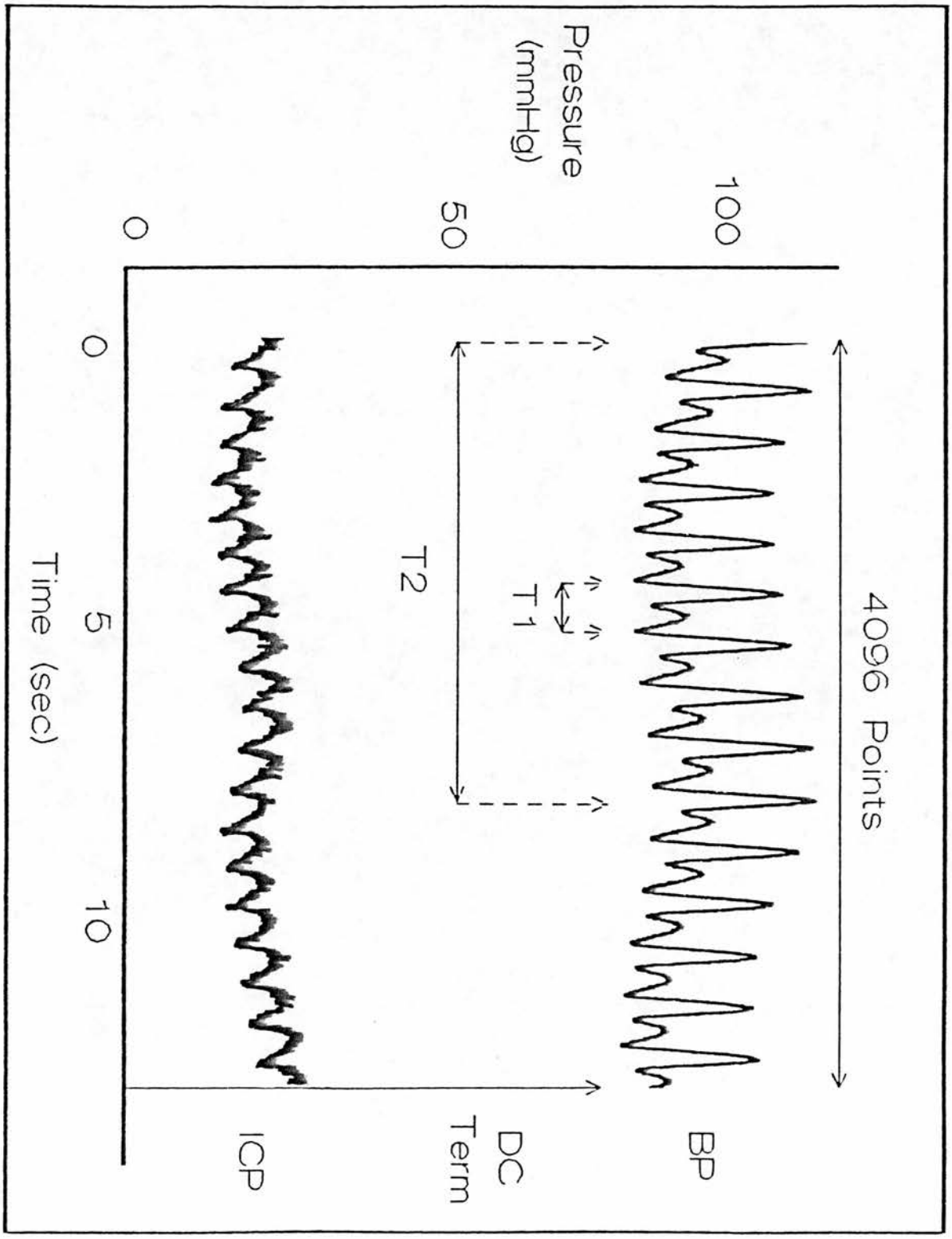

Figure 10: Sampled BP and ICP Waveform Segments. T1 = period of heart rate, T2 = period of respiration, DC term = static pressure.

The BP waveform cardiac component systolic peak nearest the apex of respiration is taken as the starting point for analysis, and the following 4096 points of both ICP and BP waveforms are then selected for spectral analysis. To improve the accuracy of the spectrum, prior to spectral analysis, the initial and final 10% of the waveform segment is multiplied by a Hanning window function (97) which helps to prevent "end effects" (80) from causing the appearance of large side lobes around peaks in the spectra.

The standard Fast Fourier Transformation (FFT) algorithm published by Cooley and Tukey (98) is used for calculation of the discrete Fourier transform. A 4096 point FFT is calculated on each ICP and BP waveform segment. The ICP and BP amplitude spectra, calculated from the Fourier transform (Appendix B), are displayed and a graphics cursor allows measurement and recording of the amplitude, frequency and phase of the spectral peaks at each measurable harmonic component in the amplitude spectrum for both the ICP and BP waveforms. The frequency resolution of the amplitude spectrum, calculated as the quotient of the sampling rate and sample number, is 0.098 Hz. Figure 11 shows the amplitude spectrum of the ICP waveform (including raw waveforms) from a patient with normal ICP compared with that of a patient exhibiting raised ICP. There is a large harmonic at the respiratory frequency (0.2 Hz = 12 breaths/minute), while the largest harmonic is seen at 1.4 Hz (84 beats/minute) which is the cardiac component fundamental. The higher harmonics are all multiples of the cardiac component fundamental.

The amplitude and phase transfer functions are then calculated from the ICP and BP amplitude spectra and raw Fourier transformed data by standard methods (79) (Appendix B). Only the cardiac component harmonics in the amplitude spectra are used in the calculation of the amplitude and phase transfer functions. Figure 12 shows the amplitude and phase transfer functions from a patient with normal ICP compared with that of a patient with raised ICP. All software is written in the C programming language. A flow chart summarizing the data analysis program is contained in Appendix G.

Figure 11: Amplitude Spectra of ICP Waveforms at Low and Raised ICP.

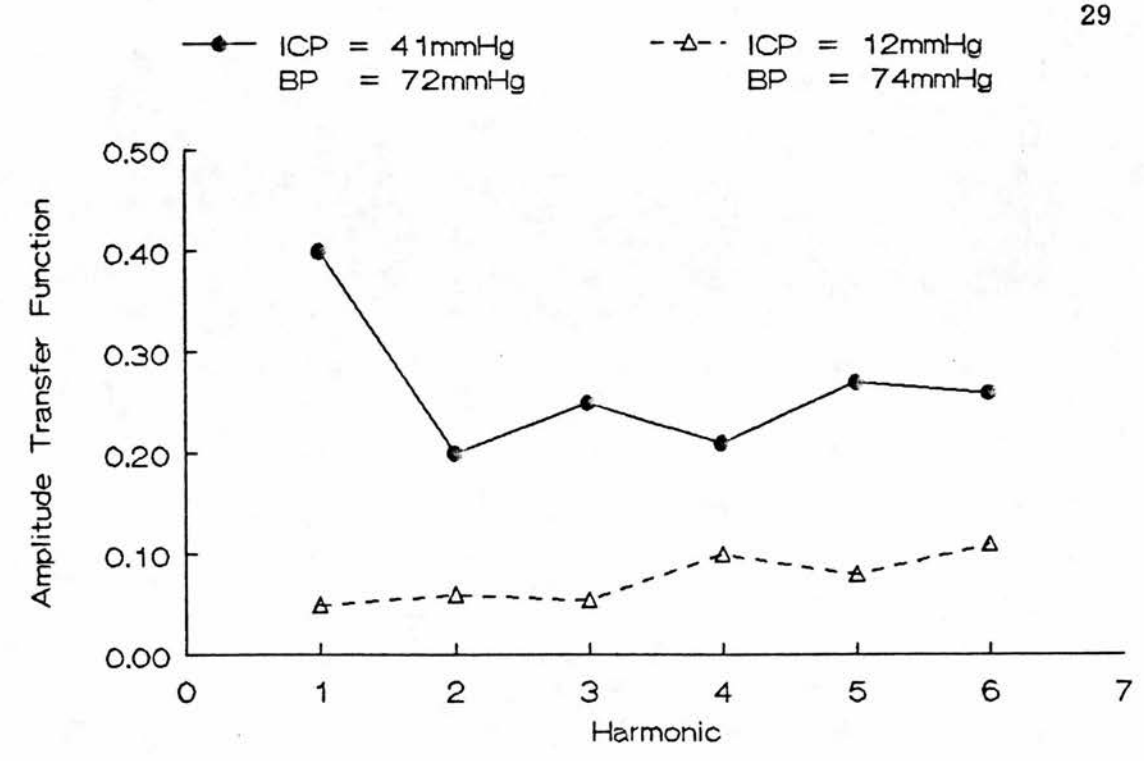

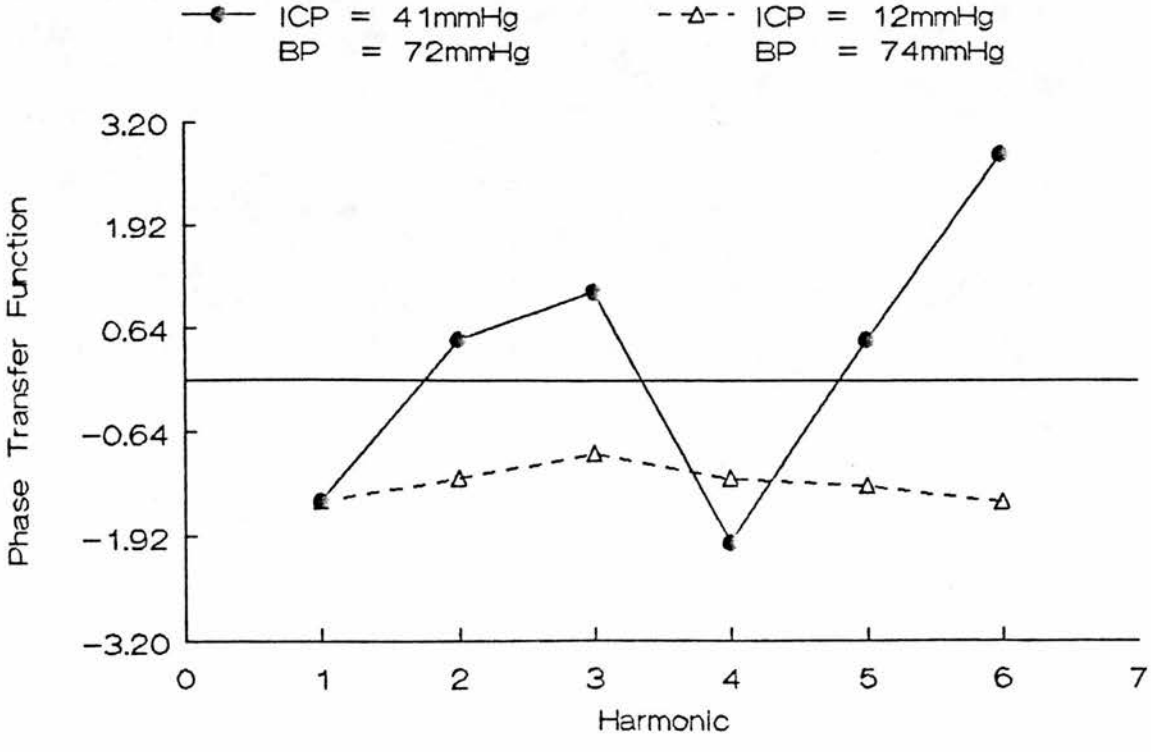

Figure 12: Amplitude and Phase Transfer Functions at Low and Raised ICP.

B. Pilot Studies

1. Reproducibility Study

A measure often used in describing the amount of variation in a population is the coefficient of variation (CV) (99):

CV = (sample standard deviation/sample mean) x 100

To assess the variance of the method in the study population, thirty sequential samples of ICP and BP waveforms were collected from a stable normotensive, normovolemic head injured patient with normal ICP (ICP < 15 mm Hg). The mean and standard deviation for each of the first 8 cardiac component harmonics were calculated and expressed as the coefficient of variation. Figure 13 is a plot of the coefficient of variation for each of the first 8 cardiac component harmonics from the amplitude and phase transfer functions. For the amplitude transfer function data, the first 5 harmonics have a coefficient of variation of less than 10%, the 6th and 7th show a variation of between 20% and 30% and the 8th harmonic shows a variation of greater than 45%. With the phase transfer function data, only the fundamental phase shows a variation of less than 20%, harmonics higher than the 4th showing very large variation between repeated measurements. Abrupt changes in phase between the 4th and 6th harmonics, often from a positive to a negative phase (phase cross-over), were frequently noted in the patient data and may be the source of the large variation above the 4th harmonic in the phase transfer function.

2. Effect of Blood Pressure Measurement Site

Use of the radial artery waveform as a measure of the input signal to the cerebrovascular bed is not ideal. The abdominal, iliac, carotid, subclavian and thoracic pressure waveforms have each been used by previous workers in this field, in experimental studies, as the input signal to the cerebrovascular bed (78,81,82,101). Both clinical and experimental studies were performed to determine the effect of different arterial pressure measurement sites on the amplitude and phase transfer functions.

a. Experimental Study

In an experimental study in cats, the intraventricular ICP waveform was recorded through an optimally damped fluid-filled catheter-transducer system. A Camino catheter-tip pressure transducer was

placed in the thoracic segment of the descending aorta, through a femoral cannulation, for measurement of the arterial blood pressure waveform. Sequential measurements of the amplitude and phase transfer functions between the BP and ICP measurement sites were obtained during withdrawal in ten 1.5 cm steps of the arterial catheter towards the periphery. As a measure of the effect of catheter withdrawal on the amplitude and phase transfer function harmonics, the mean and standard deviation between samples collected over the entire withdrawal procedure, was calculated for each harmonic and expressed as the coefficient of variation. Figure 14 is a plot of the coefficient of variation expressed as a function of harmonic number.

With the amplitude transfer function data, the fundamental showed the least variation (16%), while all higher harmonics showed equal variance (28% - 33%) to catheter withdrawal. With the phase transfer function data, only the fundamental phase showed a variation of less than 20%, while the higher harmonics showed very large variation which increased progressively with catheter withdrawal.

This data indicates that catheter position does affect the amplitude transfer function, but independently of frequency; that is, the harmonics higher than the fundamental are equally affected by catheter position, with no frequency dependent effects being demonstrated. The fundamental was affected less than higher harmonics indicating that the amplitude transfer function calculated using a peripheral BP measurement site may be biased in favour of the fundamental but by no more than the inherent variability from repeated measurements from the study population. In contrast to this, the phase shift is greatly affected in a frequency dependent manner by catheter position. The phase transfer function calculated from a peripheral BP measurement site will be significantly distorted above the fundamental phase.

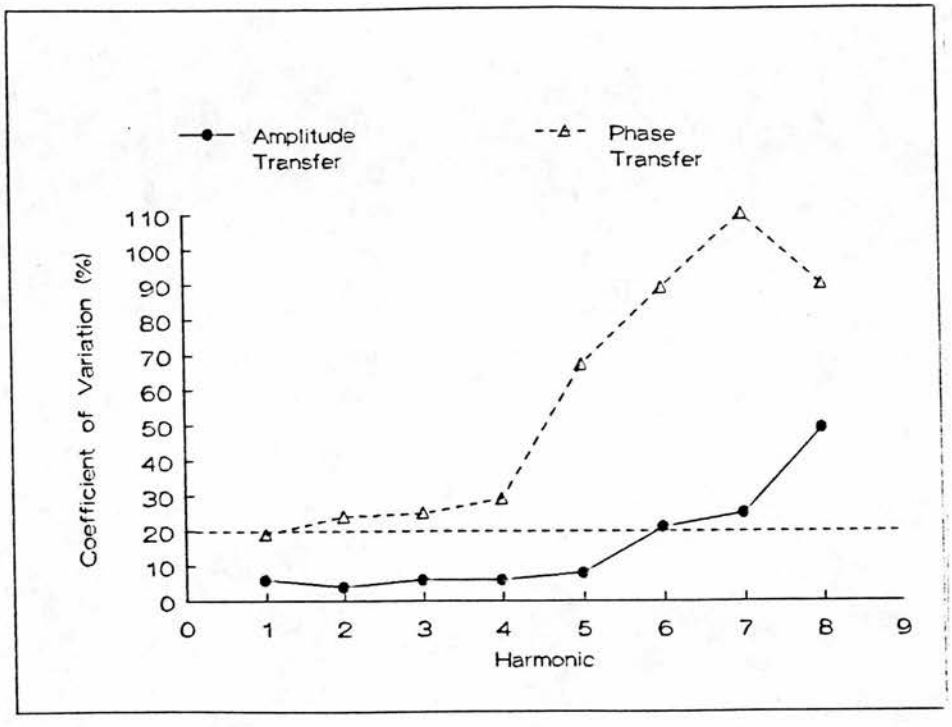

Figure 13: Coefficient of Variation of the Amplitude and Phase Transfer Functions, from Repeated Samples.

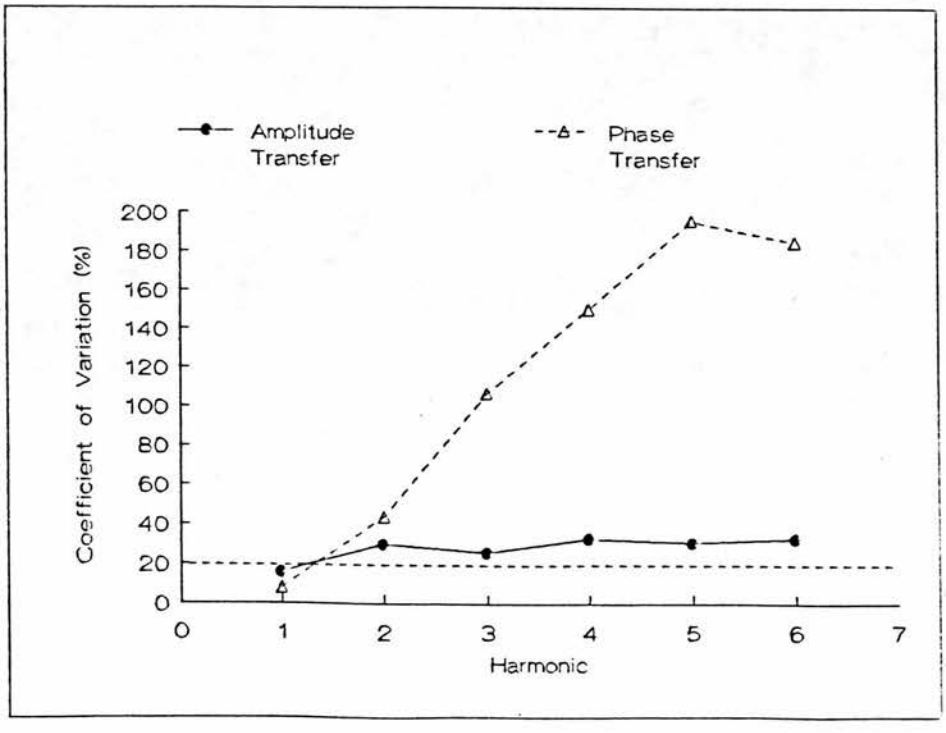

Figure 14: Coefficient of Variation of the Amplitude and Phase Transfer Functions, from BP Catheter Withdrawal.

b. Clinical Studies

In one stable normovolemic patient, for a short period during changing of BP monitoring from the radial to femoral sites, simultaneous radial pressure waveform and the lower abdominal aorta pressure waveform (through optimally damped radial and femoral artery cannulae) were recorded. The amplitude and phase transfer functions (Figure 15) calculated from both BP measurement sites to ICP (ICP/Aorta, ICP/Radial) showed very similar configuration, with the ICP/Radial amplitude transfer function showing overall a marginally greater transfer function at all frequencies. The phase transfer functions, however, were markedly different above the fundamental phase, the ICP/Radial phase transfer function showing a more positive phase than the ICP/Aortic phase transfer function.

In another patient, after accidental cannulation of the carotid artery during insertion of a jugular catheter, the carotid and radial pressure waveforms were simultaneously recorded for a brief period and the transfer functions from both BP sites and the ICP waveform were compared (Figure 16). The carotid and radial to ICP amplitude transfer functions showed similar configuration up until the 5th harmonic where the carotid/ICP transfer function demonstrated a moderately greater transfer (< 30%). Similar to the previous patient, however, the two phase transfer functions were markedly different above the fundamental phase, the ICP/Radial phase transfer function showing a more positive phase which increased progressively with frequency, the ICP/Carotid phase transfer function showing less frequency dependence.

This clinical data indicates there is no marked effect of peripheral BP measurement site on the first 6 cardiac component harmonics of the amplitude transfer function. In contrast to this the phase transfer function above the fundamental phase is greatly affected by BP measurement site.

With a variation between repeated measurements of greater than 20 percent it may be difficult to define significant changes in the amplitude transfer function harmonics greater than the 6th and phase transfer function greater than the fundamental phase. Based on this data the waveform analysis in this thesis is limited to the amplitude transfer function up to the 6th harmonic of the cardiac frequency, and the phase shift of the fundamental alone.

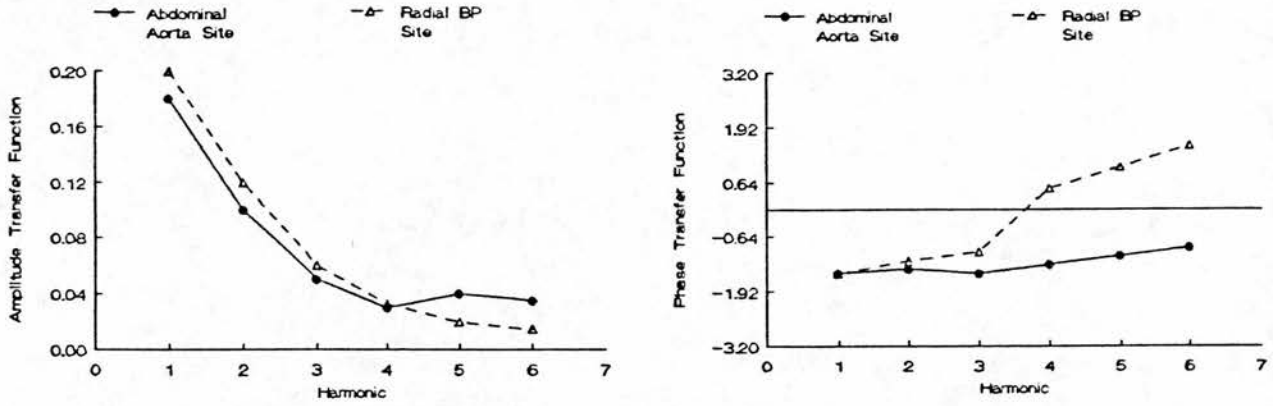

Figure 15: Amplitude and Phase Transfer Functions Calculated from Simultaneous Abdominal Aorta and Radial Artery BP Sites.

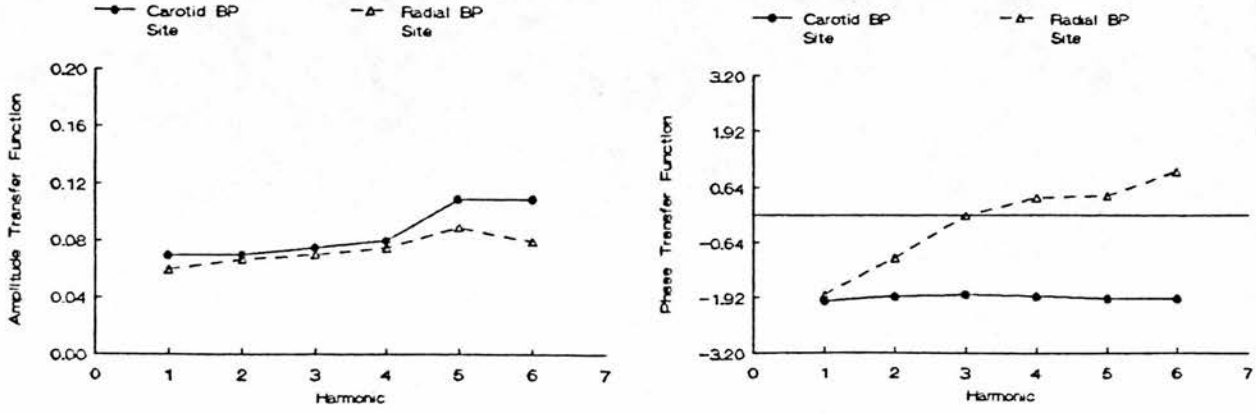

Figure 16: Amplitude and Phase Transfer Functions Calculated from Simultaneous Carotid and Radial Artery BP Sites.

3. Effect of Positive Pressure Ventilation

Positive pressure ventilation parameters can affect mean ICP (102,103). Its effects on the cerebrovascular amplitude transfer function and fundamental phase shift are unknown. Waveform data from a normotensive, normovolemic head injured patient with normal ICP (ICP < 15 mm Hg) has been obtained, showing the effects of two ventilation parameters: inspired to expired ventilation time (I/E ratio) and positive end expiratory pressure (PEEP).

Figure 17 shows the effects of three levels of I/E ratio (25%, 33% and 50%) and three levels of PEEP (+5, +10, +15 cm H2O) on the amplitude transfer function and fundamental phase shift. It can be seen that both I/E ratio and PEEP affect predominantly the fundamental in the amplitude transfer function, where increasing values of I/E ratio and PEEP lead to increasing transfer of this frequency. Increasing I/E ratio was associated with a small increase in the fundamental phase shift in a negative direction. PEEP shows no consistent effect on the fundamental phase shift. ICP increased from 12 to 14 mm Hg with no change in BP when I/E ratio was increased. ICP increased from 13 to 14 mm Hg while BP dropped from 93 to 82 mm Hg when PEEP increased. End tidal CO2 (ETCO2) remained constant at 4.1 kPa.

These data demonstrate that I/E ratio and PEEP can affect the fundamental of the amplitude transfer function and the fundamental phase shift.

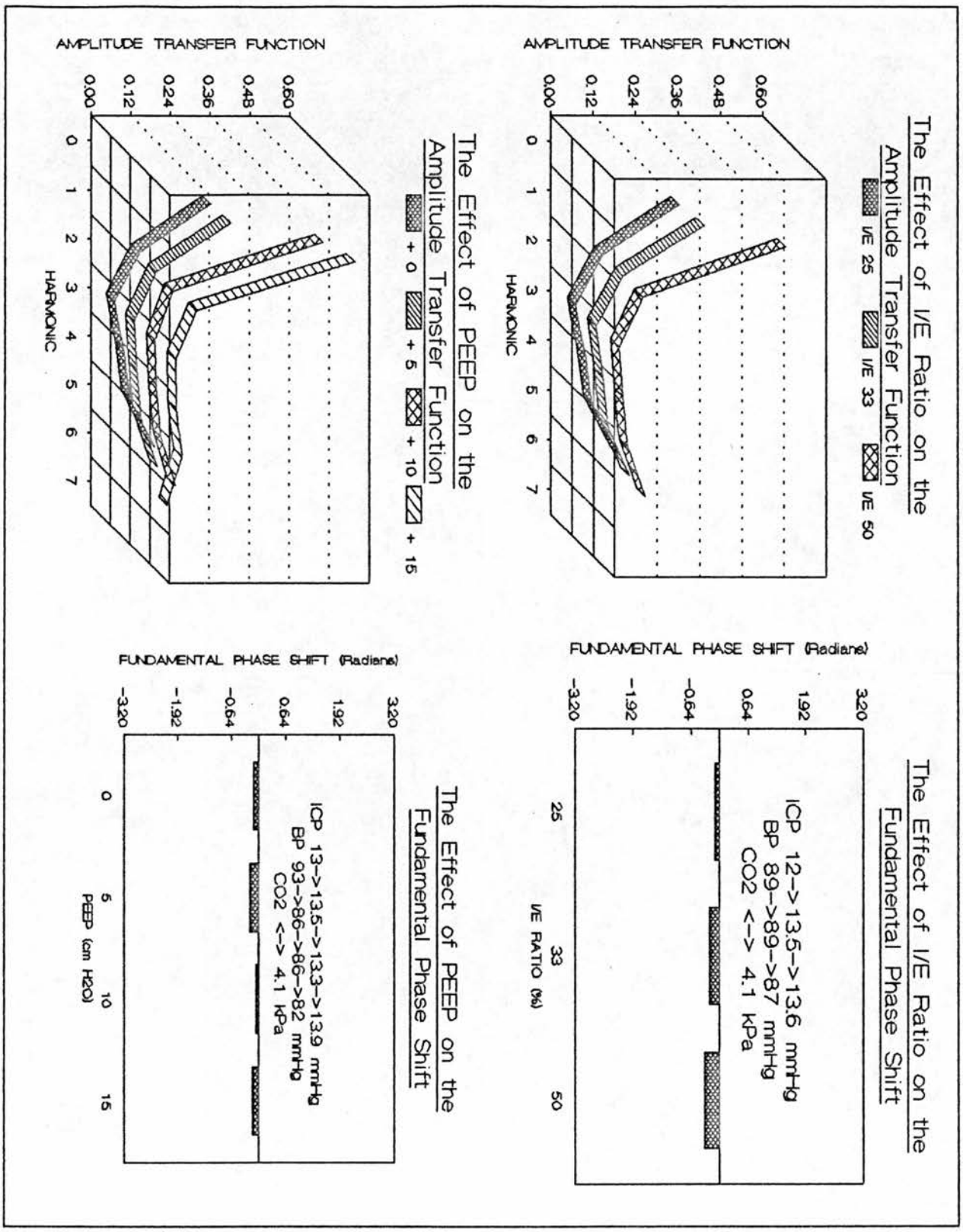

Figure 17: The Effects of I/E Ratio and PEEP on the Amplitude Transfer Function and Fundamental Phase Shift.

4. Effect of Hypocapnia

Experimental data from the work of Portnoy et al (81) and Takizawa et al (86) indicate that PACO2 affects chiefly the fundamental of the amplitude transfer function. The effect of PACO2 on the amplitude transfer function and the fundamental phase shift in head injured patients is unknown.

Samples of ICP and BP waveforms were recorded from a normotensive head injured patient with normal ICP (ICP < 15 mm Hg) during progressive hypocapnia (ETCO2 4.1 decreasing to 3.02 kPa) induced by removal of excess ventilatory dead space.

Figure 18 shows the effect of progressive hypocapnia on the first 6 harmonics of the amplitude transfer function and the fundamental phase shift. It can be seen that it is predominantly the fundamental and second harmonics of the amplitude transfer function which are affected by PACO2, higher harmonics showing little or no response to progressive hypocapnia. The fundamental phase shift shows no significant response to progressive hypocapnia. ICP decreases from 13 mm Hg to 11 mm Hg and BP from 92 to 88 mm Hg in response to progressive hypocapnia.

These data demonstrate that ETCO2 can affect the low frequency components of the amplitude transfer function.

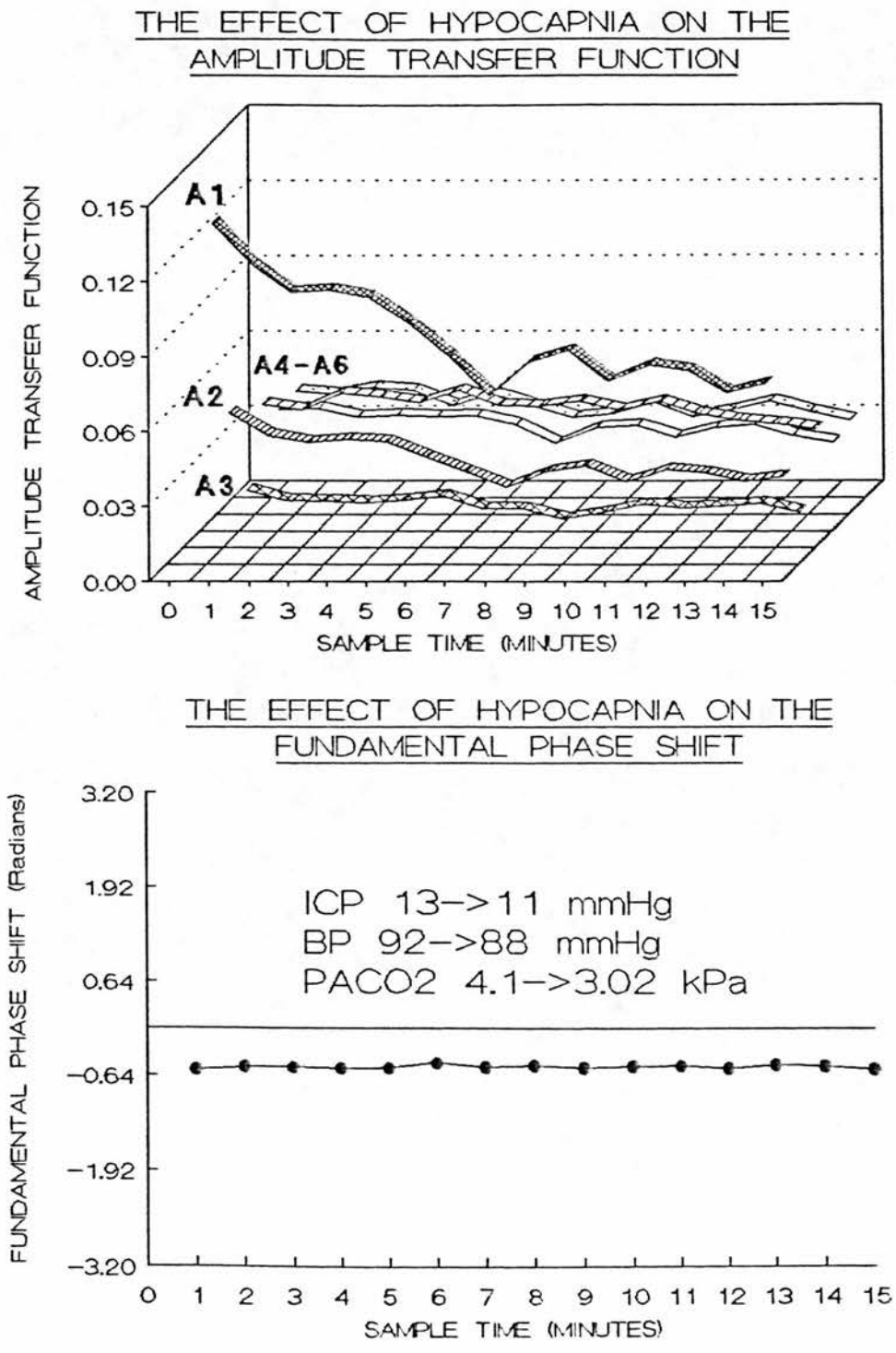

Figure 18: The Effects of Hypocapnia on the Amplitude Transfer Function and Fundamental Phase Shift.

5. Effect of Jugular Compression

Obstruction of intracranial venous outflow caused by turning of the head can increase mean ICP (104,105). The effects of obstruction of intracranial venous outflow on the amplitude transfer function and fundamental phase shift in head injured patients is unknown.

Samples of ICP and BP waveform data were recorded from a normotensive, normovolemic head injured patient with normal ICP (ICP < 15 mm Hg). Four sequential twenty second waveform samples were recorded both before and during compression of the right jugular vein. Figure 19 shows the effect of compression of the right jugular vein on the first 6 harmonics of the amplitude transfer function and on the fundamental phase shift. Values for each harmonic are expressed as mean +- standard deviation for the four sequential samples. It can be seen that it is predominantly the higher harmonics (4th, 5th and 6th) in the amplitude transfer function which are affected by jugular vein compression. The fundamental phase shift became more negative with jugular vein compression. In association with jugular compression, ICP increased significantly from 17 to 29 mm Hg ($P < 0.01$)[13] and BP increased from 87 to 90 mm Hg while ETCO2 remained unchanged at 4.0 kPa.

These data demonstrate that obstruction to intracranial venous outflow can affect the higher harmonics of the amplitude transfer function.

[13]Paired Student's t-test.

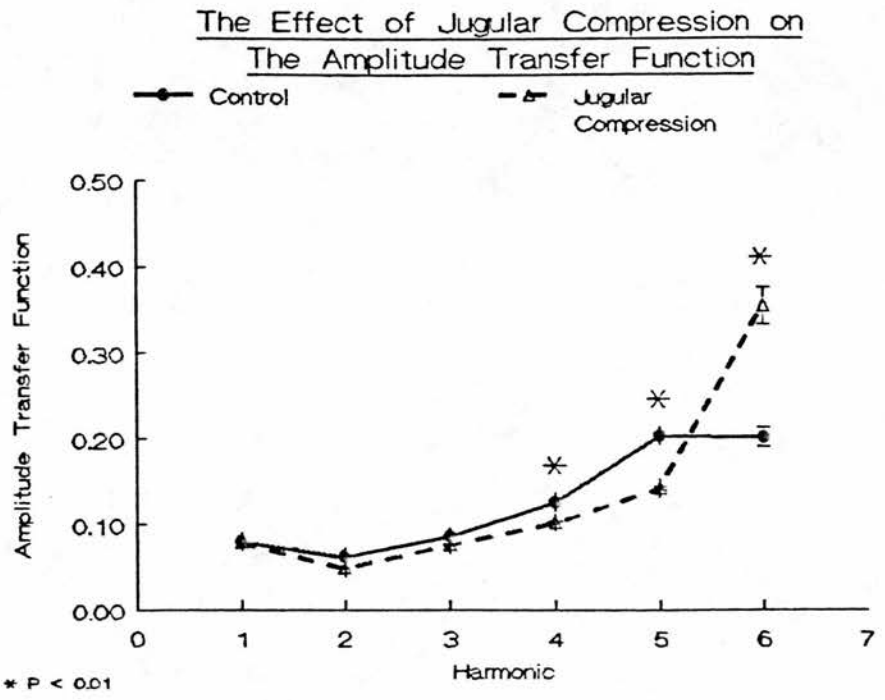

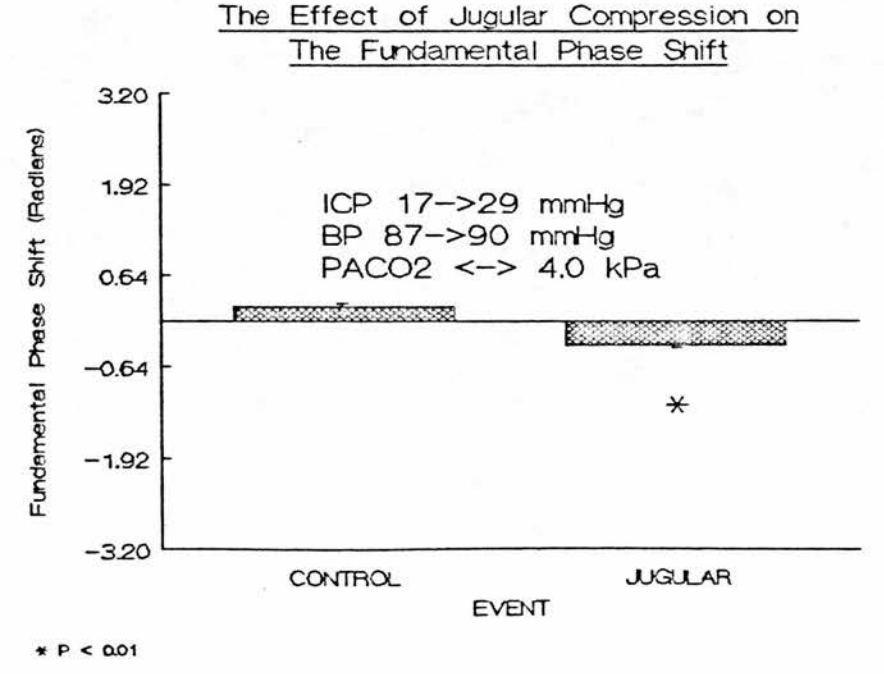

Figure 19: The Effects of Jugular Compression on the Amplitude Transfer Function and Fundamental Phase Shift.

C. An Observational Study in Head Injured Patients

The purpose of this study was to determine whether the systems analysis method could detect, in head injured patients, any pressure transmission characteristics of the cerebrovascular bed associated with raised ICP. In doing so, the inherent variability of cerebrovascular pressure transmission in the head injured population could also be defined.

1. Methods

Five minute samples of ICP and BP waveform data from 30 head injured patients, timed to coincide with clinical recordings by the nursing staff, were collected to tape, as previously described (page 18). This data was recorded once every half hour during the monitoring period which ranged from 2 to 14 days in the head injury intensive care unit.

All patients being ICP monitored had sustained a major head injury and were sedated (Phenoperidine: 2 - 4 mg/hour), paralysed (Pancuronium: 4 mg/hour) and mechanically ventilated with intermittent positive pressure ventilation. Ventilator and respiratory parameters were recorded, and were maintained constant during each segment of ICP recording (ventilation rate = 12 breaths/minute, percentage inspired time = 25%, percentage expired time = 65% with a 10% pause, peak inflation pressure = 15 to 20 cm H2O, percentage arterial oxygen saturation (SaO2) > 95%, ETCO2 = 3 to 4 kPa). Patients were positioned supine with 10 degrees of head up tilt. Head position was standardized and excessive flexion or rotation of the neck corrected.

With each waveform analysis the following physiological data were recorded: ICP, BP, CVP, heart rate (HRT) and core body temperature (Tc). In addition to each ICP and BP waveform collected, the most recently sampled arterial blood gas values (PaCO2, PaO2, pH) were recorded.
Waveform samples were excluded from the analysis under the following circumstances:

a) blocked, overdamped or faulty pressure monitoring equipment (including: catheters, transducers and fluid-filled connecting tubing);
b) samples from patients with major chest trauma;
c) samples within 30 minutes of physiotherapy;
d) samples within 120 minutes of therapy for raised ICP;

e) samples from patients with a clinical history of peripheral vascular disease;

f) samples from patients whose age was greater than 69 years.

2. Results

a. Patient Population

The study population consisted of 30 head injured patients (20 males, 10 females) with ages ranging from 6 to 62 years old (median age 23 years). On admission, 27 patients scored 8 or less on the Glasgow Coma Scale (GCS), 2 patients were GCS 9-12 and 1 patient was GCS 13-15. Computerized Tomographic (CT) scans showed that twenty patients exhibited focal brain lesions (8 acute subdural haematoma, 5 chronic subdural haematoma, 7 intracerebral haematoma) and ten patients presented with diffuse brain injury.

b. Transfer Function Data

The waveform database comprised 1500 ICP and BP waveform samples (50 per patient). Pilot samples (n = 100) from the waveform database underwent spectral analysis. The amplitude transfer function for the first 6 cardiac component harmonics were calculated and found to cluster into four classes (Figure 20): those with an overall flat amplitude transfer function (curve type 1), those with an elevated low frequency response (curve type 2), those with an elevated high frequency response (curve type 3) and those exhibiting both an elevated low and high frequency response (curve type 4). The remaining 1400 samples then underwent spectral analysis and were prospectively coded into the four curve types based on the following criteria:

Curve type 1: All harmonics were within 100% of the amplitude of the 3rd harmonic.

Curve type 2: The 1st harmonic was at least twice the amplitude of the 3rd harmonic, and all harmonics higher than the 1st had amplitudes within 100% of the 3rd harmonic.

Curve type 3: One or more harmonics above the 3rd harmonic were at least twice the amplitude of the 3rd harmonic, while the first and second harmonics were within 100% of the amplitude of the 3rd harmonic.

Curve type 4: Any amplitude transfer function not meeting the criteria of curve types 1, 2 and 3.

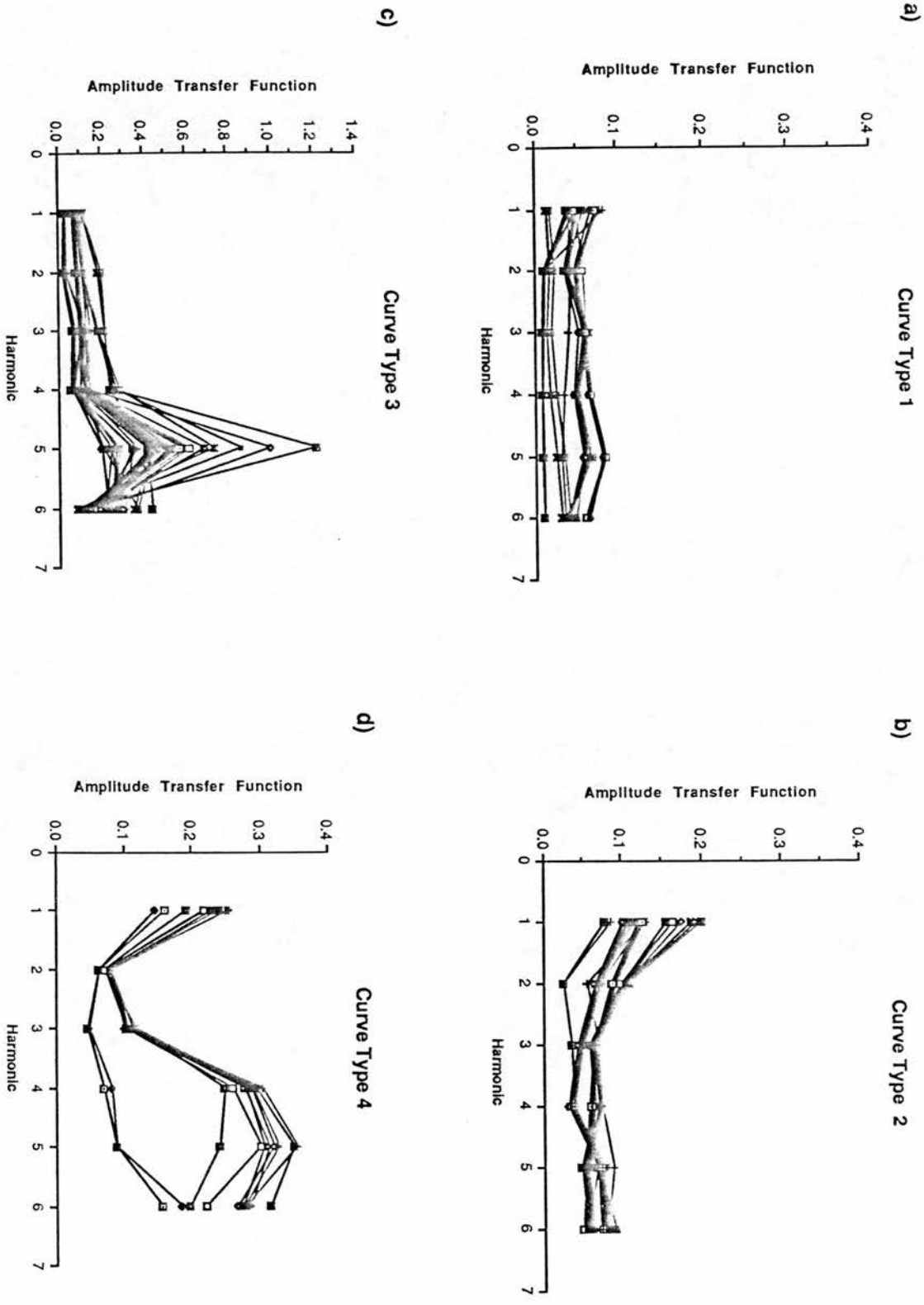

Figure 20: Observational Study Pilot Amplitude Transfer Function Data. A) Flat; B) Elevated Low Frequency; C) Elevated High Frequency; D) Elevated Low and High Frequency Cerebrovascular Pressure Transmission.

Twenty-eight amplitude transfer functions were excluded because one or more of the higher harmonics were immeasurably small.

The distribution of the amplitude transfer function harmonic samples was found to be log-normal. A log transformation of the data produced an approximately normal distribution (see Appendix H) with a Kolmogorov-Smirnov (Lilliefors modification) goodness of fit test[14] approaching acceptance of the null hypothesis, that is, not significantly different from a normal distribution (KS statistic < 0.15 with greater than 200 degrees of freedom). Table 3 lists the Kolmogorov-Smirnov goodness of fit statistic for each harmonic broken down by amplitude transfer function curve type. The 95% confidence limits were calculated from the transformed data for each of the 6 harmonics classed by amplitude transfer function curve type. Figures 21 and 22 show the plots for the averaged amplitude and fundamental phase shift data respectively, classed by curve type, together with the 95% confidence limits for each harmonic.

With the fundamental phase shift data, also grouped by amplitude transfer function curve type (Figure 22), the phase shift for curve type 2 and 4 are both more negative compared to curve type 1. Furthermore, the fundamental phase shift for curve type 3 shows a positive phase shift compared with the other curve types.

c. Physiological Data

Table 4 is a breakdown of the physiological data by amplitude transfer function curve type. BP was not significantly different between groups; however, curve types 2 and 4 (elevated low frequency, elevated low frequency in combination with elevated high frequency) were most often associated with raised ICP (ICP > 20 mm Hg) whereas curve types 1 and 3 (flat, elevated high frequency) were most often associated with ICP less than 15 mm Hg. Despite a strong association between ICP and amplitude transfer function curve type this effect failed to reach statistical significance ($P = 0.352$) tested by a "within patients design" multiple analysis of variance (MANOVA) comparison, with HRT, BP, CVP, Tc, PaCO2, PaO2 and pH acting as co-variates in the analysis. The small patient numbers per group may be relevant to this result. There was no significant difference in any of the co-variates (HRT, BP, CVP, Tc, PaCO2, PaO2 and pH) between amplitude transfer function curve types.

---

[14]SPSS Inc., Chicago, Illinois

Table 3: Breakdown of Kolmogorov-Smirnov Goodness of Fit Tests by Curve Type and Harmonic for the Transformed (Natural Log) Amplitude Transfer Function Data from Patients.

Curve Type	A1	A2	A3	A4	A5	A6	P1
1	0.0969	0.0721	0.1066	0.0452	0.0490	0.0546	0.1507
2	0.0607	0.0834	0.0917	0.0538	0.0657	0.0564	0.0919
3	0.0631	0.0800	0.0658	0.0621	0.0632	0.0733	0.1328
4	0.1342	0.1616	0.0846	0.1073	0.1111	0.0480	0.1519

A K-S statistic < 0.15 denotes an approximately normal distribution (see Appendix H)

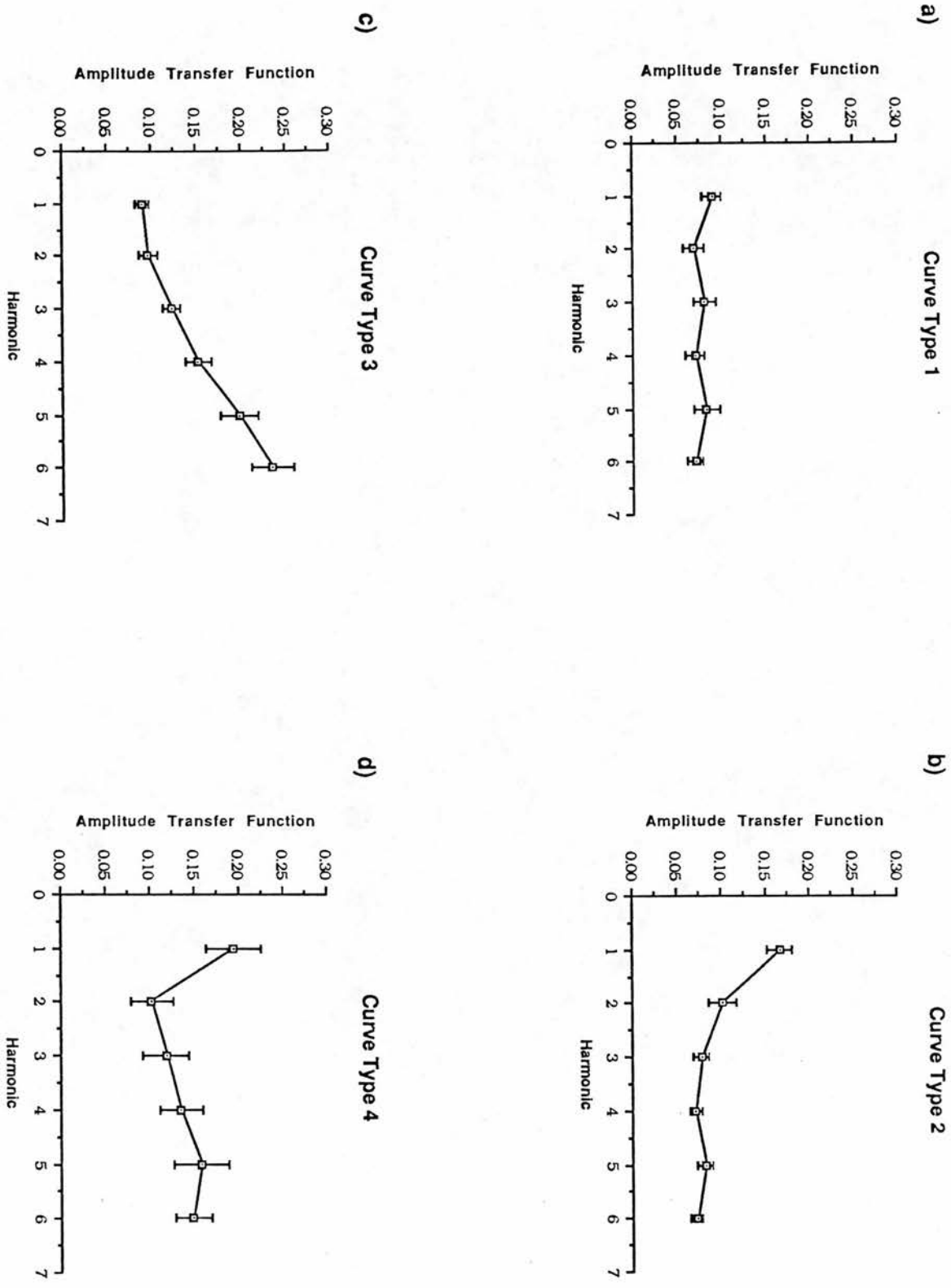

Figure 21: Observational Study Amplitude Transfer Function Data with 95% Confidence Limits for each Harmonic. A) Flat; **B)** Elevated Low Frequency; **C)** Elevated High Frequency; **D)** Elevated Low and High Frequency Cerebrovascular Pressure Transmission.

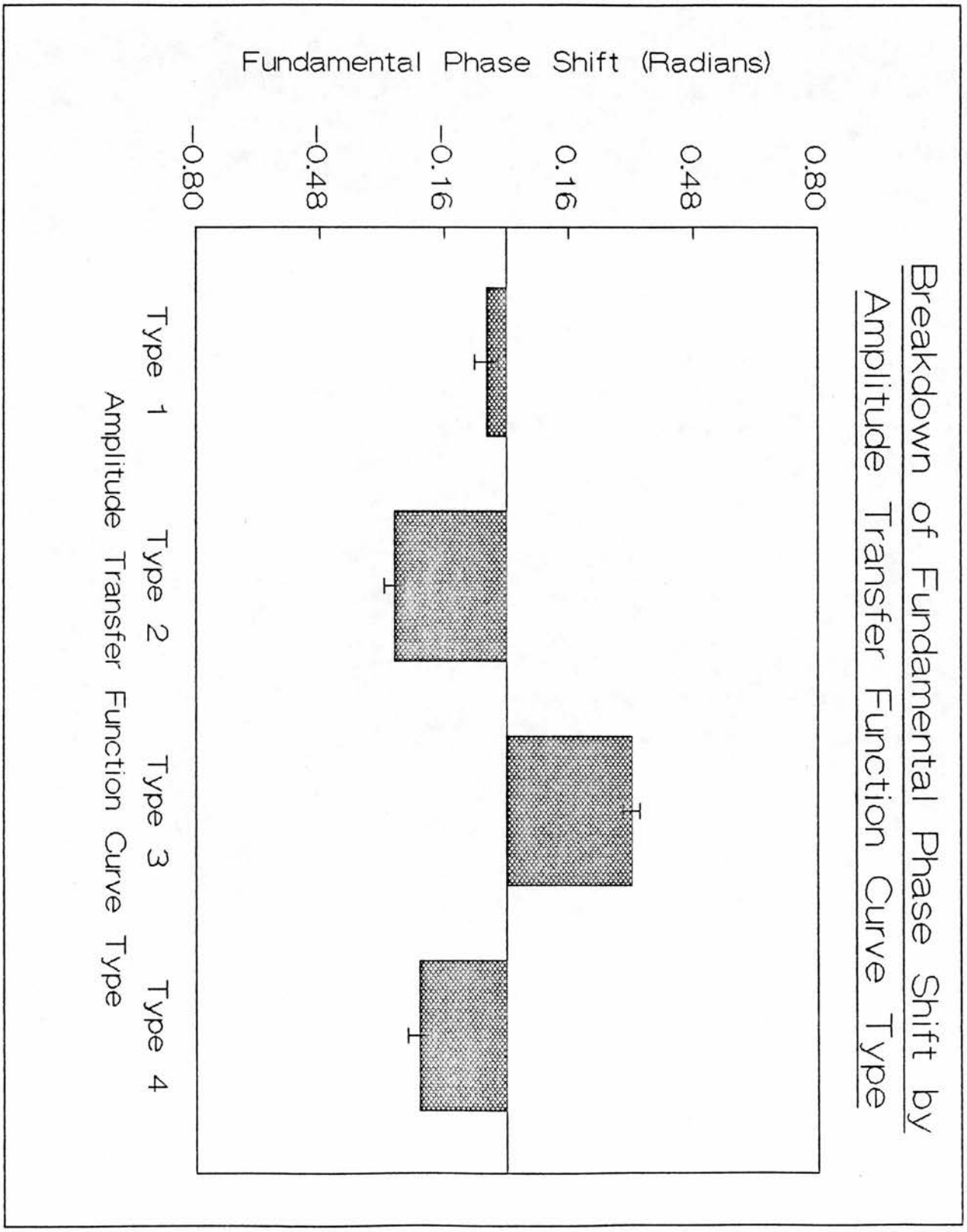

Figure 22: Observational Study Data for the Fundamental Phase Shift with 95% Confidence Limits.

Table 4: Breakdown of Physiological Data by Amplitude Transfer Function Curve Type.

Curve Type	ICP (mm Hg)	BP (mm Hg)	CVP (mm Hg)	HRT (BPM)	Tc (Deg. C)	PaCO2 (kPa)	PaO2 (kPa)	ph (nmol/L)
1 (n = 382)	15 +- 9 (13)*	90 +- 15	1.2 +- 2.8	93 += 14	37.2 +- 1.0	3.6 +- 0.7	18.8 +- 3.8	33.6 +- 3.7
2 (n = 243)	24 +- 10 (23)*	86 +- 10	2.7 +- 3.8	94 +- 22	37.3 +- 0.6	3.3 +- 0.6	19.2 +-3.9	31.5 +- 3.3
3 (n = 545)	13 +- 10 (11)*	85 +- 15	1.9 +- 2.9	112 +- 16	37.4 +- 0.7	3.5 +- 0.6	18.1 +- 3.5	34.2 +- 4.5
4 (n = 202)	30 +- 19 (26)*	86 +- 10	1.6 +- 3.1	97 +- 13	36.7 +- 1.3	3.6 +- 0.3	18.4 +- 3.2	34.0 +- 1.5

All Values are means +- standard deviations
'*' denotes median value

d. Pathological Data

Table 5 is a breakdown of principal pathology (diffuse/focal) by amplitude transfer function curve type. It is interesting to note that in the diffuse pathology group, there is a majority of amplitude transfer function curves type 3 (55%) compared with curve type 1 (12%), curve type 2 (2%) and curve type 4 (31%). Samples from patients with focal injuries show very few amplitude transfer function curves type 4 (7%) compared with a more even distribution (35%, 25%, 33%) amongst the other curve types.

Table 5: Breakdown of Principal Pathology (Diffuse/Focal) by Amplitude Transfer Function Curve Type.

Curve Type	Diffuse	Focal	Total
1	52 (12%)	330 (35%)	382
2	10 (2%)	233 (25%)	243
3	239 (55%)	306 (33%)	545
4	134 (31%)	68 (7%)	202
Total	435	937	1372

D. Discussion of Results

This is the first study to demonstrate, through the use of a systems analysis approach, definable patterns of pressure transmission across the cerebrovascular bed in a head injured population.

A consideration of the observed data, based on amplitude transfer function curve type, in relation to previous work by other investigators, may prove useful as an aid to interpreting these results.

a. Curve Type 1 (Flat)

A flat amplitude transfer function was associated mostly with ICP below 20 mm Hg (mean ICP = 15 mm Hg). A flat amplitude transfer function indicates equal transmission of all the arterial pressure waveform harmonics through to the CSF space. Kasuga et al (88) have noted a decreased pressure transmission in the low frequency range of 1 to 7 Hz in their control group of dogs with normal ICP (ICP < 10 mm Hg) which tended to increase with ICP at or near 15 mm Hg. Similarly, Portnoy et al (82,86) observed attenuation of the amplitude transfer function fundamental in the transmission of the arterial pulse through to the CSF space under conditions of low ICP (ICP < 7 mm Hg). Furthermore, Portnoy et al (83) found, in hydrocephalic dogs, attenuated low frequency transmission when ICP was below 9 mm Hg and a flat amplitude transfer function when ICP was greater than 12 mm Hg. They attributed this attenuation to functional autoregulatory tone of the precapillary cerebral resistance vessels, and further demonstrated that a flat amplitude transfer function (equal transmission of all harmonics) can be experimentally induced by intraventricular infusion of mock CSF or arterial hypercarbia. Portnoy et al propose that the conversion from an attenuated low frequency transmission to a flat amplitude transfer function is evidence for reduced arteriolar vasomotor tone.

The mean ICP in this curve type 1 group (15 mm Hg) is within the ICP range associated with a flat amplitude transfer function as reported by Portnoy and the increased low frequency pressure transmission as reported by Kasuga. This observed form of pressure transmission cannot be attributed to arterial hypercarbia as all patients were maintained normocarbic (Table 4). Table 6 is a breakdown of amplitude transfer function curve type by patient distribution. Within the 30 patients monitored, 18 patients exhibited, at some point, amplitude transfer

functions of curve type 1, and of those 18 patients, only 3 did not go on to demonstrate other forms of amplitude transfer function curve type. Of these 15 patients that did go on to show other curve types, only 3 patients exclusively demonstrated curve types 1 and curve types 3, both associated with lower ICP (ICP < 15 mm Hg). Of the remainder, 12 out of 18 patients (67%) also demonstrated either curve types 2 or 4, both associated with raised ICP (ICP > 20 mm Hg).

These data support the view that the amplitude transfer function curve type 1, despite its association with lower ICP, may indicate reduced cerebrovascular tone and be predictive of raised ICP. However, in the absence of transfer function data from a control group of patients (normal subjects with ICP monitoring), with which to compare, or independent evidence of the functional state of the cerebrovascular autoregulatory mechanisms, this statement is speculative.

Table 6: Breakdown of Amplitude Transfer Function Curve Type by Patient Distribution.

Curve Type	# Patients Exhibiting Curve Type at Any Time	# Patients Exhibiting Curve Type Exclusively
1	18	3 (16%)
2	11	2 (18%)
3	16	8 (50%)
4	10	2 (20%)

b. Curve Type 2 (Elevated Low Frequency)

This amplitude transfer function curve type was characterized by an elevated low frequency pressure transmission which was most often associated with ICP above 20 mm Hg. It was chiefly the fundamental that was elevated. Portnoy et al (81) and Takizawa (86) have both demonstrated the dependence of the fundamental in the amplitude transfer function on CO2 induced alterations in cerebrovascular resistance. This effect of CO2 on the fundamental was supported by the pilot data reported in this thesis (page 37) on the effects of hypocarbia on the amplitude transfer function. It is well established that increased CO2 tension in arterial blood increases CBF (107) by decreasing cerebrovascular resistance predominantly through dilation of the major resistance vessels; the small bore arteries and arterioles (169). Following on from this it seems likely, that the greatly increased low frequency pressure transmission seen with this curve type 2 amplitude transfer function is as a result of marked dilation of the small bore arteries and arterioles.

Portnoy et al (82) suggest that a greatly increased transfer of the fundamental may be a marker for impairment of the autoregulatory function of these resistance vessels. However, an increased fundamental transmission could be due either to loss of autoregulatory tone or paradoxically to intact autoregulation compensating for reduced cerebral perfusion pressure through active vasodilation. Some measurement of local CBF or flow/metabolism coupling such as the AJDO2 (arterial to jugular bulb oxygen difference) would be required to distinguish these conflicting mechanisms. Interestingly, Portnoy recently reports (108) an account of the amplitude transfer function taken from a patient in the neurosurgical intensive care unit after evacuation of an acute epidural haematoma. This patient demonstrated a marked increase in the fundamental relative to the other harmonics, very similar to the amplitude transfer function curve type 2. Concomitant measurement of $AJDO_2$ was 8.7 ml O2 % which suggests the presence of ischaemia. Portnoy further states that postoperatively, this form of amplitude transfer function is common and often associated with patients who can easily develop a rapid rise in ICP.

c. Curve Type 3 (Elevated High Frequency)

In this study a high proportion of amplitude transfer functions (40%) demonstrated elevated high frequency harmonics without an associated increased fundamental. This was mostly associated with an ICP below 20 mm Hg.

Within the 30 patients monitored, 16 patients exhibited, at some point, amplitude transfer functions of curve type 3, and of those 16 patients, 8 (50%) did not go on to demonstrate other forms of amplitude transfer function curve type. This distribution of waveform data supports the view that the amplitude transfer function curve type 3 may be more representative of normal cerebrovascular tone. This is supported by a report from Portnoy (108) on an amplitude transfer function identical to a curve type 3 transfer function recorded from a patient following removal of an epidural haematoma. $AJDO_2$ at this time was 6 ml O2 % suggesting ischaemia was not present. Portnoy states that the presence of this pattern of amplitude transfer function, even in the presence of elevated ICP, is usually a good prognostic sign for improved outcome.

Kasuga et al (87), applying pressure pulse waves into the CVB, demonstrated a resonance in the intracranial compartment in dogs. This resonant peak occurred under control conditions in the higher frequency range from 10 to 15 Hz, a frequency which is nearly within range of the 5th and 6th harmonics of the amplitude transfer function found in patients[15]. They demonstrated that the resonant frequency increased when ICP was experimentally increased by intraventricular infusion of mock CSF or through inflation of an extradural balloon (88).

Bray and Robertson (89,90) in a clinical study of the power density spectrum of the ICP waveform, showed two predominant frequency bands; the higher band (4 - 15 Hz) they associated with the ringing or resonant properties of the intracranial compartment and they demonstrated a strong inverse correlation between the frequency at which the resonant peak of the high frequency band occurred and intracranial compliance as measured by the PVI. That is, as intracranial compliance decreased the resonant frequency increased. They further demonstrated that an

---

[15]This is assuming the higher heart rate of the dog, approximately 2-3 Hz, is considered in the calculation.

increase in the frequency of the resonance above 9.0 Hz was predictive of poor outcome in patients.

The results from the pilot study (page 39) on the effects of jugular compression on cerebrovascular pressure transmission, would confirm the association of altered compliance with high frequency pressure transmission. Although compliance was not measured in that study, ICP increased with jugular compression and it is conceivable that the ICP change was a result of intracranial vascular engorgement secondary to the distal obstruction in venous outflow (109). Associated with jugular compression in that study, the fundamental phase became more negative, which is consistent in electrical terms with increased system capacitance, or its equivalent in mechanical terms: compliance.

These reports would support the hypothesis that an elevated high frequency pressure transmission, as seen with the amplitude transfer function curve type 3, is an indication of the start of a resonant peak in the transfer function, and its detection is indicative of high intracranial compliance and a favourable prognosis for ICP. A state of reduced compliance, either with or without raised ICP, will tend to increase the resonant frequency beyond that of the frequency of the 6th harmonic and hence the level of detection by this method. This would result in the transformation from a curve type 3 amplitude transfer function to another form (curve types 1,2 or 4) which may be predictive of, or associated with, raised ICP.

d. Curve Type 4 (Elevated Low and High Frequency)

This group was the smallest in number and most often associated with ICP raised above 20 mm Hg. Following on from the previous discussion, one could speculate that the elevated fundamental with this form of pressure transmission would indicate reduced arteriolar tone but, in association with an elevated high frequency pressure transmission, is indicative of high intracranial compliance.

The distribution of amplitude transfer function curve types between patients (Table 6) demonstrates that most patients exhibited at least two forms of transfer function, one of which was associated with raised ICP (curve types 2 and 4). It is unclear whether this amplitude transfer function curve type 4 represents a distinct form of cerebrovascular pressure transmission or a transition period from one form to another.

E. Discussion of Methods

Several assumptions are made with the systems analysis approach which should be considered as sources of error. The chief assumptions are:

1) the cerebrovascular bed can be described as a linear system;
2) the BP and ICP waveforms are periodic signals;
3) the BP waveform at the radial artery is a measure of the input signal to the cerebrovascular bed;
4) the ICP waveform within the subdural space is a measure of the output signal from the cerebrovascular bed.

Furthermore, not related to systems analysis but a potential source of error:

5) the waveform sample selection process was unbiased and representative for any given patient.

1. Linear Model of the Cerebrovascular Bed

A linear model is often assumed for reasons of mathematical convenience (appendix B, page 194). Most physiological systems contain non-linear elements. The craniospinal system, of which the cerebrovascular system is an element, is described by a non-linear volume-pressure relationship (28,110,111,112). The validity of the assumption of a linear model is especially important when comparing frequencies present in an output waveform with those of an input waveform. Major non-linearities in a system can generate sum and difference frequencies (and their multiples) between interacting input signals (97). In a non-linear system, an output signal component frequency may not be related to the same component frequency of the input signal.

Evidence of the validity of the assumption of a linear model for the cerebrovascular bed is based on the observation that the cerebrovascular system output frequency spectrum (ICP waveform) does not contain any frequency elements which are not also present in the cerebrovascular system input (BP waveform) and, if present, are of sufficiently small amplitude to be considered insignificant. Furthermore, it can be assumed that provided only small perturbations in intracranial volume are considered, then the resulting intracranial response can be approximated

as a linear segment on an otherwise non-linear input-output relationship (70). Chopp and Portnoy (78) have reported a high coherence value between the BP pulse and the ICP pulse waveforms as measured by the coherence function (79), which signifies linear transmission.

2. ICP and BP Waveforms as Periodic Signals

A periodic signal is one that repeats itself exactly after a fixed length of time. The Fourier analysis method assumes extension by periodicity; that is, a waveform sampled at time (t) is identical to another one sampled one full period (T) later: $f(t + T) = f(t)$ (Appendix B, page 193).

Giddens and Kitney (113) have shown that heart rate in healthy adults is not constant but continuously variable with a low frequency heart rate variability (HRV) component around 0.05 Hz due to thermoregulatory mechanisms, a component around 0.1 Hz arising from baroreceptor activity and a component at the respiratory frequency (> 0.2 Hz). They also demonstrated in neonates that heart rate correlated strongly with breath amplitude, leading to what they term a breath amplitude sinus arrhythmia. Branch et al have also shown increased variability in the ICP spectrum induced with the slow respiratory wave component (114). Lowensohn et al (115) demonstrated HRV was present in head injured patients and reported a correlation between raised ICP and decreases in HRV although this was not reproduced in a later study (116). It is still not clear if HRV is modified in severely head injured patients.

These reports indicate that beat to beat variability of the BP and ICP waveforms can occur. To overcome this, in this study, 20 seconds of ICP and BP waveform data was collected and 10 seconds was analysed. This analysis window allowed at least one full period of the respiratory component to be collected. The period of respiration was constant in this study as the patients were all mechanically ventilated by a standard protocol. Therefore, any beat to beat variability induced due to the respiratory fluctuation would tend to be averaged over the entire analysis window. However, an increased variation of the BP harmonic frequencies could occur equivalent to that of the beat to beat variation due to heart rate variability (+- 0.2 Hz) that is not of respiratory origin. In this analysis, any variation in harmonic frequencies seen in the BP spectrum was always matched by an equal variance in the corresponding harmonics of the ICP spectrum. Although this a potential source of error, the

graphics display software allowed manual measurement (+- 0.098 Hz) of the same harmonic frequency of the ICP waveform as was chosen for the equivalent BP harmonic frequency, thus ensuring this source of variation did not affect the calculation of the transfer function.

O'Rourke and Taylor (117) studying the impedance of the femoral bed using Fourier analysis of pressure and flow waveforms, found that despite marked sinus arrythmia, the impedance values derived from the first harmonic of a rapid beat corresponded with values derived from the third harmonic of a slow beat. They proposed that this apparent linear response, under conditions thought to be non-linear, might be accounted for by the large damping of the femoral artery causing each wave, although transient, to be regarded as part of a steady state oscillation. The same relationship may be true for the cerebrovascular bed; when transfer functions are calculated from waveform samples with different base heart rates and normalized with respect to the fundamental, there is good agreement in the frequency at which events such as a resonant peak in the transfer function occur.

3. Radial BP as an Input Signal

The question of whether the BP waveform at the radial artery is a measure of the input signal to the cerebrovascular bed can be approached by first considering what is the origin of the BP pulse.

The origin of the BP pulse can be derived from a study of the component frequencies. There are three main terms: a DC or static pressure term, a slow sinusoidal term (0.2 - 0.3 Hz) linked to respiration rate and a higher frequency term (1 - 3 Hz) linked to heart rate (Figure 10). All three component frequencies must originate from within the "chest", the site for the cardiovascular and respiratory systems. As a first approximation, a reasonable site for measurement of the "origin" of the BP pulse would be a cannula or transducer situated within a large vessel in the thoracic cavity, such as in the aortic arch, which would be under the influence of both cardiovascular and respiratory systems.

However, if a transfer function analysis of cerebrovascular pressure transmission is shown to provide information of clinical importance to the management of head injured patients, then its methods must be clinically practical. In an intensive care unit, there are practical and ethical limitations to the use of more central sites for routine pressure

monitoring. The errors caused by use of the radial artery as a measure of the input to the cerebrovascular bed have been quantified as discussed in the general methods section of this chapter. The results indicate that under controlled conditions, and within a select population of patients (predominantly young, otherwise healthy men with no previous history of peripheral vascular disease), the errors of peripheral BP measurement are no greater than the inherent variability of the method upon repeated measurement (20 - 30 percent error for the amplitude transfer function). This degree of error would be a limiting factor if subtle changes in the transfer function were believed to be important. However, the classification of cerebrovascular pressure transmissions into categories of amplitude transfer function curve types 1 to 4, which demonstrate amplitude differences of more than 100% between certain harmonics, is readily distinguishable.

4. Subdural ICP as an Output Signal

Measurement of the ICP pulse from the subdural space is not ideal, but placement of an intraventricular catheter, particularly in patients with collapsed ventricles or mid-line shift, is often not possible. Takizawa (86) has shown that simultaneous ICP waveform recording in the lateral ventricle and cisterna magna yields identical spectra, but found attenuation of the higher harmonics from the recording in the lumbar space. Provided there is CSF communication between the intracranial compartments, Takizawa's findings of identical waveform recording from the lateral ventricle and cisterna magna might be extended to the intracranial compartment as a whole. This view is supported by the recent report by Crutchfield et al (195) who used the Camino catheter-tip pressure monitoring system in dogs and showed identical ICP waveform and pressure recording during simultaneous monitoring of intraventricular, intraparenchymal and subdural pressure.

Furthermore, Yano et al (130) who studied patients with various pathological processes affecting both right and left hemispheres, could show no difference between concurrent left and right subdural pressure recordings. They concluded that the supratentorial space could generally be considered as one compartment regardless of the differences in types of intracranial lesions. Similar to Yano's findings in patients, Crutchfield et al (195) demonstrated in an experimental study in dogs, that there was

no difference between concurrent left and right subdural pressure recordings during unilateral epidural balloon inflation. In contrast to this, Broaddus et al (131) have shown pressure differentials within the subdural space in patients, ipsilateral to major pathology as seen on CT. However, they used subdural bolt pressure sensors for ICP measurement, a method prone to erroneous measurement, particularly with elevated ICP (132).

Based on these reports, ICP waveform recording in the subdural space is probably representative of the waveform throughout all the intracranial compartments. This may not be the case, however, for absolute ICP as there must be some pressure differential from the ventricles to the subarachnoid space, otherwise there would be no impetus to CSF flow in this direction (133,134). Furthermore, it is recognized that in head injured patients the CSF compartments are often compressed. In which case, in order to minimize measurement error, it is particularly important to monitor the subdural ICP waveform with a catheter-tip transducer which is less likely to be affected by compression of the CSF compartment than a fluid filled catheter-transducer system (137).

The use of the ICP waveform as a measure of the output of the cerebrovascular bed assumes that the site of transmission of the cerebrovascular pulse into the CSF space occurs at the terminal portions of the cerebral venous system. There has been much published in support of arterial (118,119,120,121,122,123), venous (124,125,126) or both arterial and venous (127,128,129) sites of transmission of the cerebrovascular pressure pulse into the CSF space.

The most convincing evidence comes from Portnoy's group (84,125,126). This group showed that when the transverse sinuses in dogs were obstructed and the venous flow redirected through a cannula to a flask before being returned to the animal via the femoral vein, the sagittal sinus pressure pulse was still present. This indicates that, under normal conditions, the CSF pulse is not a retrograde phenomenon from the right side of the heart but an antegrade pulse of arterial origin which is at some point transmitted into the CSF space. Branch et al (84) demonstrated that the amplitude spectra from pressure waveforms simultaneously recorded from the CSF space and a cortical vein were identical. This indicates that the CSF pulse is transmitted from the vein to the CSF or vice-versa. Thin walled veins are more likely to pulse than

thick walled arteries and arterioles (82). This would facilitate transmission from the veins into the CSF. This argues in favour of transmission of the pulse from the veins to the CSF rather than from the arteries to the CSF and then to the veins.

This evidence would support the concept that the cardiac pressure pulse enters the cerebrovascular bed, passes through the arteries, arterioles and small diameter venules and veins of the cerebrovascular bed in an antegrade direction before being transmitted into the CSF space from the large calibre thin walled veins.

5. Sample Selection

Thirty severely head injured patients were monitored in the intensive care unit over periods ranging from 2 to 14 days. Five minute waveform samples were collected to tape every 30 minutes timed to coincide with clinical recordings from the nursing staff. To be consistent amongst patients, samples from the same period of patient management were chosen for analysis. For the following reasons the early period of management, usually the first 2 to 3 days, produced the most controlled data:

i) patients were most intensively monitored by medical and nursing staff during this period;

ii) comments were entered more frequently and accurately to the data collection computer system by nursing and medical staff, thus allowing more precise annotation of significant events;

iii) monitoring equipment (transducers, fluid-filled tubing, acudynamic adjustable damping devices, patient monitors) were new and more frequently calibrated;

iv) after stabilization of physiological parameters patients were observed for the first 2 to 3 days under controlled sedation, being paralysed and mechanically ventilated to a standard protocol (page 41). However, after this period, provided ICP was normal for 24 hours, sedation and paralysis were reduced, in preparation for the patient to be clinically assessed. During this latter period, the patient's level of sedation was unpredictable, with occasional patient movement and respiratory effort being made against the ventilator.

Ideally, 48 hours of data collection would yield 96 waveform samples for analysis. In fact, considerably fewer valid samples were available as certain forms of nursing care, physiotherapy, routine x-rays, CT scan

investigation, and regular blood gas sampling would interrupt or interfere with one or both of the ICP and BP waveform recordings. Chiefly for these reasons, 50 waveform samples were selected per patient. The choice of samples was determined from the ICU nursing charts and selected to provide a representative sample over the range of intracranial pressures exhibited by the patient over the initial 2 to 3 day period of monitoring.

Waveform samples were excluded from analysis as described previously (page 41). The exclusion criterion d) "samples within 120 minutes of therapy for raised ICP" was set at 120 minutes based on the work of Dearden and Miller (138) in a paired comparison of hypnotic and osmotic therapy on ICP reduction after severe head injury. They showed that in a group of 17 head injured patients, hypnotic therapy (thiopentone: 5 mg/kg given over 5 minutes or gamma hydroxybutyrate: 60 mg/kg iv given over 10 minutes) had a time to maximum reduction of ICP of 18 minutes (range 5 to 26 minutes) and a total duration of ICP reduction of 32 minutes (range 1 - 104 minutes), whereas osmotic therapy (mannitol: 0.5 g/kg iv given over 5 minutes) had a time to maximum reduction of ICP of 24 minutes (range 1 - 55 minutes) and a total duration of ICP reduction of 59 minutes (range 14 - 116 minutes). Although this criterion should avoid waveform sampling during the maximum effect of hypnotic and osmotic therapy, some longer term effects on the cerebrovascular bed cannot be eliminated, particularly as mannitol's effect on blood viscosity in man lasts at least two hours (139).

Every effort was made to ensure that a representative sample was taken from the waveform database for a given patient. However, the unpredictable nature of "artifacts" not annotated in the ICU charts or on the computer print-out were not noticed until the waveform was displayed graphically, which meant that the first choice for a given sample occasionally was discarded. Therefore, some unconscious sampling bias may be present. However, the frequency with which it was necessary to discard the first choice of a waveform sample was small (< 5%) and consequently is not likely to have a significant effect.

F. Conclusions

In conclusion, these studies have demonstrated definable patterns of cerebrovascular pressure transmission in head injured patients. Certain forms of cerebrovascular pressure transmission may be predictive of raised ICP, or of its underlying cause. The interpretation of the data from this study can only be speculative as concurrent measurements of craniospinal compliance and CBF (as a measure of cerebrovascular resistance) were not performed.

What is required, to aid in the interpretation of these clinically observed forms of cerebrovascular pressure transmission, is an investigation into the relationship between cerebrovascular resistance, craniospinal compliance and cerebrovascular pressure transmission.

This data might best be obtained experimentally, under more controlled conditions, in an animal model of raised ICP.

CHAPTER III. AN IMPROVED METHOD OF COMPLIANCE MEASUREMENT

It has been proposed that changes in lumped craniospinal compliance may, at least in part, be responsible for specific patterns of amplitude transfer function in head injured patients. The most commonly used methods of measuring craniospinal compliance depend upon the rapid injection of known volumes of fluid into the CSF space with immediate measurement of the resultant increase in CSF pressure. This is expressed as mm Hg per ml of added CSF volume in the volume-pressure response (VPR) or as in the pressure volume index (PVI), this being the notional volume that when added to the CSF space would produce a tenfold rise in ICP.

It is difficult to inject equal volumes of fluid manually at a constant and rapid rate of injection. As a result, the measurement of lumped craniospinal compliance using the VPR and PVI volume-pressure tests is not routinely carried out in neurosurgical practice largely because of the high variability of measurements. For example, Borgenson and Christensen (140) in a lumbar-ventricular perfusion study in patients failed to show a relationship between PVI and ICP due to the large variation in PVI measurements. Similarly, an attempt to correlate the amplitude of high frequency harmonics, in the amplitude transfer function from BP to ICP, to craniospinal compliance, as measured by the VPR, failed for identical reasons (141).

Before an experimental study of the relationship between cerebrovascular pressure transmission and craniospinal compliance can be performed, an improved method of measuring craniospinal compliance is needed.

Modification of the VPR technique from a manual to an automatic injection sequence would be the first step in improving the reproducibility of measurements. This chapter describes the development of an automatic method for measuring craniospinal compliance and its subsequent validation in feline models, of raised ICP and arterial hypertension, hypotension and hypercarbia.

A. Theory

The volume-pressure response method consists of manual injection of fluid into the CSF space through a cannula or needle inserted into either the lumbar cistern, the cisterna magna or the lateral ventricle. Typically the injection tubing is also connected through a 3-way tap to a strain gauge transducer for measurement of the pressure response resulting from the volume injection. The VPR (dP/dV) is then calculated from the mean ICP response (dP) after rapid injection of 0.5, 1, 1.5 and 2 ml of saline (dV). The sequence of events is as follows: the 3-way tap is positioned to allow injection of the volume bolus into the CSF space, the volume injection is then given over 1 second, and immediately after injection the 3-way tap is closed off to the syringe and opened on to the pressure transducer to allow recording of the pressure response. Closing the 3 way tap to the syringe produces an infinite outflow resistance (ignoring leaks in the injection and pressure measurement system) to the now volume loaded CSF space. This volume load is gradually dissipated by the craniospinal system through the normal CSF outflow resistance channels.

This process can be described in electrical terms (Figure 23) where resistance R1 is the injection tubing resistance, capacitor C1 is the lumped craniospinal compliance (compliance and capacitance are equivalent terms[16]) and resistance R2 is the CSF outflow resistance. The volume injection flows through the injection tubing resistance (R1) and charges up the "craniospinal capacitance" (C1) which is discharged (once the 3-way tap is closed) through the CSF outflow resistance (R2).

Two modifications to the existing method have been carried out (Figure 24). A pressure generator[17], originally used for testing the frequency response of catheter-transducer systems, has been modified to allow the triggered production of rectangular wave pressure pulses of 150 mm Hg amplitude and 100 mSec duration. When these pressure pulses are applied to the end of the injection tubing resistance (R1) a small volume injection results (approx. 0.05 ml) into the CSF space. The second modification to

---

[16]Compliance in mechanical terms is analogous to capacitance in electrical terms. Compliance can be defined as the volume (V) difference resulting from a pressure (P) difference (dV/dP). Capacitance can be defined as the charge (q) difference resulting from a potential (v) difference (dq/dv).

[17]Biotek Inc., Vermont, USA.

the method involves reduction of the injection tubing resistance (R1) so that it is considerably (at least ten times) less than the CSF outflow resistance (R2). Provided the injection tubing resistance (R1) is considerably less than the outflow resistance (R2) and the injection resistance (R1) is left open to atmospheric pressure after volume injection, than the injected volume bolus will leave the system through R1 rather than through the much higher resistance R2.

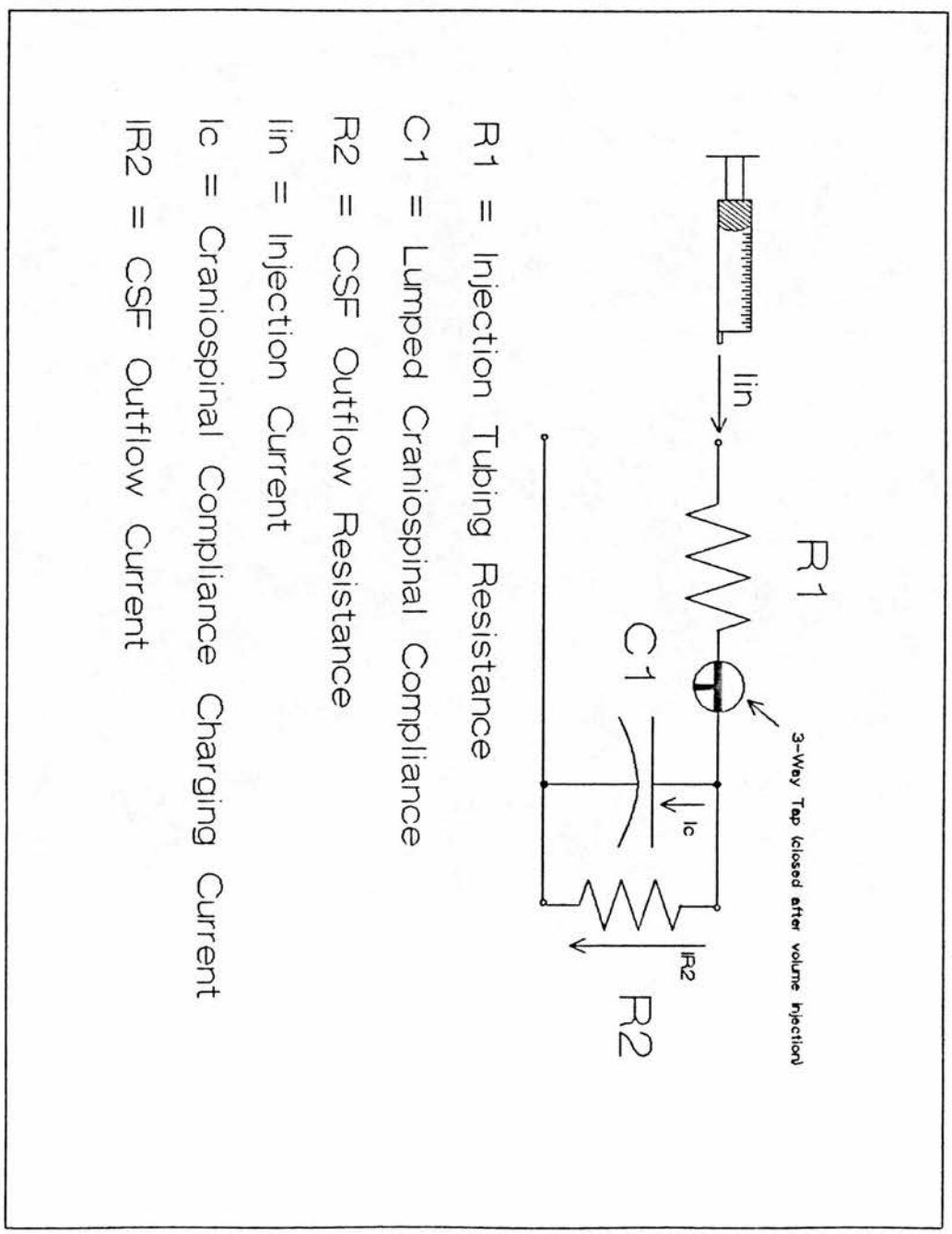

Figure 23: Electrical Model of VPR Method.

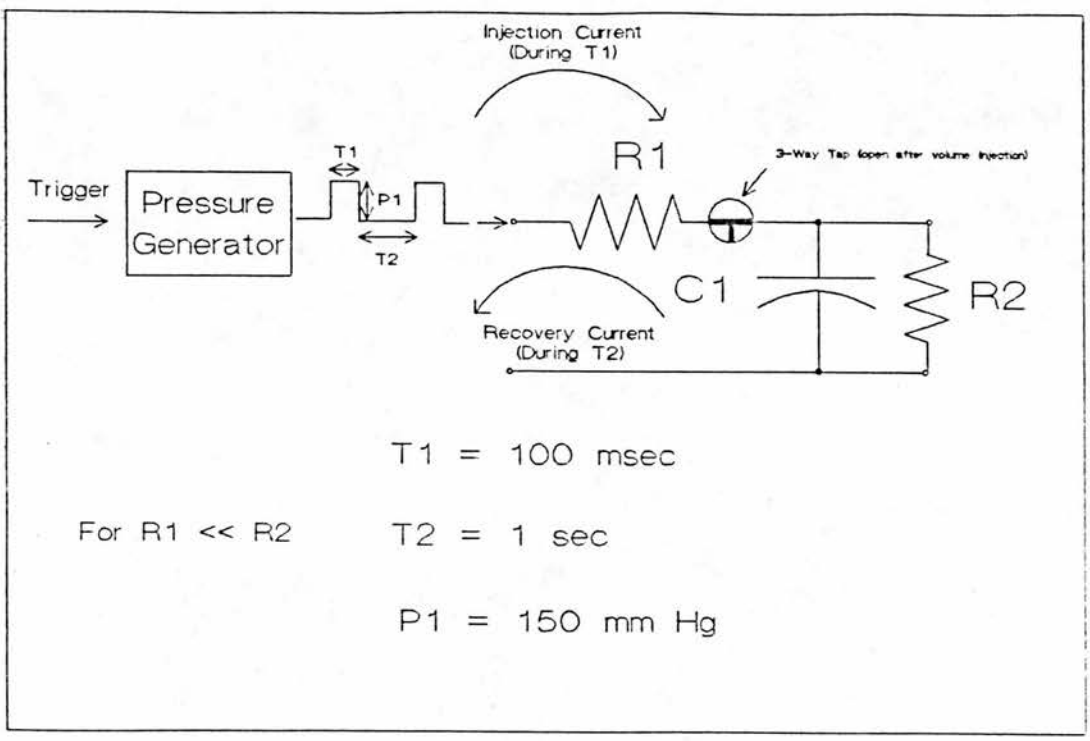

Figure 24: Electrical Model of Modified VPR Method.

It can be shown through the application of Thevenin's theorem[18] (142) that R2 is in parallel with R1 (Figure 25) and if R2 is very much greater than R1, R2 can effectively be ignored. This simplifies the first approximation model to a series RC circuit (Figure 25), where R1 is the injection tubing resistance and C1 is the lumped craniospinal compliance.

It can be further shown (Appendix I) that the value of the "craniospinal capacitance" or compliance can be easily calculated from the standard capacitance charge equation (equation 1) provided the following are known: injection tubing resistance (R1), peak input pulse pressure (Vp), input pulse duration (Ti), and the intracranial pressure (Vc) after Ti seconds.

---

[18]Thevenin's theorem states that any circuit can be analysed as a series voltage source (V_{th}) and resistance (R_{th}). V_{th} is calculated as the open circuit voltage. R_{th} is calculated as the equivalent resistance when all sources are reduced to zero potential. In this case, the pressure generator source is short circuited to ground, which results in R2 and R1 as a parallel combination Thevenin resistance (R_{th}).

$$C1 = \frac{\left[\dfrac{Ti}{Ln\left(\dfrac{Vp}{(Vp-Vc)}\right)}\right]}{R1}$$

Equation 1: SPR Method Equation.

This method has two advantages over the existing VPR technique:

1) it can be easily automated;
2) it is less invasive in that:
   i) the volume injection can be smaller and of shorter duration, particularly if averaging techniques are used to separate the ICP response (Vp) from background noise;
   ii) the injected volume leaves the system after compliance testing through the injection tubing resistance.

Physical model tests were carried out on the method to determine the optimal parameters (injection tubing resistance, input pulse amplitude and duration), the accuracy compared with an independent measure of compliance, and the sources of error.

For convenience, the new method under test will be referred to in all following text as the "Short Pulse Response" (SPR) method.

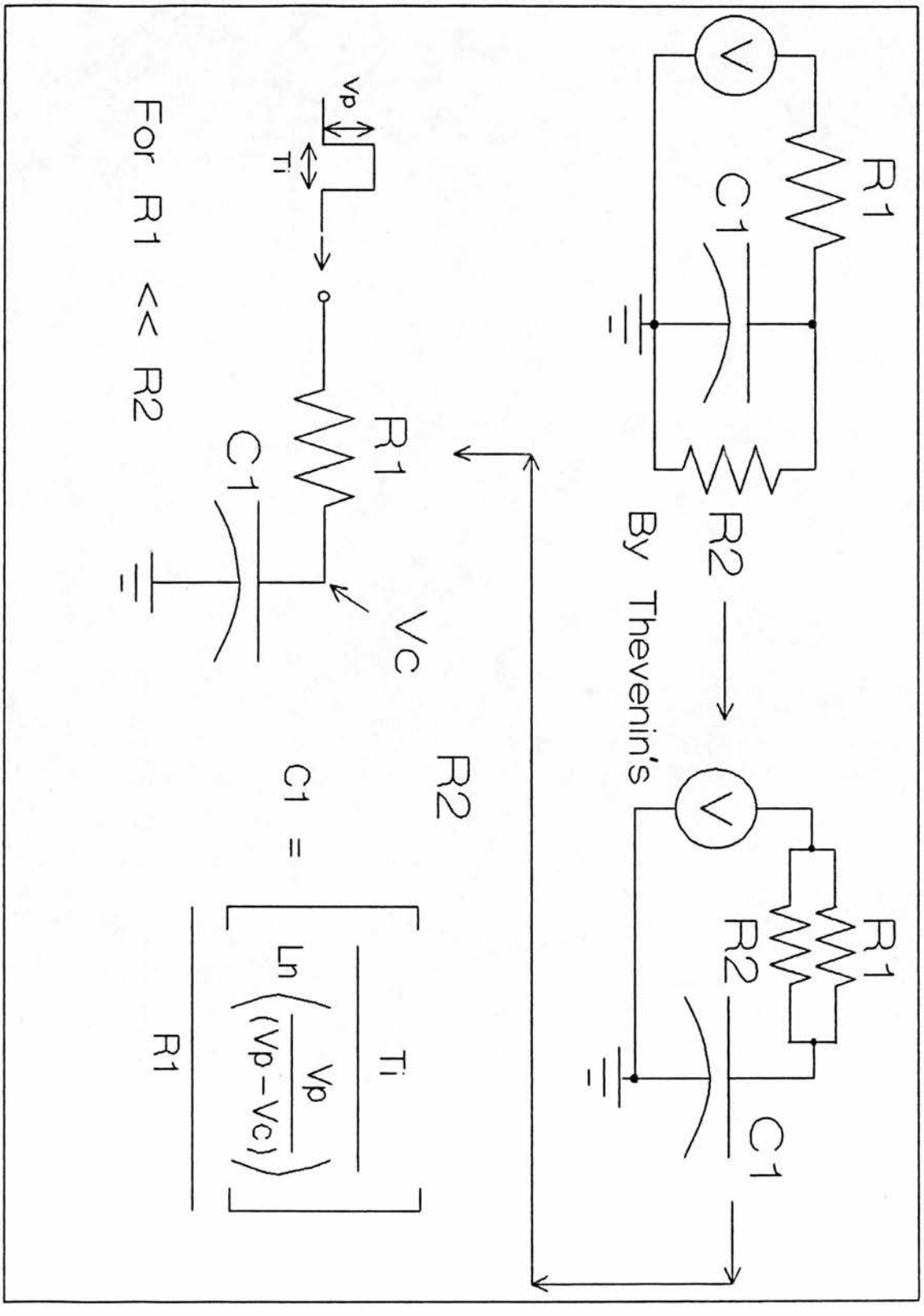

Figure 25: First Approximation Electrical Model of Craniospinal System.

B. Physical Model Testing

1. General Methods

Figure 26 is a block diagram of the SPR measurement system. A two channel biological signal averager[19] produces, during averaging mode, 5 volt trigger pulses of 0.1 mSec duration. These pulses are modified by a "pressure signal and timing conditioning unit" to produce variable voltage (0 - 2.0 volts) and duration (20 - 1000 msec) rectangular wave pulses. A schematic diagram of the "pressure signal and timing conditioning unit" is given in Appendix J. These variable voltage and duration pulses trigger the pressure generator to produce pressure pulses of equal duration and pressure amplitude with a conversion of 100 mm Hg/volt, and a rise time of 2 msec. The pressure pulses are then applied to the system under test through optimally damped fluid-filled low compliance tubing[20]. A Camino catheter-tip pressure transducer is placed within the dome of the pressure generator to measure the input pressure pulse and similarly a pressure sensor is placed within the system under test to record the pressure response to the input stimulus. Both recorded input and output pressure signals are then conditioned by the "pressure signal and timing conditioning unit" prior to input to the biological signal averager. After removal of the DC component the signals are filtered through low pass filters with a cutoff frequency of 100 Hz. The conditioned signals are then averaged with a stimulus presentation rate of 1 Hz and a sweep time (averager maximum) of 1 second. All physical model test responses are the average of 10 stimulus presentations. The input pressure pulse is averaged on the first channel and the system pressure response on the second channel of the averager. Amplitude and latency cursors on the averager allow measurement of the peak input pressure (Vp), the duration of the input pulse (Ti) and the peak system pressure resulting from the pressure stimulus (Vc). Once the injection tubing resistance (R1) is known, the system compliance can be calculated according to equation 1 (page 67).

---

[19]Medelec MS92a. Medelec Ltd., Surrey, UK.

[20]High density polyethylene tubing. Portex Ltd., Kent, UK.

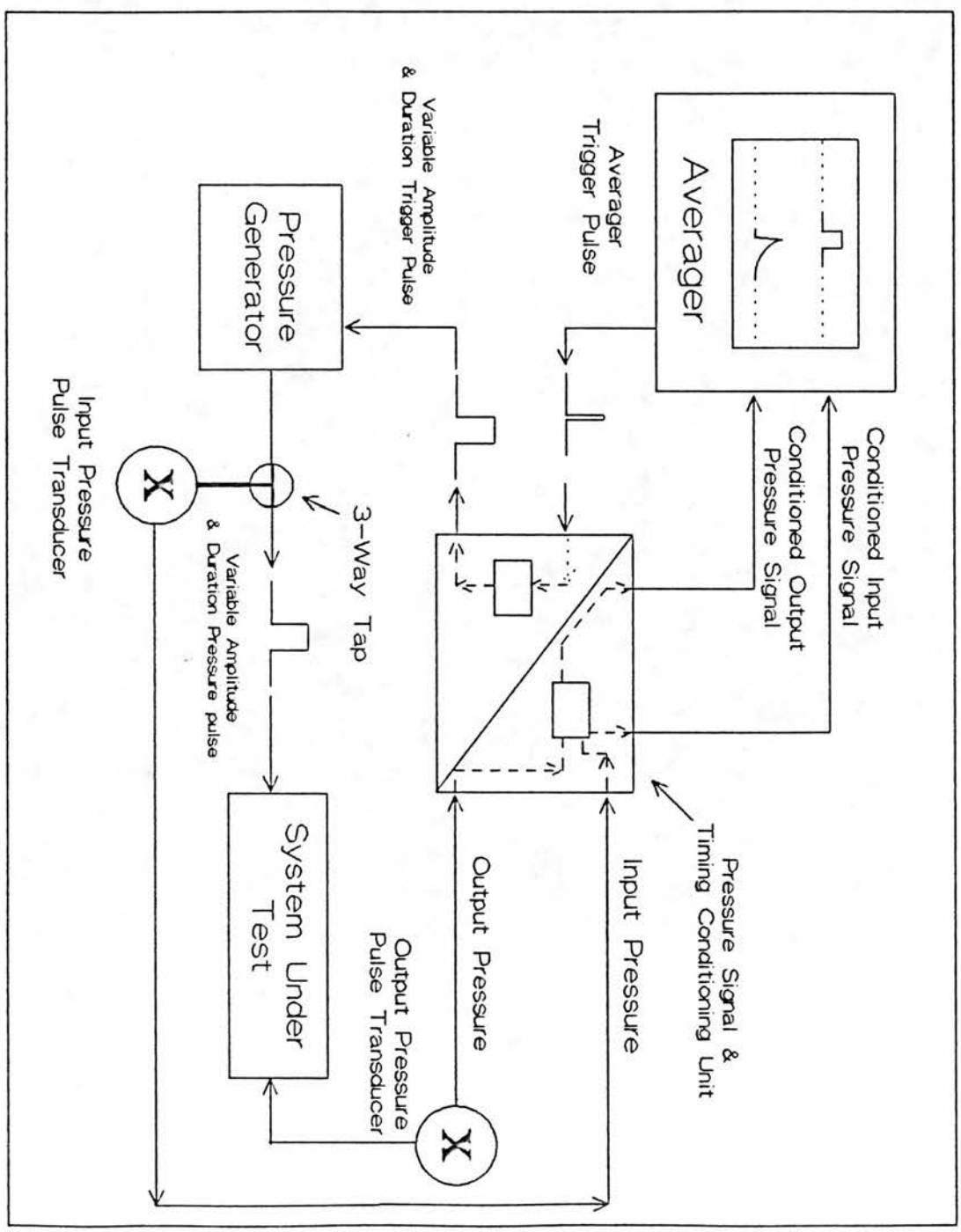

Figure 26: Block Diagram of the SPR Measurement System.

2. A Physical Model of the Craniospinal System

A simple physical model of the craniospinal system was built to allow testing of the SPR method. Figure 27 is a block diagram of the physical model. It consists of a 20 ml syringe (mock cranium) filled with 10 ml of saline (mock CSF). A fluid coupling system was inserted into the 10 ml "CSF" space of the syringe and consisted of a 19 Gauge 5 cm metal needle, a 30 cm length of low compliance tubing, two 3-way taps and an Acudynamic adjustable damping device. Also placed within the syringe was a second identical fluid coupling system connected to a strain gauge transducer system[21] for measuring the pressure within the syringe. Table 2 (page 22) summarizes the static and dynamic characteristics of this catheter-transducer system. Transient response analysis of the catheter-transducer system determined that 2.25 turns on the Acudynamic tap were required to produce optimal damping. Quantities of air could be added or removed from the syringe to alter the compliance of the model.

3. Injection Tubing Resistance

Figure 28a illustrates the method used for measurement of the injection tubing resistance. A bucket of saline was seated on a drip stand so that it could be adjusted to different heights above the injection tubing. The resulting pressure head of saline was connected to the injection tubing by a 2 metre length of large bore (2 cm) hose pipe. The saline was allowed to flow and the volume of fluid collected over one minute from a range of bucket heights. The resistance of the injection tubing was calculated from the average slope from a sequence of five pressure versus flow experiments (Figure 28b). There was no evidence of turbulent flow over the pressure range tested, as all the pressure versus flow curves were linear. The resistance of the injection tubing used throughout these experiments was 3.5 +- 0.17 mm Hg/ml/min[22]. A prerequisite of the SPR method is that the injection tubing resistance R1 is considerably (at least ten times) less than the CSF outflow resistance (R2) (page 65). This condition was met, as the normal CSF outflow

[21]Bentley Trantec physiological pressure transducer. Bentley Trantec Inc., Irvine, USA.

[22]value is mean +- standard deviation.

resistance in the cat was 105 mm Hg/ml/min[23], which is over 30 times greater than the 3.5 mm Hg/ml/min resistance of the injection tubing (R1).

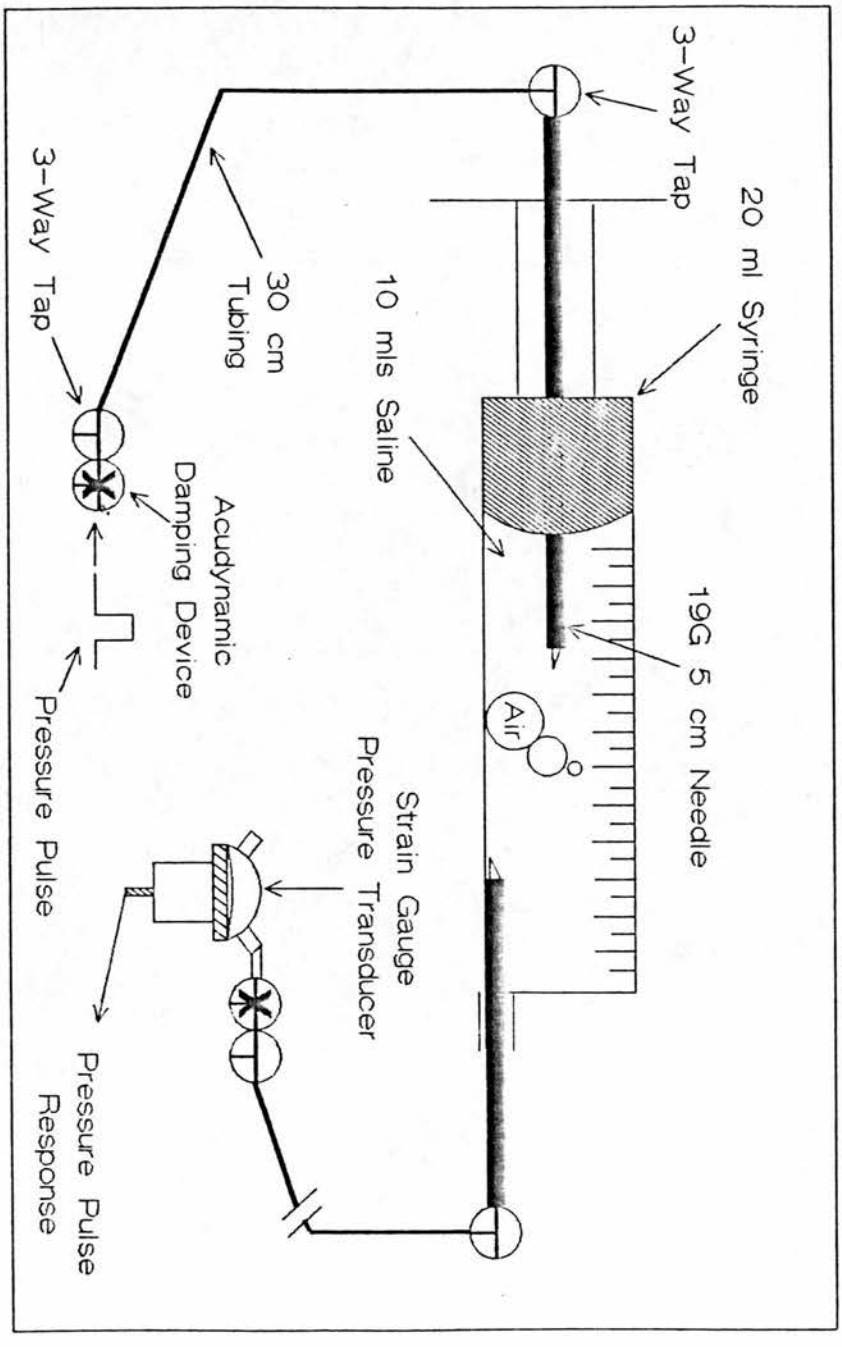

Figure 27: Block Diagram of the Physical Model Apparatus (not drawn to scale).

[23]This value of CSF outflow resistance is the average of three investigators' published normal values. References (41,42,143).

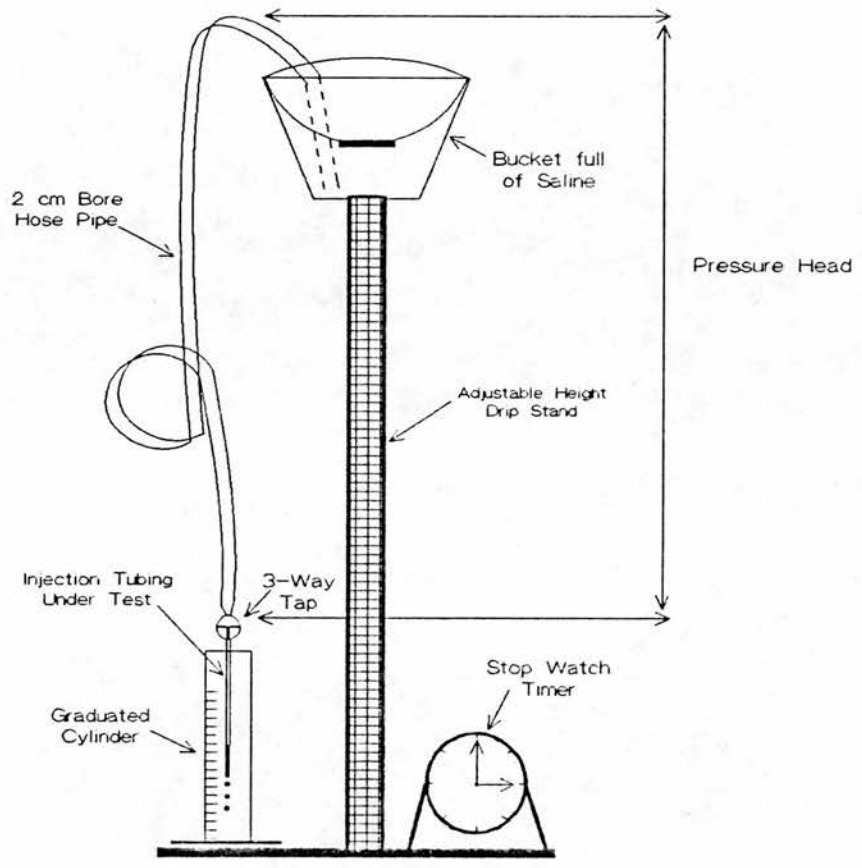

Figure 28a: Block Diagram of the Injection Tubing Resistance Measurement Apparatus.

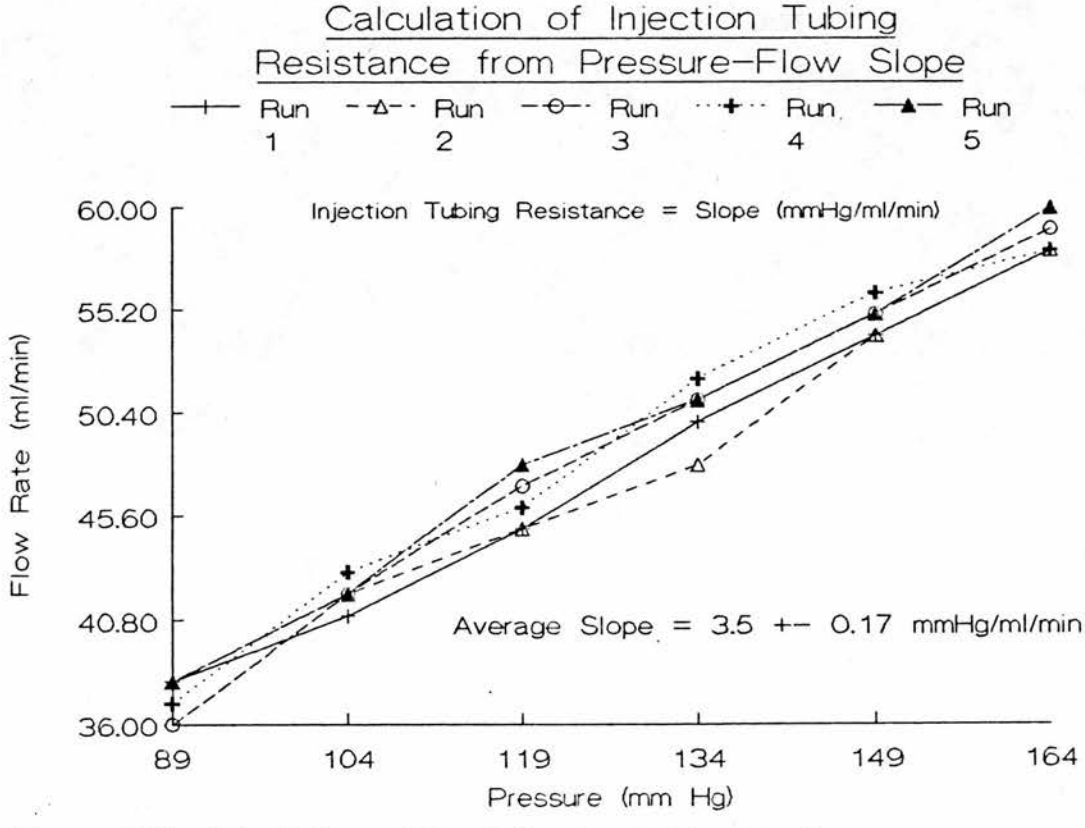

Figure 28b: Calculation of the Injection Tubing Resistance.

4. Effect of Injection Tubing on the Pressure Pulse

The injection tubing distorted the pressure pulse before it reached the system under test. Figure 29 illustrates the effect of different amounts of damping, through adjustment of an Acudynamic adjustable damping device placed in series with the injection tubing (Figure 27), on correcting the distortion. It was found that 1.75 turns of the Acudynamic tap produced optimal conditions.

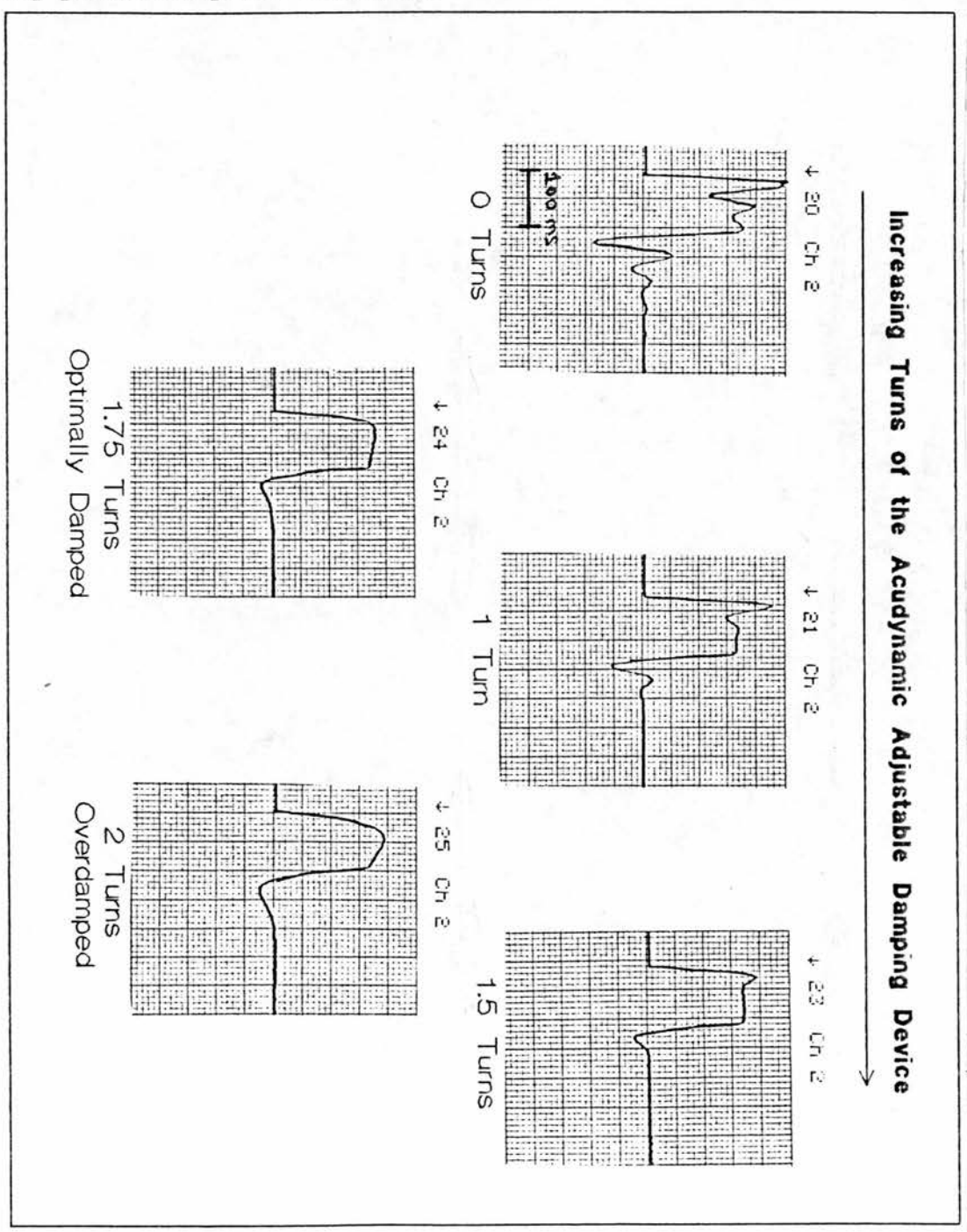

Figure 29: Effect of Damping on the Injection Tubing Pressure Pulse. Arrows indicate onset of stimulus.

5. Input Pulse Amplitude Series

The effect of different pressure pulse amplitudes on the measured compliance was determined. Figure 30a illustrates a typical input pressure pulse and output pressure response measured from the physical model. The physical model was set up with 1 ml of injected air in the syringe. Sequences of compliance measurements were performed at input pressure pulse amplitudes of 100, 125, 150, 175 and 200 mm Hg. Figure 30b shows the average of 5 measurements of compliance at each input pressure amplitude. There was a difference of less than 5% between the compliance calculated at 100 mm Hg and that calculated at 200 mm Hg.

The larger the input pulse amplitude, the larger the system response, so that less averaging is required to separate a response from background noise. This will be particularly relevant in the animal model tests where the pressure response will require separation from the background ICP waveform. The maximum pressure pulse amplitude that the pressure generator can produce is 200 mm Hg. To prevent reduction of the lifespan of the pressure generator through overuse at the limit of its operating range, 150 mm Hg was selected as the optimal pressure pulse amplitude.

6. Input Pulse Duration Series

The effect of different input pressure pulse durations on the measured compliance was determined. The physical model was set up with 1 ml of injected air in the syringe. Sequences of compliance measurements were performed at input pressure pulse durations of 50, 100, 150, 200 and 250 msec. Figure 31b shows the average of 5 measurements of compliance at each input pressure duration. There was a difference of 27% between the compliance calculated at 50 msec and that calculated at 250 msec. The reason for this large difference can be seen in the input pulse shape from the 250 msec duration run (Figure 31a). The pressure generator is failing to maintain a constant pressure as can be seen by a distinct sag and overshoot during and at the completion of the pressure pulse period. This phenomenon is better understood in relation to the mechanism of the pressure generator.

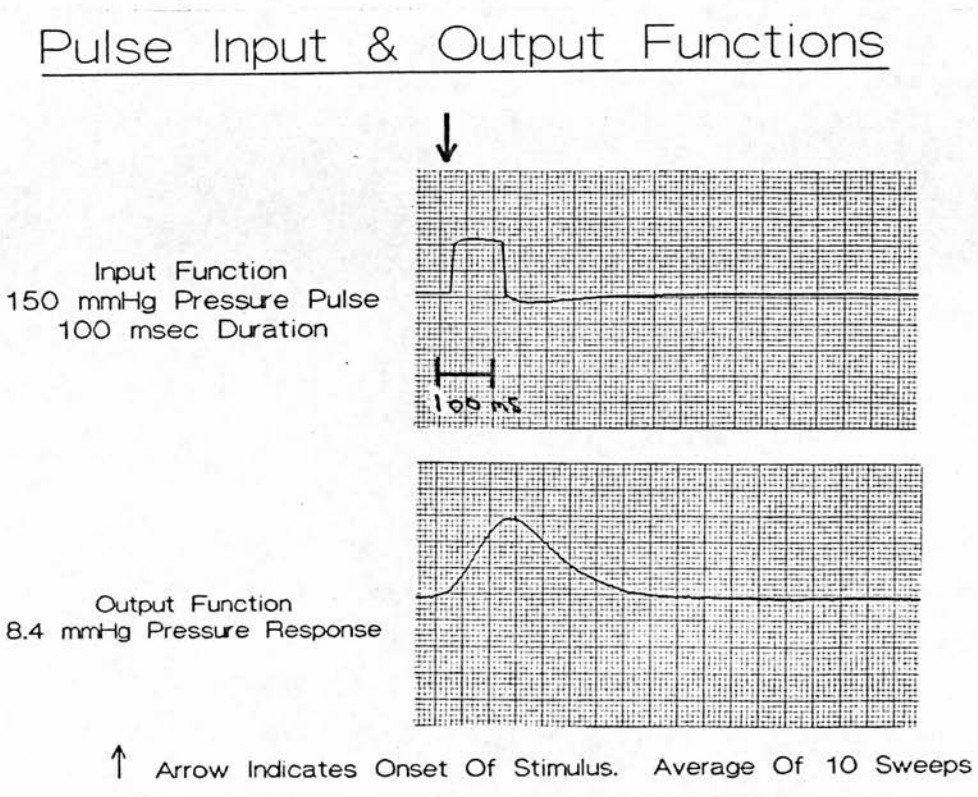

Figure 30a: Sample Input and Output Pressure Pulses.

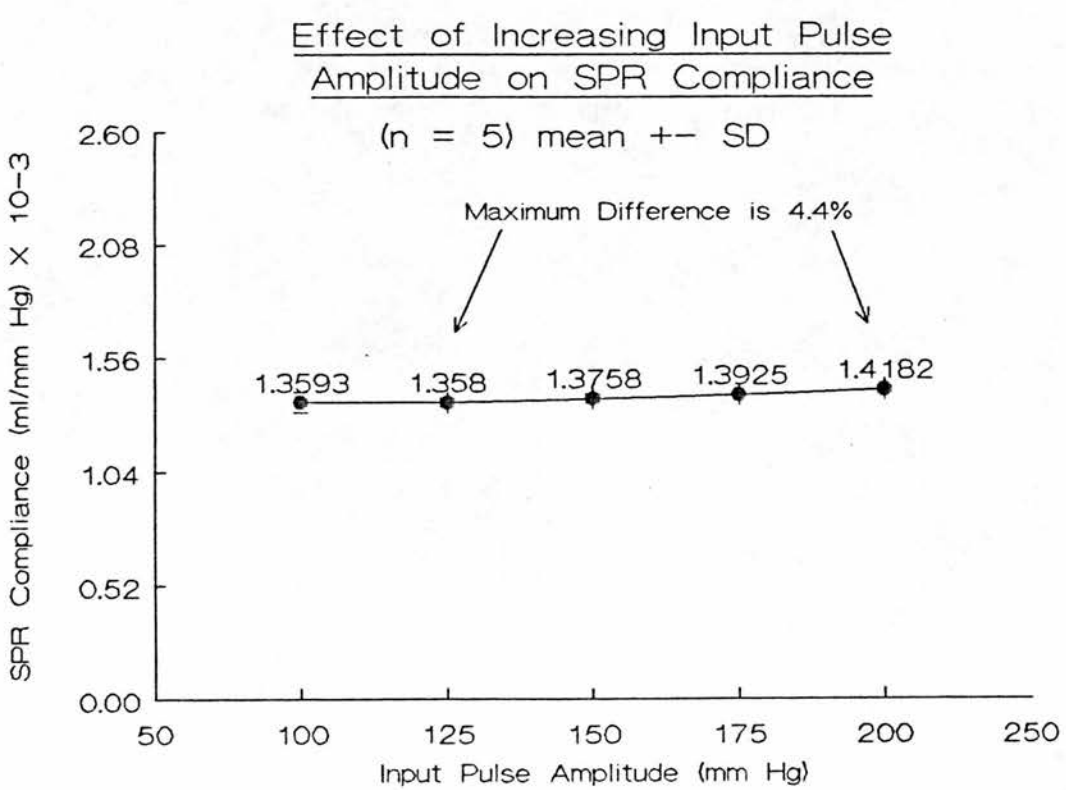

Figure 30b: Effect of Increasing Pulse Amplitude on SPR Compliance.

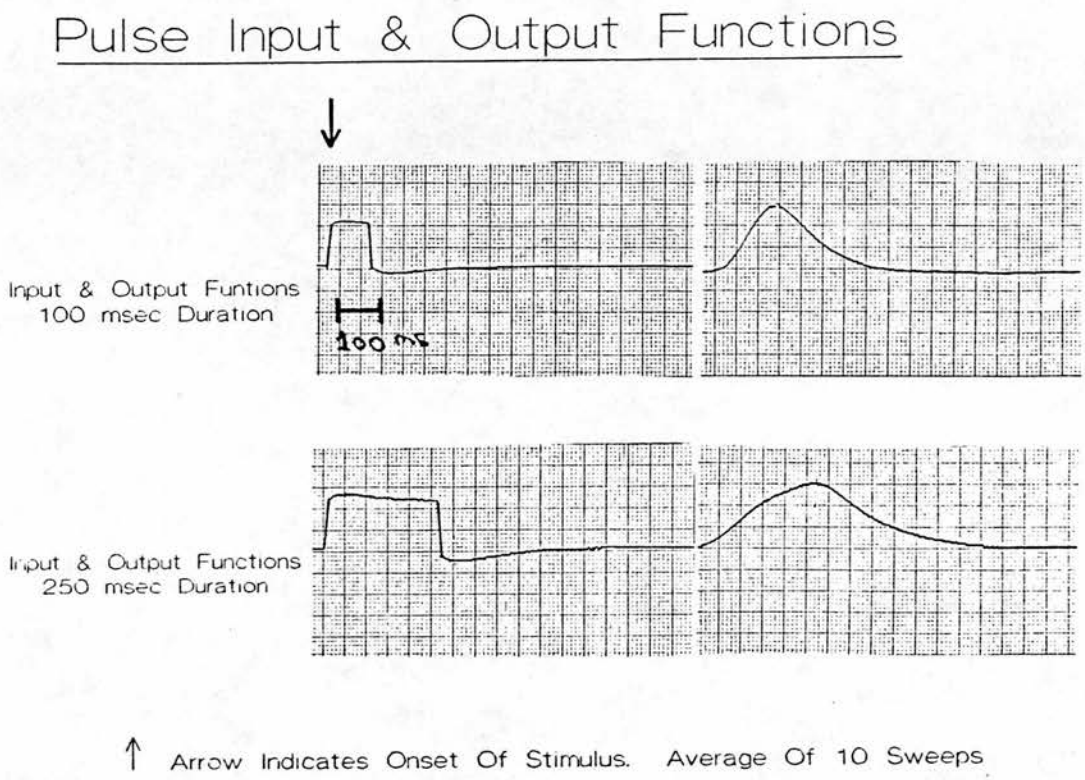

Figure 31a: Effect of Pulse Duration on Input Pulse Distortion.

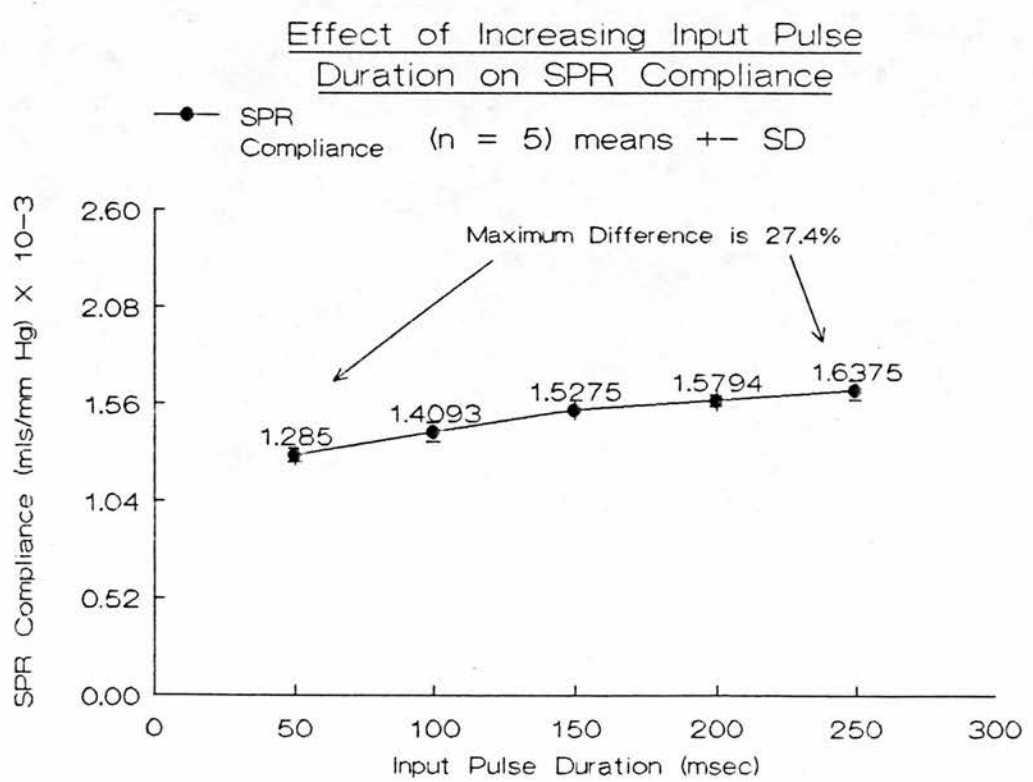

Figure 31b: Effect of Increasing Pulse Duration on SPR Compliance.

This pressure generator (Figure 32) is based on a moving coil piston attached to a metal diaphragm which is actuated by a constant force generated by the moving coil current. The pressure change within the dome results from the interaction of force and area (pressure = force/area). However, the force acts against the compliant properties of both the generator diaphragm and the system under test. The sag and overshoot demonstrated with the 250 msec pulse duration can be accounted for by the stiffness of the generator diaphragm absorbing part of the pressure output (hence the sag) and also, upon removal of the pulse, results in the diaphragm sucking extra fluid back from the test system (hence the overshoot).

This pulse duration study demonstrates that, with long pulse durations at least, the compliance of the pressure generator diaphragm should be considered in the calculation of system compliance.

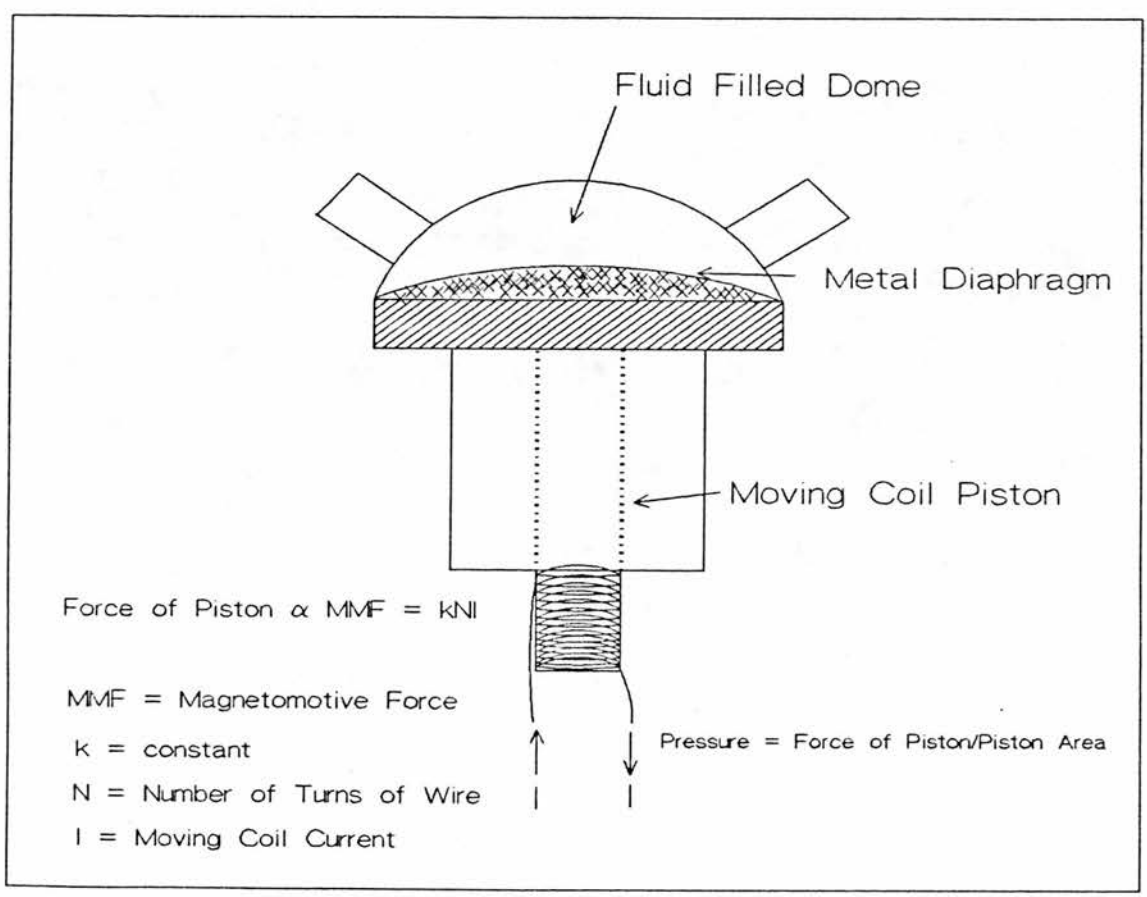

Figure 32: Diagrammatical Representation of Pressure Generator Mechanism.

As shown in Appendix K, however, provided the pulse duration is considerably less than the total RC time constant of the system under test, then the generator diaphragm compliance can be effectively ignored. In practice this is the case, as can be seen, for example, by analysing the condition where the craniospinal compliance of the cat decreases from the normal value[24] of 0.025 ml/mm Hg by 200 percent to 0.0063 ml/mm Hg. The RC time constant for the system is then calculated as the resistance (R) 210 mm Hg/ml/sec[25] multiplied by the compliance (C) 0.0063 ml/mm Hg which equals an RC time constant of 1.32 seconds which is still over 13 times the input pulse duration of 100 msec.

The pulse duration of 100 msec was selected on the basis that it was the minimum duration which was still significantly greater than the 2 msec rise time of the pressure generator.

7. An Independent Measure of Compliance

The SPR method required validation against an independent measure of compliance. The simplest measure of compliance within a linear model is to infuse fluid slowly within a closed system and record continuously the linear increase in pressure within the system. The slope of the resultant volume-pressure relationship is the compliance of the system. Figure 33a is a block diagram summarizing this method which for convenience is referred to in all following text as the "Infusion Method".

The physical model was set up with 1 ml of injected air in the syringe. The infusion method consists of a Harvard servo-controlled synchronous motor infusion pump[26], which infuses fluid into the system at a constant rate of 0.0393 ml/min. for a duration of four minutes. Pressure is measured within the syringe by an optimally damped fluid-filled catheter-transducer system which is sampled at 1 Hz for 4 minutes (240 seconds)

---

[24]This value is the average of 4 investigators' published compliance values at normal ICP from experimental studies in cats. References (41,42,46,73).

[25]The injection tubing resistance is 3.5 mm Hg/ml/min. To convert this to units expressed as mm Hg/ml/sec the value is multiplied by 60, giving 210 mm Hg/ml/sec.

[26]Harvard synchronous motor infusion pump model 940. Harvard Apparatus Ltd., Kent, UK.

under microcomputer control by a 12 bit A/D converter.[27] The resolution of pressure measurement is 0.0610 mm Hg[28]. For each pressure value sampled, the volume increment is calculated as the infusion rate of 0.0393 ml/min divided by 60 seconds which equals 0.000655 ml. The sampled pressure and volume data is stored to a data file. The 240 volume increments are then plotted against the corresponding 240 pressure increments and the compliance calculated from the slope of this volume versus pressure relationship. Appendix L is a flow diagram of the infusion method data collection program. Figure 33b contains an example plot of an infusion method volume-pressure run.

8. Comparison of SPR and Infusion Methods

The SPR method was compared with the infusion method in the physical model over a range of compliances produced by the introduction of increasing quantities of air into the physical model. The physical model was set up initially with 1 ml of injected air in the syringe. Through the positioning of a 3-way tap, compliance was measured alternately, over a range of compliances (1 - 5 ml air), by the infusion method followed by the SPR method. This entire sequence was carried out five times, with the average and standard deviation between runs calculated at each level of compliance for both methods. Figure 34 shows sample input and output pressure responses from the SPR method for the 1 and 5 ml injected air runs. The infusion method volume-pressure curves are also shown for the 1 and 5 ml injected air runs.

Figure 35 is a plot comparing the measured compliances[29] for both the SPR and infusion methods. The maximum difference was 7% between the two methods. The degree of difference was independent of compliance.

---

[27]Tecmar Lab Master. Tecmar Inc., Cleveland, USA.

[28]Pressure resolution was calculated as the calibrated transducer pressure range (250 mm Hg) divided by the 12 bit A/D resolution (2^{12} = 4096 discrete levels) yielding 0.0610 mm Hg (250/4096).

[29]Values are means +- standard deviations.

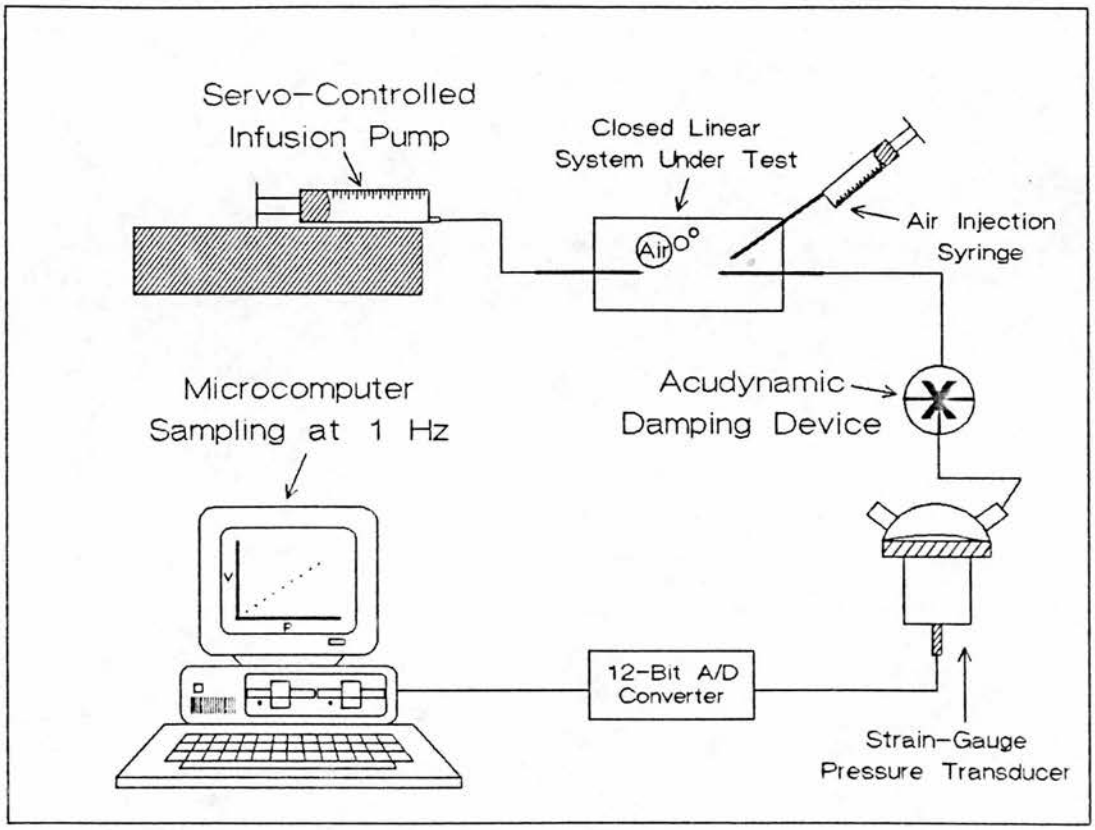

Figure 33a: Block Diagram of Infusion Compliance Method Apparatus.

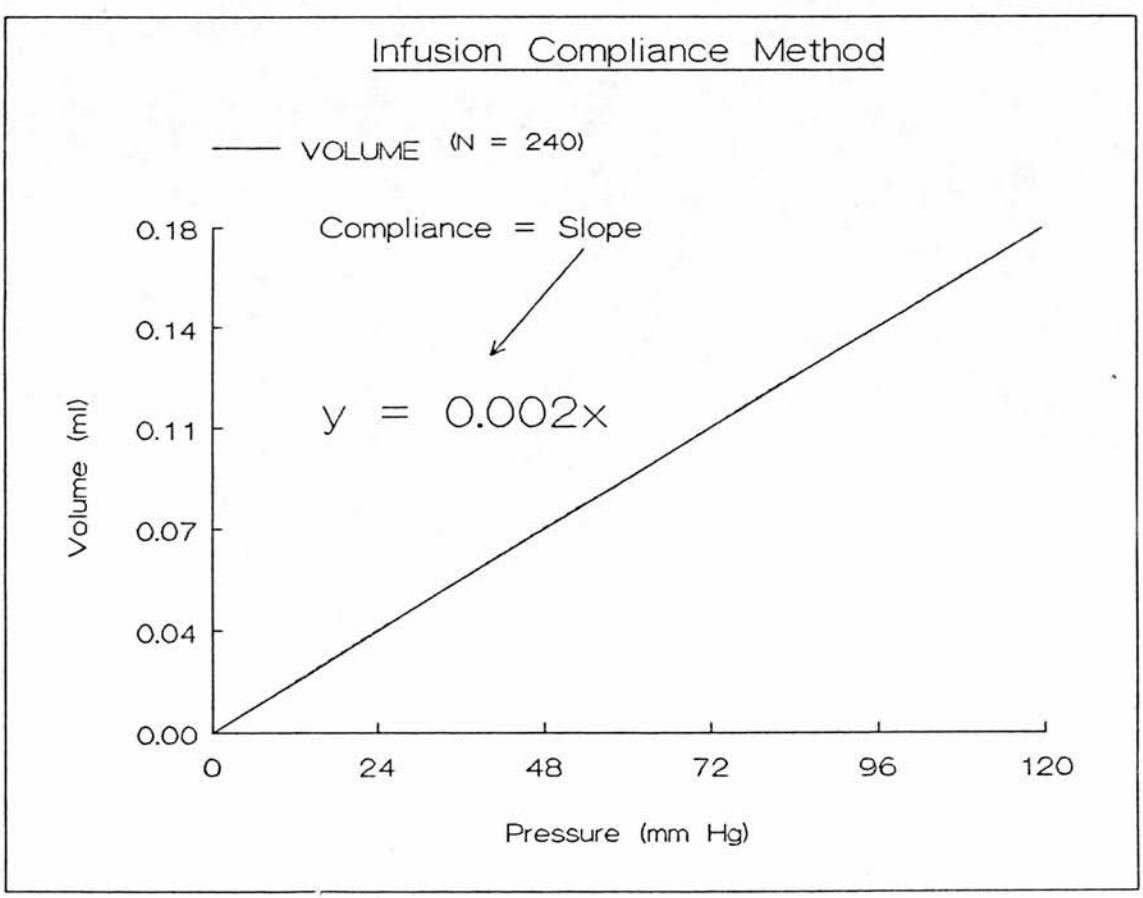

Figure 33b: Sample Plot of an Infusion Method Volume-Pressure Run.

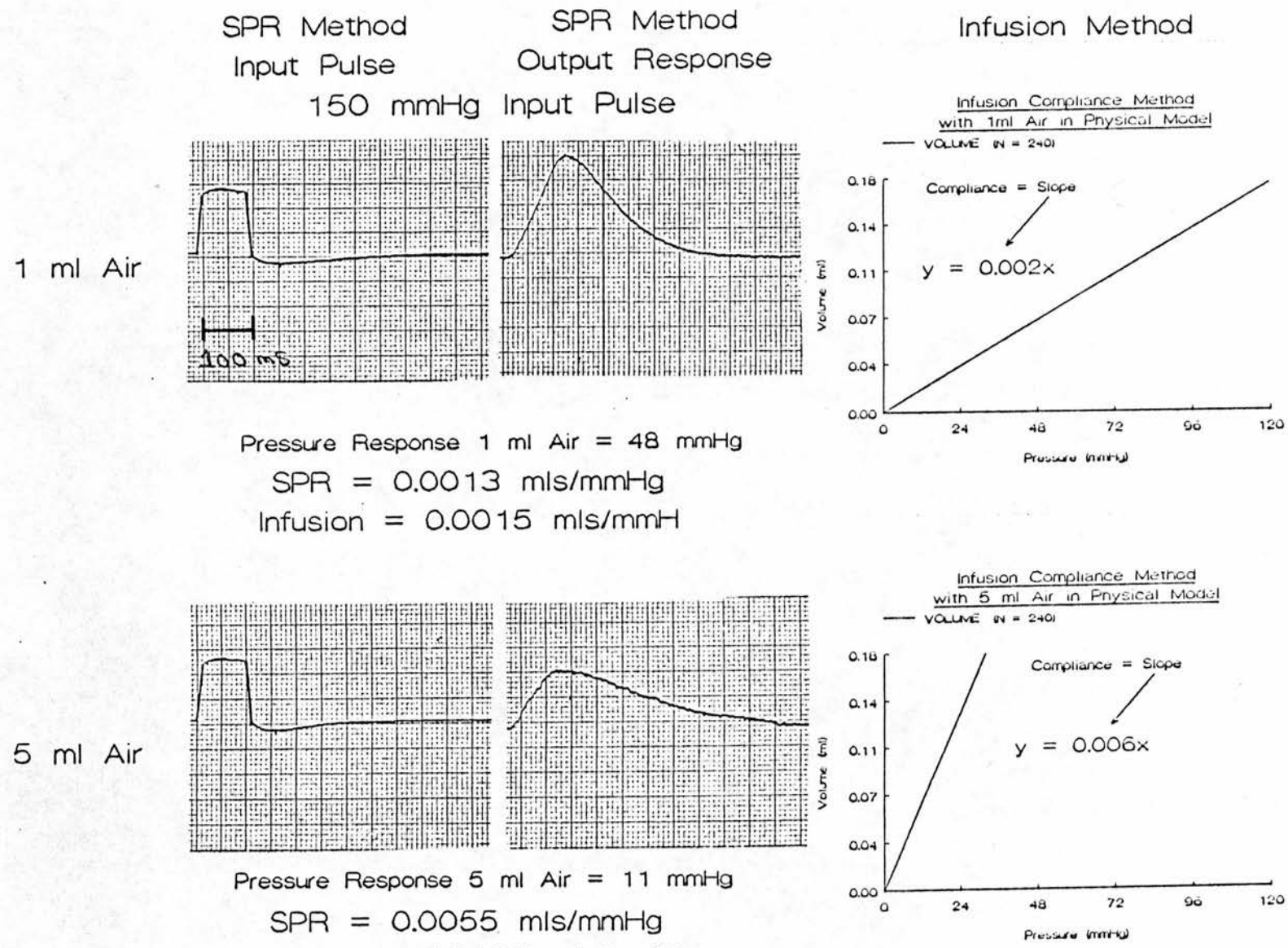

Figure 34: Sample Input and Output Functions for SPR and Infusion Compliance Methods.

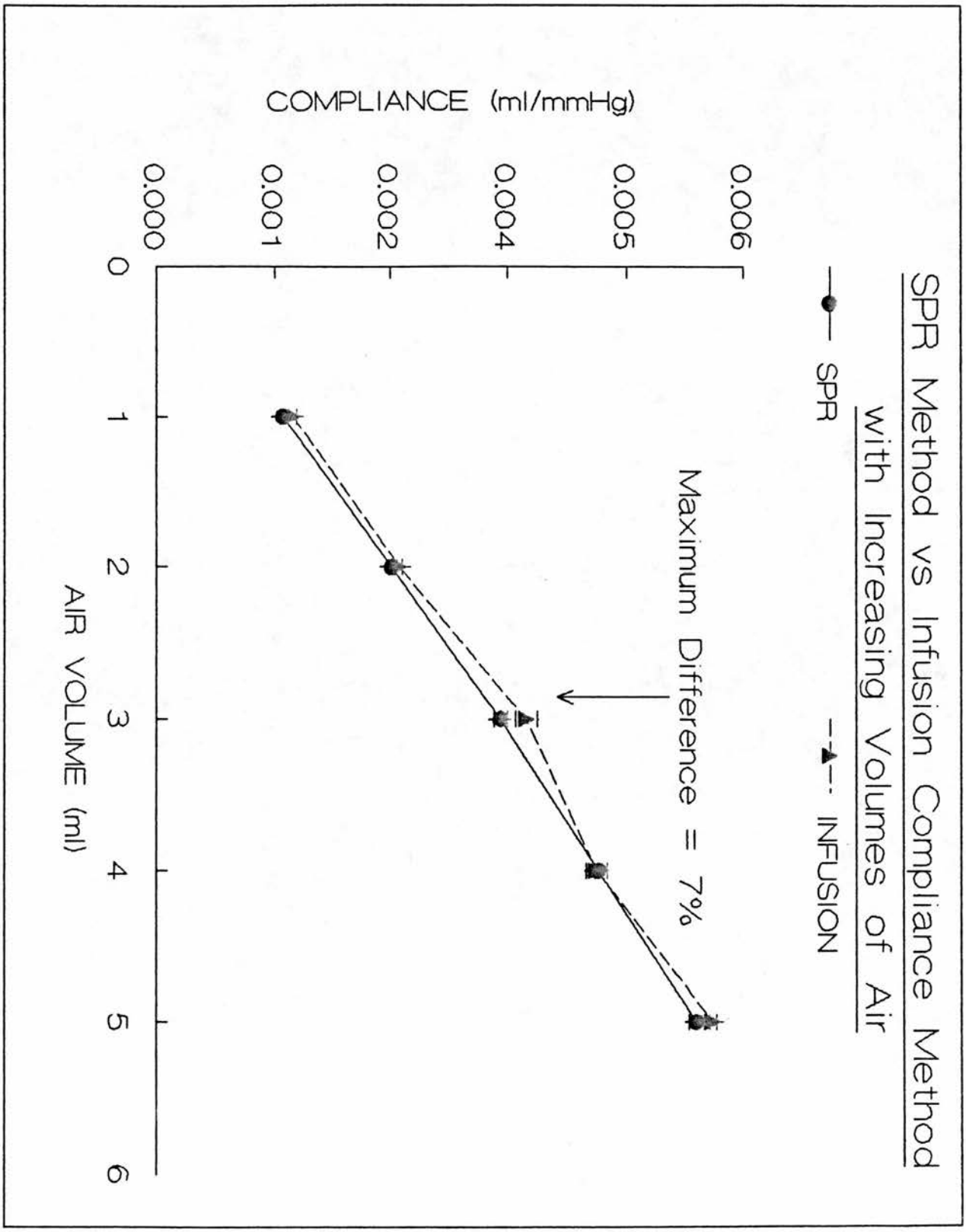

Figure 35: Comparison of SPR and Infusion Method in a Physical Model.

9. Sources of Error

a. Camino Transducer Error

Pilot experiments in the physical model using the Camino system for measurement of pressure within the syringe demonstrated large errors when the SPR method was compared with the infusion method. Figure 36 is a plot of the two methods compared over 3 levels of compliance produced by addition of 1, 2 and 3 ml of air into the physical model. The SPR method overestimated compliance compared to the infusion method, the difference between the two methods becoming greater with increasing compliance. This difference disappeared when the Camino system was replaced by an analogue strain-gauge transducer system (Figure 35).

The Camino catheter-tip transducer system is a digital system with 8-bit resolution over the 260 mm Hg pressure range[30]. This yields a pressure resolution of 1 mm Hg[31]. If a measurement error of 1 mm Hg were made with the Camino system this could cause large errors in the measured compliance. This can be best seen with a sample calculation. With a normal cat compliance of 0.025 ml/mm Hg and an SPR method volume injection of approximately 0.05 ml, the pressure response would be 2 mm Hg[32]. If the pressure response measured by the Camino system were underestimated or overestimated by 1 mm Hg, giving measured pressure responses of 1 or 3 mm Hg, this would yield calculated compliances of 0.05 and 0.0167 ml/mm Hg respectively. This represents a difference of 100% and 50% respectively from the actual compliance of 0.025 ml/mm Hg. As a result of this large source of error, the Bentley Trantec analogue strain gauge transducer system was used for pressure measurement within the physical model. The static and dynamic characteristics of this catheter-transducer system have been previously described (page 71). A similar calculation can be performed to determine that the pressure resolution required to keep the measurement error less than 10 percent is 0.1 mm

---

[30]Camino transducers cover the pressure range from -10 mm Hg to 250 mm Hg.

[31]An 8-Bit system can resolve 256 (2^8) discrete levels. The pressure resolution is then the pressure range covered (260 mm Hg) divided by the digital resolution (256 discrete levels) which yields 260/256 = 1.015 mm Hg or approximately 1 mm Hg.

[32]Compliance (C) is change in Volume (dV) divided by change in pressure (dP). C = dV/dP. Knowing dV and C then dP can be solved: dP = dV/C.

Hg[33]. An analogue transducer calibrated over a pressure range from 0 to 200 mm Hg when sampled by the 12 bit (4096 points of resolution) A/D converter of the SPR method signal averager yields a pressure resolution of 0.048 mm Hg (200/4096).

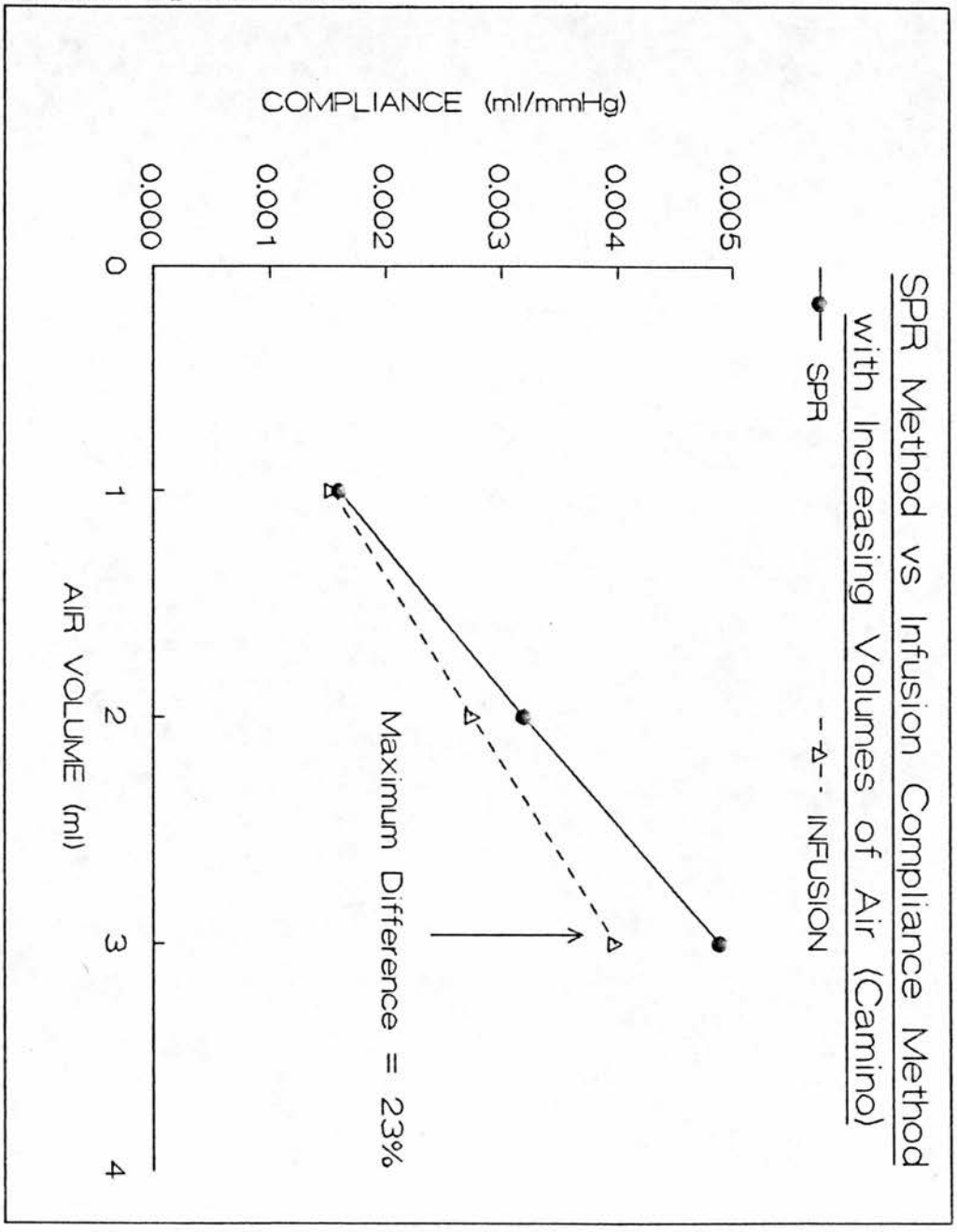

Figure 36: Comparison of SPR and Infusion Method using the Camino Transducer System.

[33]A compliance (C) change of 0.002 from the normal cat compliance of 0.025 is an 8% change. The pressure increment (P) resulting from this compliance change, assuming a constant volume (V) injection of 0.025 mls (worst case), is P = V/C. This yields a change from 1 to approximately 1.1 mm Hg. A pressure resolution of 0.1 mm Hg is required to detect this change.

b. Effect of Air Bubbles

To ascertain the error in compliance measurement caused by air bubbles in the measurement tubing, increasing quantities of air (0.1, 0.3, 0.5 and 0.7 ml) were injected into the injection tubing resistance (R1) during measurement of a fixed compliance within the physical model. The entire sequence of volume injections was carried out five times. The total injection tubing volume was 1.4 ml. With the largest volume injected (0.7 ml) half of the injection tubing resistance contained air. Figure 37 is a plot of air bubble volume versus measured compliance[34]. Compliance was overestimated when there was air contaminating the injection tubing resistance. There was an average of 5% overestimation in compliance for each 0.1 ml of added air.[35]

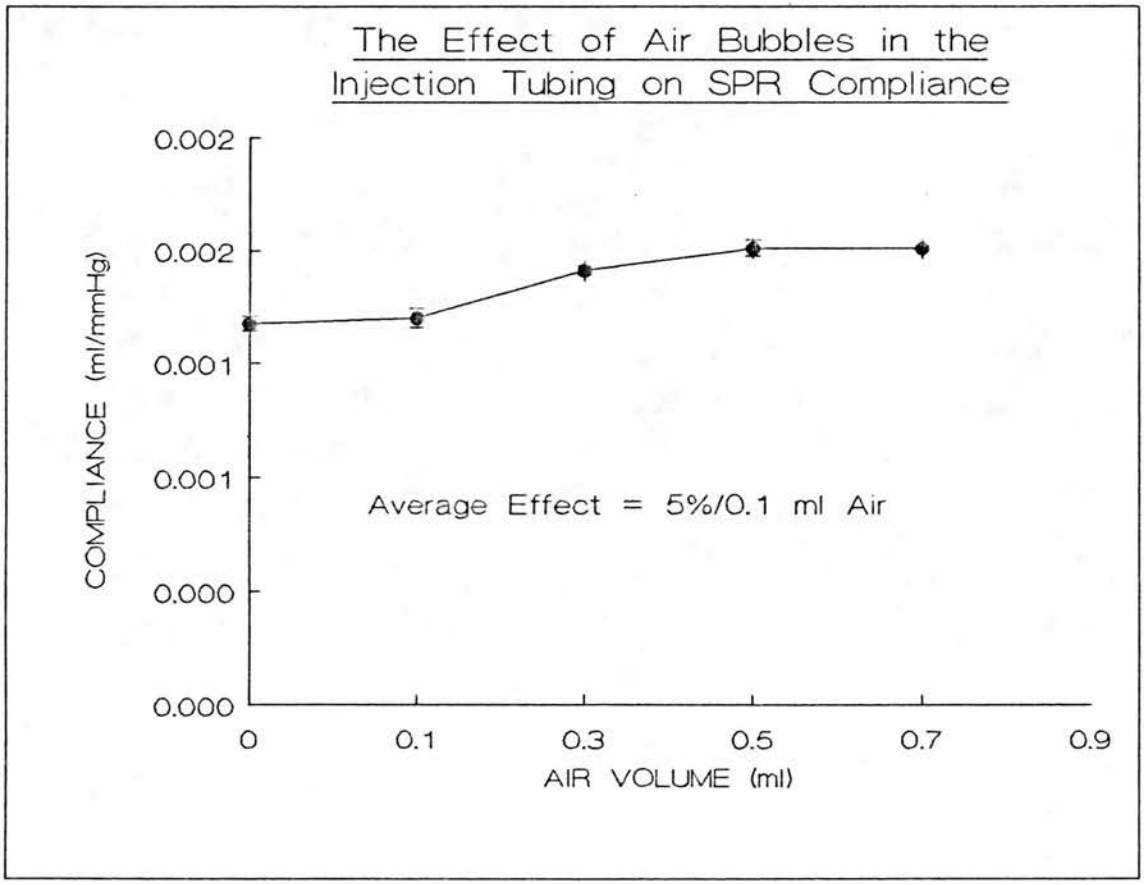

Figure 37: The Effect of Air Bubbles in the Injection Tubing on SPR Compliance.

---

[34]Values are means +- standard deviations.

[35]See page 111 of the discussion section for consideration of the measurement error due to invisible trapped air in the injection fluid.

c. Measurement Error

Compliance is calculated using equation 1 (page 67). The calculation will be affected by measurement error from two sources: the measurement of the injection tubing resistance (R1), and the measurement of input pulse duration (Ti), input pulse amplitude (Vp) and output pulse amplitude (Vc). The latter group of measurements is all obtained from the signal averager.

Five sequential measurements of the resistance of the injection tubing (R1) produced a mean resistance of 3.5 +- 0.17 mm Hg/ml/min. Taking two standard deviations away from the mean produces a range of resistance values of 3.16 to 3.84 mm Hg/ml/min. The error caused in the calculation of compliance using these two limiting values of injection tubing resistance was 10 percent.

The measurement accuracy of the pressure pulse duration (Ti) is governed by the 4 msec averager time base resolution, which would cause a maximum error of 4% in the measurement of the 100 mSec pulse duration. Similarly, the measurement accuracy of the input (Vp) and output pressure (Vc) amplitudes is governed by the 2 mV resolution of the display gain amplifier, which would cause a maximum error of 10%[36] in the measurement of Vp and Vc.

Having determined the major sources of error in the SPR method and compared the accuracy of the method with the infusion method of compliance measurement, the SPR method was next compared with the VPR method in animal models.

C. Animal Model Testing

1. Methods

Twelve cats of both sexes, each weighing between 2.5 and 5.5 Kg, were split into three groups: an ICP group (n = 4), a BP group (n = 4) and a CO2 group (n = 4). All animals were induced with ketamine hydrochloride[37] (30 mg/kg I.M.) and atropine sulphate[38] (0.05 mg/kg I.M.),

---

[36]This calculation assumes a worst case Vc amplitude of 20 mV.

[37]Ketalar. Parke-Davis, Eastleigh, UK.

[38]Antigen Ltd., Roscrea, Ireland.

followed by alpha-chloralose[39] anaesthesia given as a 1% solution (75 mg/kg I.V.). Figure 38 is a diagram summarizing the animal preparation. Both femoral veins were cannulated with polyethylene tubing[40] (internal diameter 0.86 mm) for infusion of fluids and drugs. Both femoral arteries were cannulated for arterial blood gas sampling[41] and to allow monitoring of arterial pressure through placement of a Camino catheter-tip pressure transducer into the descending thoracic aorta. The animals were given a tracheostomy, intubated and then were ventilated with intermittent positive pressure ventilation at a stroke rate of 25 breaths/min and a tidal volume of 30 ml[42]. Ventilatory volume was adjusted as required to keep the animals normocarbic (PaCO2 35 - 40 mm Hg). The animals were ventilated during surgical preparation with a gas mixture of 60% oxygen/ 40% nitrous oxide and were maintained post surgery on oxygen alone. Muscle paralysis was induced with pancuronium bromide[43] (0.7 mg I.V.) repeated hourly. Each animal's body temperature was maintained constant at 38 degrees Celsius with a homeothermic blanket system[44]. The auditory canals were infiltrated with 1% lignocaine gel[45] after which the animal was placed in a stereotactic frame in the sphinx position, the scalp and temporal muscles were reflected and bilateral burr holes were drilled in the skull 7 mm posterior and 4 mm lateral to bregma for cannulation of the lateral ventricles with 2 inch 19 gauge needles[46] (78). The continuous infusion method[47] was used for location of ventricles. In addition, a midline incision was made in the posterior fossa, and a 19 gauge 2 inch

---

[39]Sigma Ltd., Poole, UK.

[40]Portex Ltd., Hythe, UK.

[41]Blood gas analyser IL system 1302. Instrument Laboratories, Milan, Italy.

[42]Harvard ventilator model 665A. Harvard Apparatus Ltd., Edenbridge, UK.

[43]Pavulon. Organon Teknika Ltd., Cambridge, UK.

[44]Harvard homeothermic blanket system. Harvard Apparatus Ltd., Edenbridge, UK.

[45]Astra Pharmaceuticals Ltd., Kings Langley, UK.

[46]Needles were modified spinal needles cut to a 2 inch length with the sharp bevels filed smooth.

[47]Reference 70 page 105.

metal needle was placed into the cisterna magna through the foramen magnum. The needle insertion holes were sealed by cyanoacrylate adhesive[48] to prevent CSF leaks. ICP was monitored through the left ventricular cannula using an optimally damped fluid-filled catheter transducer system as previously described (page 71). The right ventricular cannula was used for infusion of saline or Hartman's solution into the CSF space for altering the baseline ICP. The cisterna magna cannula was connected to the SPR method pressure pulse generator for applying input pressure pulses to the CSF system for measurement of craniospinal compliance, the method having been previously described (page 69). Through the positioning of a 3-way tap, the cisterna magna cannula could be redirected to the VPR method test apparatus which consisted of a 30 cm low compliance tube, a 3 way tap and a 1 ml syringe, the VPR method also having been previously described (page 64). The ICP response to the SPR and VPR pressure and volume pulses were recorded through the left lateral ventricular cannula. All pressure transducers were calibrated against a water column and zeroed with reference to the plane of the stereotactic frame ear bars.

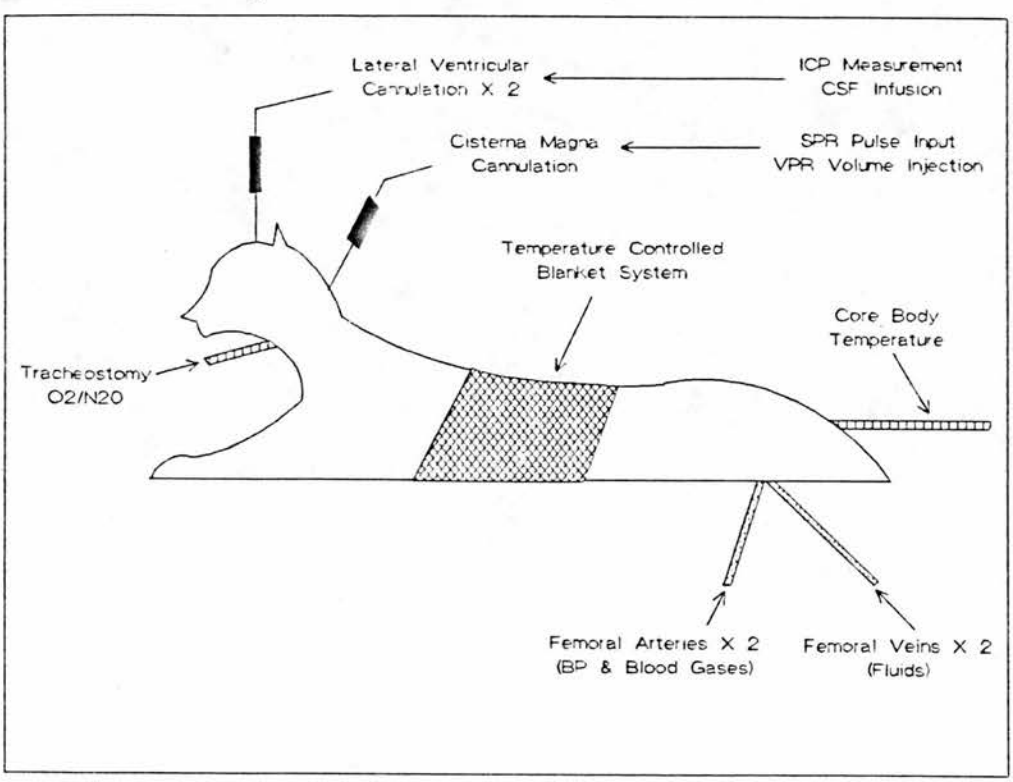

Figure 38: Diagram Summarizing the Animal Preparation.

[48]RS components Ltd., Corby, UK.

2. Statistical Analysis

All comparisons between two groups of data were tested statistically with a students paired t-test. Curve fits were performed on some data to characterize the trend of the data. A power function was found to be the approximating function that best fit the shape or general trend of the data. The curve fits were performed using a least squares regression according to the power formula[49]: $y = ao\ x^{a1}$.

3. Comparison of SPR and VPR Methods with Raised ICP

a. Protocol

The ICP of four animals was raised in five stages from 10 to 100 mm Hg by infusion of saline (3 - 60 ml/hour) into the right lateral ventricle. Placement of a cannula into the cisterna magna caused a variable loss of CSF. So that all animals could start from the same ICP baseline, ICP was raised, by slow intraventricular infusion (3 ml/hour) of saline, to a starting baseline level of between 10 and 15 mm Hg.

At each level of ICP, four sequential measurements of craniospinal compliance were performed by both the SPR and VPR methods with five minutes separating each measurement. With two of the animals the SPR preceded the VPR method, while with the remaining two animals the VPR preceded the SPR method. For the SPR method, the compliance for a given level of ICP was the average of the four sequential compliance measurements, where each measurement was the signal average of 50 stimulus presentations. For the VPR method, the compliance for a given level of ICP was calculated from the mean pressure response after rapid injection of 0.5, 1, 1.5 and 2 ml of saline[50]. In addition to compliance, the following physiological data was recorded: ICP, BP, Tc, PaCO2, PaO2 and pH.

b. Results

Figure 39 shows sample output pressure pulses recorded from an animal at normal ICP (13 mm Hg) and at elevated ICP (90 mm Hg)

---

[49]Power function converted to a linear equation ie:
$y = ao\ xa1 \Rightarrow \ln y = a1 \ln x + \ln ao$

[50]VPR (dP/dV) is the inverse of compliance dV/dP. The VPR was calculated and this value was then inverted to yield the compliance.

demonstrating that even at elevated ICP the signal average of 50 stimulus presentations is sufficient to remove the background ICP pulse waveform.

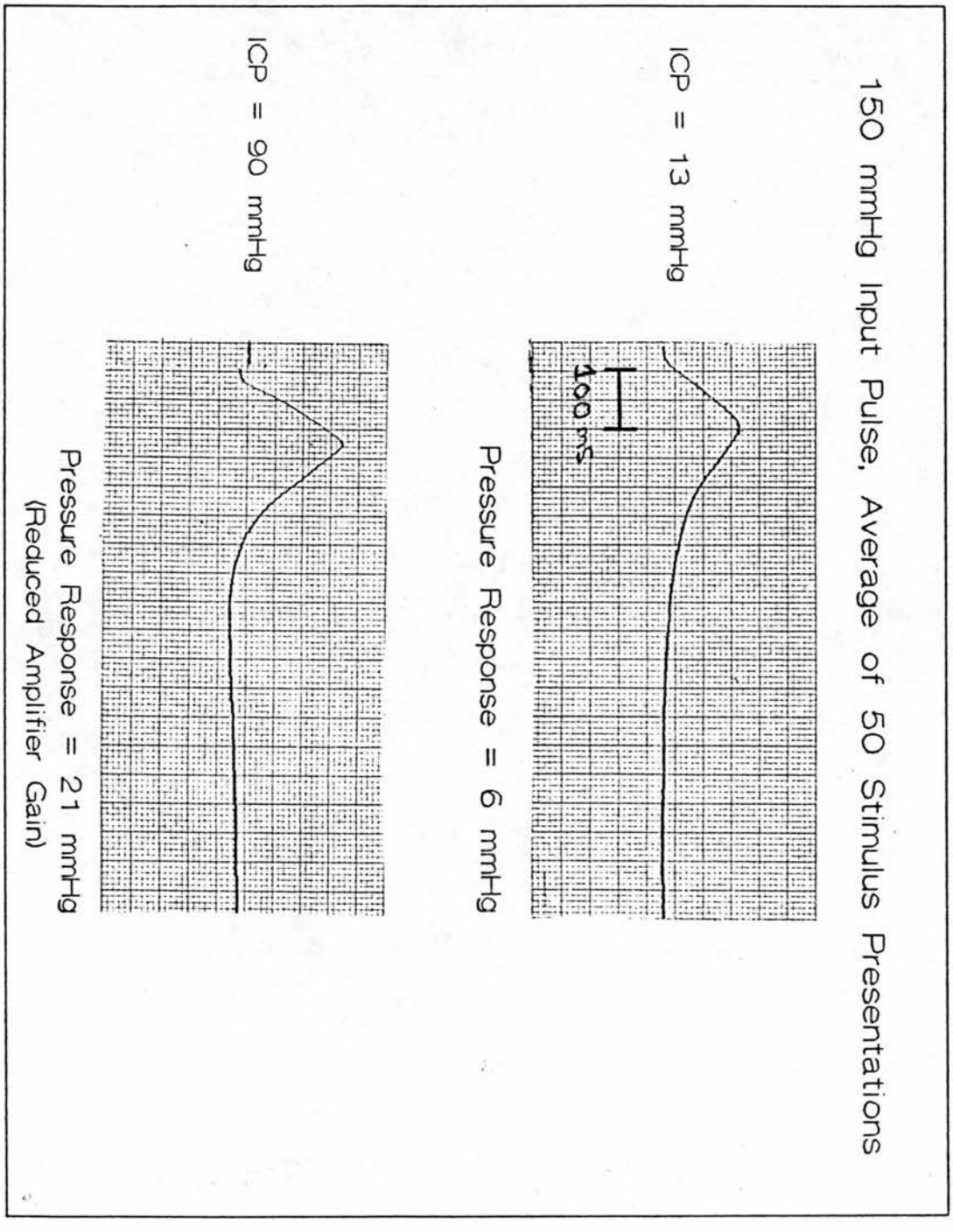

Figure 39: Sample SPR Output Pressure Responses at Low and High ICP in the Animal Model.

Figures 40a and 40b are plots of the calculated compliance versus ICP as measured by both the SPR and VPR methods. Data points[51] from all four animals are pooled. Both methods show a decrease in compliance with increasing ICP. The VPR method overestimates compliance compared to the SPR method and also demonstrates greater variability between measurements. All VPR compliance values from all four animals were greater than the corresponding SPR compliance values, indicating that the overestimation is independent of whether compliance was first measured by the SPR or VPR method. The amount of overestimation ranged from 20% to 162% with a mean of 77%. The coefficient of variation (CV) as previously described (page 30) was used as a measure of the reproducibility between the four sequential measurements of compliance of both methods. The CV for the SPR method ranged from 0.6% to 9.3% with a mean variation between measurements of 2.6%. The VPR method showed a CV ranging from 5.6% to 48% with a mean variation between measurements of 17%. Table 7 is a breakdown of the physiological data averaged across all four animals and grouped by ICP level[52].

---

[51]Values are means +- standard errors.

[52]Values are means +- standard deviations.

Table 7: Breakdown of Physiological Data for SPR Validation Series ICP Group.

ICP (mm Hg)	BP (mm Hg)	Tc (Deg. C)	PaCO2 (mm Hg)	PaO2 (mm Hg)	pH
11.7 +−0.83	143 +−25	37.3 +−0.04	39.6 +−6.3	416 +−67	7.27 +−0.03
33.0 +−1.9	149 +−19	37.4 +−0.14	36.9 +−3.2	397 +−90	7.31 +−0.03
51.3 +−0.4	154 +−20	37.5 +−0.08	36.3 +−4.8	453 +−38	7.30 +−0.06
75.0 +−1.9	150 +−24	37.4 +−0.14	39.3 +−1.9	471 +−51	7.27 +−0.04
106.8 +−5.1	157 +−16	37.1 +−0.08	41.0 +−3.7	413 +−78	7.27 +−0.04

All values are means +− standard deviations

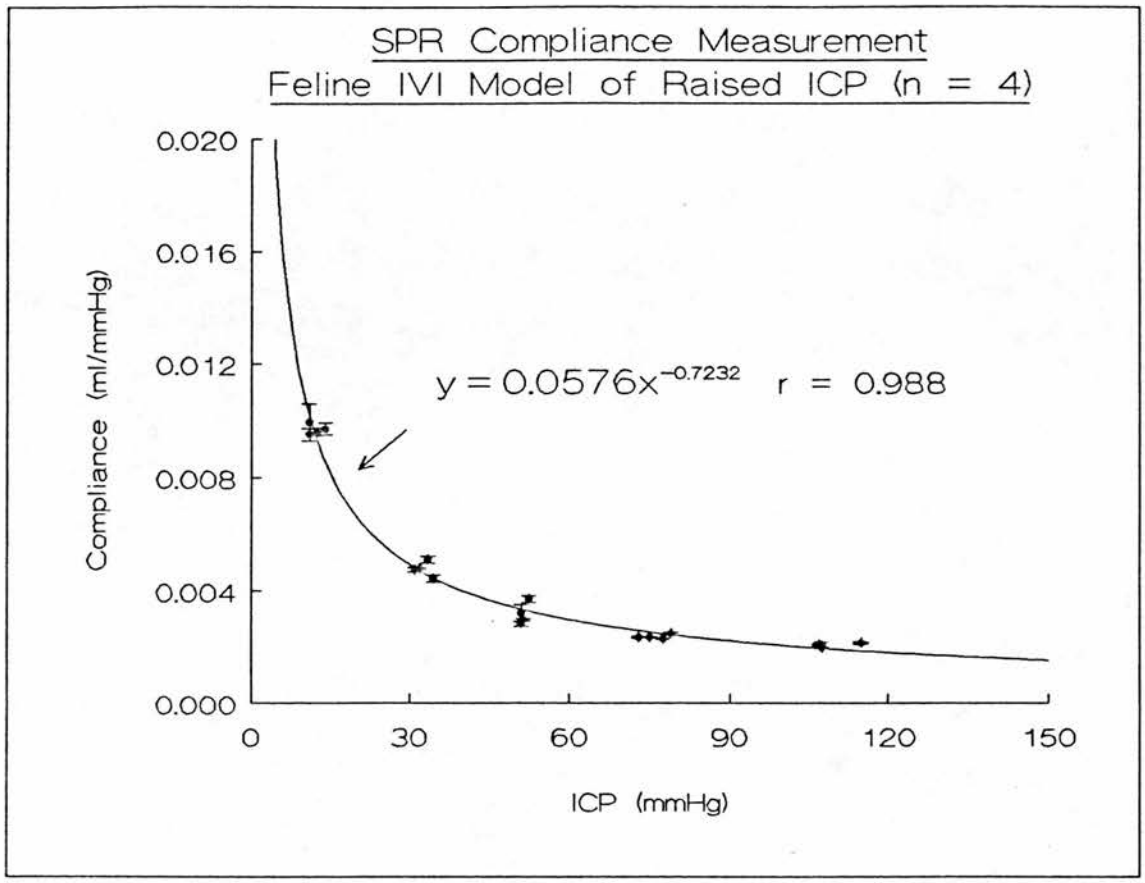

Figure 40a: SPR Compliance vs Increasing ICP in the Animal Model.

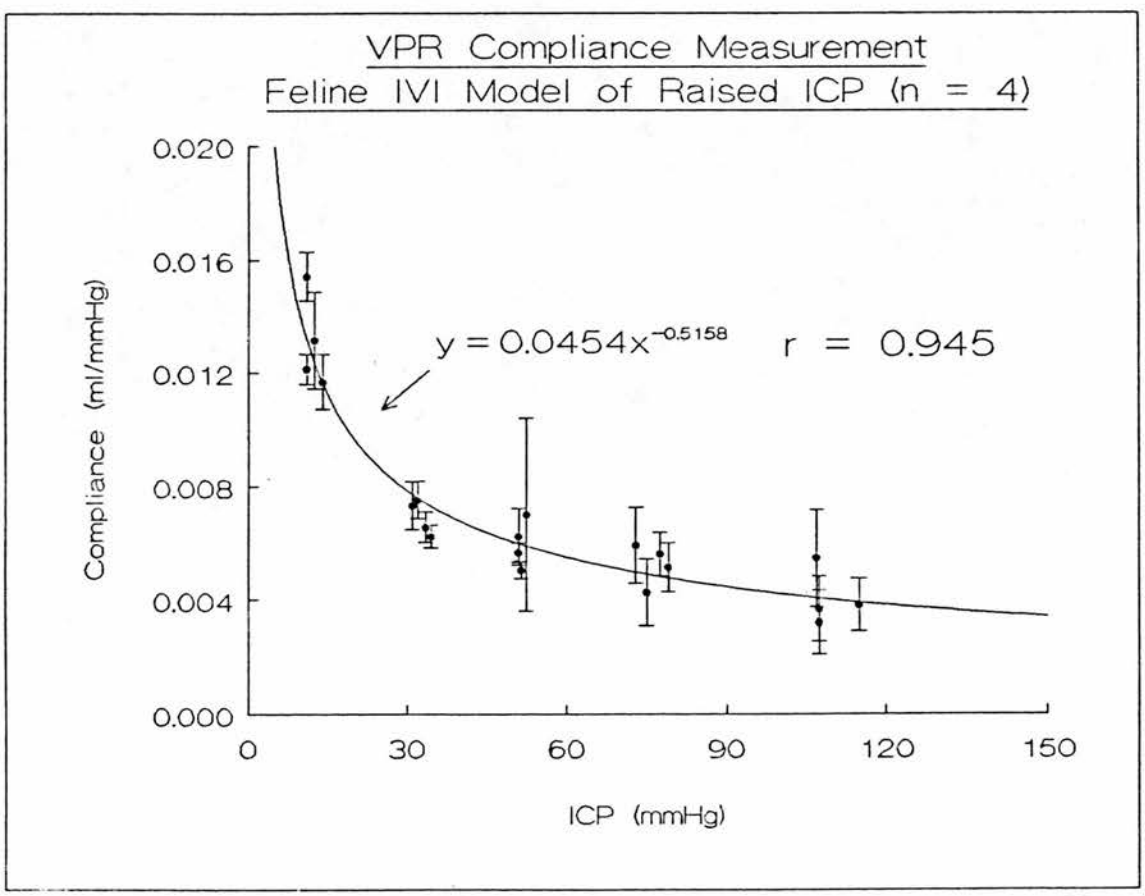

Figure 40b: VPR Compliance vs Increasing ICP in the Animal Model.

4. Comparison of SPR and VPR Methods with Arterial Hypertension and Hypotension

a. Protocol

The BP of four animals was first lowered and then raised in stages. Pooling the data from all animals gave a range of BP from 20 mm Hg to 220 mm Hg. BP was lowered with intravenous infusion (10 - 40 ml/hour) of trimetaphan camsylate[53] (2.5 mg/ml). BP was raised with intravenous infusion (6 - 40 ml/hour) of Angiotensin II[54] (100 ug/ml) and supplemented as required with adrenalin[55] (0.2 mg/ml at 10 - 40 ml/hour). ICP was raised, by slow intraventricular infusion (3 ml/hour) of saline, to a baseline level of between 10 and 15 mm Hg.

At each level of BP, four sequential measurements of craniospinal compliance were performed by both the SPR and VPR methods with five minutes separating each measurement. In addition to compliance, the following physiological data was recorded: ICP, BP, Tc, PaCO2, PaO2 and pH.

b. Results

Figures 41a and 41b are plots of the calculated compliance versus BP as measured by both the SPR and VPR methods. Data points[56] from all four animals are pooled. Both methods show a decrease in compliance with increasing BP. Similar to the results with raised ICP the VPR method overestimates compliance compared to the SPR method and also demonstrates greater variability between measurements. The amount of overestimation ranged from 28% to 214% with a mean of 89%. The coefficient of variation (CV) between the four sequential measurements at each level of BP for the SPR method ranged from 0.4% to 4.6% with a mean variation between measurements of 2.56%. The VPR method showed a CV ranging from 3.8% to 49.3% with a mean variation between measurements of 16%. Table 8 is a breakdown of the pooled physiological data.

---

[53]Arfonad (Trimetaphan camsylate). Roche Products Ltd., Welwyn Garden City, UK.

[54]Sigma Ltd., Poole, UK.

[55]Antigen Ltd., Roscrea, Ireland.

[56]Values are means +- standard errors.

Table 8: Breakdown of Physiological Data for SPR Validation Series BP Group.

BP (mm Hg)	ICP (mm Hg)	Tc (Deg. C)	PaCO2 (mm Hg)	PaO2 (mm Hg)	pH
20	8	37.5	34.8	234	7.32
35	10	38.0	35.6	252	7.30
61	14	38.0	39.7	209	7.29
66	11	37.5	37.6	200	7.31
71	15	37.3	30.1	393	7.34
118	14	37.0	37.6	472	7.29
125	12	37.8	34.4	495	7.33
147	17	37.6	32.2	510	7.36
175	19	37.7	32.1	484	7.34
190	17	37.3	38.4	536	7.32
220	18	37.6	30.1	393	7.34
Mean	14.1	37.6	34.5	380	7.32
+- SD	+- 3.4	+- 0.3	+- 3.2	+- 125	+- 0.02

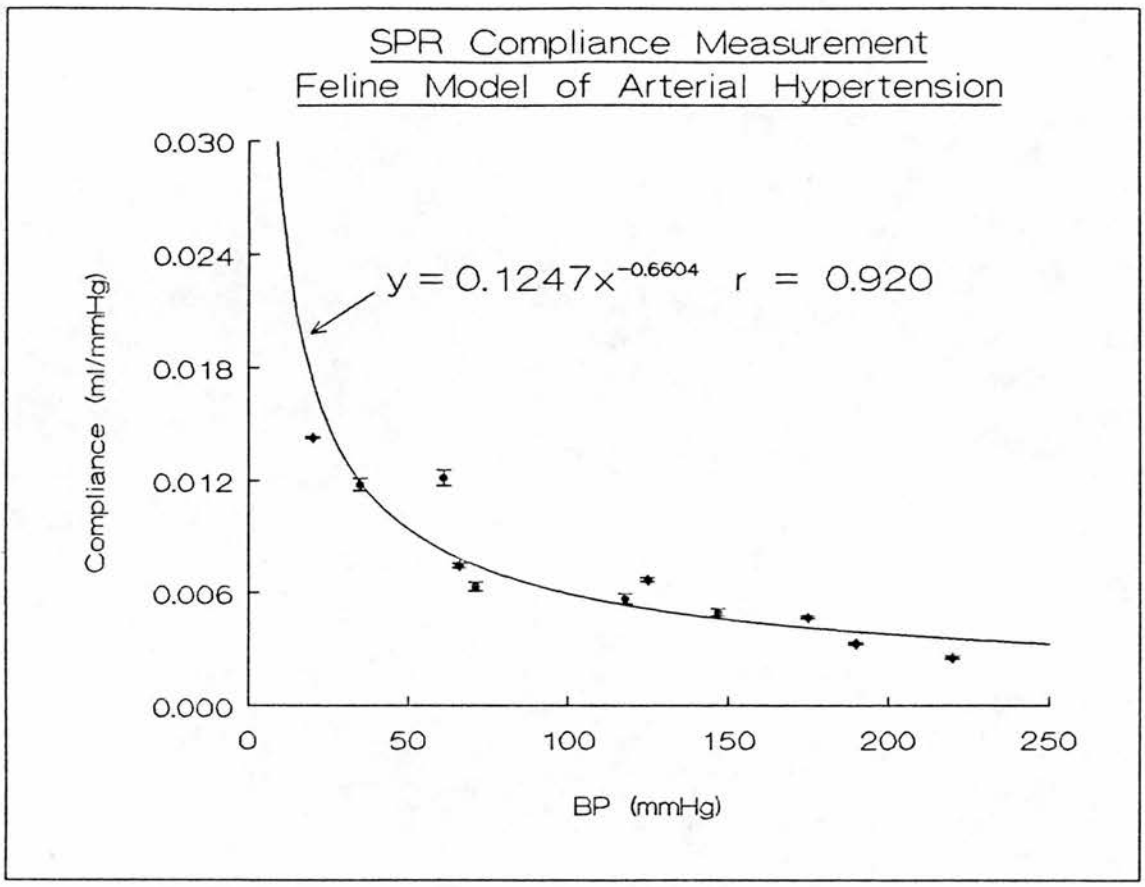

Figure 41a: SPR Compliance vs BP in the Animal Model.

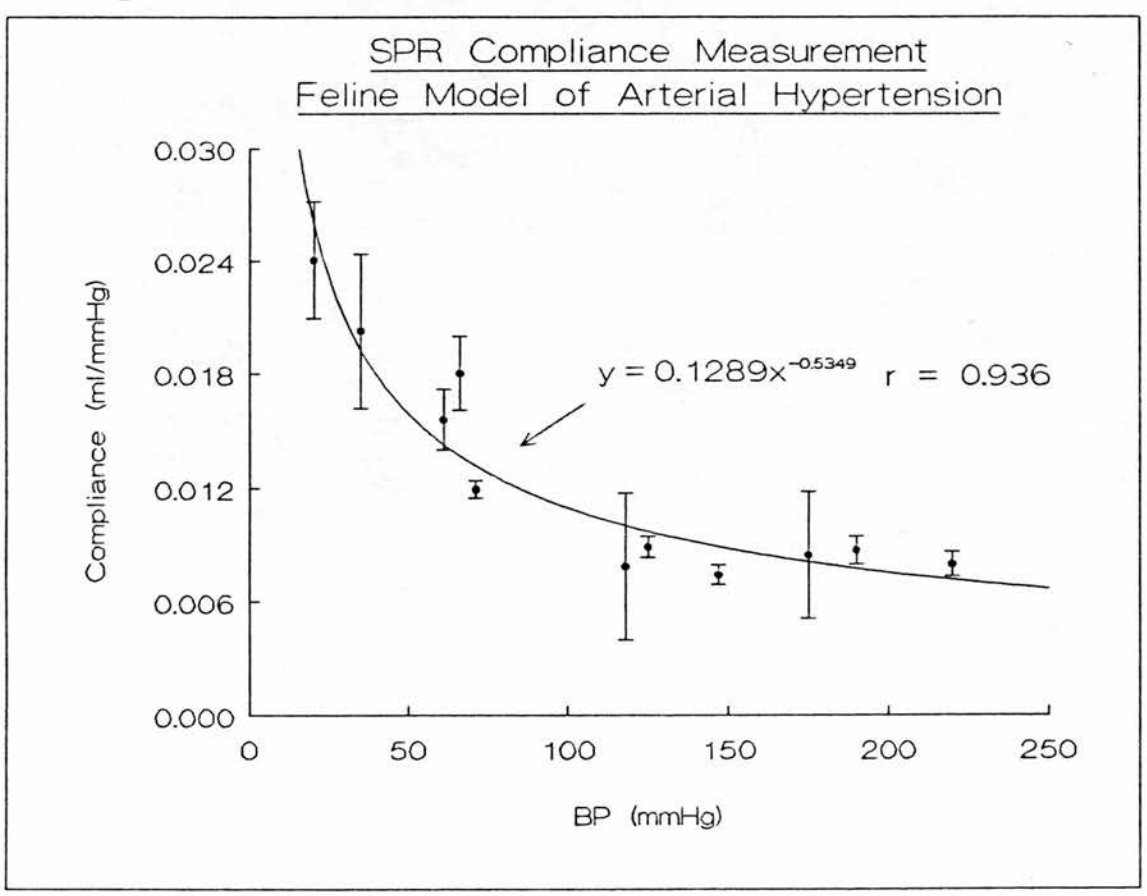

Figure 41b: VPR Compliance vs BP in the Animal Model.

5. Comparison of SPR and VPR Methods with Arterial Hypercarbia

a. Protocol

The arterial CO2 tension of four animals was raised in two stages by the administration of 5% and 10% CO2 in the inspired gas mixture. ICP was raised, by slow intraventricular infusion (3 ml/hour) of saline, to a baseline level of between 10 and 15 mm Hg.

At each level of CO2, four sequential measurements of craniospinal compliance were performed by both the SPR and VPR methods with five minutes separating each measurement. In addition to compliance, the following physiological data was recorded: ICP, BP, Tc, PaCO2, PaO2 and pH.

b. Results

Figure 42 is a barchart graph of the grouped compliance data[57] as measured by both the SPR and VPR methods at normocarbia and at two levels of hypercarbia. Table 9 is a breakdown of the physiological data averaged across all four animals and grouped by the inspired CO2 level. With 5% inspired CO2 the PaCO2 increased from a baseline of 37.6 mm Hg to 59.8 mm Hg ($P < 0.01$) increasing further still with 10% CO2 to 117 mm Hg ($P < 0.01$). ICP also increased significantly rising from a baseline value of 13 mm Hg to 25 mm Hg ($P < 0.01$) and increasing to 34 mm Hg ($P < 0.01$) with 10% CO2. Associated with these changes, both methods showed a decrease in compliance with 5% CO2 although only the SPR method showed a statistically significant decrease ($P < 0.01$). With 10% inspired CO2, compliance increased towards control levels, although this change did not reach statistical significance. There was a large variation in compliance across animals. However, within one individual animal, similar to the ICP and BP groups, the SPR method showed less variation (CV = 1.8% to 10.9% with a mean of 4.9%) compared with the VPR method (CV = 3.4% to 41% with a mean of 14.2%). The amount of overestimation of the VPR method compared with the SPR method ranged from 21% to 171% with a mean of 52%.

---

[57]Compliance was averaged across all four animals; values are means +- standard errors.

Table 9: Breakdown of Physiological Data for SPR Validation Series CO2 Group.

	ICP (mm Hg)	BP (mm Hg)	Tc (Deg. C)	PaCO2 (mm Hg)	PaO2 (mm Hg)	pH
0% CO2	13.1 +−2.2	128 +−28	37.5 +−0.1	37.6 +−2.2	415 +−37	7.30 +−0.01
5% CO2	25.0 +−4.9	131 +−23	37.2 +−0.2	59.8 +−7.1	350 +−142	7.12 +−0.02
10% CO2	34.3 +−9.2	145 +− 17	38.0 +−0.4	117.1 +−36.5	263 +−69	6.90 +−0.11

All values are means +− standard deviations

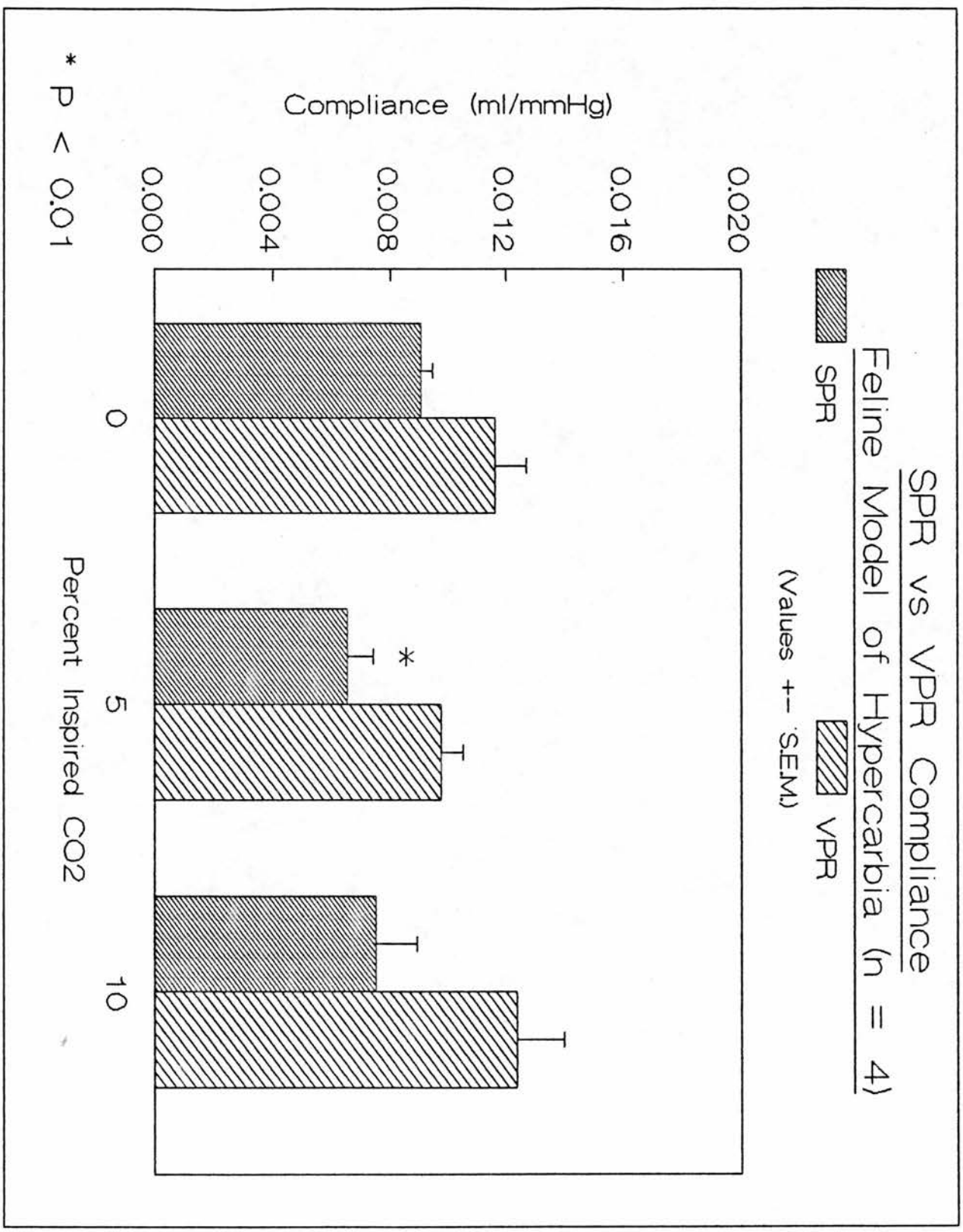

Figure 42: SPR and VPR Compliance vs CO2 in the Animal Model.

6. SPR Method and Blood Brain Barrier Damage

Two animal experiments were carried out to determine whether the repeated application of pressure pulses into the CSF space induced by the SPR method produced damage to the blood brain barrier or to the neuronal parenchyma.

a. Protocol

Both animals were prepared as previously described (page 87) with the exception that intraventricular cannulae were not placed and cranial surgery, other than exposure of the foramen magnum, was not performed. This was to eliminate surgery and ICP monitoring as a source of trauma to the brain. Pressure pulses were applied through the cisterna magna cannula as normal. A sequence of fifty pressure pulses was applied, once every 15 minutes for 8 hours. In one animal, forty minutes before the end of the protocol, 8 ml (2 ml/Kg body weight) of a 2% Evans Blue Dye[58] was given intravenously to assess major blood brain barrier disruption (144). In the second animal, at the end of the protocol, trans-cardiac perfusion-fixation using a formaldehyde, acetate, methanol buffer mixture (40:1:1) was performed as described by the method of Brierly and Brown (145). After the brain was perfusion fixed, it was removed, sectioned and stained with Haematoxylin, Eosin and Luxul Fast blue stains. Sections of both brains were examined by a neuropathologist for evidence of blood brain barrier breakdown or focal tissue damage.

b. Results

Figure 43 is a photograph of coronal slices taken from the brain of the animal injected with Evans Blue Dye. Nine slices are shown extending in 5 mm steps from the forebrain to the cerebellum. The brain slices show normal brain parenchyma, no evidence of brain shift and no focal or hemispheric swelling. There is also no evidence of intraparenchymal staining with Evans Blue Dye. Although some very patchy and light superficial subarachnoid staining is evident. The histological examination of perfusion-fixed brain showed no evidence of cortical, deep nuclear or white matter damage. There was, however, a patchy polymorphic infiltration of the Virchow-Robin spaces.

---

[58]Sigma Ltd., Poole, UK.

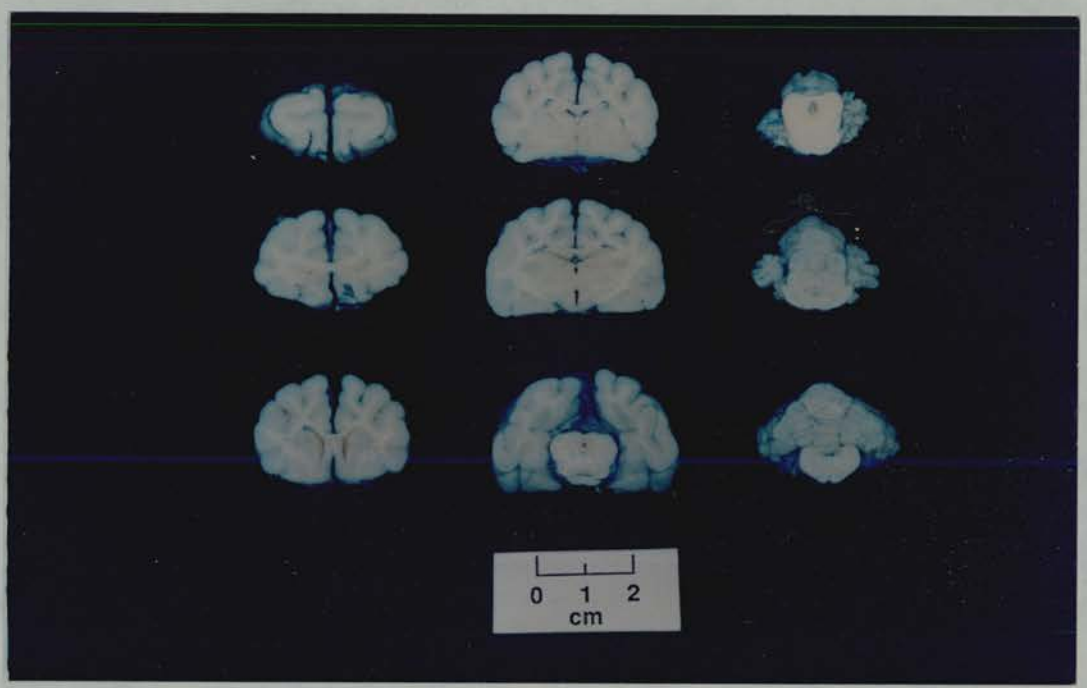

Figure 43: Photograph of Coronal Slices of a Cat Brain injected with Evans Blue Dye after Repetitive SPR Compliance Measurement.

D. Discussion of Results and Methods

The idea of short pulse analysis of craniospinal compliance is not new. Marmarou (40) in his thesis[59] considered that the theoretical pressure response resulting from an impulse volume function[60] was a rapid increase in pressure followed by an exponential return to resting level. The peak pressure recorded was a function of the injected volume, the initial pressure and the system compliance, while the exponential decay was a function of the compliance and outflow resistance. The SPR method described in this chapter has transformed this theory into a practical method where the forcing function is not an idealized impulse volume but a practical short duration pressure pulse. The peak pressure recorded is a function of the input pressure, the injection resistance and the system compliance and the decay is a function of compliance and the outflow resistance, although with the SPR method the outflow resistance is the injection tubing resistance and not the CSF outflow resistance.

The physical model for testing of the SPR method was kept simple, as the intention was not to model the craniospinal system, but only to provide a means of optimizing the methodological parameters (tubing resistance, input pulse amplitude and duration) and determining the sources of error. The compliance range over which the SPR method was tested in the physical model extended from 0.001 to 0.006 ml/mm Hg. This range is approximately five times less compliant than would be found physiologically, larger compliances being found too difficult to reproduce in a physical model. Nonetheless, it is more important to perform physical model testing at reduced compliances where the accuracy and reproducibility of compliance measurement is more critical.

Further evidence towards the validity of the assumption that the CSF outflow resistance (R2) is considerably greater than the injection tubing resistance (R1) was derived from pilot animal work. The CSF outflow resistance was determined by two independent methods both at normal ICP (8 mm Hg) and at elevated ICP (90 mm Hg). Appendix M describes the two methods used for calculation of CSF outflow resistance at both normal and

---

[59]Marmarou's thesis (40) Fig 28, page 60.

[60]An impulse function is a theoretical function approximated by a pulse of infinite amplitude and infinitely small duration.

elevated ICP. The CSF outflow resistance at normal ICP was the lowest with both methods, giving values of 55 and 78 mm Hg/ml/min respectively, the average of the two methods yielding 66 mm Hg/ml/min which is approximately 20 times greater than the injection tubing resistance (R1) of 3.5 mm Hg/ml/min. At elevated ICP the outflow resistance increased to 157 and 104 mm Hg/ml/ min respectively with a mean between methods of 130 mm Hg/ml/min which is approximately 40 times greater than the injection tubing resistance R1.

A further source of error of the SPR method is the assumption that the generator diaphragm compliance does not affect the measured craniospinal system compliance. The condition under which this was shown to be valid was that the total RC time constant of the system was considerably greater than the input pulse duration time (Ti). However, with ICP's greater than 60 mm Hg, the system compliance may become sufficiently small as to negate these conditions. In this case, the generator diaphragm compliance (C2) will need to be considered in the calculation of the system compliance (C1). The animal experiments have shown that even at high ICP the SPR method measures compliance with the same relationship to ICP as the VPR method. Figure 44 is a superimposed plot of the SPR method and VPR method compliance measurements[61] versus ICP.

[61]Values are the average compliance (+- standard error) across all four animals at each stage of ICP.

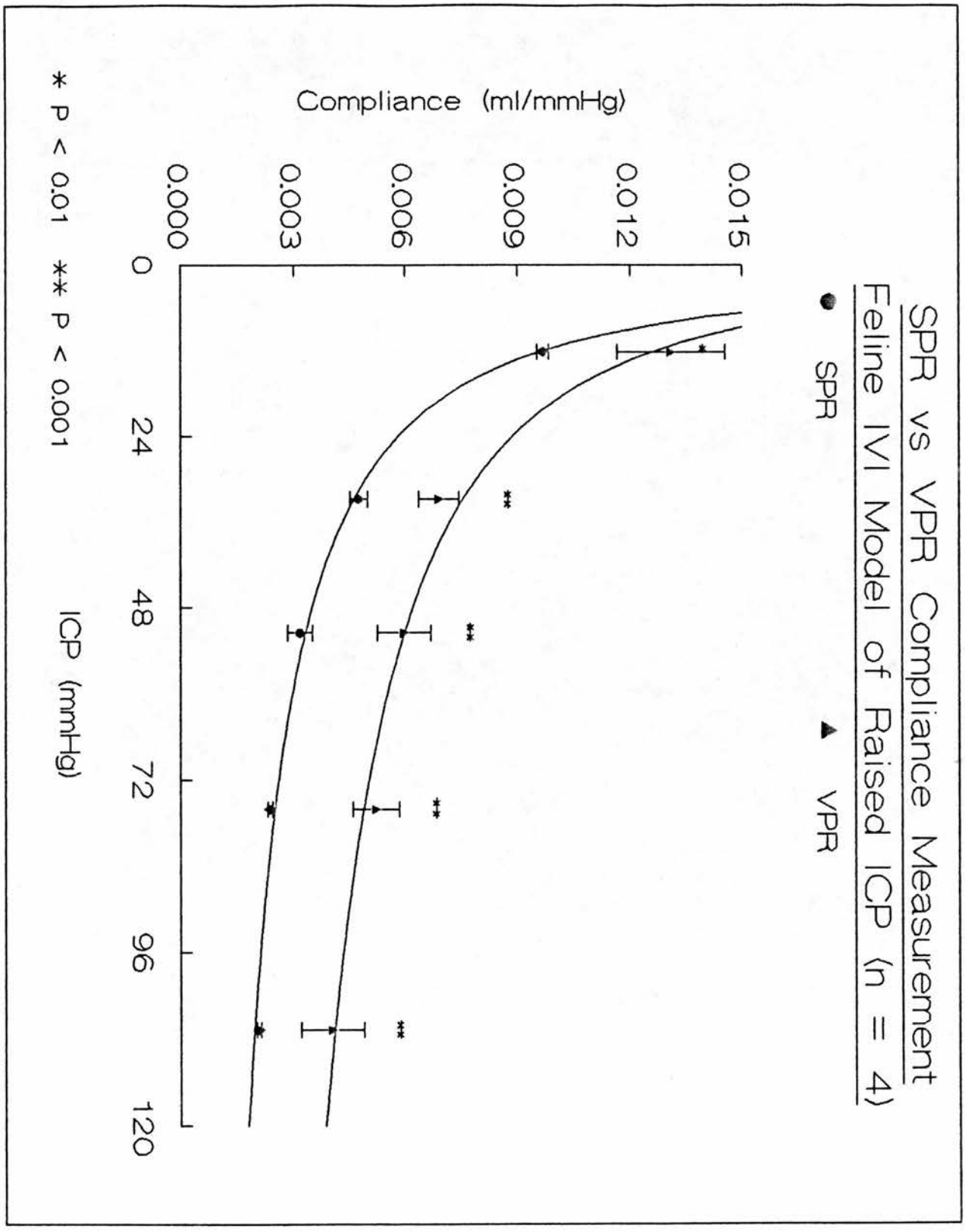

Figure 44: Superimposed Plot of SPR and VPR Methods vs Increasing ICP.

It can be seen that the two methods follow a parallel course with increasing ICP. If, with reduced system compliance, the generator compliance were increasingly affecting the SPR compliance measurement, then one would expect to see a divergence of the two methods as ICP increases. A possible reason why this is not observed may be that as the system compliance (C1) and generator diaphragm compliance (C2) are effectively in series[62], both are subject to the effects of raised ICP. It is likely that both compliances are reduced to the same degree with raised ICP, which causes the relative pressure drop across the two series capacitors to be unchanged[63]. Future modifications of this method should attempt to reduce the generator compliance as a source of error.

The SPR method shows less variability between measurements than the VPR method. In all three experimental groups, the SPR method demonstrated a coefficient of variation between measurements at least five times smaller than that of the VPR method. The SPR method appears to be less invasive than the VPR method. This is seen from Figure 45a which shows that after a set of 5 sequential SPR method compliance runs, ICP returned to baseline. This was not the case, however, with the VPR method where occasionally, particularly with the larger 2 ml volume injection, secondary ICP rises occurred immediately following the VPR injection, in some cases taking 30 minutes or longer to return to baseline ICP levels (Figure 45b). This phenomenon has been reported by other investigators (70,148) under both experimental and clinical conditions.

---

[62]This can be shown by using Thievenon's theorem, see footnote 4.

[63]Taking C2 into account the series capacitance is now (C1*C2)/(C1+C2). If C2 >> C1 then the effective capacitance is C1. If both C1 and C2 decrease by the same amount, the same holds true, C1 is still the effective capacitance.

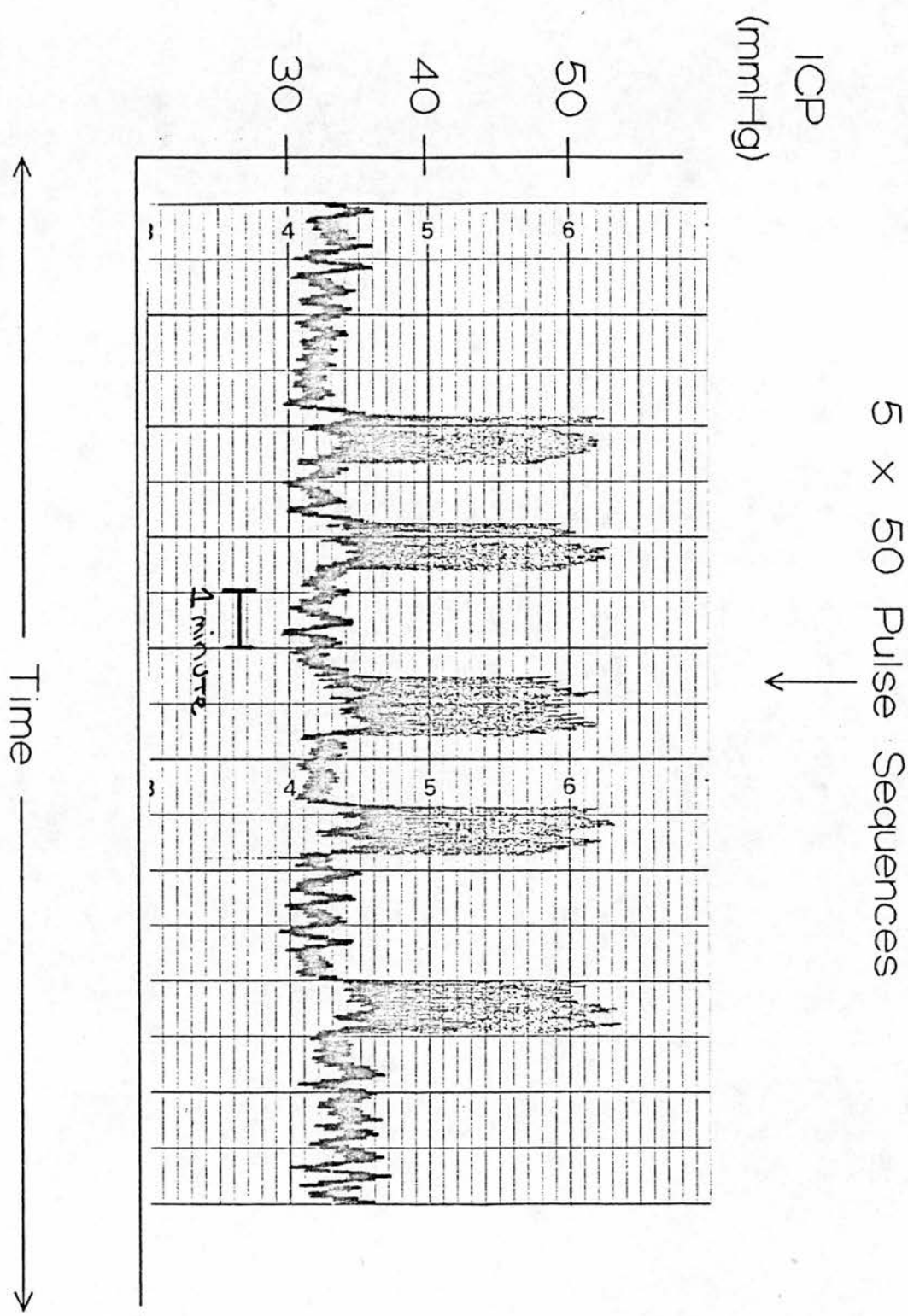

Figure 45a: The Effect of the SPR Compliance Method on ICP.

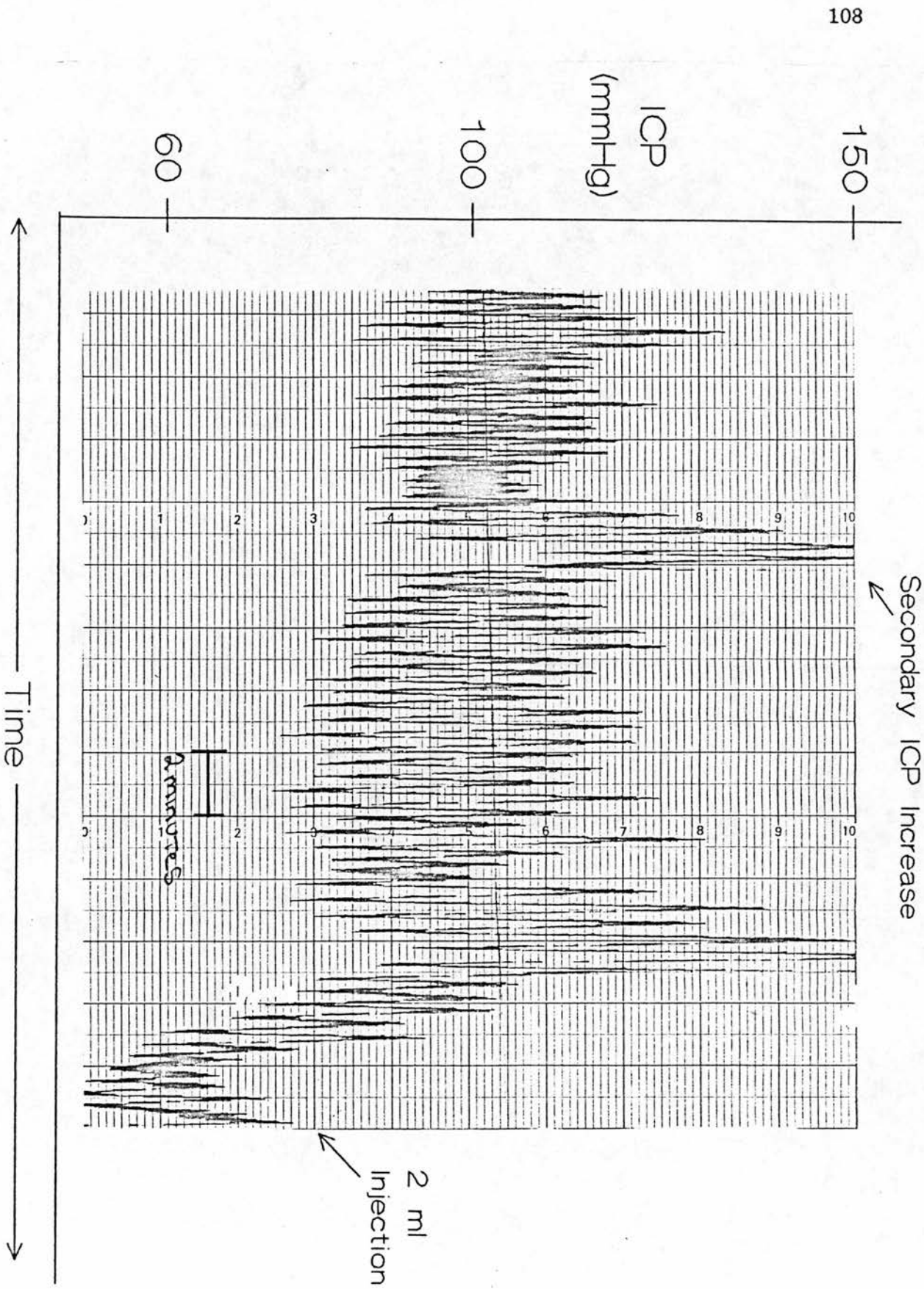

Figure 45b: The Effect of the VPR Compliance Method on ICP.

Although 150 mm Hg pressure pulses are generated by the SPR measurement method, the pressure that develops within the CSF space is dependent on the system compliance. The animal experimental work has shown that the maximum pressure that develops as a result of the SPR method is 40 mm Hg which occurs when the animal's compliance is most compromised (ICP > 100 mm Hg). Under more compliant circumstances, a smaller pressure response will develop. It can be seen from Table 10 that, although repeated pressure pulses are applied by this method directly over the brain stem, there is no significant effect on heart rate, systolic or diastolic blood pressure.

The brain pathology results showed that there was no effect of the SPR method on either blood brain barrier permeability or focal grey and white matter tissue. In particular, the hippocampus, cerebellar purkinje cells and lamina III of the cortical laminae appeared normal. The presence of the patchy subarachnoid polymorphic infiltration may be an epiphenomenon of the invasive experimental method as this type of subarachnoid infiltration has also been reported by another investigator (146) using a similar cat protocol, but not using the SPR method. The polymorphic infiltration may also explain the slight extravasation of Evans Blue Dye into the subarachnoid space. Further experimental work is needed to study the longer term effects of this pulse technique on the brain.

Table 10: The effect of the SPR method on Heart Rate and BP. Individual and averaged data from a set of 5 sequential SPR method compliance runs. The compliance from each run is calculated from the average of 50 150 mm Hg pressure pulses applied at a repetition rate of 1 Hz. There is no statistically significant effect of the SPR compliance method (paired t-test) on either BP or Heart rate.

Run	BP Sys/Dias Before SPR	BP Sys/Dias After SPR	Heart Rate Before SPR	Heart Rate After SPR
1	118/90	118/89	230	230
2	119/90	117/88	220	220
3	138/91	122/87	260	260
4	125/79	122/77	260	250
5	142/82	124/76	250	260
mean +−SD	128+−9 86+−5	121+−3 83+−6	244 +−16	244 +−16

With the SPR method, similar to other investigators (147,149), the craniospinal system is modelled as a simple first order system, where a lumped compliance is the only reactive component[64]. Other investigators have modelled the craniospinal and cerebrovascular systems more fully as second or higher order systems containing a series of distributed compliances (150,151,152,153). The inertial properties[65] of the craniospinal system have also been considered (62,87,88). If there is inertance present in the craniospinal system, there was no evidence of it exerting an effect during compliance measurement with the SPR method. This can be seen from Figure 39 which shows the pressure response plots at both normal and elevated ICP. There is no oscillation seen on the decay portion of either response, although oscillation would be expected if significant inertance was present (79). There may be inertance to the craniospinal system, but its effects may be insignificant when such a small and rapid volume perturbation to the system (approx. 0.05 ml over 100 msec) is involved.

In the physical model tests, it was found there was an average of 5% overestimation in compliance for each 0.1 ml of added air to the injection tubing. This degree of error is with reference to air added to the injection tubing and does not consider the effects of tubing compliance and leaky connectors on the absolute system compliance. Furthermore, the high compressibility of air makes it impossible to remove all trapped air unless boiled distilled water and tedious filling techniques are applied (93). In order to make the SPR method practical, particularly if future development of the method is aimed towards producing a system that can be used clinically, all tests were carried out with room temperature normal saline as the injection fluid. The VPR compliance method in both experimental and clinical studies use room temperature normal saline as

---

[64]A reactive component is one that responds or reacts to change. The current that charges a capacitor is dependent on the rate of change in voltage (dV/dt). Similarly, inductors are also reactive elements. The voltage developed across an inductor is dependent on the rate of change of current (dI/dt).

[65]In electrical terms the inertance is equivalent to inductance. An inductor (L) will inhibit changes in current (I) by developing a potential difference opposite in polarity, and thus opposing the source causing the change in current. The amplitude of the induced potential difference (VL) is dependent on the rate of change of the current (dI) produced by the source. VL = L x dI/dt.

the injection fluid. As a consequence, the error in measuring compliance caused by using normal saline as the injection fluid will not affect the comparison of the SPR with the VPR technique.

The large overestimation of compliance by the VPR method compared to the SPR method should be considered. Some of the overestimation may be because the VPR method is more susceptible to contamination with air, which would tend to increase the measurement of compliance. It is more likely, however, that the difference between the two techniques is a result of the dynamic properties of the two methods. The VPR method involves injection of much larger volumes than the SPR method which would cause a greater perturbation to the system, and furthermore the volume injection is given over the much longer time interval of 1 second, ten times longer than the SPR method. Anile et al (62) have reported that compliance measurement is time dependent. They have shown that if the VPR injection volume of 0.3 ml is given slowly over one second (similar to these studies where 0.05 - 0.2 ml was given over one second) then the measured compliance is dependent on whether the CSF system was open or closed to atmospheric pressure. If the CSF system is closed, the measured compliance is similar to that of a rapid injection sequence (0.05 ml injected as quickly as possible). If, however, the CSF system is open to atmosphere, the slow VPR injection causes fluid to be displaced more readily from the craniospinal compartment resulting in gross overestimates of compliance compared to the rapid injection sequence. The level of overestimation was dependent on ICP but ranged from 20% to several hundred percent with the higher levels of ICP. The explanation proposed for this phenomenon is based on Anile's division of compliance into physical and physiological compliance. Physical compliance they define as being the true compliance of the system related to the expansion of the spinal dura matter and any small compression of the brain or expansion of the skull that may occur. It is recognized that blood can be ejected from the cerebrovascular bed as fluid is injected into the CSF space (40,41,126). Physiological compliance, therefore, is probably dependent on cerebrovascular properties, in particular venous outflow resistance. With a large volume injection given over a longer period, there is time for the inertance of the cerebral blood volume to be overcome. As a result some blood is ejected from the craniospinal compartment so that the total intracranial blood volume is reduced and

compliance is therefore greater. Rapid injection would tend to inhibit fluid flow because of the inertance of the fluid. The faster the rate of injection, the greater the inhibition of fluid flow. Based on the preceding discussion, it is feasible that the SPR method is measuring principally the "physical compliance" of the craniospinal system, which would be expected to be less than the lumped physical and physiological compliance as measured by the VPR method.

E. Conclusions

The aim of the work described in this chapter was to improve the reproducibility of compliance measurement in order to facilitate an experimental study in animals of the relationship between craniospinal compliance, cerebrovascular pressure transmission and cerebrovascular resistance. The SPR method appears to be a more accurate, less variable and less invasive method of measuring craniospinal compliance compared to the VPR method. The major sources of compliance measurement error with the SPR method have been quantified and are not negligible. Nonetheless, the errors are likely to be small compared to the overall biological variation that will be inherent to the proposed experimental studies.

CHAPTER IV. EXPERIMENTAL STUDIES

After showing that waveform analysis of human cerebrovascular pressure transmission is feasible and following the development of an improved method for measuring lumped craniospinal compliance, the purpose of this experimental study was to measure both parameters under conditions expected to change either or both craniospinal compliance and cerebrovascular pressure transmission. Raised ICP will reduce craniospinal compliance. An increase in arterial PCO2 can cause cerebral vasodilation and thereby alter cerebrovascular pressure transmission. An increase in arterial pressure can produce changes in both compliance and pressure transmission dependent on the state of cerebral autoregulation and whether or not ICP is elevated.

The SPR method of measuring lumped craniospinal compliance with its improved reproducibility between measurements, was applied to an investigation of the relationship between cerebrovascular pressure transmission, craniospinal compliance and cerebrovascular resistance in experimental models of raised ICP, arterial hypercarbia and arterial hypertension. The results from the three arms of this study are presented first, each with a short commentary, followed by a final discussion.

A. General Methods

Twelve cats of both sexes, each weighing between 2.0 and 5.2 kg, were split into three groups: an ICP group (n = 4), a CO2 group (n = 4) and a BP group (n = 4). Animals were prepared surgically as previously described (page 87). In addition to the measurement of craniospinal compliance as described in the last chapter (page 69), cerebrovascular pressure transmission between BP and ICP was measured (page 18) using a catheter-tip pressure transducer placed in the descending segment of the thoracic aorta for recording of the BP waveform while the ICP waveform was recorded through placement of an optimally damped fluid-filled catheter-transducer system placed in the left lateral ventricle through a 19 gauge 2 inch needle catheter. Cerebrovascular resistance

was calculated[66] as the quotient of cerebral perfusion pressure to cerebral blood flow (CBF) where CBF was the average from four measurement sites.

1. CBF Measurement

CBF was determined through the use of the hydrogen clearance technique (155,156,157). Appendix N describes the hydrogen clearance method for measurement of CBF, the H2 electrode design and electrode etching process. Cranial burr holes were drilled while being irrigated continuously with cool saline. Four platinum electrodes[67] were placed in two pairs straddling the sagittal suture, 20 mm posterior to Bregma and 5 mm lateral to the midline. Electrodes were positioned with the aid of an operating microscope, and inserted, using a microdrive, directly through unopened dura to a depth of 1.5 mm into the cerebral cortex, and were sealed in place with cold curing dental acrylic[68]. Electrodes were polarized to +400 mV relative to a Ag/AgCl reference electrode[69] which was wrapped in a saline soaked gauze and placed in a subcutaneous pouch. Electrodes were allowed to stabilize for 30 minutes post insertion. The first blood flow measurement from each experimental animal was discarded. During a blood flow measurement, hydrogen gas was administered in a 10% concentration through one of two parallel inspired gas circuits proximal to the ventilator input. Hydrogen was given for 10 minutes after which the animals inspired gases were switched to the parallel circuit not containing hydrogen. The hydrogen electrode current during the desaturation phase was sampled online at 1 Hz for the entire desaturation

---

[66]From Ohm's law, resistance (R) is the quotient of potential difference (V) and current (I). R = V/I. In equivalent terms, cerebrovascular resistance (CVR) is equal to the quotient of the pressure drop across the cerebral vascular bed, that is, cerebral perfusion pressure (CPP) (CPP = BP - ICP) divided by cerebral flood flow (CBF). CVR = CPP/CBF. This assumes that ICP is an accurate measure of cerebral venous pressure due to the vascular waterfall effect (159,160).

[67]Platinum wire (0.2 mm diameter) Engelhard Sales Ltd., Chessington, UK. The platinum wire is electrolytically etched to a tip diameter between 10 - 20 microns which tapers back over 1.5 mm to a base diameter of 100 microns. Total exposed length of platinum is 1.5 mm, the remaining wire is sealed with an epoxy-resin cement.

[68]Simplex Rapid (pink). Nobel Pharma Ltd., Harrow, UK.

[69]Clark Electromedical Instruments, Pangbourne, UK.

period by a microcomputer based blood flow measurement system (158).

After the re-establishment of a stable baseline, approximately 15 minutes after hydrogen gas inhalation had ceased, a baseline correction algorithm was used to correct for any drift in the hydrogen electrode during desaturation when compared to the pre-hydrogen baseline[70]. The natural log plot (Ln) was then calculated from the logarithm of the difference between each sampled point and its corresponding baseline value. The first 20 seconds of desaturation was discarded as potentially contaminated with arterial recirculation artefact (157). The initial slope index of CBF (ISI) was then calculated from the slope of the subsequent one minute period (155). Clearance curves in these studies were predominantly biexponential. The ISI values reported are the average of the ISI flows from the four hydrogen electrodes. Appendix O is a flow chart describing the H2 clearance analysis program.

2. Statistical Analysis

All comparisons between two groups of data were tested with a students paired t-test. All averaged data is expressed as means +- SEM.

B. Induced Intracranial Hypertension

This set of experiments was designed chiefly to determine whether ICP, raised through intraventricular infusion of mock CSF, as a model of a diffuse intracranial hypertension, would affect predominantly low or high frequency pressure transmission across the cerebrovascular bed. In addition, the relationship and time course between the changes in pressure transmission, craniospinal compliance and cerebrovascular resistance would be observed.

1. Protocol

The ICP of four animals was raised in four stages from 10 to 70 mm Hg by infusion of saline or Hartman's solution (3 - 60 ml/hour) into the right lateral ventricle. ICP was raised through slow intraventricular infusion of saline to a starting baseline level of between 10 and 15 mm Hg.

---

[70]Baseline drift is assumed to be linear. A sloping baseline is forced from the pre-hydrogen baseline to the final minute of the sampled desaturation curve using a linear regression algorithm.

At each level of ICP, four sequential 20 second samples of ICP and BP waveform data were stored to FM magnetic tape for subsequent offline calculation of cerebrovascular pressure transmission. This was immediately followed by four sequential measurements of craniospinal compliance using the SPR method. Compliance for a given level of ICP was the average of the four sequential measurements, where each measurement was the signal average of 50 stimulus presentations. Five minutes after compliance measurement, CBF was determined using the hydrogen clearance technique, with 10 minutes of hydrogen saturation. Just prior to desaturation, arterial blood gas samples were taken. During the initial slope phase of desaturation, BP and ICP were recorded for calculation of the CPP.

2. Results

Figure 46 is a combined plot of cerebrovascular pressure transmission (amplitude transfer function and fundamental phase shift), craniospinal compliance and cerebrovascular resistance versus increasing ICP. Table 11 contains physiological data (ICP, BP, CPP, Tc, PaCO2, PaO2, pH) recorded at each stage in the protocol. To prevent obscuring the relationship between amplitude transfer function curves, the associated standard error bars were not plotted. Table 12 contains the amplitude transfer function data with standard errors for each harmonic, broken down by ICP level.

ICP increased from 10 to 65 mm Hg ($P < 0.001$) which was associated with a fall in CPP from 139 to 88 mm Hg. These changes were followed by and exponential decrease in craniospinal compliance from 0.0097 to 0.0024 ml/mm Hg ($P < 0.01$). The amplitude transfer function increased at all frequencies with increasing ICP. The first harmonic was used as a measure of low frequency pressure transmission and the 4th harmonic as a measure of high frequency pressure transmission. Both low and high frequencies increased significantly compared to baseline ($P < 0.05$) with increasing ICP. There was no significant change in the fundamental phase shift with increasing ICP. Cerebrovascular resistance did not change significantly with increasing ICP as seen by the decrease in the initial slope flow from 35.2 to 21 ml/100g/min, which was followed by a parallel decrease in CPP. The lack of cerebrovascular response with

increasing ICP would indicate that in this group of animals, CBF autoregulation to reduced CPP had been impaired.

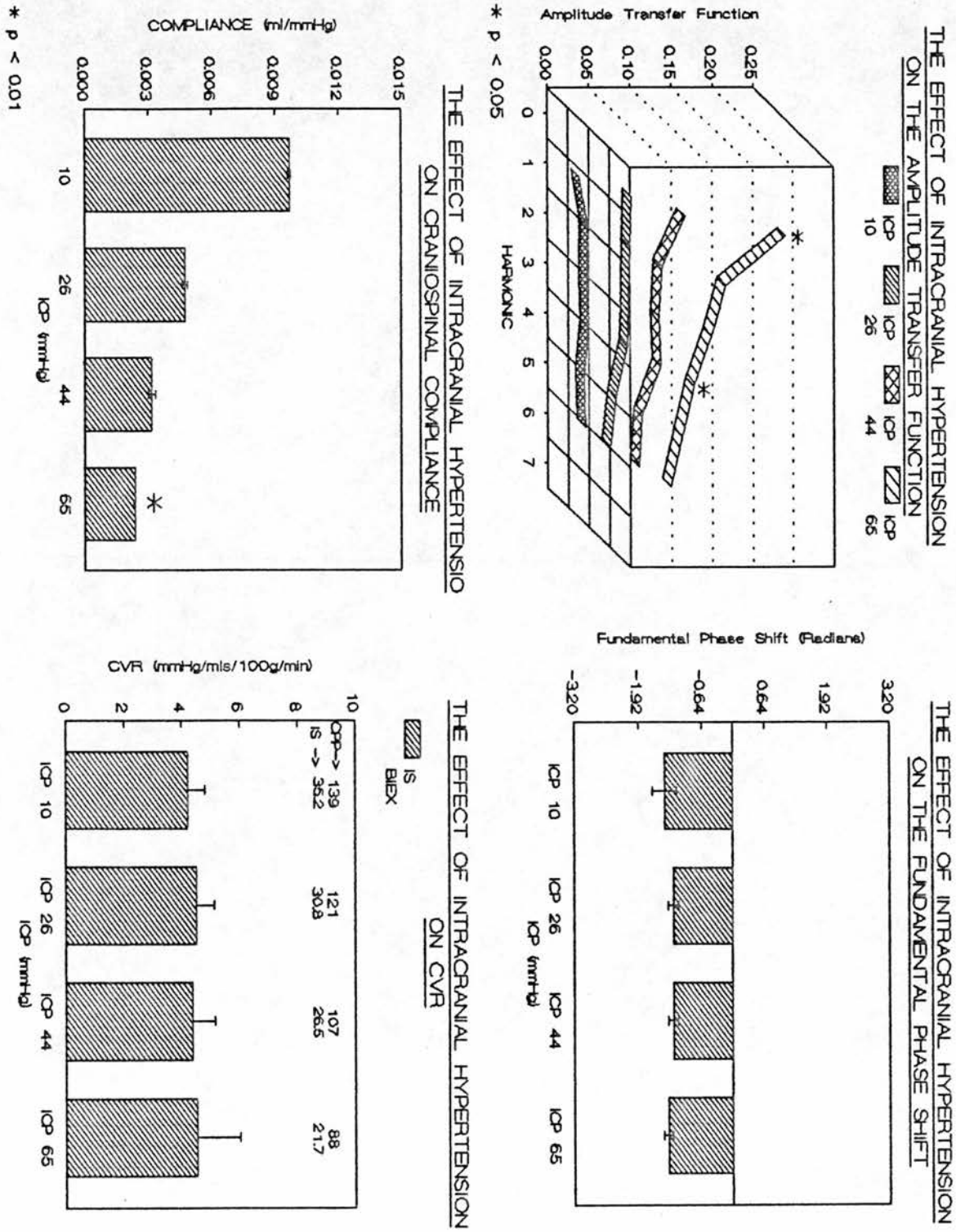

Figure 46: Cerebrovascular Resistance, Pressure Transmission and Craniospinal Compliance vs ICP.

Table 11: ICP Experimental Group Physiological Data.

ICP (mmHg)	BP (mmHg)	CPP (mmHg)	Tc (Deg. C)	PaCO2 (mmHg)	PaO2 (mmHg)	pH
10 +−2.2	149 +− 14	139 +−12	37.3 +−0.1	40.2 +−3.2	433 +−36	7.27 +−0.02
26 +−5.3	147 +−8	121 +−3	37.4 +−0.1	38.3 +− 1.9	421 +−43	7.30 +−0.01
44 +−5.3	151 +− 10	107 +−7	37.4 +−0.1	37.8 +− 1.4	470 +−26	7.27 +−0.03
65 * +−5.7	153 +− 13	88 +−13	37.4 +−0.1	37.5 +−2.4	418 +−38	7.27 +−0.03

* denotes P < 0.001

Table 12: ICP Experimental Group Amplitude Transfer Function Data.

ICP (mmHg)	A1	A2	A3	A4	A5	A6
10 +−2.2	0.0212 +−0.009	0.0311 +−0.009	0.0307 +−0.007	0.0323 +−0.007	0.0262 +−0.008	0.0278 +−0.004
26 +−5.3	0.0586 +−0.012	0.0569 +−0.014	0.0559 +−0.011	0.0544 +−0.012	0.0403 +−0.009	0.0328 +−0.007
44 +−5.3	0.0988 +−0.025	0.0708 +−0.020	0.0666 +−0.018	0.0695 +−0.015	0.0464 +−0.007	0.0431 +−0.0071
65 +−5.7	* 0.1978 +−0.059	0.1235 +−0.041	0.1066 +−0.035	* 0.0851 +−0.023	0.0702 +−0.014	0.0563 +−0.013

* denotes P < 0.05

3. Commentary

These results demonstrate that an increase in both low and high frequency pressure transmissions across the cerebrovascular bed occurs with diffusely raised ICP. This increase in pressure transmission is associated in a stepwise fashion with reduced craniospinal compliance, and occurs in the absence of any detected change in lumped cerebrovascular resistance. Over the range of CPP tested in this group of non-autoregulating animals (88 - 140 mm Hg), cerebrovascular pressure transmission is dependent only on mechanisms governing craniospinal compliance.

C. Induced Arterial Hypercarbia

Since the previous group of animals demonstrated no change in cerebrovascular resistance to raised ICP, none of the observed changes in cerebrovascular pressure transmission could be attributed to cerebrovascular resistance. To investigate this further, the following set of experiments was designed to force alterations in cerebrovascular resistance and craniospinal compliance independently. Cerebrovascular resistance was altered through the administration of CO2 in the inspired gases and craniospinal compliance was altered through the application of abdominal compression.

1. Protocol

The arterial CO2 tension of four animals was raised in two stages with administration of 5% and 10% CO2 in the inspired gas mixture. At each level of CO2, four sequential 30 second samples of ICP and BP waveform data were stored to FM magnetic tape for subsequent offline calculation of cerebrovascular pressure transmission, which was immediately followed by four sequential measurements of craniospinal compliance using the SPR method. During the normocapnic stage of the protocol, five minutes after the last SPR measurement, a fixed weight was placed upon the animal's back, which compressed the abdomen against a rigid spherical object, approximately the size of a closed fist, which had been inserted between the animal's abdomen and the base of the stereotactic frame. While abdominal compression was applied, a further set of four sequential waveform and compliance measurements was obtained. Abdominal compression was then stopped, five minutes after which a set of waveform

and compliance measurements was obtained. As before, compliance for a given stage of the protocol was the average of the four sequential measurements, where each measurement was the signal average of 50 stimulus presentations. Five minutes after the post abdominal compression waveform and compliance measurements were obtained, CBF was determined through the use of the hydrogen clearance technique, with 10 minutes of hydrogen saturation. Just prior to desaturation, arterial blood gas samples were taken. During the initial slope phase of desaturation, BP and ICP were recorded for calculation of the CPP.

2. Results

Cerebrovascular pressure transmission and CBF changes with altered CO2 were sufficiently different between animals to cause grouped analysis to obscure the relationship between the two variables. As a result, the relationship between cerebrovascular pressure transmission, craniospinal compliance and cerebrovascular resistance will be reported individually for the four animals.

Table 13 contains the physiological data (ICP, BP, CPP, Tc, PaCO2, PaO2, pH) recorded at each stage in the protocol averaged across all animals in this group. To prevent obscuring the relationship between amplitude transfer function curves, the associated standard error bars were not plotted. Tables 14a & 14b contains the amplitude transfer function data with standard errors for each harmonic, broken down into three levels of hypercarbia (normocapnia, 5%, 10%) and the three measurements taken before, during and after abdominal compression.

Table 13: CO2 Experimental Group Physiological Data.

	ICP (mmHg)	BP (mmHg)	CPP (mmHg)	Tc (Deg. C)	PaCO2 (mmHg)	PaO2 (mmHg)	pH
Normo-capnia	15 +-1.0	160 +-15	145 +-14	38.4 +-0.27	36.1 +-0.9	388 +-36	7.31 +-0.002
5% CO2	21 +-5.0	143 +-11	122 +-12	38.2 +-0.36	63.9* +-1.7	288 +-40	7.133* +-0.009
10% CO2	26 +-5.0	140 +-7	114 +-10	38.0 +-0.24	97.1* +-2.2	273 +-35	7.006* +-0.010
Compression On	19 +-0.5	154 +-10	135 +-9	.	.	.	.
Compression Off	13 +-2.0	129 +-22	128 +-13	.	.	.	.

* denotes P < 0.01

Table 14a: CO2 Experimental Group Amplitude Transfer Function Data, Hypercarbia.

	A1	A2	A3	A4	A5	A6
Control P014	.0372+-.0008	.0438+-.0008	.0384+-.0017	.0291+-.0028	.0223+-.0026	.0385+-.0104
Control P015	.0403+-.0001	.0290+-.0002	.0350+-.0012	.0178+-.0007	.0115+-.0019	.0237+-.0012
Control P016	.0227+-.0001	.0242+-.0002	.0242+-.0019	.0218+-.0010	.0167+-.0016	.0577+-.0079
Control P017	.0330+-.0003	.0292+-.0002	.0353+-.0010	.0313+-.0014	.0289+-.0014	.0223+-.0004
5% CO2 P014	.1273+-.0187 %	.1026+-.0014	.0962+-.0007	.0878+-.0055 *	.0513+-.0080	.0423+-.0075
5% CO2 P015	.0851+-.0008 *	.0605+-.0007	.0432+-.0008	.0452+-.0050 △	.0350+-.0102	.0337+-.0085
5% CO2 P016	.0300+-.0003 *	.0293+-.0006	.0391+-.0023	.0211+-.0010	.0181+-.0010	.0349+-.0048
5% CO2 P017	.1004+-.0007 *	.0572+-.0008	.0634+-.0014	.0771+-.003 *	.0389+-.0008	.0285+-.0012
10% CO2 P014	.1032+-.0027	.0733+-.0016	.0653+-.0019	.0412+-.0033 *	.0313+-.0013	.0288+-.0014
10% CO2 P015	.0717+-.0116	.0478+-.0075	.0353+-.0062	.0190+-.0024 *	.0123+-.0012	.0223+-.0134
10% CO2 P016	.0613+-.0127 *	.0605+-.0071	.0530+-.0101	.0374+-.0012 %	.0446+-.0079	.0166+-.0037
10% CO2 P017	.1425+-.0020 *	.0698+-.0009	.0547+-.0011	.0795+-.0027	.0451+-.0015	.0404+-.0032

* denotes P < 0.001 % denotes P < 0.01 △ denotes P < 0.05

Table 14b: CO2 Experimental Group Amplitude Transfer Function Data, Abdominal Compression.

	A1	A2	A3	A4	A5	A6
Control P014	.0372+-.0008	.0438+-.0008	.0384+-.0017	.0291+-.0028	.0223+-.0026	.0385+-.0104
Control P015	.0403+-.0001	.0290+-.0002	.0350+-.0012	.0178+-.0007	.0115+-.0019	.0237+-.0012
Control P016	.0227+-.0001	.0242+-.0002	.0242+-.0019	.0218+-.0010	.0167+-.0016	.0577+-.0079
Control P017	.0330+-.0003	.0292+-.0002	.0353+-.0010	.0313+-.0014	.0289+-.0014	.0223+-.0004
Press On P014	.0445+-.0011 *	.0501+-.0026	.0482+-.0042	.0328+-.0012	.0217+-.0021	.0346+-.0083
Press On P015	.0424+-.0002 %	.0370+-.0078	.0467+-.0025	.0222+-.0019	.0160+-.0014	.0245+-.0034
Press On P016	.0281+-.0005 *	.0275+-.0003	.0286+-.0023	.0239+-.0006 *	.0196+-.0009	.0506+-.0070
Press On P017	.0656+-.0064 %	.0603+-.0052	.0607+-.0060	.0502+-.0059	.0305+-.0052	.0232+-.0030
Press Off P014	.0356+-.0008 %	.0379+-.0009	.0432+-.0013	.0312+-.0017	.0273+-.0008	.0493+-.0117
Press Off P015	.0450+-.0006	.0356+-.0039	.0428+-.0069	.0194+-.0007	.0169+-.0016	.0582+-.0111
Press Off P016	.	.	.	.	.	.
Press Off P017	.0390+-.0003	.0277+-.0009	.0342+-.0005	.0406+-.0017	.0389+-.0024	.0275+-.0065

* denotes P < 0.01 % denotes P < 0.05

a. Animal P014

Figure 47 is a combined plot for this animal showing cerebrovascular pressure transmission (amplitude transfer function and fundamental phase shift), cerebrovascular resistance and craniospinal compliance at normocapnia and with 5% and 10% inspired CO2. With 5% CO2, cerebrovascular resistance decreased significantly ($P < 0.05$) and was associated with a large increase in both low and high frequency (first and fourth harmonic) components of the amplitude transfer function ($P < 0.01$, $P < 0.001$). There were no significant changes in craniospinal compliance or the fundamental phase shift with 5% CO2. With 10% CO2 there was no significant change in cerebrovascular resistance from the 5% level, nor was there a change in low frequency pressure transmission. However, high frequency pressure transmission decreased significantly ($P < 0.001$) with 10% CO2 which was also associated with a significant increase in craniospinal compliance ($P < 0.001$).

Abdominal compression (Figure 48) caused a small increase in low frequency pressure transmission ($P < 0.01$) and was associated with the fundamental phase shift becoming less negative ($P < 0.01$).

b. Animal P015

This animal (Figure 49) showed similar responses with CO2 and abdominal compression to the previous animal P014 (Figure 48). With 5% CO2 there was a large increase in low frequency pressure transmission ($P < 0.001$) but with no major change in either compliance or phase. The principal change occurred when 10% CO2 caused reduced high frequency pressure transmission ($P < 0.001$) associated with increased compliance ($P < 0.001$). Similar to the previous animal, there was no change in the low frequency pressure transmission with 10% CO2 despite a marked reduction in CVR ($P < 0.01$) consistent with vasodilation.

Like the previous animal, abdominal compression (Figure 50) caused a small increase ($P < 0.05$) in the low frequency pressure transmission, followed this time by the fundamental phase shift becoming more negative ($P < 0.01$).

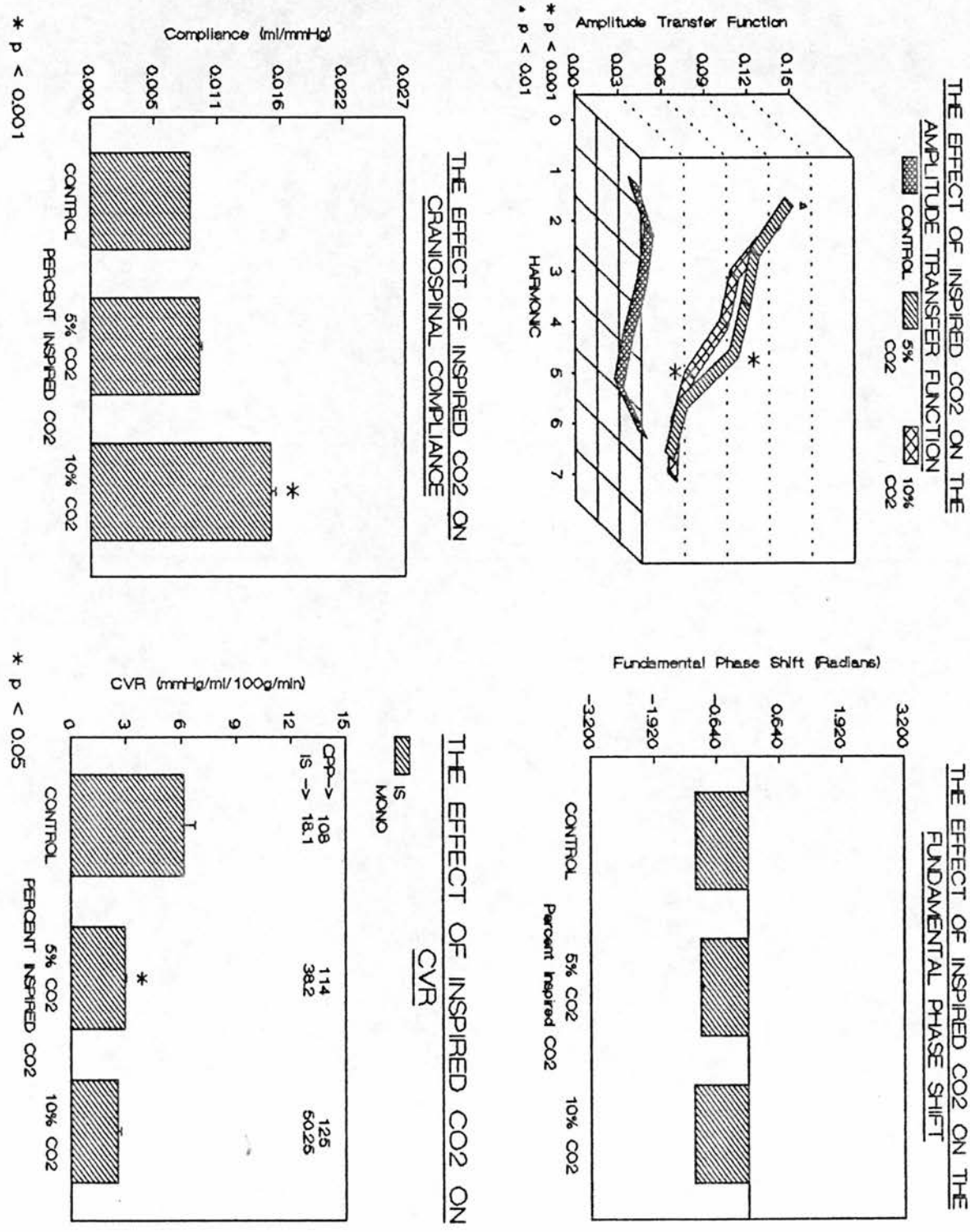

Figure 47: Cerebrovascular Resistance, Pressure Transmission and Craniospinal Compliance vs Inspired CO2, Animal P014.

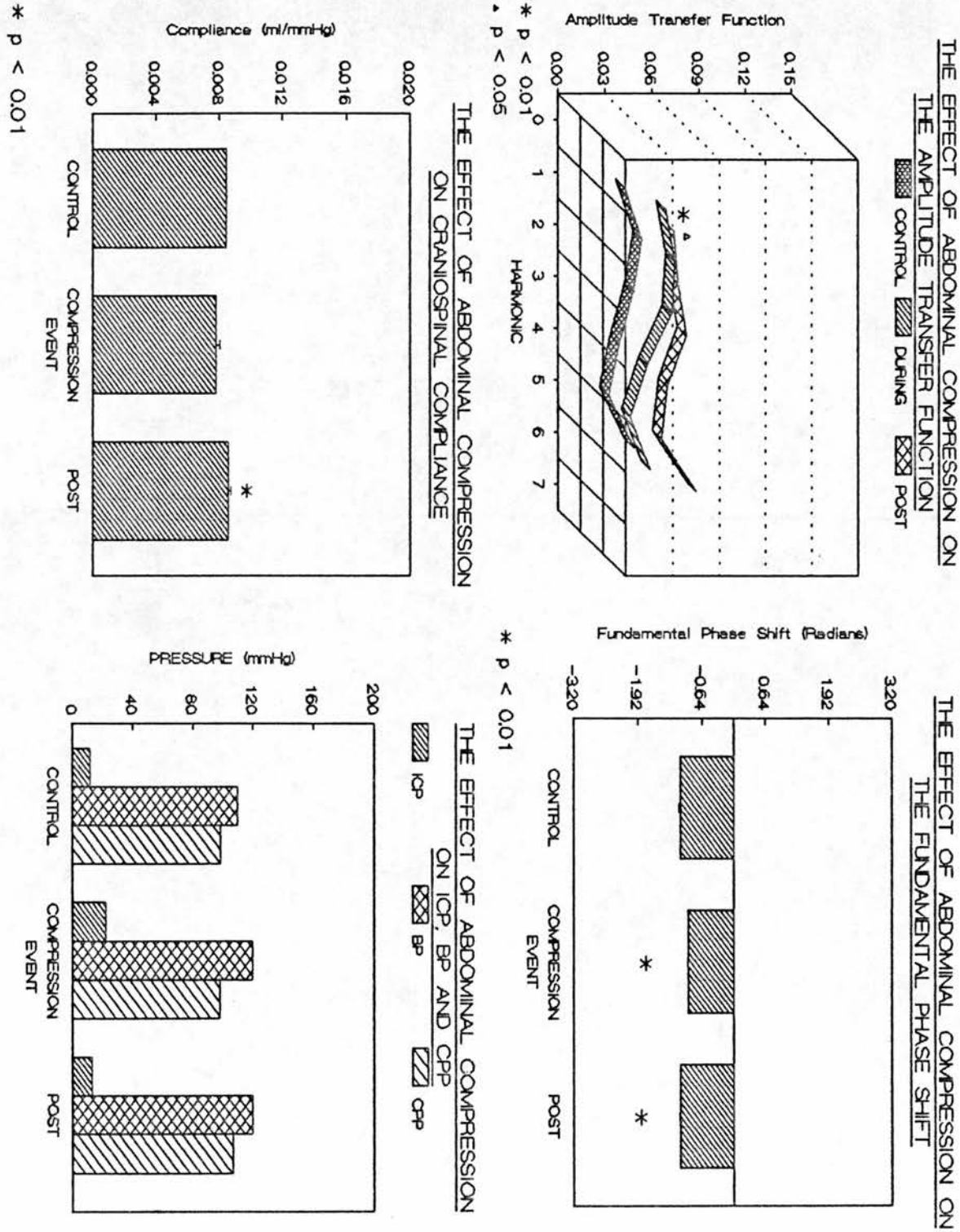

Figure 48: Cerebrovascular Resistance, Pressure Transmission and Craniospinal Compliance vs Abdominal Compression, Animal P014.

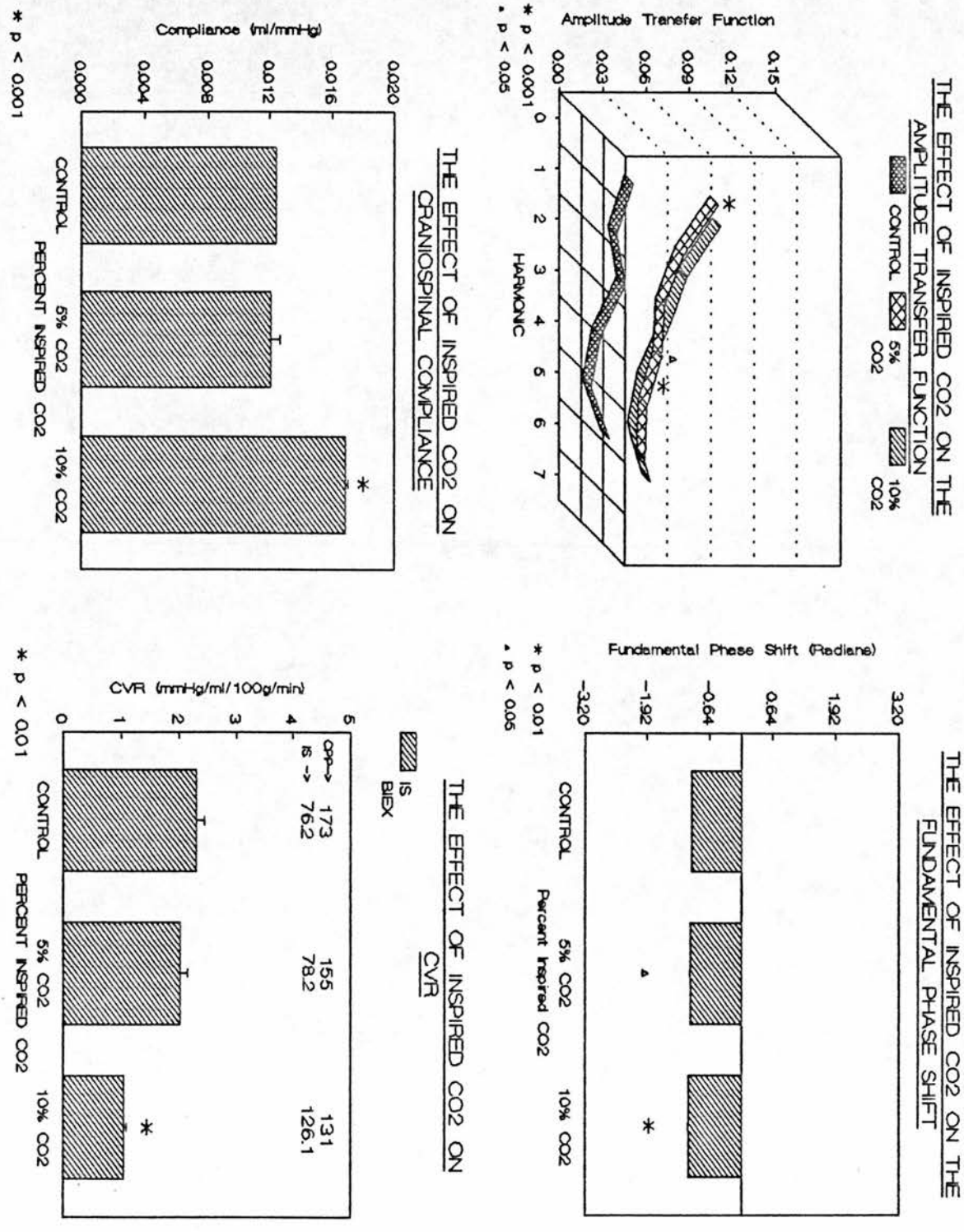

Figure 49: Cerebrovascular Resistance, Pressure Transmission and Craniospinal Compliance vs Inspired CO2, Animal P015.

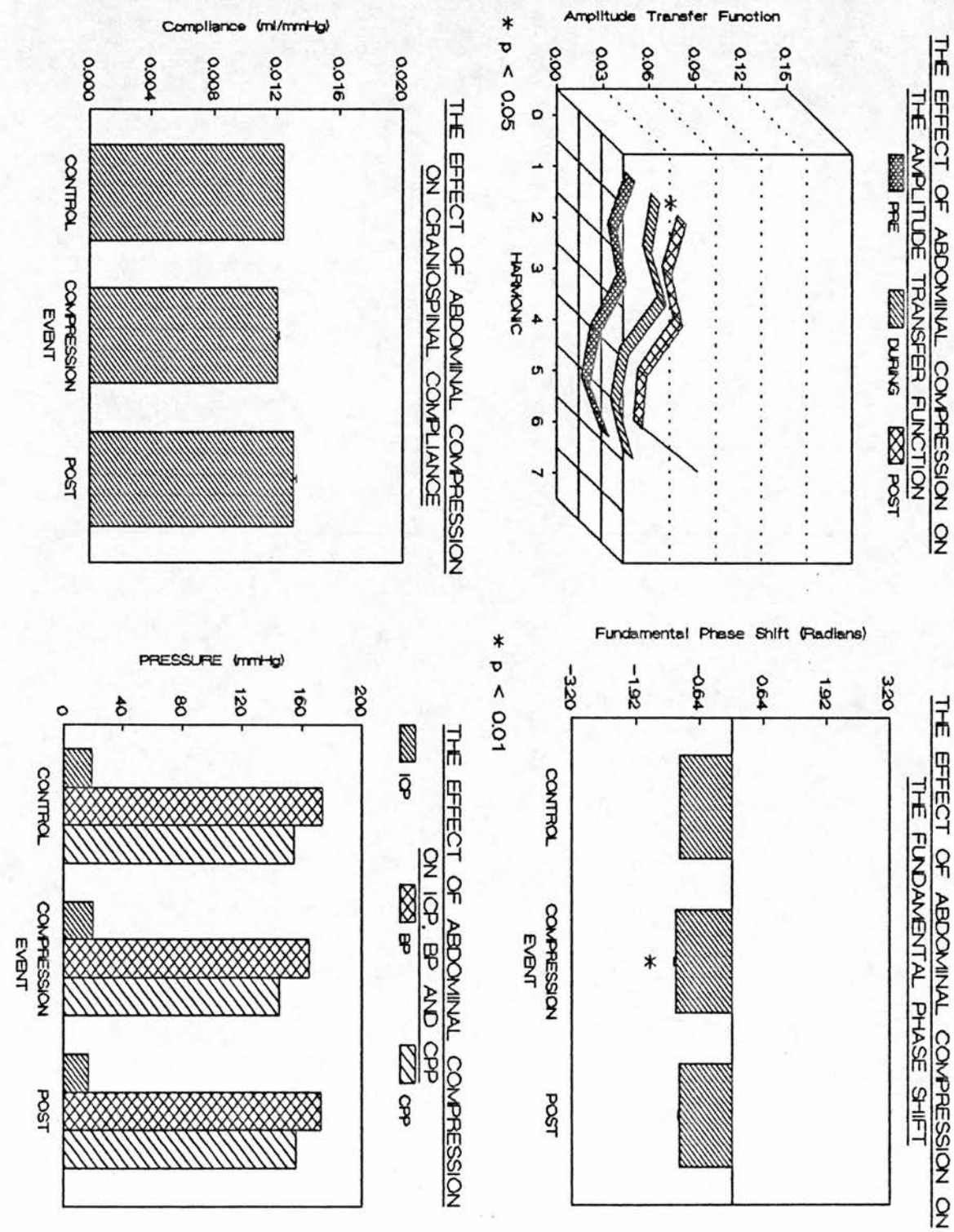

Figure 50: Cerebrovascular Resistance, Pressure Transmission and Craniospinal Compliance vs Abdominal Compression, Animal P015.

c. Animal P016

With 5% CO2, this animal (Figure 51) similar to the previous two animals, showed a significant decrease in cerebrovascular resistance ($P < 0.01$) which was associated with an increase in low frequency pressure transmission ($P < 0.001$). The high frequency pressure transmission showed no significant change. Compliance showed only a small decrease ($P < 0.05$), and the fundamental phase shift became more negative ($P < 0.001$) with 5% CO2. However, with 10% CO2 there was no significant change in cerebrovascular resistance, although the increase in IS flow from 52 to 58 ml/100g/min despite very little change in CPP would suggest that some vasodilation may have been occurring. Consistent with vasodilation there was a further increase in low frequency pressure transmission above that of the 5% level ($P < 0.001$). Also with 10% CO2, there was now a large increase ($P < 0.01$) in the high frequency pressure transmission, associated this time with a large decrease ($P < 0.001$) in compliance.

Abdominal compression (Figure 52) showed significant increases in both low and high frequency pressure transmission ($P < 0.01$), which was associated with the fundamental phase shift becoming less negative.

d. Animal P017

The final animal in this group showed responses with CO2 and abdominal compression similar to those of the previous animal P016. With 5% CO2 (Figure 53) there was a significant decrease in cerebrovascular resistance ($P < 0.05$) which was associated with a large increase in low frequency pressure transmission ($P < 0.001$). Like the previous animal, the high frequency pressure transmission also showed a large increase ($P < 0.001$). Following this increase in the high frequency pressure transmission there was a large decrease in compliance ($P < 0.001$), with the fundamental phase shift becoming more negative ($P < 0.001$) with 5% CO2. However, with 10% CO2 there was no significant change in cerebrovascular resistance, although similar to the previous animal the maintenance of flow from 44 to 42 ml/100g/min despite a falling CPP would suggest that some vasodilation was occurring. This is consistent with the further increase in low frequency pressure transmission above that of the 5% level ($P < 0.001$). Also with 10% CO2, however, there was no significant change in the high frequency pressure transmission from that of the 5%

level which was mirrored by very little change in compliance with 10% CO2.

Abdominal compression (Figure 54) showed a significant increase in only the low frequency pressure transmission ($P < 0.05$), which was associated with the fundamental phase shift becoming less negative ($P < 0.01$).

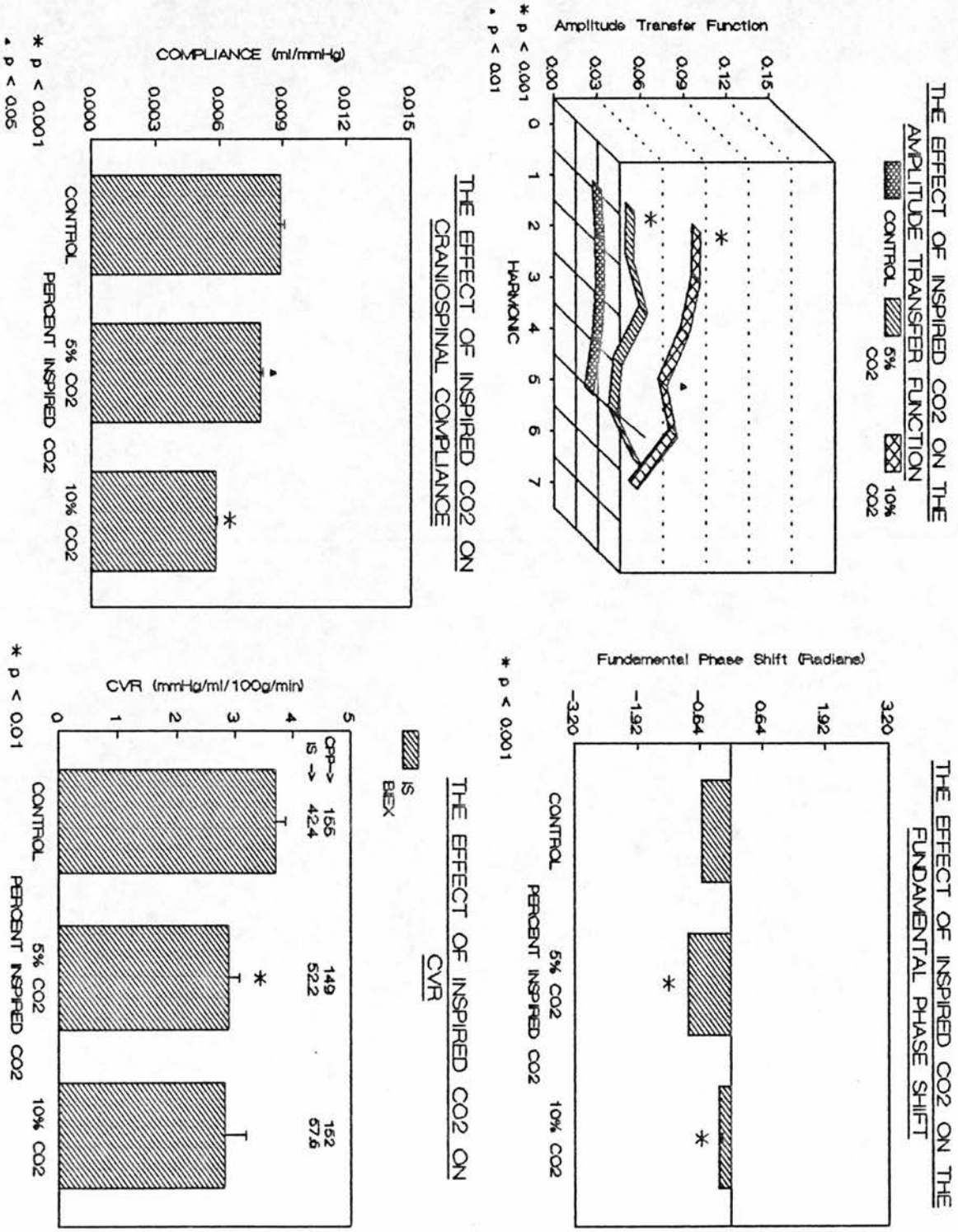

Figure 51: Cerebrovascular Resistance, Pressure Transmission and Craniospinal Compliance vs Inspired CO2, Animal P016.

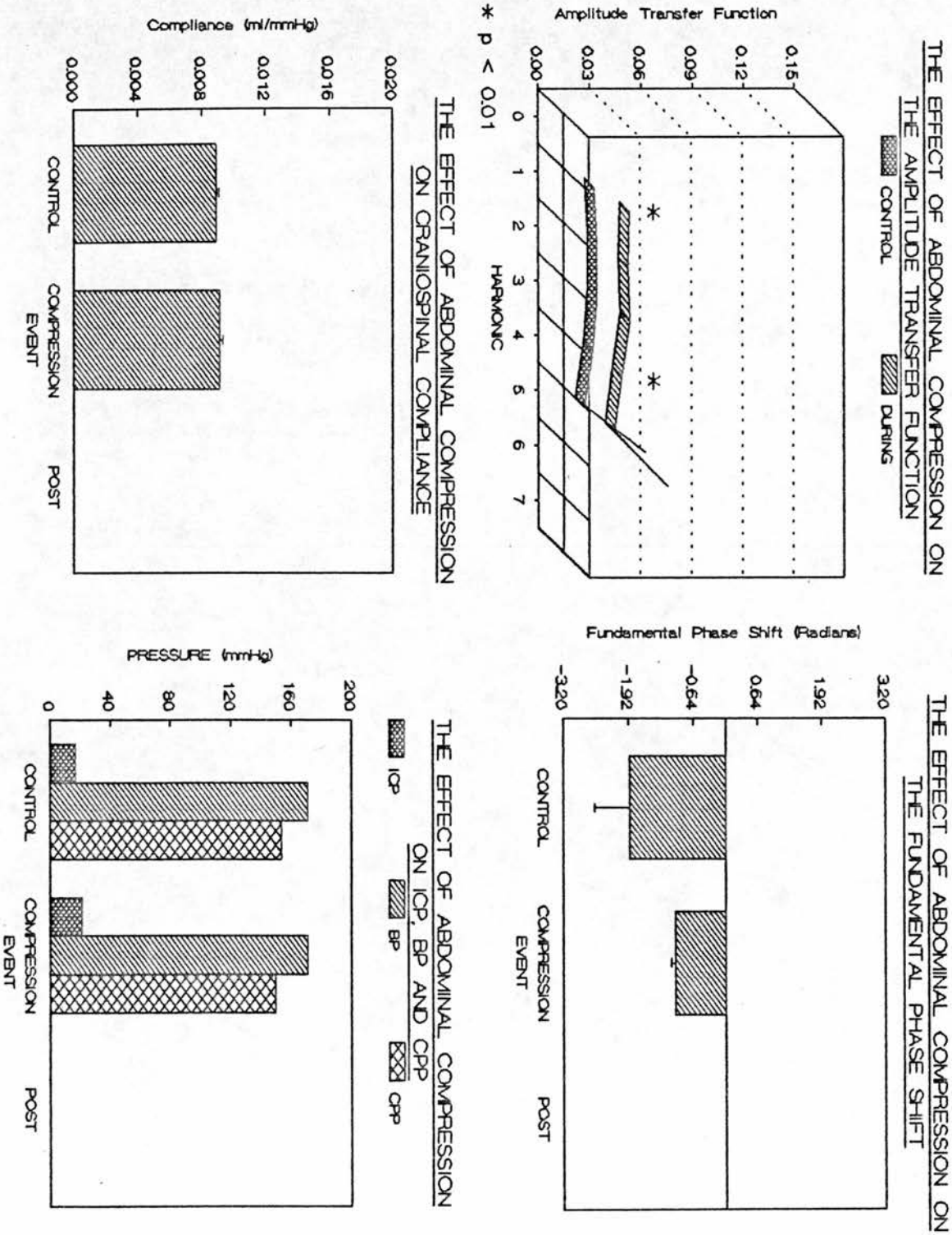

Figure 52: Cerebrovascular Resistance, Pressure Transmission and Craniospinal Compliance vs Abdominal Compression, Animal P016.

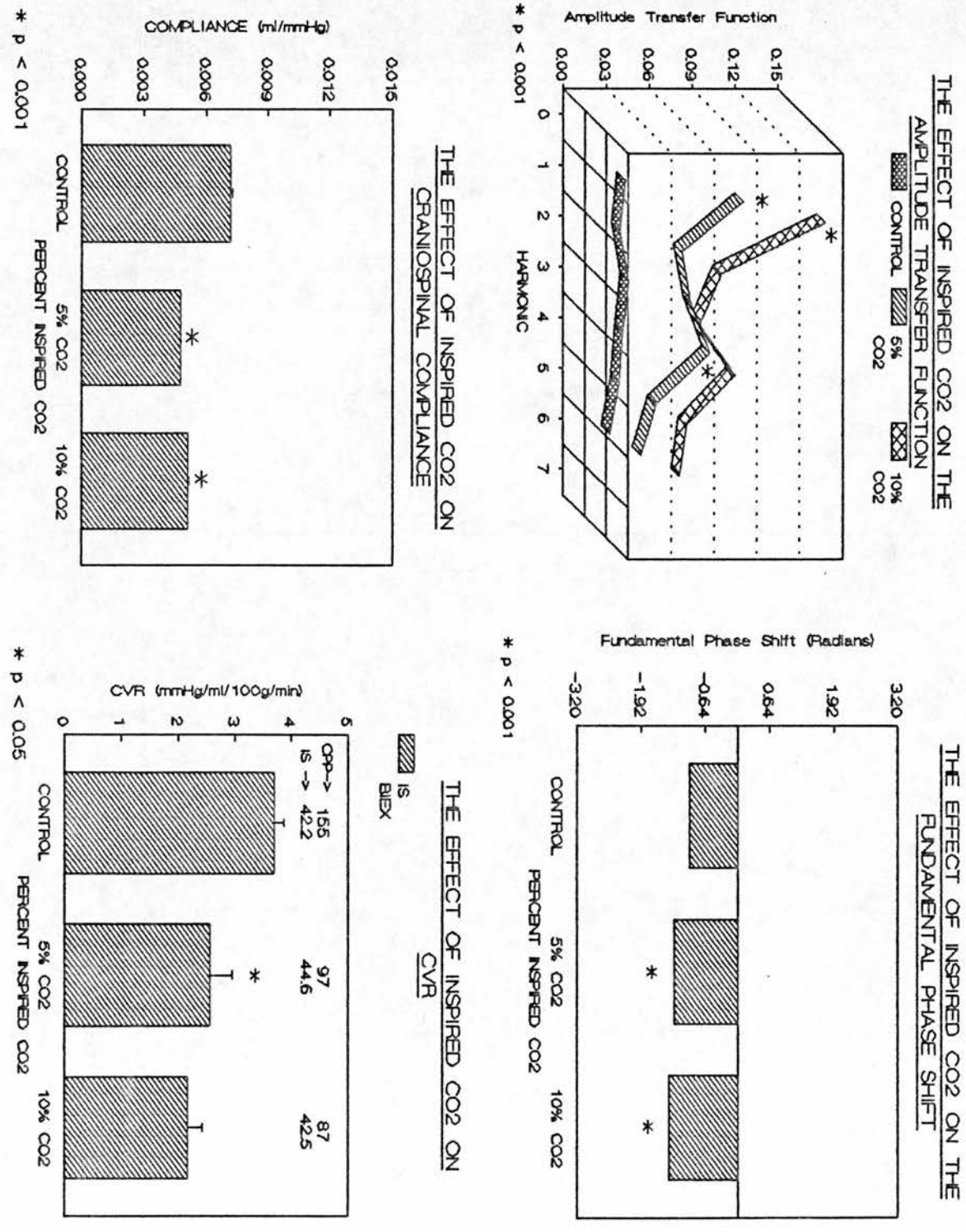

Figure 53: Cerebrovascular Resistance, Pressure Transmission and Craniospinal Compliance vs Inspired CO2, Animal P017.

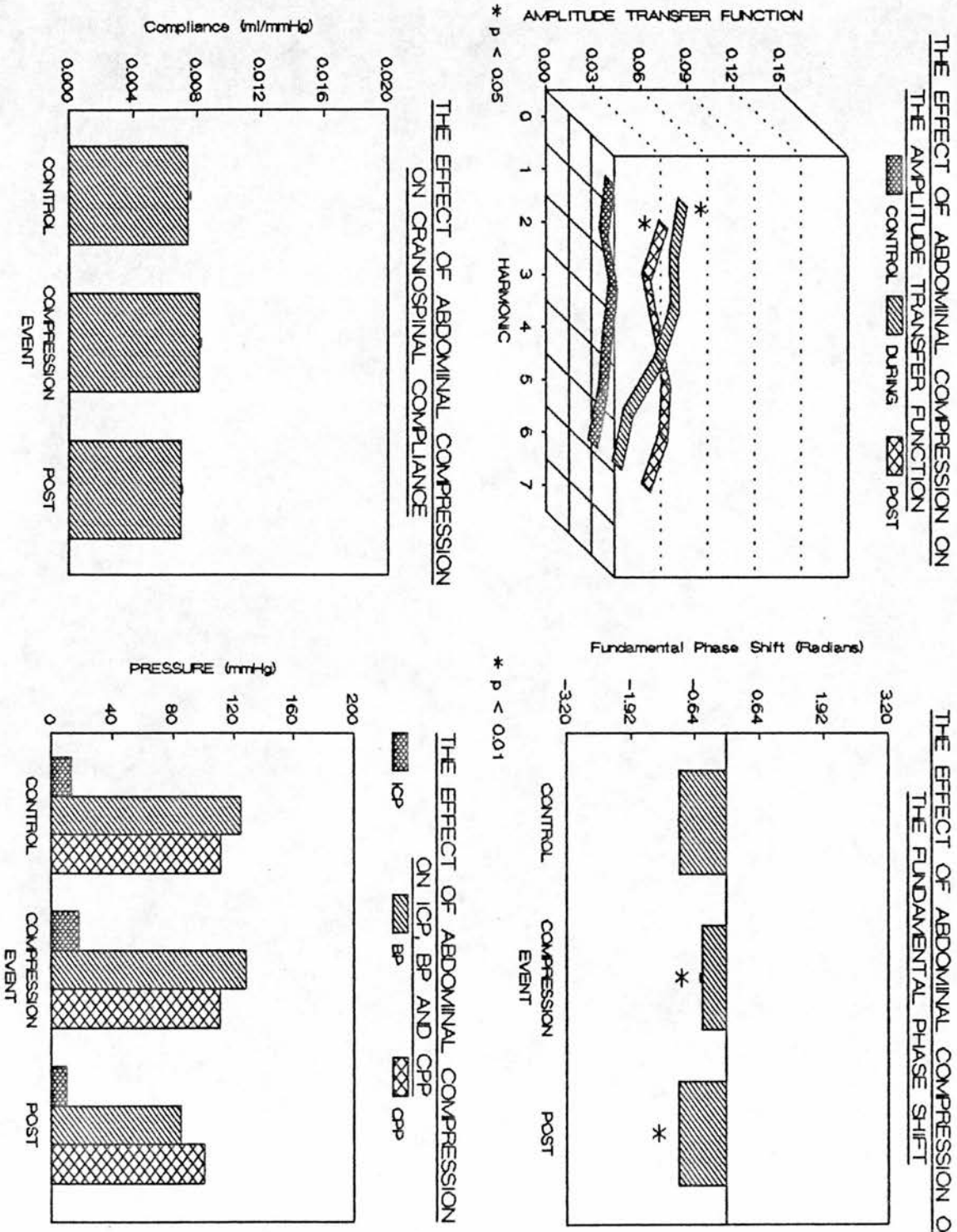

Figure 54: Cerebrovascular Resistance, Pressure Transmission and Craniospinal Compliance vs Abdominal Compression, Animal P017.

3. Commentary

All animals showed a decrease in cerebrovascular resistance with 5% CO2, and an associated increase in low frequency pressure transmission. However, the animals can be divided into two groups depending on their response to 10% CO2. Both animals (Figures 47,49) that failed to show a further increase in low frequency pressure transmission with 10% CO2, despite an indication of a reduction in cerebrovascular resistance consistent with vasodilation, were also the only two animals that demonstrated a marked increase in compliance with 10% CO2. In the other two animals (Figures 51,53) 10% CO2 induced further decrease in cerebrovascular resistance with an increase in low frequency pressure transmission but also were associated with either no significant change or a decrease in compliance.

The other consistent waveform change in this group of animals was with the relationship between compliance and high frequency pressure transmission. With one exception, every significant change in compliance was followed by an inverse change in the high frequency pressure transmission, as measured by the amplitude of the fourth harmonic in the amplitude transfer function. Figure 55 is a plot of the percentage change in amplitude of the fourth amplitude transfer function harmonic versus the associated change in compliance. As can be seen from this plot, a decrease in compliance (negative change) is associated with an increase (positive change) in the fourth harmonic amplitude and vice-versa.

The changes in the fundamental phase shift can also be divided into two groups. With 5% CO2, the two animals (Figures 51,53) that showed a consistent decrease in compliance with CO2, both showed the fundamental phase shift become more negative ($P < 0.001$). The phase of the other two animals (Figures 47,49), that both showed large increases in compliance especially with 10% CO2, showed either no change or become less negative. There were no consistent significant changes in the fundamental phase shift with 10% CO2.

Finally, with abdominal compression, because the perturbation to the craniospinal system with this method was small there were no significant changes in compliance. However, in three of the four animals (Figures 48,52,54), abdominal compression increased predominantly low frequency pressure transmission with an associated fundamental phase shift becoming less negative.

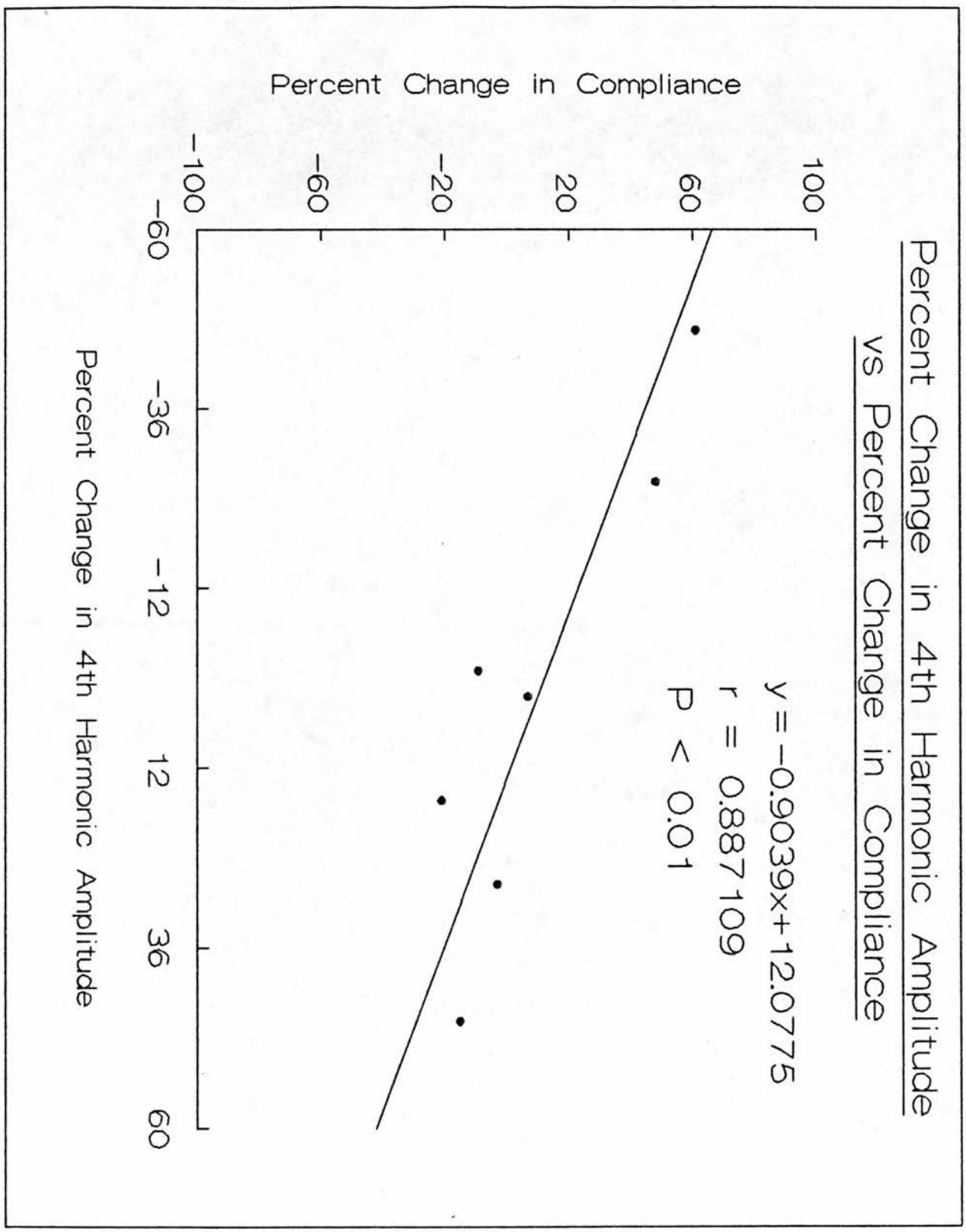

Figure 55: Plot of the Percentage Change of the Amplitude Transfer Function Fourth Harmonic vs Percentage Change in Compliance. Also shown is the linear equation of best fit (least squares method) to the data with the correlation coefficient (r) and the probability level (P) that the relationship is not statistically different from a linear relationship.

D. Induced Arterial Hypertension

This arm of the study was designed to examine the relationship between cerebrovascular pressure transmission, craniospinal compliance and cerebrovascular resistance both within and beyond the normal autoregulatory range of CBF to arterial BP.

1. Protocol

The BP of four animals was raised in stages. BP was raised with intravenous infusion (6 - 40 ml/hour) of Angiotensin II (100 ug/ml) and supplemented as required with adrenalin (0.2 mg/ml at 10 - 40 ml/hour). ICP was raised, by slow intraventricular infusion (3 ml/hour) of saline or Hartman's solution, to a baseline level of between 10 and 15 mm Hg. At each level of BP, four sequential 30 second samples of ICP and BP waveform data were stored to FM magnetic tape for subsequent offline calculation of cerebrovascular pressure transmission, which was immediately followed by four sequential measurements of craniospinal compliance using the SPR method. As previously, compliance for a given stage of the protocol was the average of the four sequential measurements, where each measurement was the signal average of 50 stimulus presentations. Five minutes after the final compliance measurement had been obtained, CBF was determined using the hydrogen clearance technique, with 10 minutes of hydrogen saturation. Just prior to desaturation, arterial blood gas samples were taken. During the initial slope phase of desaturation, BP and ICP were recorded for calculation of the CPP.

2. Results

Cerebrovascular pressure transmission and CBF changes with altered BP were sufficiently different between animals to cause grouped analysis to obscure the relationship between the two variables. As a result, the relationship between cerebrovascular pressure transmission, craniospinal compliance and cerebrovascular resistance will be reported individually for the four animals.

BP was increased from a mean control level of 137 +- 7 mm Hg to 202 +- 3.7 mm Hg ($P < 0.01$). In all animals, a further set of measurements was obtained at an average BP level of 118 +- 16 mm Hg during a second experimental run post arterial hypertension. Table 15 contains the

physiological data (ICP, BP, CPP, Tc, PaCO2, PaO2, pH, pupil size) recorded at each stage in the protocol averaged across all animals in this group. To prevent obscuring the relationship between amplitude transfer function curves, the associated standard error bars were not plotted. Table 16 contains the amplitude transfer function data with standard errors for each harmonic, broken down by BP level.

a. Animal P027

Figure 56 is a combined plot for this animal showing cerebrovascular pressure transmission (amplitude transfer function and fundamental phase shift), cerebrovascular resistance and craniospinal compliance at control BP, raised BP, and again at a control BP level post arterial hypertension during a second experimental run. When BP increased from 133 to 206 mm Hg, cerebrovascular resistance decreased significantly ($P < 0.01$), consistent with pressure passive vasodilation, which was followed by a small but significant increase ($P < 0.01$) in low frequency pressure transmission. Also associated with arterial hypertension, there was a small but significant decrease in compliance ($P < 0.01$), but there was no significant change in the fundamental phase shift.

During the second experimental run (BP 170 mm Hg), cerebrovascular resistance increased again and was not significantly different from the pre-hypertensive controls. However, there was a large increase in the low frequency pressure transmission ($P < 0.01$) above that of the hypertensive state, and the amplitude transfer function demonstrated large fluctuations in the amplitude of the high frequency harmonics. Associated with this inappropriate increase in low frequency pressure transmission, there was a marked increase in compliance ($P < 0.001$) and the fundamental phase shift showing a large positive phase ($P < 0.001$).

Table 15: BP Experimental Group Physiological Data.

	BP (mmHg)	ICP (mmHg)	CPP (mmHg)	Tc (Deg. C)	PaCO2 (mmHg)	PaO2 (mmHg)	pH	Pupils (mm)
Control	137 +-7	14 +-1	138 +-8	37.6 +-0.28	36.2 +-1.2	487 +-12	7.346 +-0.01	6 +-1
BP Up First Run	** 202 +-3.7	20 +-3	** 179 +-2	37.6 +-0.34	31.2 +-1.6	379 +-60	7.398 +-0.02	* 11 +-1.5
Control Second Run	118 +-16	** 5 +-2.7	111 +-13	37.6 +-0.11	35.0 +-5.4	200 +-55	* 7.046 +-0.05	12 +-0

** denotes P < 0.01 * denotes P < 0.05

Table 16: BP Experimental Group Amplitude Transfer Function Data.

	A1	A2	A3	A4	A5	A6
Control P027	.0981+-.0018	.1176+-.0026	.1581+-.0024	.1168+-.0027	.0839+-.0089	.0588+-.0107
Control P028	.1206+-.0047	.1373+-.0067	.2231+-.0078	.2682+-.0174	.3912+-.0332	.2627+-.0103
Control P029	.0617+-.0047	.0732+-.0043	.0901+-.0046	.1251+-.0097	.1075+-.0066	.0738+-.0137
Control P030	.0783+-.0030	.0954+-.0031	.0513+-.0012	.0341+-.0048	.0632+-.0112	.1432+-.0331
BP Up P027	.1326+-.0025 %	.1176+-.0045	.1121+-.0083	.1589+-.0129 *	.1064+-.0109	.1656+-.0583
BP Up P028	.3329+-.0073 *	.2881+-.0020	.3277+-.0185	.3577+-.0056 Δ	.4669+-.0192	.4712+-.0800
BP Up P029	.0291+-.0010 Δ	.0389+-.0024	.0263+-.0002	.0338+-.0039 %	.0668+-.0016	.0683+-.0032
BP Up P030	.1314+-.0025 %	.1205+-.0032	.0885+-.0034	.0663+-.0031 %	.1314+-.0086	.1959+-.0229
Run2 P027	.2969+-.0105 %	.0416+-.0014	.2658+-.0174	.0672+-.0089 %	.1480+-.0144	.1044+-.0282
Run2 P028	.0959+-.0022 *	.1019+-.0027	.1090+-.0038	.0907+-.0079 Δ	.0895+-.0192	.0700+-.0129
Run3 P029	.1193+-.0055 %	.0990+-.0118	.0821+-.0082	.0554+-.0112	.1403+-.0645	.0757+-.0232
Run3 P030	.0845+-.0036 %	.0814+-.0033	.1846+-.0160	.1712+-.0059 %	.1017+-.0025	.0775+-.01910

* denotes P < 0.001 % denotes P < 0.01 Δ denotes P < 0.05

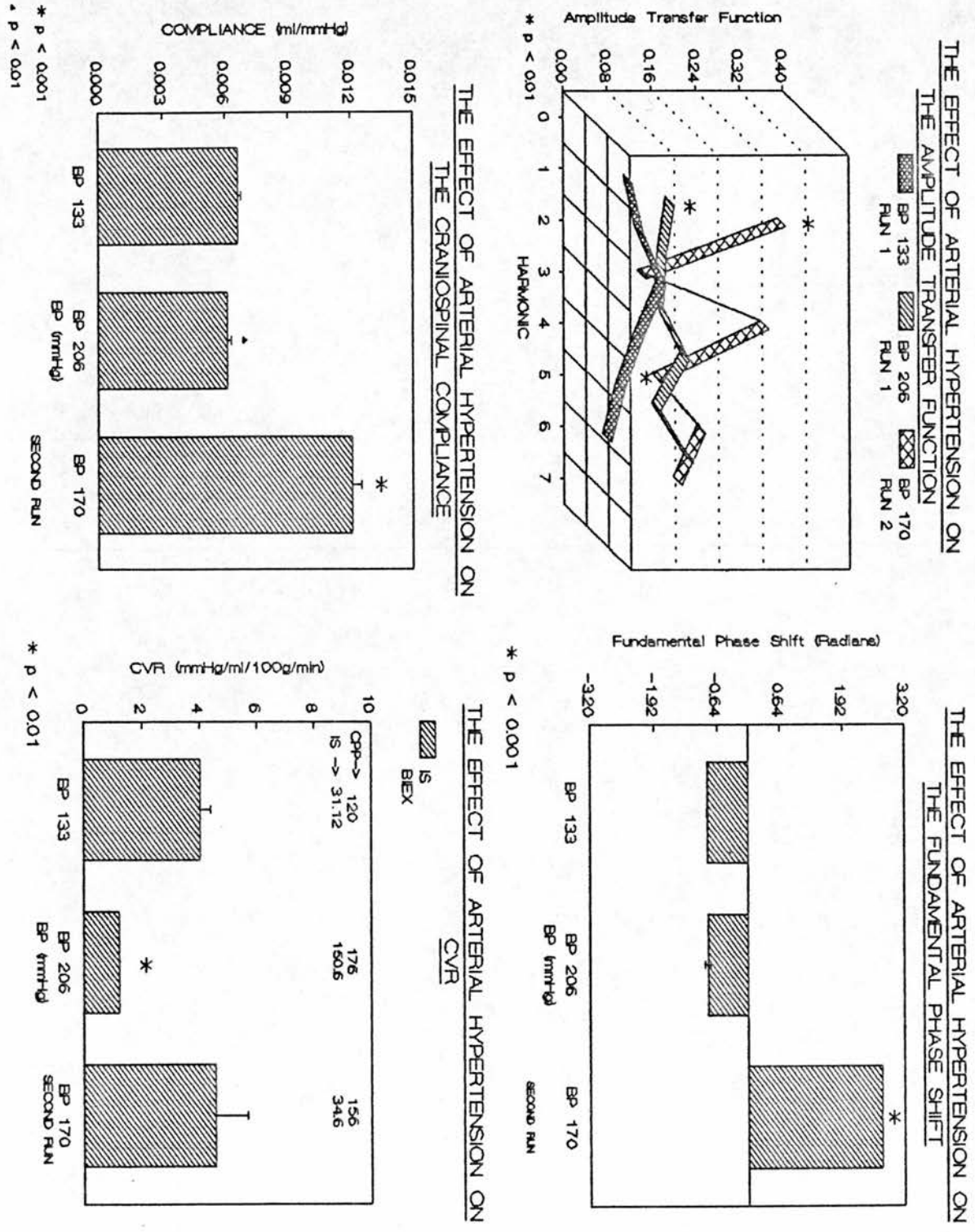

Figure 56: Cerebrovascular Resistance, Pressure Transmission and Craniospinal Compliance vs Arterial Hypertension, Animal P027.

b. Animal P028

In this animal (Figure 57), when BP was increased from 150 to 210 mm Hg there was a large increase in both low ($P < 0.001$) and high ($P < 0.05$) frequency pressure transmissions. However, there was no significant change in cerebrovascular resistance. The ISI flows were already elevated in this animal at 191 ml/100g/min which increased further in a pressure passive manner to 226 ml/100g/min with arterial hypertension. This indicates that at control BP levels, this animal may be above the upper level of autoregulation, or may be demonstrating the onset of loss of autoregulation. Also associated with arterial hypertension, there was a significant decrease in compliance ($P < 0.01$), and the fundamental phase shift became more negative ($P < 0.001$).

During the second experimental run (BP 110 mm Hg), cerebrovascular resistance increased significantly ($P < 0.05$) from the pre-hypertensive controls. However, the amplitude transfer function took on a flatter course than before with a significant decrease ($P < 0.001$) in both low and high frequency pressure transmission. As with the previous animal, there was a marked increase in compliance ($P < 0.001$) and the fundamental phase shift showed a large positive phase ($P < 0.001$).

c. Animal P029

When BP was increased from 150 mm Hg to 190 mm Hg in this animal (Figure 58), there was no significant change in cerebrovascular resistance, but there was a significant decrease in both low ($P < 0.05$) and high ($P < 0.01$) frequency pressure transmissions. As with all previous animals, compliance decreased ($P < 0.01$) with arterial hypertension.

During the second experimental run (BP 100 mm Hg), cerebrovascular resistance increased significantly ($P < 0.05$) from the pre-hypertensive controls. There was a large increase in the low frequency pressure transmission ($P < 0.01$) above that of the hypertensive state, and this inappropriate increase in low frequency pressure transmission was again associated with a marked increase in compliance ($P < 0.01$) and a large positive fundamental phase shift ($P < 0.001$).

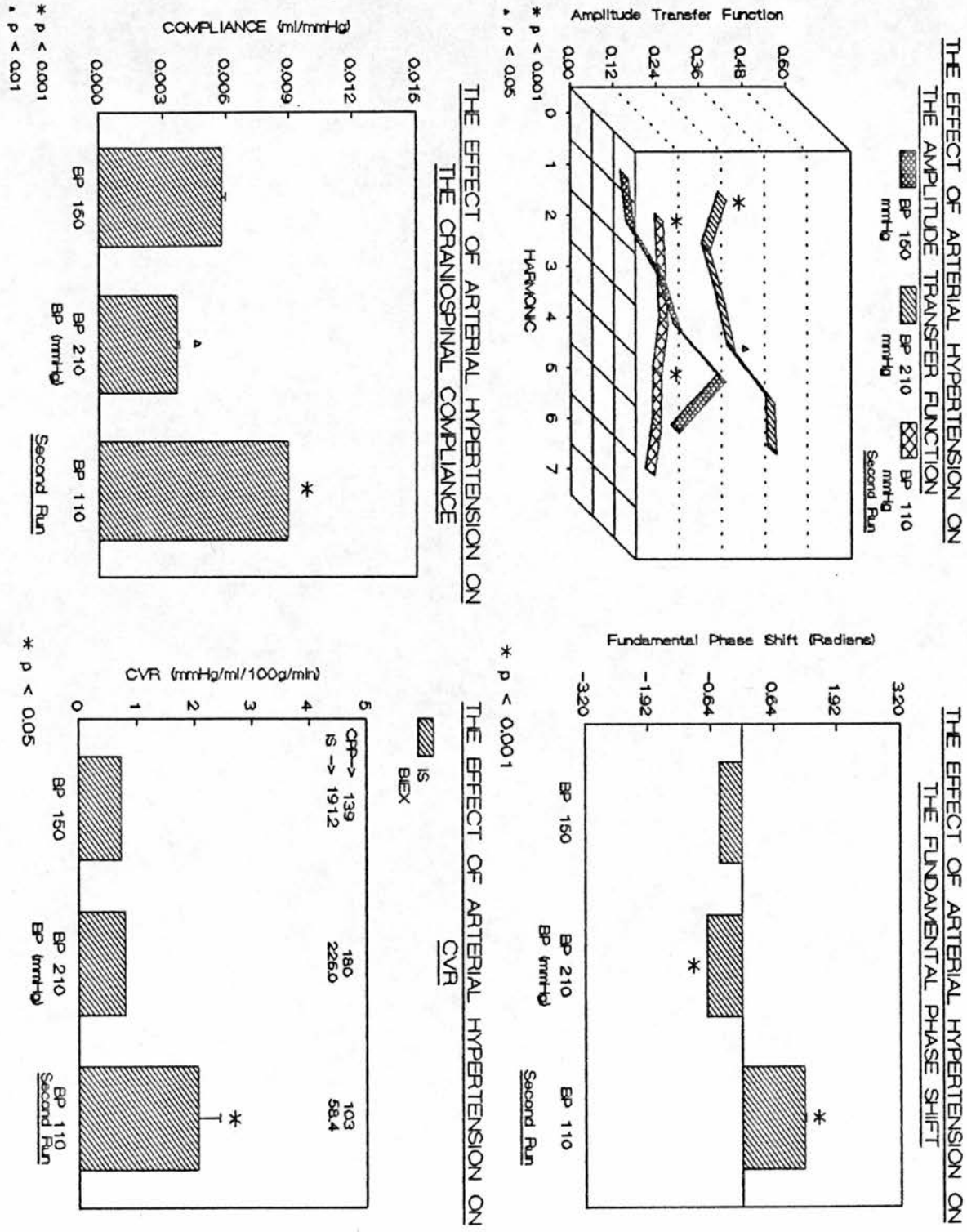

Figure 57: Cerebrovascular Resistance, Pressure Transmission and Craniospinal Compliance vs Arterial Hypertension, Animal P028.

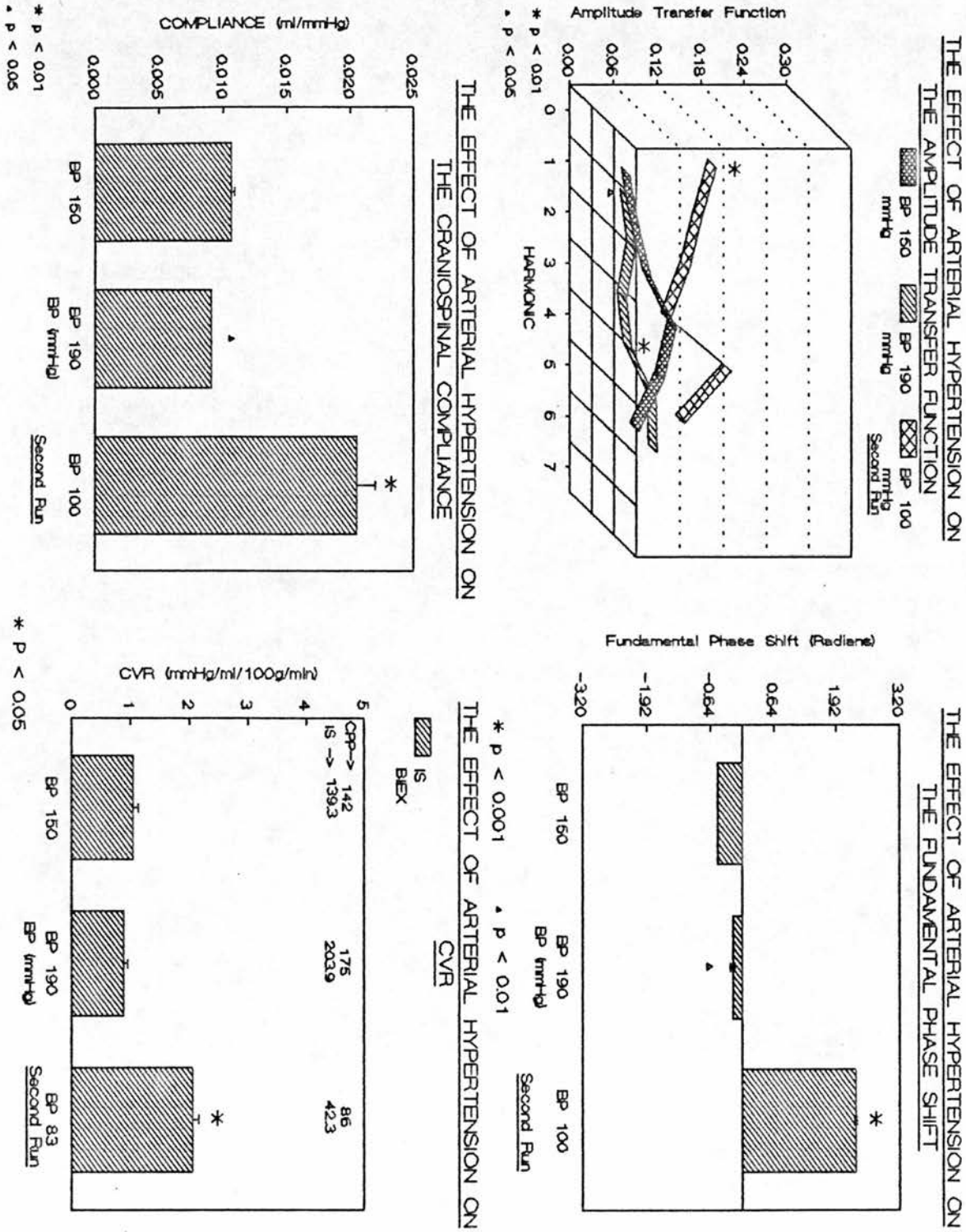

Figure 58: Cerebrovascular Resistance, Pressure Transmission and Craniospinal Compliance vs Arterial Hypertension, Animal P029.

d. Animal P030

With this final animal (Figure 59), when BP was increased from 115 to 200 mm Hg, cerebrovascular resistance decreased significantly ($P < 0.01$), consistent with pressure passive vasodilation, which was followed by large increases in both the low and high frequency pressure transmission ($P < 0.01$). There was no significant change in compliance or the fundamental phase shift with arterial hypertension.

During the second experimental run (90 mm Hg), cerebrovascular resistance increased again ($P < 0.01$) and was not significantly different from the pre-hypertensive controls. There was a small but significant decrease in low frequency pressure transmission at this stage ($P < 0.01$), although there was a large significant increase in the high frequency pressure transmission ($P < 0.001$) above that of the hypertensive state. Similar to all previous animals, there was also a marked increase in compliance ($P < 0.001$) and an increase ($P < 0.05$) in a positive direction of the fundamental phase shift.

3. Arterial Hypertension and Brain Damage

In one animal (P030), to assess blood brain barrier function, 8 ml of a 2% Evans Blue Dye was given intravenously forty minutes before the end of the protocol (144). The brain was removed and examined for evidence of extravasation of Evans Blue Dye.

a. Results

Figure 60 is a photograph of coronal slices taken from the brain of the animal injected with Evans Blue Dye. Four slices are shown extending from the forebrain to the cerebellum. All brain slices show marked extravasation of Evans Blue Dye, both superficially and extending into the full thickness of the cerebral and cerebellar cortex and occasionally spreading to subcortical white matter.

In addition to blood-brain barrier breakdown, one animal had blood stained CSF and another had an intraparenchymal haemorrhage located just inferior to the ventricular needle catheter. As seen from Table 15, all animals demonstrated a significant increase ($P < 0.05$) in pupil diameter from a mean diameter at control BP of 6 +- 1 mm becoming fully dilated at 12 mm with arterial hypertension. The pupils remained fully dilated through the second experimental run of control measurements.

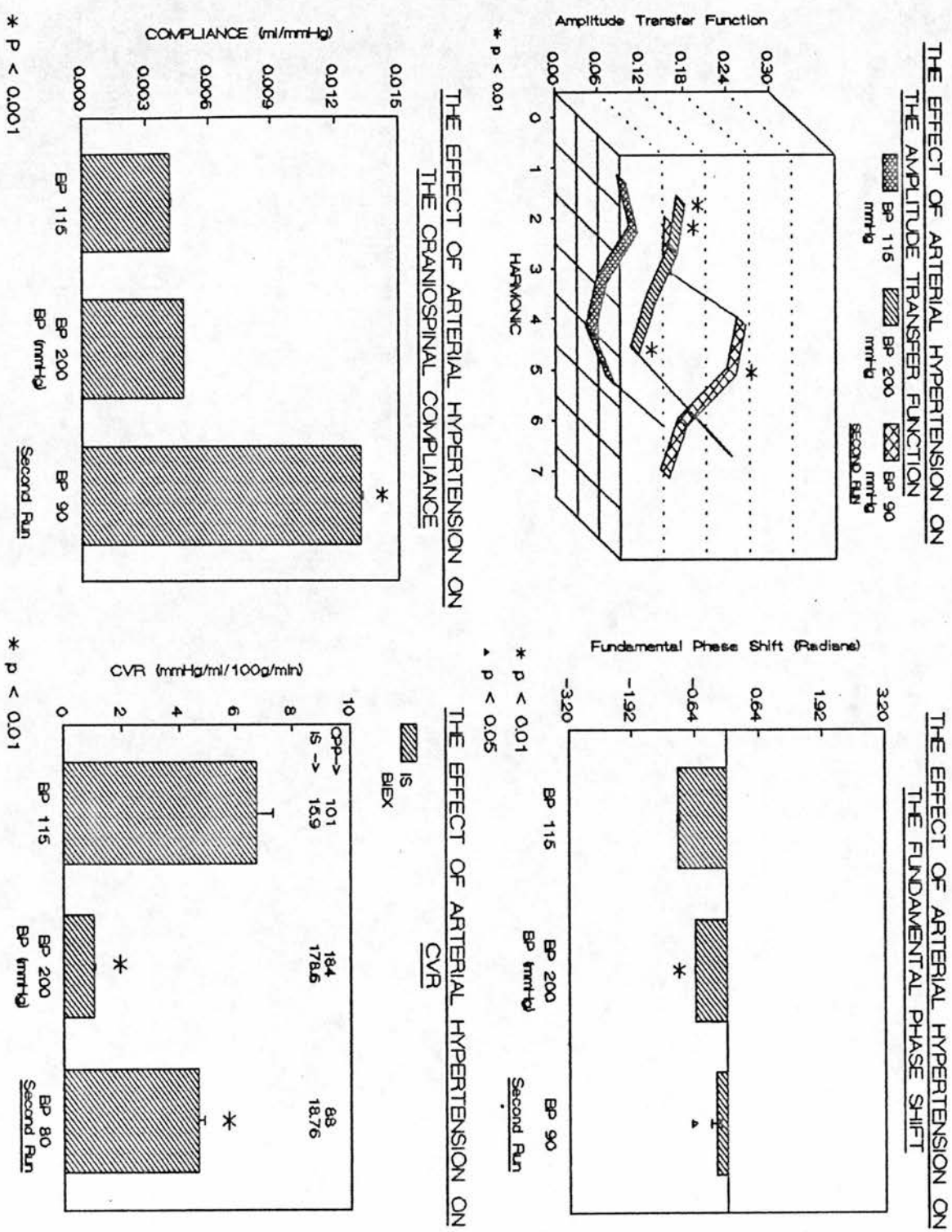

Figure 59: Cerebrovascular Resistance, Pressure Transmission and Craniospinal Compliance vs Arterial Hypertension, Animal P030.

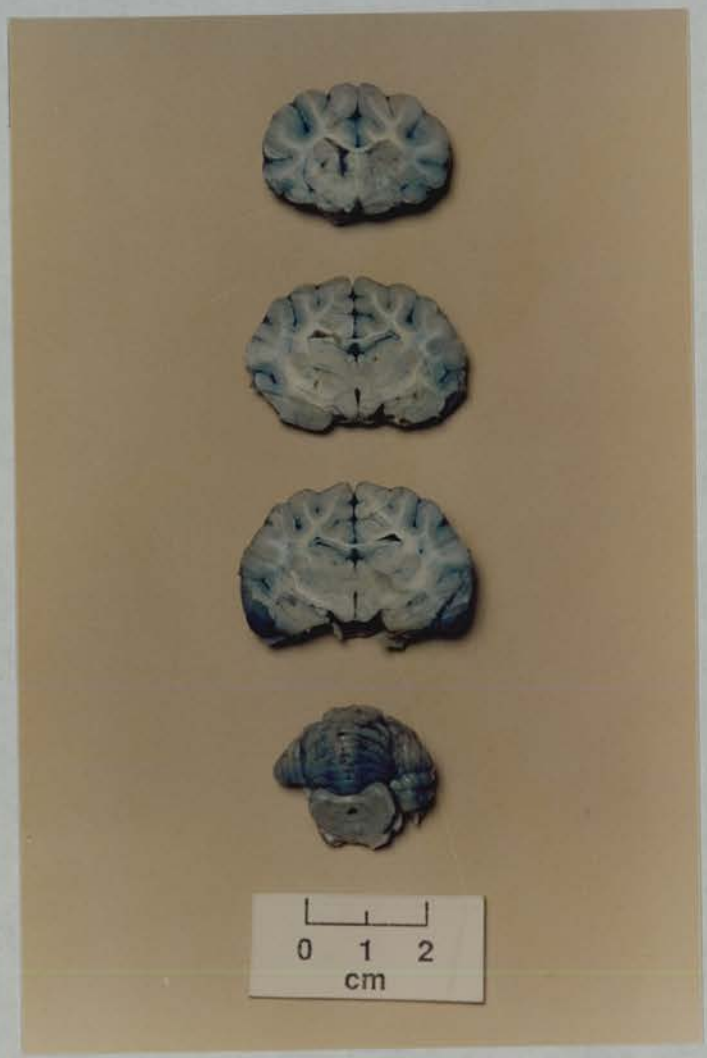

Figure 60: Photograph of Coronal Slices taken from the Brain of an Animal Injected with Evans Blue Dye after Prolonged Arterial Hypertension.

4. Commentary

The normal upper limit of autoregulation in the cat, under alpha-chloralose anaesthesia and using the H2 clearance technique for measurement of CBF, has been shown to be approximately 160 mm Hg (144).

Three of the four animals in this group (Figures 56,57,59) showed large increases in both low and high frequency pressure transmission with arterial hypertension well above the upper limit of autoregulation. All of these animals showed either no change or marked decreases in cerebrovascular resistance which is consistent with a pressure passive non-autoregulatory increase in CBF. The one animal that did not demonstrate increased pressure transmission with arterial hypertension also showed no change in cerebrovascular resistance. This animal had unusually high ISI control flows (139 ml/100g/min) which increased passively with arterial hypertension. It is possible that this animal has already lost or has impaired autoregulation with resistance vessels fully open and unable to dilate further or to increase pressure transmission.

The most consistent and striking changes in this group of animals occurred during the second experimental run when BP was once again at or near control levels. All animals showed a marked increase in a positive direction of the fundamental phase shift and a marked increase in craniospinal compliance. Also occurring at the post arterial hypertension stage was a significant decrease in ICP in all animals from 20 mm Hg +- 3 during arterial hypertension to 5 mm Hg +- 3 post arterial hypertension ($P < 0.01$).

There were less consistent changes in high frequency pressure transmission. Three of the four animals (Figures 56,57,59) showed an elevation in high frequency pressure transmission during arterial hypertension although in one animal (Figure 56) the elevation was not statistically different. Associated with the elevated high frequency pressure transmission, compliance showed either no change (Figure 59) or significantly decreased (Figures 56,57) with arterial hypertension. The remaining animal (Figure 58) showed a significant decrease in high frequency pressure transmission ($P < 0.01$) with arterial hypertension, despite a significant decrease in compliance. This animal was the same animal with abnormally elevated ISI flows and which failed to show an increased low frequency pressure transmission with arterial hypertension.

E. Discussion of Results

1. Intracranial Hypertension

The intracranial hypertension group of animals demonstrated both increased low and high frequency pressure transmission which increased in a stepwise fashion with raised ICP and was associated with decreased craniospinal compliance. It is well documented that raised ICP decreases compliance (41,42,49,56). More recently the relationship between raised ICP and cerebrovascular pressure transmission has been studied (78,81,85), but this study is the first to investigate the relationship between cerebrovascular pressure transmission, craniospinal compliance and cerebrovascular resistance.

Autoregulation of CBF to reduced CPP is known to exist for a CPP as low as 50 mm Hg (160,163). The animals in this group did not demonstrate autoregulation to a CPP range from 139 to 88 mm Hg. However, the mean BP in this group was 149 +- 14 mm Hg bringing the preparation close to the upper limit of CBF to raised BP of 160 mm Hg (144). It is conceivable that the starting point for reduction of CPP in this group was already above the upper limit of autoregulation for these animals. Alternatively, loss of autoregulation may have been the result of H2 electrode placement, which can occasionally cause sufficient cortical damage to impair autoregulation (144). This is usually associated with slow monoexponential clearances, whereas the majority of H2 electrodes placed in this study demonstrated bicompartmental ISI flows over a range of CBF values from 30 to 130 ml/100g/min. Whatever the cause, the measurements obtained indicate a pressure passive decrease in CBF as ICP increased, which may have been as a result of compression of the large cerebral veins and sinuses (164,165,166), where the major site of compression is believed to have been located at the intradural portion of the venous drainage system adjacent to the major dural sinuses (lateral lacunae) (167,168). This compression will have increased venous impedance and hence upstream venous pressure, which explains the increased pressure transmission from BP to ICP[71]. The major source of cerebrovascular resistance (> 65%) at

---

[71]If the cerebrovascular bed is modelled as the series combination of two resistances R1 and R2, where R1 is the arteriolar segment and R2 is the venous segment, and if R1 remains unchanged and R2 increases, then for a given input pressure (P) an increased pressure will now be dropped across R2. P2 = P * (R2/R1+R2). This results in an increased pressure transmission into the CSF space.

normocapnia has been shown to be predominantly the small calibre arteries and arterioles (169). Pial arteries have also been shown to dilate in cats with an intraventricular infusion model of raised ICP (170), but this vasodilation appears not to be occurring in this non-autoregulating group of animals. As a consequence the increased cerebrovascular pressure transmission observed with this group of animals appears to be solely as a result of the increased venous impedance brought on by vascular compression.

2. Arterial Hypercarbia

In both this group of animals and the arterial hypertension group, it was necessary to present results according to individual animals. Studies of pressure transmission across the cerebrovascular bed have a large inherent variability because the impedance of vascular beds are highly dependent on the animal body size and weight (117). These studies had a large variation (2.0 - 5.5 Kg) in animal body weight. Furthermore, in the CO2 group of animals, there were unique responses made by some animals to 10% CO2. Although this adds to the variability of the absolute values for cerebrovascular pressure transmission, the relationship between the changes in arterial PaCO2 and pressure transmission, compliance and cerebrovascular resistance remains unchanged.

All animals in this group showed a decrease in cerebrovascular resistance with 5% CO2 and an associated increase in low frequency pressure transmission. Cerebrovascular resistance is known to decrease with arterial hypercarbia (107) and it is most likely the small calibre arteries and arterioles which are mainly affected (169). In this group, for the same level of arterial hypercarbia (Table 13), increases in low frequency pressure transmission from control levels ranged from 50% to over 300%. All increases were associated with decreased cerebrovascular resistance with no significant change in BP, indicating an active arteriolar vasodilation.

A greatly increased low frequency pressure transmission was proposed by Portnoy et al (81,82) to be an indicator for loss of autoregulatory vasomotor tone. It is known that loss of CBF autoregulation to raised blood pressure can often occur in conjunction with loss of CO2 reactivity (171,189) where the latter process was described by Langfitt as vasomotor

paralysis (39). Loss of autoregulation can be induced by high levels of arterial hypercarbia (191,192). Two animals in this study (Figures 47,50), showed no further increase in low frequency pressure transmission with 10% CO2 despite additional decreases in cerebrovascular resistance. The apparent dissociation of cerebrovascular resistance and low frequency pressure transmission found in these two animals, in conjunction with an existing elevated low frequency pressure transmission, would support Portnoy's theory. However, an increased low frequency pressure transmission could be due either to loss of autoregulatory tone through vasomotor paralysis or paradoxically to intact autoregulation compensating for reduced CPP through active vasodilation. The large variation in both the degree of elevation of low frequency pressure transmission and in the CBF responsiveness to CO2 found in these studies would make it difficult to distinguish these two mechanisms.

An elevated high frequency pressure transmission without an associated low frequency elevation, has been found clinically, as reported in this thesis, and by other investigators both experimentally (87,88) and clinically (83,89,90), and is believed to be due to the presence of a resonant peak in the amplitude transfer function. However, in this CO2 group of animals, the increased high frequency pressure transmission occurred in conjunction with an elevated low frequency transmission, often with a considerable degree of variation in the amplitude of the higher harmonics. It is unlikely that this form of pressure transmission is indicating a resonant rise in pressure transmission. In these studies, the high frequency pressure transmission as measured by the amplitude of the fourth harmonic demonstrated a consistent inverse relationship to craniospinal compliance. However, the large variation in the amplitude of the higher harmonics, particularly with the presence of large swings in their amplitude, weakens the relationship between compliance and high frequency pressure transmission, particularly if one uses only a single harmonic amplitude as the only measure of high frequency response. Some measure of average high frequency pressure transmission may be required before further study of this relationship between compliance, resonance and high frequency pressure transmission.

Abdominal compression causes increased transmission of abdominal pressure to the lumbar CSF space and to venous channels, like the longitudinal vertebral veins (178). Increased intracranial venous

pressure may lead to intracranial vascular engorgement and raised ICP (104,105). In these studies, abdominal compression failed to produce large changes in craniospinal compliance, but despite this, in each animal, small but significant increases in mainly low frequency pressure transmission occurred with abdominal compression. These results contrast with pilot clinical data reported in this thesis (page 39) where jugular compression was found to affect predominantly the higher harmonics in the amplitude transfer function. ICP increased considerably more (from 17 to 29 mm Hg) (Figure 19) in the clinical study than it did in this experimental study (15 to 19 mm Hg) (Table 13), suggesting possibly that an altered high frequency pressure transmission may result only with greater perturbation to the craniospinal system. Jugular compression was not attempted in this experimental study, as it was found difficult to avoid compression of the carotid arteries in the process. This would alter the input function to the cerebrovascular bed which would not be detected because of the proximal location of the thoracic BP transducer.

3. Arterial Hypertension

Acutely raised arterial pressure has been previously shown, in an experimental study in cats using identical anaesthesia to this study, to cause loss of CBF autoregulation, damage to the blood-brain barrier and overdistension of the cerebral resistance vessels (144). The present study from the arterial hypertension group has shown that three of the four animals (Figures 56,57,59) demonstrated large increases in low frequency pressure transmission when arterial hypertension was well above the upper limit of autoregulation. All of these animals showed either no change or marked decreases in cerebrovascular resistance, which indicates a pressure passive non-autoregulatory increase in CBF. This further supports Portnoy's hypothesis that an increased low frequency pressure transmission may be a marker for loss of autoregulation.

The most consistent and marked changes in the arterial hypertension group of animals occurred during the second experimental run when BP was once again at or near control levels. All animals showed a large increase in a positive direction of the fundamental phase shift and a marked increase in craniospinal compliance. Similar large increases in compliance and phase were also found in two animals (Figures 47,49) in the CO2 group during 10% CO2 inhalation where both animals failed to

show an increase in low frequency pressure transmission despite reductions in cerebrovascular resistance. Phase changes have also been found clinically by Anile and co-workers (179) who reported that, in patients with normal pressure hydrocephalus that showed a favourable outcome, all demonstrated a change in the fundamental phase shift from a positive to a negative phase. They subsequently demonstrated (180), experimentally in dogs, that if the craniospinal system is opened to atmospheric pressure (increased transmural pressure) there is an associated increase in the fundamental phase shift in a positive direction.

The marked changes in compliance and phase seen with the BP group of animals are best understood in electronic terms, where a more negative system phase indicates increased capacitance, and an increase in system phase in a positive direction indicates an increased inductance. In mechanical terms, capacitance is equivalent to compliance and inductance to inertance[72]. During the second BP run, the increased phase shift in a positive direction may indicate a greatly increased inertance brought on by the distention of the blood vessels with an increased mass of blood[73]. A possible sequence of events might be that the increased mass of blood, forced in under arterial hypertension, in combination with blood vessels exhibiting reduced tone, results in both greater inertance and decreased compliance. The decreased compliance being the result of increased transmural pressure with raised BP. At this time, the decreased compliance is the dominant factor determining the system phase. When BP is then reduced, the transmural pressure decreases and hence the

---

[72]Inertance is a measure of the force required to set a mass in motion or alter its direction once it is in motion (161).

[73]The value of system phase at any one time is dependent on the sum of the phase shift due to inertial or inductive effects and those due to the compliant or capacitive effects. The phase shift due to the inertial effects is calculated from: $\Phi_I = \mathrm{Tan}^{-1}(X_I/R)$, where $X_I = 2\pi FI$. X_I is the inductive reactance and R is the system resistance, and F and L are the frequency and inductance respectively. Similarly the phase shift due to the capacitive effects is calculated from: $\Phi_C = \mathrm{Tan}^{-1}(-X_C/R)$, where $X_C = 1/(2\pi FC)$. X_C is the capacitive reactance and R is the system resistance, and F and C are the frequency and capacitance respectively.

Fluid Inertance will be dependent on the mass of fluid and factors affecting the movement (vessel diameter) of the fluid within the containing vasculature. Vascular compliance will be dependent on the physical dimensions of the containing vasculature and factors affecting the compressibility of the contained fluid and containing structures, and for thick walled vessels, the pressure across the vessel wall (transmural pressure) (162).

compliance increases. However, after 30 minutes of severe arterial hypertension, the inertance is now the main determinant of the system phase, possibly as a result of the now altered visco-elastic properties of the brain and cerebrovascular system. Some factors that may indicate altered visco-elastic properties of the brain and cerebrovascular bed are the disruption to the blood-brain barrier, intracerebral haemorrhage and possibly brain-stem damage, as signified by the bilateral fully dilated pupils. The greatly increased craniospinal compliance seen at this time may have resulted from the increased intracranial blood volume. An increased blood volume contained within a vasculature that has lost tone will become more compliant, especially at low transmural pressure. As a result, blood can be more readily displaced from the intracranial cavity.

These marked changes in compliance and phase may be interpreted as indicators for a generalized cerebral vasodilation as a consequence of reduced vasomotor tone. Evidence for this can be seen from Tables 14 and 15 where, during the second BP run, three out of four animals in the BP group showed an increased low frequency pressure transmission compared to the control run, despite there being no significant change in CPP between the two runs. This indicates reduced arteriolar vasomotor tone. Furthermore, the blood brain barrier disruption found in these animals on post-mortem is further evidence for a disturbed cerebrovascular bed. This is supported by the work of Häggendal and Johansson (194) who have shown blood brain barrier disruption in cats with acute aramine induced arterial hypertension. Associated with the blood brain barrier disruption, they found that arterial hypertension was always accompanied by cerebral venous hypertension. The increased pressure transmission to the venous portion of the vascular bed is presumably as a result of decreased arteriolar resistance. This is further supported by the work of MacKenzie et al (144), who studied pial artery dilation during angiotensin induced hypertension in cats. They found that at pressures above 180 mm Hg there were two vascular responses. Vessels less than 100 microns in diameter displayed a characteristic "sausage string" morphology, that is a series of regularly spaced vasoconstricted segments interdispersed with vasodilated segments. They conclude that the vasoconstricted segments are the remnants of autoregulatory constrictions. However, vessels larger than 100 microns in diameter did not show the "sausage string" pattern but displayed

marked vasodilation. Furthermore, the autoregulatory constrictions were temporary and after 20 minutes of hypertension all constricted segments gave way to a generalized marked vasodilation.

F. Discussion of Methods

All animals in this study had anaesthesia induced with ketamine hydrochloride. Ketamine has been shown to have no significant effect on ICP in paralysed and mechanically ventilated preparations and has a duration of anaesthesia of less than 25 minutes (181). The main anaesthetic used was alpha-chloralose which has been shown to provide stable anaesthesia with no effect on vascular smooth muscle and minimal effect on the autonomic reflexes (182).

Arterial hypertension was induced with angiotensin II which is known to have no pharmacological action on the cerebral circulation (184,185,186). However, tachyphylaxis to angiotensin occurred within 15 minutes, after which angiotensin was supplemented with adrenalin, which does alter vascular smooth muscle tone. All BP and ICP waveforms were collected prior to use of adrenalin, although the later stages of the CBF measurements after the initial two to three minutes may have been affected by the adrenalin administration.

H2 electrodes for measurement of CBF were positioned as described by MacKenzie et al (144), which in the cat would record CBF in the boundary region of the middle and anterior cerebral arteries. The electrode positions were maintained close to the midline to reduce any effects of lateral brain displacement on disruption of the electrode position in the cortex. The majority of blood flow curves were found to be biexponential (> 80%). However, unpredictably during intracranial and arterial hypertension, some electrodes which were previously biexponential would become monoexponential. As a result, bicompartmental analysis was not possible. The ISI of CBF was used throughout the studies, which has been shown to be a good measure of average flow from fast and slowly clearing tissue (155,157).

G. Conclusions

These experimental studies show that, despite inter-animal variability, there are consistent relationships between cerebrovascular pressure transmission, craniospinal compliance and cerebrovascular resistance.

1) Increased low frequency pressure transmission either with or without elevated high frequency pressure transmission, can occur with raised ICP, arterial hypercarbia or arterial hypertension.

2) This increased pressure transmission is associated with reduced craniospinal compliance, reduced cerebrovascular resistance and a negative fundamental phase shift. Furthermore, during intracranial hypertension and arterial hypertension, the increased pressure transmission is associated with impaired autoregulation.

3) Post arterial hypertension, and in two instances of severe arterial hypercarbia, there was an abnormally high craniospinal compliance and a positive fundamental phase shift. This combination of factors may be characteristic of a generally vasodilated cerebrovascular bed with normal or reduced ICP and BP.

CHAPTER V. FINAL DISCUSSION

In the introduction, two questions were posed. The first concerned defining the inherent variability of cerebrovascular pressure transmission in severely head injured patients. The results of that study raised questions which could be better answered from the knowledge gained by attempting to answer the second question. The second question concerned the definition of the relationships between cerebrovascular pressure transmission, craniospinal compliance and cerebrovascular resistance under a series of normal and abnormal physiological conditions. Prior to performing experimental studies aimed at providing an answer to the second question, it was necessary to develop an improved method of measuring craniospinal compliance. This was subsequently validated in both physical and animal experiments. Having applied this improved method of compliance measurement to three sets of experimental studies aimed at answering the second question, it is now appropriate to discuss whether the data obtained from those experimental studies might aid the interpretation of the results obtained from the clinical studies of cerebrovascular pressure transmission.

A. Relationships between Patterns of Cerebrovascular Pressure Transmission in Head Injured Patients and Experimental Animals.

Four forms of cerebrovascular pressure transmission were observed in head injured patients (Figure 21).

1. Curve Type 1 (Flat)

In patients, a flat amplitude transfer function was associated with ICP below 20 mm Hg (mean ICP = 15 mm Hg) and with a negative fundamental phase shift. The data from the intracranial hypertension group of animals (Figure 46) demonstrate that a flat amplitude transfer function was found under craniospinal conditions with ICP less than 15 mm Hg, and was associated with normal craniospinal compliance and cerebrovascular resistance. In this group of animals, under baseline physiological conditions, there was also a negative value of the fundamental phase shift.

In these experimental studies, due to unavoidable CSF leaks during cannulation of the CSF space and placement of blood flow electrodes, it

was necessary to correct for CSF loss. ICP was raised through slow intraventricular infusion of fluid to a baseline of between 10 and 15 mm Hg before starting the experimental protocol. As a result, these experiments may have started with a craniospinal system that was volume loaded. However, Marmarou (41) reported control values for ICP in cats of 15 mm Hg, Sullivan (42) and Shapiro (187) reported baseline values of ICP of 10 mm Hg, and Takizawa (143) found slightly lower mean ICP values of 8 mm Hg. This data would suggest that an artificially adjusted baseline ICP of between 10 and 15 mm Hg represents a close approximation to normal ICP in the cat.

These experimental results would support the hypothesis that the curve type 1 amplitude transfer function found in patients represents normal and not, as previously discussed in chapter 2, reduced cerebrovascular tone. A flat amplitude transfer function indicates equal transmission of all harmonics of the arterial pressure waveform through to the CSF space. In contrast to these results, Portnoy et al (82,106) found an attenuated fundamental harmonic under control conditions. They attributed this form of pressure transmission to functional autoregulatory tone of the precapillary cerebral resistance vessels, proposing that the conversion from an attenuated low frequency transmission to a flat amplitude transfer function was evidence for loss of arteriolar vasomotor tone. Portnoy et al (81,82), however, report a mean ICP level in cats of 4 to 5 mm Hg, which is significantly less than those reported by the other investigators. This difference in ICP level may account for the attenuated low frequency amplitude transfer function demonstrated in their data which they describe as representing a functionally normal cerebrovascular bed. Which in light of their ICP data, may represent the response for a volume depleted craniospinal system. Furthermore, cerebral blood flow was not measured, as a means of assessing autoregulation, in any studies reported by Portnoy and co-workers.

It appears, from these data, that a curve type 1 (flat) amplitude transfer function may indicate, for an ICP in the range of 10 - 15 mm Hg, a functionally normal cerebrovascular bed and not, as indicated by Portnoy, reduced arteriolar vasomotor tone.

2. Curve Type 2 (Elevated Low Frequency)

In patients, this amplitude transfer function curve type was characterized by an elevated low frequency pressure transmission which was most often associated with ICP above 20 mm Hg. It was chiefly the fundamental that was elevated. Furthermore, compared to curve type 1, the fundamental phase shift became more negative. In the experimental work, both the intracranial hypertension group (Figure 46) and arterial hypercarbia group (Figure 47) demonstrated amplitude transfer functions with configuration similar to the curve type 2 transfer function found in patients. However, in the experimental data, the entire amplitude transfer function increased, although the fundamental always showed much greater increase than the higher harmonics. Despite this difference, it is likely that these patterns represent similar forms of cerebrovascular pressure transmission when it is considered that the curve type 2 transfer function shows average data from all patients, whereas in the experimental data, the curves show average data from within single animals.

In the experimental data, the curve type 2 transfer function occurred with intracranial hypertension (> 20 mm Hg), whether ICP was increased through intraventricular infusion or through inhalation of 5% CO2. Associated with these changes craniospinal compliance was decreased and, in the case of the arterial hypercarbia group, cerebrovascular resistance was usually decreased in conjunction with the fundamental phase shift becoming more negative. This more negative phase is consistent with an increase in vascular compliance. This is supported by the work of Ursino (153,154) who demonstrated, in a mathematical model of the human cerebrovascular bed, that the ICP pulse amplitude[74] is dependent on the lumped compliance of the arterial and venous segments of the vascular bed. Ursino's model demonstrated that increased ICP pulse amplitude was associated with increased vascular compliance.

An increased vascular compliance might result from active vasodilation or from loss of autoregulatory vasomotor tone. Loss or impairment of autoregulation does occur widely in head injured adults (175) and children (176,177). The intracranial hypertension group of animals demonstrated this form of elevated low frequency pressure transmission

[74]ICP pulse amplitude is chiefly dependent on the ICP waveform fundamental harmonic component (78).

in the absence of functional autoregulation. Although, the arterial hypercarbia group of animals clearly demonstrated intact CO2 reactivity with 5% CO2 administration. However, the relationship between CBF responsiveness to CO2 and autoregulation is unclear. Harper (189) and Fieschi (171) have reported that loss of autoregulation is often accompanied by loss of CO2 reactivity, although Fieschi reports paradoxical CBF responses to CO2 when autoregulation was impaired. Tuor (188) has shown in rabbits that impairment of autoregulation is preceded by reduced CBF responsiveness to CO2. In contrast to these reports, Ekstöm-Jodal (191) and Raichle (192) have shown that arterial hypercarbia itself can impair autoregulation while CBF responsiveness to CO2 was retained. This was not reproduced by Symon (193) who demonstrated autoregulation was retained during arterial hypercarbia. In light of these conflicting reports, it remains uncertain whether the increased low frequency pressure transmission observed clinically and with the arterial hypercarbia group of animals indicates impaired autoregulation.

It appears, from these data, that the curve type 2 (elevated low frequency) form of cerebrovascular pressure transmission seen in patients is indicative of raised ICP, reduced craniospinal compliance, reduced arteriolar vasomotor tone and increased vascular compliance.

3. Curve Type 3 (Elevated High Frequency)

In patients, a high proportion of amplitude transfer functions (40%) demonstrated elevated high frequency harmonics without an associated increased fundamental. This was mostly associated with an ICP below 20 mm Hg. In the experimental studies, there were no groups of animals that demonstrated exclusively an elevated high frequency response. However, in the clinical study, a positive fundamental phase shift was unique to the amplitude transfer function curve type 3. Experimentally, a positive phase was exclusively associated with the post arterial hypertension stage of the arterial hypertension group of animals where ICP had decreased to below 10 mm Hg, and there was an associated abnormally high craniospinal compliance. As discussed in the last chapter (page 156), this combination of factors may indicate a generalized cerebral vasodilation as a consequence of reduced vasomotor tone.

Both Kasuga et al (87,88) and Bray et al (89,90) have shown that an increase in high frequency pressure transmission may indicate the occurrence of resonance within the craniospinal system. Bray and co-workers have shown that the frequency at which resonance occurs increases with decreased craniospinal compliance as measured by the PVI. These reports would support the hypothesis that an elevated high frequency pressure transmission, as seen with the amplitude transfer function curve type 3, is an indication of the start of a resonant peak in the transfer function, and its detection is indicative of high intracranial compliance. A state of reduced compliance, either with or without raised ICP, will tend to increase the resonant frequency beyond that of the frequency of the 6th harmonic and hence the level of detection by this method.

However, a decrease in the resonant frequency does not necessarily indicate an increased craniospinal compliance. By modelling the craniospinal system as a second order system, containing both a lumped compliance and lumped inertance, it can be shown that the resonant frequency of such a system can decrease through increased compliance or through increased inertance[75]. The positive phase shift seen with this form of pressure transmission would indicate that a greatly increased inertance and not compliance may be the dominant factor determining the resonant frequency.

It appears, from these data, that the interpretation of this form of pressure transmission has changed from that discussed in chapter 2. A curve type 3 amplitude transfer function, despite being associated with low ICP, may indicate high craniospinal compliance and a generalized cerebral vasodilation.

4. Curve Type 4 (Elevated Low and High Frequency)

In patients, this group was the smallest in number and most often associated with ICP raised above 20 mm Hg (Figure 21). Similar to the curve type 2 transfer function, there was a more negative fundamental

---

[75]A second order system will contain two reactive terms: capacitance or compliance (C) and inductance or inertance (L). The resonant frequency (fo) of such a system can be calculated from the formula: $fo = 1/(2\pi\sqrt{(LC)})$. The resonant frequency of the system will therefore decrease if either L or C increases (142).

phase shift compared to curve type 1. In the experimental studies, there were no animals that demonstrated an equivalent form of pressure transmission. However, with the intracranial hypertension group of animals, the fundamental often increased in combination with all higher harmonics and was associated with raised ICP, decreased craniospinal compliance and a negative fundamental phase shift.

It would appear, following on from the previous discussion, that the curve type 4 amplitude transfer function may indicate decreased cerebrovascular resistance, increased vascular compliance and decreased craniospinal compliance.

B. Recommendations for Future Research

1) The clinical studies described in chapter two, demonstrated clearly definable patterns of cerebrovascular pressure transmission in head injured patients. However, the observational design of that study with waveform sampling only once every 30 minutes, makes it difficult to comment on the temporal relationships between the observed amplitude transfer function curve types and raised ICP. Certain forms of cerebrovascular pressure transmission may be predictive of raised ICP or of its underlying cause. To investigate this, a further clinical study is required using on-line minute by minute analysis of cerebrovascular pressure transmission in head injured patients. Such a study would ideally measure, concurrently with cerebrovascular pressure transmission, craniospinal compliance and either cerebrovascular resistance or flow/metabolism coupling as a means of identifying autoregulation.

2) The SPR method of measuring craniospinal compliance, was designed for measuring compliance in the experimental studies in cats, but may, with some modification of the technique, be applicable clinically. The method has been shown in both physical and animal models to be less variable than the VPR method. The automatic nature of the technique which requires less operator intervention, may reduce the risk of infection to the patient. Similarly, the smaller volume injection with the SPR method, which is subsequently withdrawn, should be less likely to precipitate a secondary rise in ICP. Further developmental work is needed to design a unit based on a single ventricular access device which would allow simultaneous pressure pulse application and recording of the intracranial pressure response. Such a unit, if feasible, should undergo further experimental validation in animals, particularly with regard to its safety, before it is tested on patients.

3) The experimental work described in chapter four of this thesis should be extended. The intracranial hypertension group of animals failed to show functional autoregulation to reduced CPP. Furthermore, two of the four animals in the arterial hypercarbia group produced unique compliance responses to inhalation of 10% CO2 gas. The data from these animals turned out to be the most helpful and important

because a study of cerebrovascular pressure transmission under conditions of abnormal autoregulation is just as important clinically as it would be with normal autoregulation. A further study investigating the relationship between intracranial hypertension, cerebrovascular pressure transmission, craniospinal compliance and cerebrovascular resistance should be performed in a group of animals with functional autoregulation. Additional experiments in the arterial hypercarbia group should be performed to investigate further the unique compliance response obtained with 10% CO2 administration.

REFERENCES

1) Mellander S, Johansson B "Control of resistance, exchange, and capacitance functions in the peripheral circulations." Pharmacol Rev 1968;20:117-196.

2) Masserman J H, "Intracranial hydrodynamics: Central nervous system shock and edema following rapid fluid decompression of ventriculo-subarachnoid spaces." J Nerv Ment Dis 1935;80:138-158.

3) Stern W E, "Intracranial fluid dynamics. The relationship of intracranial pressure to the Monro-Kellie doctrine and the reliability of pressure assessment." J Royal College Surgeons Edinburgh 1963;9:18-36.

4) Langfitt T W, "Increased intracranial pressure." Clin Neurosurg 1969;16:436-471.

5) Monro A, "Observations on the structure and function of the nervous system." Creech and Johnston, Edinburgh, 1783.

6) Kellie G, "An account of the appearances observed in the dissection of two of three individuals presumed to have perished in the storm of the third and whose bodies were discovered in the vicinity of Leith on the morning of the 4th, November 1821, with some reflections on the pathology of the brain." Trans Med Chir Soc Edinb 1824;1:84-169.

7) Burrows G, "On disorders of the cerebral circulation and on the connection between affections of the brain and diseases of the heart." Longmans, London, 1846.

8) Weed L H, McKibben P S, "Pressure changes in cerebrospinal fluid following intravenous injection of solutions of various concentrations." Am J Physiol 1919;48:512-530.

9) Weed L H, "Some limitations of the Monro-Kellie hypothesis." Arch Surg 1929;18:1049-1068.

10) Kocher T, "Hirnerschutterung, Hirndruck und chirurgische Eingriffe bein Hirnerkrankungen." In: "Nothnagel: Spezielle Pathologie und Therapie." Vienna, 1901.

11) Duret H, "Etudes experimentales et cliniques sur les traumatismes cerebraux." Paris, 1878.

12) Cushing H, "Concerning a definite regulatory mechanism of the vasomotor centre which controls blood pressure during cerebral compression." Johns Hopk Hosp Bull 1901;12:290-292.

13) Cushing H, "Some experimental and clinical observations concerning states of increased intracranial tension." Am J Med Sci 1902;124:375-400.

14) Cushing H, "The blood pressure reaction of acute cerebral compression, illustrated by cases of intracranial haemorrhage." Am J Med Sci 1903;125:1017-1044.

15) Johnston R T, Yates P O, "Brain stem haemorrhages in expanding supratentorial conditions." Acta Radiol 1956;46:250-256.

16) Jennet W B, "Experimental brain compression." Arch Neurol 1961;4:599-607.

17) Browder J, Meyers R, "Observations on behaviour of the systemic blood pressure, pulse and spinal fluid pressure following craniocerebral injury." Am J Surg 1936;31:403-427.

18) Smyth C E, Henderson W R, "Observations on the cerebrospinal fluid pressure on simultaneous ventricular and lumbar punctures." J Neurol Psychiat 1938;1:226-237.

19) Evans J P, Espey F F, Kristoff F V, Kimball F D, Ryder H W, "Experimental and clinical observations on rising intracranial pressure." Arch Surg 1951;63:107-114.

20) Ayala G, "Uber den diagnostischen Wert des Liquordruckes und einen Apparat zu seiner Messung." Z Ges Neurol Psychiat 1923;84:42-95.

21) Ayala G, "Die Physiopathologie der Mechanik des Liquor cerebrospinalis und der Rachidealquotient." Mschr Psychiat Neurol 1925;58:65-105.

22) Weed L H, Flexner L B, Clark J H, "The effect of dislocation of cerebrospinal fluid upon its pressure." Am J Physiol 1932;100:246-261.

23) Weed L H, Flexner L B, "Cerebrospinal elasticity in the cat and macaque." Am J Physiol 1932;101:668-677.

24) Flexner L B, Clark J H, Weed L H, "The elasticity of the dural sac and its contents." Am J Physiol 1932;101:292-303.

25) Flexner L B, Weed L H, "Factors concerned in positional alterations of intracranial pressure." Am J Physiol 1933;104:681-692.

26) Masserman J H, "Cerebrospinal hydrodynamics IV: Clinical experimental studies." Arch Neurol Psychiat 1934;32:523-553.

27) Masserman J H, "Cerebrospinal hydrodynamics V: Studies of the volume elasticity of the human ventriculo-subarachnoid system." J Comp Neurol 1935;61:543-552.

28) Ryder H W, Espey F F, Kimbell F D, Penka E J, Rosenauer A, Posolsky B et al, "The elasticity of the craniospinal venous bed." J Lab Clin Med 1953;42:944.

29) Ryder H W, Espey F F, Kristoff F V, Evans P P, "Observations on the interrelationships of intracranial pressure and cerebral blood flow." J Neurosurg 1951;8:46-58.

30) Bayliss W M, Hill L, Gulland G L, "On intracranial pressure and the cerebral circulation." J Physiol 1895;18:334-362.

31) Lundberg N, "Continuous recording and control of ventricular fluid pressure in neurosurgical practice." Acta Psychiat Neurol Scand 1960;36;suppl:149

32) Lundberg N, Troupp H, Lorin H, "Continuous recording of the ventricular fluid pressure in patients with severe acute traumatic brain injury." J Neurosurg 1965;22:581-590.

33) Johnston I H, Johnston J J, Jennett W B, "Intracranial pressures following head injury." Lancet 1970;2:433-436.

34) Richardson A, Hide T A H, Eversden I D, "Long-term continuous intracranial pressure monitoring by means of a modified subdural pressure transducer." Lancet 1970;2:687-689.

35) Langfitt T W, Kumar V S, James H E, Miller J D, "Continuous recording of intracranial pressure in patients with hypoxic brain damage." In: "Brain Hypoxia." Brierley J S, Meldrum B S (eds). Heinemann:London, 1974; pp 118-135.

36) Johnston I H, Paterson A, "Benign intracranial hypertension:aspects of diagnosis and treatment." In: "Optic Nerve." Cant J S (ed). Himpton:London, 1972;pp 155-165.

37) Langfitt T W, Weinstein J D, Kassell N F, Simeone F A, "Transmission of increased intracranial pressure I: within the craniospinal axis." J Neurosurg 1964;21:989-997.

38) Langfitt T W, Weinstein J D, Kassell N F, Gagliardi L J, "Transmission of increased intracranial pressure II: within the supratentorial space. J Neurosurg 1964;21:998-1005.

39) Langfitt T W, Weinstein J D, Kassel N F, "Cerebral vasomotor paralysis produced by intracranial hypertension." Neurology 1965;15:622-641.

40) Marmarou A, "A theoretical and experimental evaluation of the cerebrospinal fluid system, PhD Thesis, Drexel University, 1973.

41) Marmarou A, Shulman K, LaMorgese J, "Compartmental analysis of compliance and outflow resistance of the cerebrospinal fluid system." J Neurosurg 1975;43:523-534.

42) Sullivan H G, Miller J D, Becker D P, Flora R E, Allen G A, "The physiological basis of intracranial pressure change with progressive epidural brain compression." J Neurosurg 1977;47:532-550.

43) Takagi H, Walstra G, Marmarou A, Shulman K, "The effect of blood pressure and PaCO2 upon bulk compliance (PVI)." In: "Intracranial Pressure IV." Lundberg N, Ponten U, Brock M (eds). Springer-Verlag:Berlin Heidelberg New York, 1980;pp 163-166.

44) Kosteljanetz M, "Pressure-volume conditions in patients with subarachnoid and or intraventricular haemorrhage. J Neurosurg 1985;63:398-403.

45) Shapiro K, Fried A, Takai F, Kohn I, "Effect of the skull and dura on neural axis pressure-volume relationships and CSF hydrodynamics. J Neurosurg 1985;63:75-81.

46) Takizawa H, Gabra-Sanders T, Miller J D, "Analysis of changes in intracranial pressure and pressure-volume index at different locations in the craniospinal axis during supratentorial epidural balloon inflation." Neurosurgery 1986;19:1-8.

47) Shapiro K, Marmarou A, "Clinical applications of the pressure-volume index in treatment of pediatric head injuries." J Neurosurg 1982;56:819-825.

48) Tans J T, Poortvliet D C, "Intracranial volume-pressure relationship in man. Part 2: Clinical significance of the pressure-volume index." J Neurosurg 1983;59:810-816.

49) Miller J D, Garibi J, "Intracranial volume/pressure relationships during continuous monitoring of ventricular fluid pressure." In: "Intracranial pressure." Brock M, Dietz H (eds). Springer:Berlin, 1972;pp 270-274.

50) Miller J D, Garibi J, Pickard J D, "Induced changes of cerebrospinal fluid volume: effects during continuous monitoring of ventricular fluid pressure. Arch Neurol 1973;28:265-269.

51) Miller J D, Pickard J D, "Intracranial volume/pressure studies in patients with head injury." Injury 1974;5:265-268.

52) Miller J D, "Volume and pressure in the craniospinal axis." Clin Neurosurg 1975;22:76-105.

53) Miller J D, Leech P J, Pickard J D, "Volume pressure response in various experimental and clinical conditions." In: "Intracranial Pressure II." Lundberg N, Ponten U, Brock M (eds). Springer-Verlag:Berlin Heidelberg New York, 1975;pp 97-99.

54) Hase U, Reulen H J, Meinig G, Schürmann K, "The influence of the decompressive operation on the intracranial pressure and the pressure volume relation in patients with severe head injuries." Acta Neurochir 1978;45:1-13.

55) Löfgren J, "Pressure-volume relationships of the cerebrospinal fluid system." Thesis, University of Goteborg, 1973.

56) Löfgren J, Essen C von, Zwetnow N N, "The pressure-volume curve of the cerebrospinal fluid space in dogs." Acta Neurol Scand 1973;49:557-574.

57) Löfgren J, Zwetnow N N, "Cranial and spinal components of the cerebrospinal fluid pressure-volume curve." Acta Neurol Scand 1973;49:575-585.

58) Löfgren J, Zwetnow N N, "Intracranial blood volume and its variation with changes in intracranial pressure." In: "Intracranial pressure III." Beks J W F, Bosch D A, Brock M (eds). Springer-Verlag:Berlin Heidelberg New York, 1976;pp 25-28.

59) Gray W J, Rosner M J, "Pressure-volume index as a function of cerebral perfusion pressure. Part 1: The effects of cerebral perfusion pressure changes and anaesthesia." J Neurosurg 1987;67:369-376.

60) Gray W J, Rosner M J, "Pressure-volume index as a function of cerebral perfusion pressure. Part 2: The effects of low cerebral pressure and autoregulation." J Neurosurg 1987;67:377-380.

61) Marmarou A, Maset A L, Ward J D, Choi S, Brooks D, Lutz H A et al, "Contribution of CSF and vascular factors to elevation of ICP in severely head-injured patients." J Neurosurg 1987;66:883-890.

62) Anile C, Portnoy H D, Branch C, "Intracranial compliance is time-dependent." Neurosurgery 1987;20:389-395.

63) Heifetz M D, Weiss M, "Detection of skull expansion with increased intracranial pressure. J Neurosurg 1981;55:811-812.

64) Chopp M, Portnoy H D, "Hydraulic model of the cerebrovascular bed: An aid to understanding the volume-pressure test." Neurosurgery 1983;13:5-11.

65) Zee C M, Shapiro K, "The viscoelasticity of normal and hydrocephalic brain tissue." In: "Intracranial Pressure VII." Hoff J T, Betz A L (eds). Springer-Verlag:Berlin Heidelberg, 1989;pp 263-266.

66) Walsh E K, Schettini A, "Brain tissue elasticity and CSF elastance." In: "Intracranial Pressure VII." Hoff J T, Betz A L (eds). Springer-Verlag:Berlin Heidelberg, 1989;pp 271-274.

67) Van Harreveld A, Ochs S, "Cerebral impedance changes after circulatory arrest." Am J Physiol 1956;187:180-192.

68) Wyler G R, Kely W, "Use of antibiotics with external ventriculosomies." J Neurosurg 1972;37:185-187.

69) Troupp H, McDowell D G, "Summary of session on patient management." In: "Intracranial Pressure III." Beks J W F, Bosch D A, Brock M (eds). Springer-Verlag:Berlin Heidelberg New York, 1976; pp 279-280.

70) Avezaat C J J, Van Eijndhoven J H M, "Cerebrospinal fluid pulse pressure and craniospinal dynamics: A theoretical, clinical and experimental study." Thesis, Erasmus University, Rotterdam, 1984.

71) Langfitt T W, "Intracranial volume-pressure relationship." In: "Intracranial Pressure II." Lundberg N, Ponten U, Brock M (eds). Springer-Verlag:Berlin Heidelberg New York,1975;pp 69-76.

72) Leyden E, "Beitrage und Untersuchungen zur Physiologie und Pathologie des Gehirns. Über Hirndurck und Hirnbewegungen." Virchows Arch 1866;37:519-559.

73) Avezaat C J J, Van Eijndhoven J H M, Wyper D J, "Cerebrospinal fluid pulse pressure and intracranial volume-pressure relationships." J Neurol Neurosurg Psychiat 1979;42:687-700.

74) Szewczykowski J, Sliwka S, Kunicki A, Dytko P, Dorsak-Sliwka J, "A fast method of estimating the elastance of the intracranial system. J Neurosurg 1977;47:19-26.

75) Wocjan J, Roszkowski M, Sliwka S, Batorski L, Pawlowski G, "Analysis of CSF dynamics by computerized pressure-elastance resorption test in hydrocephalic children. Indications for surgery." Childs Nerv Syst 1986;2:98-100.

76) Batorski L, Czosnyka M, Wollk-Laniewski P, Zaworski W, "Application of advanced forms of intracranial pressure analysis in craniosynostosis." In: "Intracranial Pressure VII." Hoff J T, Betz A L (eds). Springer-Verlag:Berlin Heidelberg, 1989;pp 189-192.

77) Czosnyka M, Wollk-Laniewski P, Batorski L, Zaworski W, Nita C, "Remarks on amplitude-pressure characteristic phenomenon." In: "Intracranial Pressure VII." Hoff J T, Betz A L (eds). Springer-Verlag:Berlin Heidelberg, 1989;pp 255-259.

78) Chopp M, Portnoy H, "Systems analysis of intracranial pressure. Comparison with volume-pressure test and CSF-pulse amplitude analysis." J Neurosurg 1980;53:516-527.

79) Marmareliz PZ, Marmareliz VZ, In: "Analysis of physiological systems: The white noise approach." Plenum:New York, 1987, pp 1-128.

80) Press W H, Flannery B P, Teukolsky S A, Vetterling W T, "Numerical Recipes. The art of scientific computing." Cambridge University Press, 1987, pp 381-453.

81) Portnoy H D, Chopp M, "Cerebrospinal fluid pulse wave form analysis during hypercapnia and hypoxia." Neurosurgery 1981;9:14-27.

82) Portnoy H D, Chopp M, Branch C, Shannon M B, "Cerebrospinal fluid pulse waveform as an indicator of cerebral autoregulation." J Neurosurg 1982;56:668-678.

83) Portnoy H D, Branch C, Chopp M, "The CSF pulse wave in hydrocephalus." Childs Nerv Syst 1985;1:248-254.

84) Branch C A, Chopp M, Portnoy H D, "Fourier analysis of intracranial pressures during experimental intracranial hypertension." In: "Intracranial Pressure VII." Hoff J T, Betz A L (eds). Springer-Verlag:Berlin Heidelberg, 1989;pp 175-180.

85) Takizawa H, Gabra-Sanders T, Miller J D, "Changes in the cerebrospinal fluid pulse wave spectrum associated with raised intracranial pressure." Neurosurgery 1987;20:355-361.

86) Takizawa H, Gabra-Sanders T, Miller J D, "Spectral analysis of the CSF pulse wave at different locations in the craniospinal axis." J Neurol Neurosurg Psychiat 1986;49:1135-1141.

87) Kasuga Y, Nagai H, Hasegawa Y, Nitta M, "Transmission characteristics of pulse waves in the intracranial cavity of dogs." J Neurosurg 1987;66:907-914.

88) Kasuga Y, Nagai H, Hasegawa Y, "Transmission characteristics of pulse waves in the intracranial cavity of dogs during normal intracranial condition, intracranial hypertension, hypercapnia and hydrocephalus." In: "Intracranial Pressure VII." Hoff J T, Betz A L (eds). Springer-Verlag:Berlin Heidelberg, 1989;pp 196-200.

89) Bray R S, Sherwood A M, Halter J A, Robertson C, Grossman R G, "Development of a clinical monitoring system by means of ICP waveform analysis." In: "Intracranial Pressure VI." Miller J D, Teasdale G M, Rowan J O (eds). Springer-Verlag:Berlin Heidelberg New York Tokyo, 1986;pp 260-264.

90) Robertson C S, Narayan R K, Contant C F, Grossman R G, Gokaslan Z L, Pahwa R, et al, "Clinical experience with a continuous monitor of intracranial compliance." J Neurosurg 1989;71:673-680.

91) Fry D L, "Physiological recording by modern instruments with particular reference to pressure recording." Physiol Rev 1960;40:753-788.

92) Geddes L A, "The direct and indirect measurement of blood pressure." Year Book Publications:Chicago,1970.

93) Gabe I T, "Pressure measurement in experimental physiology." In: "Cardiovascular fluid dynamics." Academic Press:London, 1972.

94) Frank O, "Kritik der elastischen Manometer." Z Biol 1903;44:445-613.

95) Hanson A T, Warburg E, "The theory for elastic liquid membrane manometers. General Part." Acta Physiol Scand 1950;306-343.

96) Allan M W B, Gray W M, Asbury A J, "Measurement of arterial pressure using catheter-transducer systems: Improvement using the accudynamic." Br J Anaesth 1988;60:413-418.

97) Stremler F G, "Introduction to communication systems." Addison Wesley Press, 1979, pp 11-132.

98) Cooley J W, Tukey J W, "An algorithm for the machine calculation of complex Fourier series." Math of Comput 1965;19:297-301.

99) Snedecor G W, Cochran W G, "Statistical methods." Iowa State University Press. 1982, pp 37.

100) Schwartz M, Shaw L, "Signal processing, discrete spectral analysis, detection and estimation." McGraw-Hill, 1975, pp. 33-43, pp. 150-153.

101) Hirai O, Handa H, Ishikawa M, Kim S, "Epidural pulse waveform as an indicator of intracranial pressure dynamics." Surg Neurol 1984;21:67-74.

102) Cooper K R, Boswell P A, Choi S C, "Safe use of PEEP in patients with severe head injury." J Neurosurgery 1985;63:552-555.

103) Dearden N M, "Management of raised intracranial pressure after severe head injury." Br J Hosp Med 1986;Aug:94-103.

104) Gooding C A, Stimac G K, "Jugular vein obstruction caused by turning of the head." AJR 1984;142:403-406.

105) Cowan F, Thoresen M, "Changes in superior sagittal sinus blood velocities due to postural alterations and pressure on the head of the newborn infant." Pediatrics 1985;75:1038-1047.

106) Portnoy H D, Chopp M C, Branch C, "Hydraulic model of autoregulation and the cerebrovascular bed: The effects of altering systemic arterial pressure." Neurosurgery 1983;13:482-497.

107) Miller J D, Bell B A, "Cerebral blood flow variations with perfusion pressure and metabolism" In: "Cerebral Blood Flow: Physiologic and Clinical Aspects." Wood J (ed). McGraw-Hill:New York 1987;pp:119-130.

108) Portnoy H D, "CSF pulse wave. ICP and autoregulation." J Pediatric Neurosciences 1988;4:227-250.

109) Cardosa E R, Piatek D, "Intracranial and venous pressures. Part 1:Intracranial pulse wave changes during hemodynamic manoeuvres in humans." In: "Intracranial Pressure VII." Hoff J T, Betz A L, (eds). Springer-Verlag:Berlin Heidelberg New York Tokyo, 1989;pp 203-205.

110) Guinane J E, "An equivalent circuit analysis of cerebrospinal fluid hydrodynamics." Am J Physiol 1972;223:425-430.

111) Sklar F H, Beyer C W, Clark W K, "Physiological features of the pressure-volume function of brain elasticity in man." J Neurosurg 1980;53:166-172.

112) Sahay K B, Kothiyal K P, Banarjee A K, "A finite deformation model of infantile hydrocephalus." Int J Neurosci 1988;40:19-29.

113) Giddens D P, Kitney R I, "Neonatal heart rate variability and its relation to respiration." J Theor Biol 1985;113:759-780.

114) Branch C A, Chopp M, Portnoy H D, "Single pulse spectral analysis of intracranial pressures." In: "Intracranial Pressure VII." Hoff J T, Betz A L, (eds). Springer-Verlag:Berlin Heidelberg New York Tokyo, 1989;pp 172-174.

115) Lowensohn R I, Weiss M, Hon E H, "Heart-rate variability in brain damaged adults." Lancet 1977;March:626-628.

116) Leipzig T J, Lowensohn R I, "Heart rate variability in neurosurgical patients." Neurosurgery 1986;19:356-362.

117) O'Rourke M F, Taylor M G, "Vascular impedance of the femoral bed." Circ Res 1966;18:126-139.

118) Antoni N, "Pressure curves from the cerebrospinal fluid." Acta Med Scand 1946;170:439-462.

119) O'Connell J E A, "The vascular factor in intracranial pressure and the maintenance of the cerebrospinal fluid circulation." Brain 1943;66:204-228.

120) Goldensohn E S, Whitehead R W, Parry T M, Spencer J N, Grover R F, Draper W B, "Studies on diffusion respiration. IX. Effect of diffusion respiration and high concentrations of CO2 on cerebrospinal fluid pressure of anaesthetized dogs." Am J Physiol 1951;165:334-340.

121) Bering E A, "Choroid plexus and arterial pulsation of cerebrospinal fluid." Arch Neurol Psychiat 1955;73:165-172.

122) Dunbar H S, Guthrie T C, Karpell B, "A study of the cerebrospinal fluid pulse wave." Arch Neurol 1966;14:624-630.

123) Du Boulay G H, "Pulsatile movements in the CSF pathways." Br J Radiol 1966;39:255-262.

124) Hamit H F, Beall A C, De Bakey M E, "Hemodynamic influences upon brain and cerebrospinal fluid pulsations and pressures." J Trauma 1965;5:174-184.

125) Portnoy H D, "The CSF pulse wave in hydrocephalus (letter)." Child's Nerv Syst 1986;2:107-108.

126) Chopp M, Portnoy H D, Branch C, "Hydraulic model of the cerebrovascular bed: an aid to understanding the volume pressure test." Neurosurgery 1983;13:1-11.

127) Adolph R J, Fukusumi H, Fowler N O, "Origin of cerebrospinal fluid pulsations." Am J Physiol 1967;212:840-846.

128) Dardenne G, Dereymaeker A, Lacheron J M, "Cerebrospinal fluid pressure and pulsatility." Europ Neurol 1969;2:193-216.

129) Dereymaeker A, Stevens A, Rombouts J J, Lacheron J M, Pierquin A, "Study on the influence of the arterial pressure upon the morphology of cisternal CSF pulsations." Europ Neurol 1971;5:107-114.

130) Yano M, Ikeda Y, Kobayashi S, Otsuka T, "Intracranial pressure in head-injured patients with various intracranial lesions is identical throughout the supratentorial intracranial compartment." Neurosurgery 1987;21:688-692.

131) Broaddus W C, Pendleton G A, Delashaw J B, Short R V, Kassell N F, Grady M S, et al," Differential intracranial pressure recordings in patients with dual ipsilateral monitors." In: "Intracranial Pressure VII." Hoff J T, Betz A L (eds). Springer-Verlag:Berlin Heidelberg, 1989;pp 41-44.

132) Mendelow A D, Rowan J O, Murray L, Ker A E, "A clinical comparison of subdural screw pressure measurements with ventricular pressure." J Neurosurg 1983;58:45-50.

133) Njemanze P C, Beck O J, "MR-gated intracranial CSF dynamics: evaluation of CSF pulsatile flow." AJNR 1989;10:77-80.

134) Wachi A, Marmarou A, "Clinical evaluation of a fibreoptic device for measuring PVI." In: "Intracranial Pressure VII." Hoff J T, Betz A L (eds). Springer-Verlag:Berlin Heidelberg, 1989;pp 55-57.

135) Dearden N M, "Intracranial pressure monitoring." Care of the critically ill 1985;1:8-13.

136) Marshall L F, Zovickian J, Ostrup R, Seelig J M, "Multiple simultaneous recordings of ICP in patients with acute mass lesions." In: "Intracranial Pressure VI." Miller J D, Teasdale G M, Rowan J O (eds). Springer-Verlag:Berlin Heidelberg New York Tokyo, 1986;pp 184-186.

137) Piper I R, Dearden N M, Leggate J R S, Robertson I, Miller J D, "Methodology of spectral analysis of the intracranial pressure waveform in a head injury intensive care unit." In: "Intracranial Pressure VII." Hoff J T, Betz A L (eds). Springer-Verlag:Berlin Heidelberg, 1989;pp 668-671.

138) Dearden N M, Miller J D, "Paired comparison of hypnotic and osmotic therapy in the reduction of intracranial hypertension after severe head injury." In: "Intracranial Pressure VII." Hoff J T, Betz A L (eds). Springer-Verlag:Berlin Heidelberg, 1989;pp 474-481.

139) Burke A M, Quest D O, Chien S, et al, "The effects of mannitol on blood viscosity." J Neurosurg 1981;55:550-553.

140) Borgensen S E, Christensen L, "Analysis of the power spectrum of the pulse pressure wave during induced intracranial hypertension in humans." In: "Intracranial Pressure VII." Hoff J T, Betz A L (eds). Springer-Verlag:Berlin Heidelberg, 1989;pp 181-183.

141) Piper I R, Dearden N M, Miller J D, "Can waveform analysis of ICP separate vascular from non-vascular causes of intracranial hypertension?" In: "Intracranial Pressure VII." Hoff J T, Betz A L (eds). Springer-Verlag:Berlin Heidelberg, 1989;pp 157-163.

142) Malvino A P, "Electronic principles." McGraw-Hill:New York, 1979;pp 9-11.

143) Takizawa H, Gabra-Sanders T, Miller J D, "Variations in pressure-volume index and CSF outflow resistance at different locations in the feline craniospinal axis." J Neurosurg 1986;64:298-303.

144) Mackenzie E T, Strandgaard S, Graham D I, Jones J V, Harper A M, Farrar J K, "Effects of acutely induced hypertension in cats on pial arteriolar calibre, local cerebral blood flow, and the blood-brain barrier." Circ Res 1976;39:33-41.

145) Brown A W, Brierley J B," The nature, distribution and earliest stages of anoxic-ischemic nerve cell damage in the rat brain as defined by the optical microscope." Br J Exp Path 1968;49:87-106.

146) Whittle I R, "The contribution of secondary mediators to the etiology and pathophysiology of brain oedema: experimental studies using an infusion model." PhD Thesis, 1989, University of Edinburgh.

147) Marmarou A, Shulman K, Rosende R M, "A non-linear analysis of the cerebrospinal fluid system and intracranial pressure dynamics." J Neurosurg 1978;48:332-344.

148) Shapiro K, Fried A, "Pressure-volume relationships in shunt-dependent childhood hydrocephalus. The zone of instability in children with acute deterioration." J Neurosurg 1986;64:390-396.

149) Guinane J E, "An equivalent circuit analysis of cerebrospinal fluid hydrodynamics." Am J Physiol 1972;223:425-430.

150) Takemae T, Kosugi Y, Ikebe J, Kumagai Y, Masuyama K, Saito H, "A simulation study of intracranial pressure increment using an electrical circuit model of cerebral circulation." IEEE Trans Biomed Eng 1987;34:958-62.

151) Hoffmann O, "Biomathematics of intracranial CSF and Haemodynamics. Simulation and analysis with the aid of a mathematical model." Acta Neurochir Suppl 1987;40:117-130.

152) Sorek S, Bear J, Karni Z, "A non-steady compartmental flow model of the cerebrovascular system." J Biomech 1988;21:695-704.

153) Ursino M, "A mathematical study of human intracranial hydrodynamics. Part 1. The cerebrospinal fluid system pulse pressure." Ann Biomed Eng 1988;16:379-401.

154) Ursino M, "A mathematical study of human intracranial hydrodynamics. Part 2. Simulation of clinical tests." Ann Biomed Eng 1988;16:403-416.

155) Pasztor E, Symon L, Dorsch N W C, Branston N M, "The hydrogen clearance method in assessment of blood flow in cortex, white matter and deep nuclei of baboons." Stroke 1973;4:556-567.

156) Young W, "H2 clearance measurement of blood flow: A review of technique and polarographic principles." Stroke 1980;11:552-564.

157) Farrar J K, "Hydrogen clearance technique.", In: "Cerebral Blood Flow. Physiologic and Clinical Aspects." Wood J H (ed). McGraw-Hill:New York, 1986;pp 275-287.

158) Piper I R, Guha A, Tator C H, Gentles W, "A microcomputer system for on-line collection of blood flow and related physiological data." Comput Biol Med 1987;14:279-291.

159) Permutt S, Riley R L, "Hemodynamics of collapsible vessels with tone: the vascular waterfall." J Appl Physiol 1963;18:924-932.

160) Miller J D, "Intracranial pressure and cerebral blood flow." PhD thesis, University of Glasgow, 1973.

161) Geddes L A, Baker L E, "Principles of applied biomedical instrumentation." Wiley:New York;1968;pp 446-467.

162) Latimer K E, "The transmission of sound waves in liquid-filled catheter tubes used for intravascular blood-pressure recording." Med & Biol Eng 1968;6:29-42.

163) McPherson R W, Koechler R C, Traystman R J, "Effect of jugular venous pressure on cerebral autoregulation in dogs." Am J Physiol 1988;255:H1516-1524.

164) Langfitt T W, Weinstein J D, Kassell N F, Gagliardi L J, Shapiro H M, "Compression of cerebral veins by intracranial hypertension. I:dural sinus pressures." Acta Neurochir 1966;15:215-222.

165) Shapiro H M, Langfitt T W, Weinstein J D, "Compression of cerebral veins by intracranial hypertension. II: morphological evidence for collapse of vessels." Acta Neurochir 1966;15:223-232.

166) Osterholm J L, "Reaction of the cerebral venous sinus system to acute intracranial hypertension." J Neurosurg 1970;32:654-659.

167) Yada K, Nakagawa Y, Tsuru M, "Circulatory disturbance of the venous system during experimental intracranial hypertension." J Neurosurg 1973;39:723-729.

168) Nakagawa Y, Tsura M, Yada K, "Site and mechanism for compression of the venous system during experimental intracranial hypertension." J Neurosurg 1974;41:427-434.

169) Tuor U I, Farrar J K, "Contribution of the inflow arteries to alterations in total cerebrovascular resistance in the rabbit." Pflugers Arch 1985;403:283-288.

170) Auer L M, Ishiyama N, Pucher R, "Cerebrovascular response to intracranial hypertension." Acta Neurochir 1987;84:124-128.

171) Fieschi C, Agnoli A, Battastini N, Bozzao L, Prencipe M, "Derangements of regional cerebral blood flow and of its regulatory mechanisms in acute cerebrovascular lesions." Neurology 1968;18:1166-1179.

172) Waltz A G, "Effect of blood pressure on blood flow in ischemic and in non-ischemic cerebral cortex; the phenomena of autoregulation and luxury perfusion." Neurology 1968;18:613-621.

173) Reivich M, "Arterial PCO2 and cerebral hemodynamics." Am J Physiol 1964;206:25-30.

174) Harper A M, "Autoregulation of cerebral blood flow: influence of arterial blood pressure on the blood flow through the cerebral cortex." J Neurol Neurosurg Psychiat 1966;29:398-403.

175) Obrist W D, Langfitt T W, Jaggi J L, Cruz J, Gennarelli T A, "Cerebral blood flow and metabolism in comatose patients with acute head injury. Relationship to intracranial hypertension." J Neurosurg 1984;61:241-253.

176) Muizelaar J P, Marmarou A, DeSalles A A, Ward J D, Zimmerman R S, Li Z, et al, "Cerebral blood flow and metabolism in severely head-injured children. Part 1: Relationship with GCS score, outcome, ICP and PVI." J Neurosurg 1989;71:63-71.

177) Muizelaar J P, Ward J D, Marmarou A, Newlon P G, Wachi A, "Cerebral blood flow and metabolism in severely head-injured children. Part 2: Autoregulation. J Neurosurg 1989;71:72-76.

178) Guerci A D, Shi A Y, Levin H, Tsitlik J, Weisfeldt M L, Chandra N, "Transmission of intrathoracic pressure to the intracranial space during cardiopulmonary resuscitation in dogs." Circ Res 1985;56:20-30.

179) Anile C, Maira G, Mangiola A, Rossi G F, "Normal pressure hydrocephalus: a retrospective study on clinico-radiological data, CSF dynamics and CSF pulse waveform morphology." In: "Intracranial Pressure VII." Hoff J T, Betz A L (eds). Springer-Verlag:Berlin Heidelberg, 1989;pp 186-188.

180) Anile C, Mangiola A, Andreasi F, Branch C A, Portnoy H D, "CSF pulse waveform morphology as an indicator of intracranial system impedance: an experimental study." In: "Intracranial Pressure VII." Hoff J T, Betz A L (eds). Springer-Verlag:Berlin Heidelberg, 1989;pp 193-1195.

181) Pfenninger E, Grunert A, Bowdler I, Kilian J, "The effect of ketamine on intracranial pressure during haemorrhagic shock under the conditions of both spontaneous breathing and controlled ventilation." Acta Neurochir 1985;78:113-118.

182) Cox R H, "Influence of chloralose anaesthesia on cardiovascular function in trained dogs." Am J Physiol 1972;223:660-667.

183) Van Aken H, Puchstein C, Anger C, Heinecke A, Lawin P, "Changes in intracranial pressure and compliance during adenosine triphosphate-induced hypotension in dogs." Anesth Analg 1984;63:381-385.

184) Olesen J, "Effect of intracarotid epinephrine, norepinephrine and angiotensin on the regional cerebral blood flow in man." Neurology 1972;22:978-987.

185) Dinsdale H B, Robertson D M, Hass R A, "Cerebral blood flow in acute hypertension." Arch Neurol 1974;31:80-87.

186) Strandgaard S, Mackenzie E T, Jones J V, Harper A M, "Studies on the cerebral circulation of the baboon in acutely induced hypertension." Stroke 1976;7:287-290.

187) Shapiro K, Takei F, Fried A, Kohn I, "Experimental feline hydrocephalus. The role of biomechanical changes in ventricular enlargement in cats." J Neurosurg 1985;63:82-87.

188) Tuor U I, Farrar J K, "Pial vessel calibre and cerebral blood flow during haemorrhage and hypercapnia in the rabbit." Am J Physiol 1984;247:H40-H51.

189) Harper A M, Glass H I, "Effect of alterations in the arterial carbon dioxide tension on blood flow through the cerebral cortex at normal and low arterial blood pressures." J Neurol Neurosurg Psychiat 1965;28:449-452.

190) Norusis M J, "SPSS/PC update manual." SPSS Inc., Chicago, USA, 1988, pp B24-26.

191) Ekstöm-Jodal B, HÄggendal E, Linder L, Nilsson N J, "Cerebral blood flow autoregulation at high arterial pressures and different levels of carbon dioxide tension in dogs." Europ Neurol 1971;6:6-10.

192) Raichle M E, Stone H L, "Cerebral blood flow autoregulation and graded hypercapnia." Europ Neurol 1971;6:1-5.

193) Symon L, Held K, Dorsch N W C, "On the myogenic nature of the autoregulatory mechanism in the cerebral circulation." Europ Neurol 1971;6:11-18.

194) Häggendal E, Johansson B, "Pathophysiological aspects of the blood brain barrier change in acute arterial hypertension." Europ Neurol 1971;6:24-28.

195) Crutchfield J S, Narayan R K, Robertson C S, Michael L H, "Evaluation of a fibreoptic intracranial pressure monitor." J Neurosurg 1990;72:482-487.

COMMUNICATIONS

The following communications based on the work in this thesis have been presented at Scientific meetings:

1. Spectral Analysis of the Intracranial Pressure Waveform.
   Scottish Anaesthetists Conference, Edinburgh: October 1987.
   (Poster and Demonstration)

2. Methodology of Spectral Analysis of the Intracranial Pressure Waveform in a Head Injury Intensive Care Unit.
   International Symposium on Intracranial Pressure, Ann Arbor: June 1988.
   (Poster)

3. Can Waveform Analysis of ICP Separate Vascular from Non-Vascular Causes of Intracranial Hypertension?
   International Symposium on Intracranial Pressure, Ann Arbor: June 1988.
   (Paper)

4. Measurement of Craniospinal Compliance: An Improved Method.
   Society of British Neurological Surgeons, Newcastle: September 1989.
   (Paper)

5. A Microcomputer Based Pressure Waveform Analysis System.
   Physiological Society, Edinburgh: September 1989.
   (Poster and Demonstration)

6. Spectral Analysis of the Intracranial Pressure Waveform in Severely Head Injured Patients.
   Belgian Society of Intensive Care Medicine, Luxembourg: October 1989.
   (Paper)

7. Cerebrovascular Resistance, Pressure Transmission and Compliance in an Experimental Model.
   Surgical Research Society (Neurosurgical Satellite), Liverpool: January 1990. (Paper)

The following communications based on the work in this thesis have been published or are IN PRESS:

1. Piper I R, Dearden N M, Leggate J R S, Robertson I, Miller J D: Methodology of Spectral Analysis of the ICP waveform in a Head Injury Intensive Care Unit. In: Intracranial Pressure VII, eds: Hoff J T, Betz A L, 668-671, Springer-Verlag, Berlin Heidelberg, 1989 (Paper)

2. Piper I R, Dearden N M, Miller J D: Can waveform Analysis Separate Vascular from Non-vascular Causes of Intracranial Hypertension? In Intracranial Pressure VII, eds: Hoff J T and Betz A L, 157-163 Springer-Verlag, Berlin Heidelberg, 1989 (Paper)

3. Piper I R, Dearden N M, Lawson A and Miller J D: A Microcomputer based Pressure Waveform Analysis System. J Physiol 420, 3P, 1990. (Abstract of peer reviewed demonstration)

4. Piper I R, Miller J D, Dearden N M, Leggate J R S, Robertson I: Systems analysis of cerebrovascular pressure transmission: An observational study in head injured patients. J Neurosurg (IN PRESS), 1990. (Paper)

(The material in these publications form the basis of chapter 2 in this thesis.)

APPENDICES

Appendix A: Derivation of the ICP Pulse vs ICP Relationship

(Adapted from Avezaat and Van Eijndhoven, reference 70)

since VPR = dP/dV, if dV = 1 ml then VPR = dP.

if the steady state volume-pressure relationship can be described by equation:

$$P = Peq\ e^{E1Ve} + Po \qquad 1)$$

where: P = ICP
Peq = equilibrium pressure
E1 = elastic coefficient
Ve = elastic volume (defined as addition to total craniospinal volume)
Po = constant

when system volume increases by an amount dvb (pulsatile blood volume) then ICP increases by a pressure increment of dP:

$$P + dP = Peq\ e^{E1(Ve + dvb)} + Po \qquad 2)$$

$$\Rightarrow P + dP = Peq\ e^{E1\ Ve}\ e^{E1\ dvb} + Po \qquad 3)$$

$$\Rightarrow (P - Po) + dP = Peq\ e^{E1\ Ve}\ e^{E1\ dvb} \qquad 4)$$

substituting (P - Po) for $Peq\ e^{E1\ Ve}$ (see equation 1)

$$\Rightarrow (P - Po) + dP = (P-Po)\ e^{E1\ dvb} \qquad 5)$$

since (AB - A) = A(B-1)

$$\Rightarrow dP = (P-Po)(e^{E1\ dVb} - 1) \qquad 6)$$

equation 6 describes the relationship between the ICP pulse and the elastic properties of the craniospinal system.

Appendix B: Systems Analysis and the Fourier Method of Signal Analysis

(Adapted from Stremler, reference 97)

A system can be described as a group of objects or elements that are combined in a manner intended to achieve a desired object. A signal is an event that is capable of starting some action. In systems analysis, a system is characterized by its response to an input signal where a signal is a single valued function of time. The signals of interest in this study are real valued signals, that is, signals that have energy or power (which they must have in order to be measured at all). Although the signals of interest are all real valued ones, they are often expressed in complex notation as this form of representation leads to simpler analysis.

Sinusoidal signals play a major role in waveform analysis as they are periodic signals which can be fully described by a single expression for all values of time:

$f(t) = A \cos(wt + \theta)$ where: $f(t)$ = sinusoidal signal
A = Amplitude
$w = 2\pi f$ (radian frequency)
θ = phase

A more complex signal f(t) can be described approximately in vector notation:

$$f(t) \approx \sum_{n=1}^{N} (f_n \theta_n) (t)$$

for n = 1 to a value N which completely describes the signal f(t) at time (t).

where: θ_n is a set of orthogonal functions (functions that act at 90 degrees to one another such as the x and y coordinate axis or sine and cosine functions) and f_n is a set of numbers describing the amplitude of the component along a given vector axis.

As an example, it can be shown that the two dimensional vector A_1 in the vector space of orthogonal functions θ_1 and θ_2 can be represented as:

$$A_1 = A_{11}\theta_1 + A_{12}\theta_2$$

where: $A_{11} = (A1 \cdot \theta_1)/(\theta_1 \cdot \theta_1)$ or $A1 \cdot (\theta_1 / K_1)$

$$Kn = (\theta_n \cdot \theta_n)$$

and $A_{12} = (A1 \cdot \theta_2)/(\theta_2 \cdot \theta_2)$ or $A1 \cdot (\theta_2 / K_2)$

The principal Dirichlet[76] condition is that a signal has finite energy over a period $t_1 \rightarrow t_2$ or, as is more often applied, has finite power ie:

$\int |f(t)|^2 \, dt < \infty$ (most real valued laboratory signals meet this condition)

Provided a signal represented in vector notation also meets the Dirichlet conditions, the vector notation described above can be extended by Parseval's theorem:

$$\int_{t_1}^{t_2} |f(t)|^2 \, dt = \sum_{n=1}^{\infty} (|f_n|^2 \; K_n) \text{ for } n = 1 \text{ to } \infty.$$

This theorem demonstrates that a function f(t) can be represented by an infinite set of mutually orthogonal functions. This is called the generalized Fourier series representation of f(t):

$$f(t) = a_0 + \sum_{n=1}^{\infty} (a_n \cos n w t + b_n \sin n w t)$$

for f(t) over the interval $(t_1 \rightarrow t_2)$

where: $a_0 = 1/(t_2 - t_1) \int_{t_1}^{t_2} f(t) \, dt$

$$a_n = 2/(t_2 - t_1) \int_{t_1}^{t_2} f(t) \cos n w t \, dt$$

---

[76] The conditions, known as the Dirichlet conditions, for the existence of the Fourier series representation that will converge on a signal f(t) over the interval (0,T) are:

1) f(t) has only a finite number of maxima and minima in the interval T;
2) f(t) has only a finite number of finite discontinuities in the interval T;
3) f(t) satisfies the inequality: $\int_0^T |f(t)| \, dt < \infty$

$$b_n = 2/(t_2 - t_1) \int_{t_1}^{t_2} f(t) \sin n w t \, dt$$

where: $w = 2\pi/(t_2 - t_1)$ = angular frequency and over this interval sin and cos are orthogonal functions.

This representation can be extended from the interval $t_1 \rightarrow t_2$ for all (t) provided the signal is periodic, that is $f(t + T) = f(t)$, where T is the period over which the signal repeats itself exactly. Under these conditions the Fourier series can be expressed:

$$f(t) = a_0 + \sum_{n=1}^{\infty} (a_n \cos n w_0 t + b_n \sin n w_0 t) \text{ for all (t) where } w_0 = 2\pi/T$$

and the coefficients are now expressed as:

$$a_0 = 1/T \int_0^T f(t) \, dt$$

$$a_n = 2/T \int_0^T f(t) \cos n w_0 t \, dt$$

$$b_n = 2/T \int_0^T f(t) \sin n w_0 t \, dt$$

This trigonometric Fourier series can also be expressed more compactly in polar notation:

$$f(t) = \sum_{n=1}^{\infty} C_n \cos(n w_0 t + \theta_n)$$

where: $C_n = \sqrt{a_n^2 + b_n^2}$ C_n is the magnitude of the sinusoid

and $\theta_n = \tan^{-1} (-b_n / a_n)$ θ_n is the phase of the sinusoid

Expressed in polar notation the relationship between the trigonometric and exponential Fourier representations can be more readily seen. From Euler's identity:

$$e^{jwot} = \cos(w_0 t + \theta)$$

$$\Rightarrow \quad f(t) = \sum_{n=-\infty}^{\infty} F_n e^{jwot}$$ where: e^{jwot} is a complex exponential function.

The Fourier method of signal analysis lends itself to systems analysis, as it allows the description of a complex signal as a summation of sinusoidal components and therefore provides a means of describing a systems response to a given input signal. Mathematically, a system is a "rule" used for assigning a function g(t) (the output) to a function f(t) (the input):

$$g(t) = H\{ f(t) \} \text{ where } H\{\} \text{ is the "rule".}$$

A system is "linear" if the superposition theorem applies:

if $g_1(t) = H\{ f_1(t) \}$ and $g_2(t) = H\{ f_2(t) \}$

then $a_1 G_1(t) + a_2 G_2(t) = H\{ a_1 f_1(t) + a_2 f_2(t) \}$

where a_1 and a_2 are constants.

A system is "time invariant" if a time shift in the input signal results in the same time shift in the output:

$$g(t - t_0) = H\{ f(t - t_0) \} \text{ for any } t_0 = \text{time shift.}$$

A fundamental property of a linear time invariant system is that the input signal f(t) and output signal g(t) are related by linear differential equations with constant coefficients:

$$a_0 g(t) + a_1 dg/dt + \ldots = b_0 f(t) + b_1 df/dt + \ldots$$

where a's and b's are constants.

There are advantages to using the complex exponential function e^{jwot} as the input signal (f(t)) for solving for such a differential equation, because the complex exponential function repeats itself under the operation of differentiation. Such a function at the input will yield the same function at the output multiplied by an algebraic expression in terms of the differential equation and the input function. Under these conditions, when the output response is divided by the input signal, the

original input function cancels and what results is an algebraic equation which describes the system characteristics. This result is termed the frequency transfer function H(w):

$$g(t) = H(w)\ e^{jwot}$$

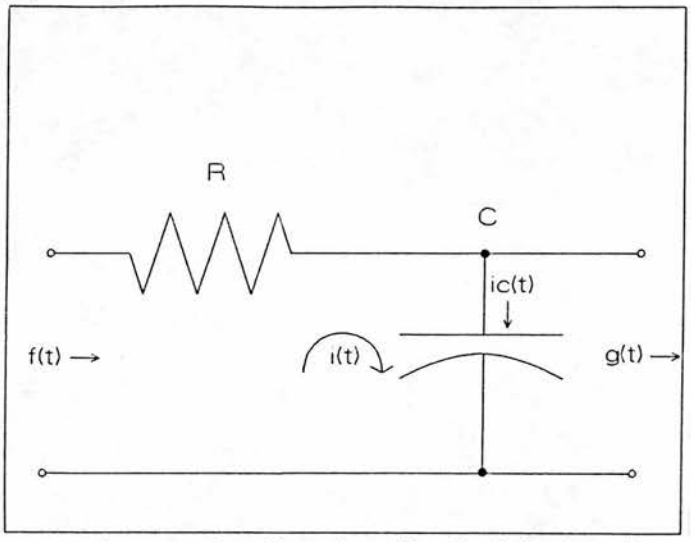

As an example of this, the differential equation for the simple RC circuit shown above can be solved through summing the currents.

$$f(t)/R - g(t)/R = ic(t)$$

$$\Rightarrow \quad 1/R(\ f(t) - g(t)\ ) = ic(t)$$

since $ic = C\ (dg/dt)$

$$\Rightarrow \quad 1/R(\ f(t) - g(t)\ ) = C\ (dg/dt)$$

$$\Rightarrow \quad f(t) - g(t) = RC\ (dg/dt)$$

$$\Rightarrow \quad f(t) = RC\ (dg/dt) + g(t)$$

let $f(t) = e^{jwot}$

and since for a linear time invariant system:

$$g(t) = H(w)e^{jwot}$$

$$\Rightarrow \quad e^{jwot} = jwRC\ H(w)e^{jwot} + Hwe^{jwot}$$

$$\Rightarrow \quad e^{jwot} = H(w)e^{jwot}(jwRC + 1)$$

dividing output by input function e^{jwot}

$$\Rightarrow \quad 1 = (H(w)e^{jwot}(jwRC + 1)) / e^{jwot}$$

solving for H(w)

$$\Rightarrow \quad H(w) = 1 / (jwRC + 1)$$

The frequency transfer function H(w) is therefore independent of the complex exponential input function e^{jwot}

If an analytical expression for a complex signal is not known, the frequency transfer function H(w) can be determined through measurement of the Fourier transform of the input and output signals. Where the Fourier transform is expressed in complex exponential form:

$$X(w) = \int_{-\infty}^{\infty} x(t)\, e^{-jwot}\, dt \qquad \text{(input signal)}$$

$$Y(w) = \int_{-\infty}^{\infty} y(t)\, e^{-jwot}\, dt \qquad \text{(output signal)}$$

This permits the input and output signals to be expressed as a series of complex exponential functions which, because of the nature of complex exponentials as previously described, allows one to relate the input and output functions of the system by a simple linear relation:

$$Y(w) = H(w) \times X(w)$$

where X(w) and Y(w) are the Fourier transforms of the input and output signals respectively. The frequency transfer function H(w) is calculated simply as:

$$H(w) = Y(w) / X(w)$$

The frequency transfer function H(w) is a complex valued function of frequency and is usually expressed in polar notation:

$$H(w) = |H(w)| e^{j\theta(w)} = |Y(w)| / |X(w)| e^{j [\theta_y (w) - \theta_x (w)]}$$

where: $|X(w)|$ refers to the modulus or amplitude of the signal
and $\theta(w)$ is the phase of the signal

The Fast Fourier Transform algorithm used in this analysis yields the result in rectilinear notation where each signal is expressed in terms of real (r) and imaginary (x) terms:

$$r + jx$$

The conversion to polar notation is:

$$|X(w)| = \sqrt{r^2_{(w)} + x^2_{(w)}}$$

$$\theta(w) = \tan^{-1} (-x_{(w)} / r_{(w)})$$

The frequency transfer function is then calculated in polar notation where the amplitude component or amplitude transfer function is:

$$|Y(w)| / |X(w)|$$

and the phase component or phase transfer function is:

$$\theta_{y(w)} - \theta_{x(w)}$$

Appendix C: Transient Response Analysis of Catheter-Transducer Systems

A catheter-transducer system can be described as a second order mechanical system and, if underdamped, will oscillate at its own natural frequency producing significant pressure waveform amplitude and phase distortion. The degree of distortion will depend on the damping factor (ß) of the system. The figures below show the effect of different amounts of damping on the relative amplitude and absolute phase of a sine wave pressure signal as the frequency of the signal approaches the resonant frequency of the catheter-transducer system. For most purposes it can be seen that a damping factor of 0.64 (optimal damping) is desirable, as the amplitude error will be less than 2% for up to two-thirds of the natural frequency of the system and the phase lag will be approximately linear over this range. A linear system phase shift will not distort a waveform but will only cause an overall time delay to the pressure signal[77].

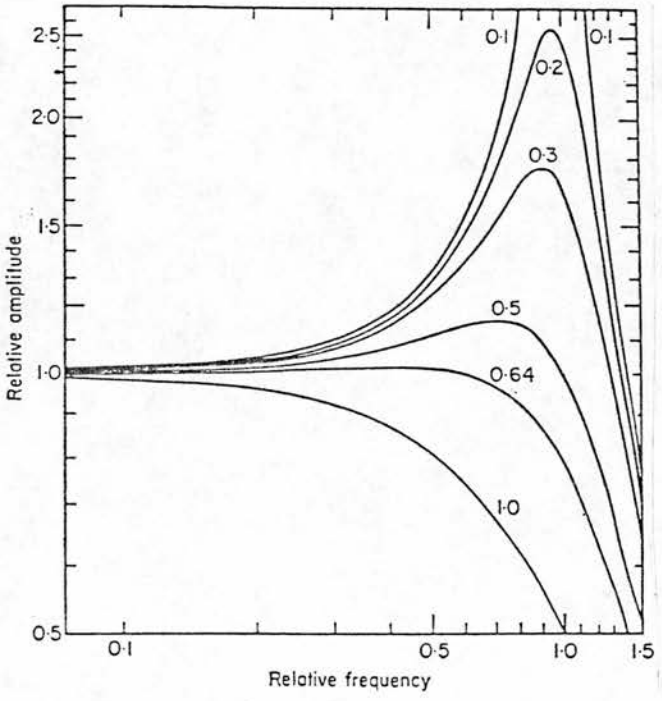

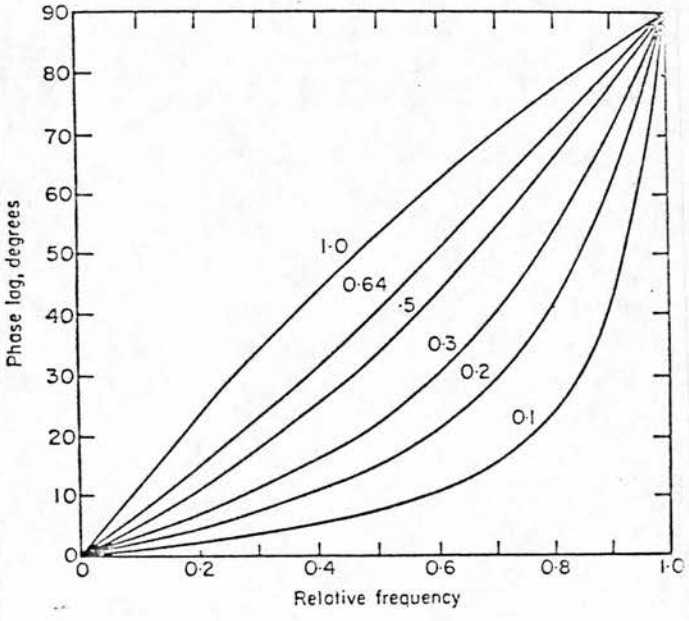

[77]Higher frequencies are phase shifted over more of their period than lower frequencies. Higher frequencies, however, have smaller periods than lower frequencies, so if the degree of phase shift with frequency is linear, all frequencies are phase shifted by the same amount in terms of time, which on summation will cause no waveform distortion but only a time delay.

The natural frequency and damping properties of a system can be tested by applying a step or transient pressure to the input of the system and recording the output pressure response. This transient response or "pop" test technique will cause the catheter-transducer system to oscillate at its natural resonant frequency. The resonant frequency (fo) and damping (ß) can then be calculated, as shown below, by the method of Hanson (95) through measurement of the pop-test output response parameters: td, d1 and d3.

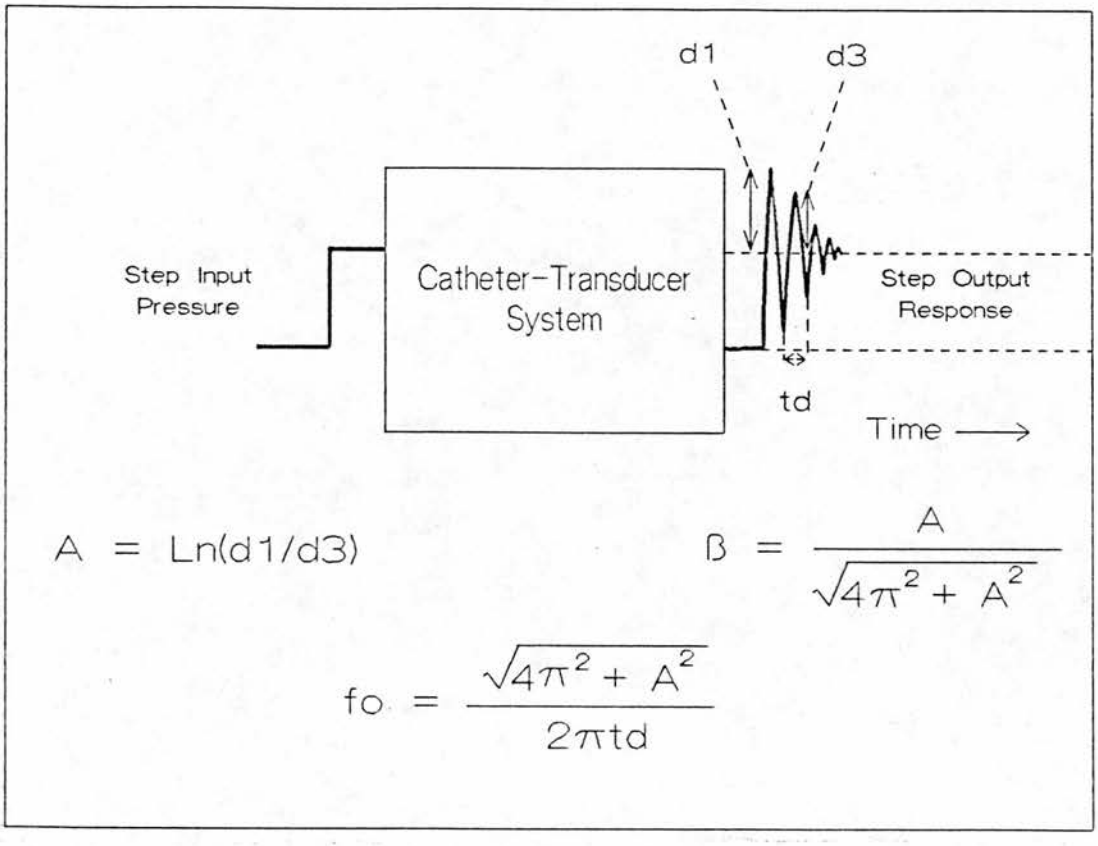

As shown overleaf, transient response analysis of the fluid-filled catheter-transducer system used in these studies has shown that it is underdamped (ß = 0.310 +- 0.021) with a resonant frequency (fo) of 21 Hz. Two and a half turns of an Acudynamic adjustable damping unit placed in series with the catheter-transducer system tubing, provided optimal damping (ß = 0.622 +- 0.04). The flat frequency response up to 14 Hz, with optimal damping, was confirmed through a test of the system frequency response with a sine-wave pressure generator over a frequency range from DC to 50 Hz

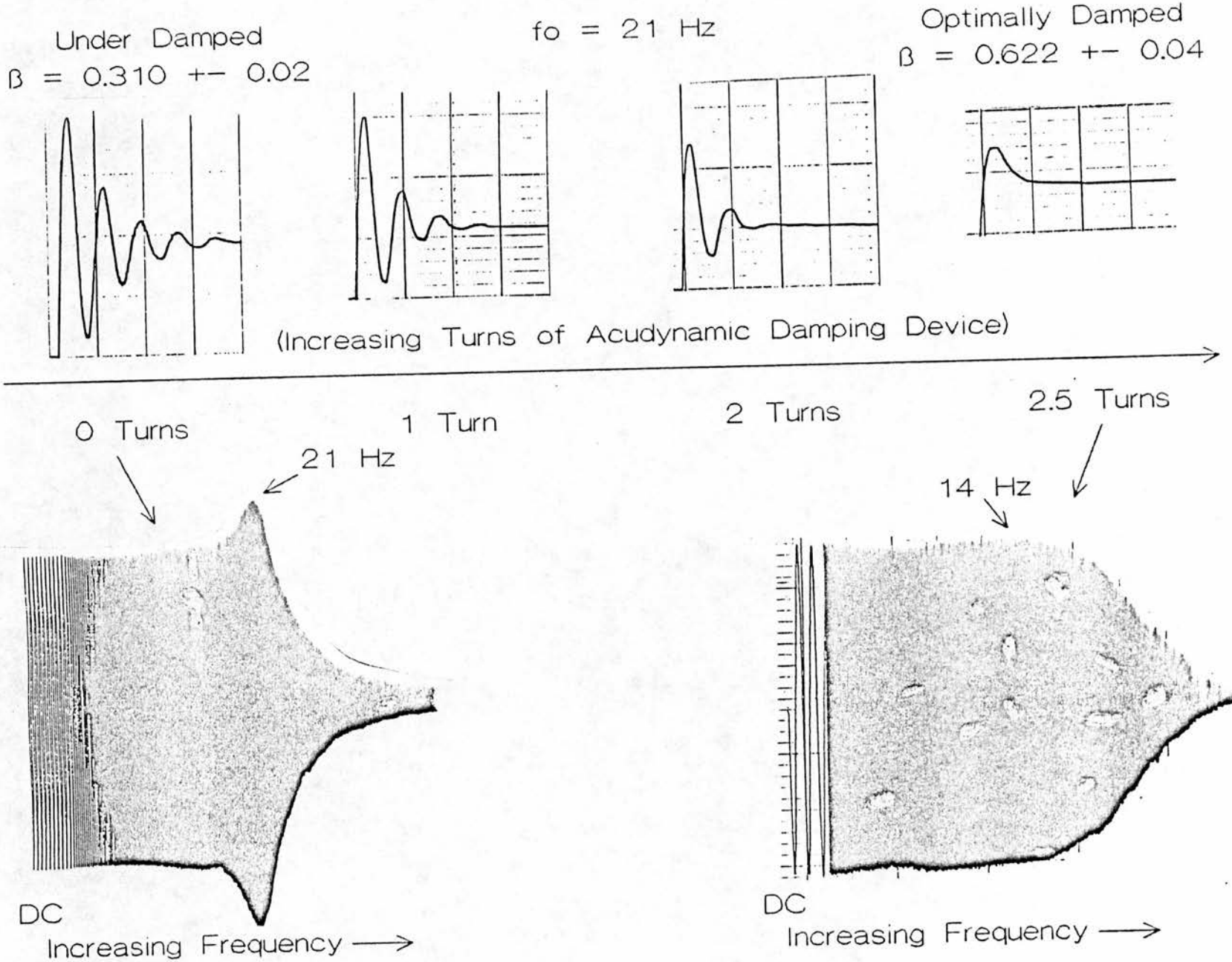
Under Damped
β = 0.310 +− 0.02
fo = 21 Hz
Optimally Damped
β = 0.622 +− 0.04
(Increasing Turns of Acudynamic Damping Device)
0 Turns
1 Turn
2 Turns
2.5 Turns
21 Hz
14 Hz
DC
Increasing Frequency ⟶
DC
Increasing Frequency ⟶

Appendix D: Flow Chart of the Data Collection Program

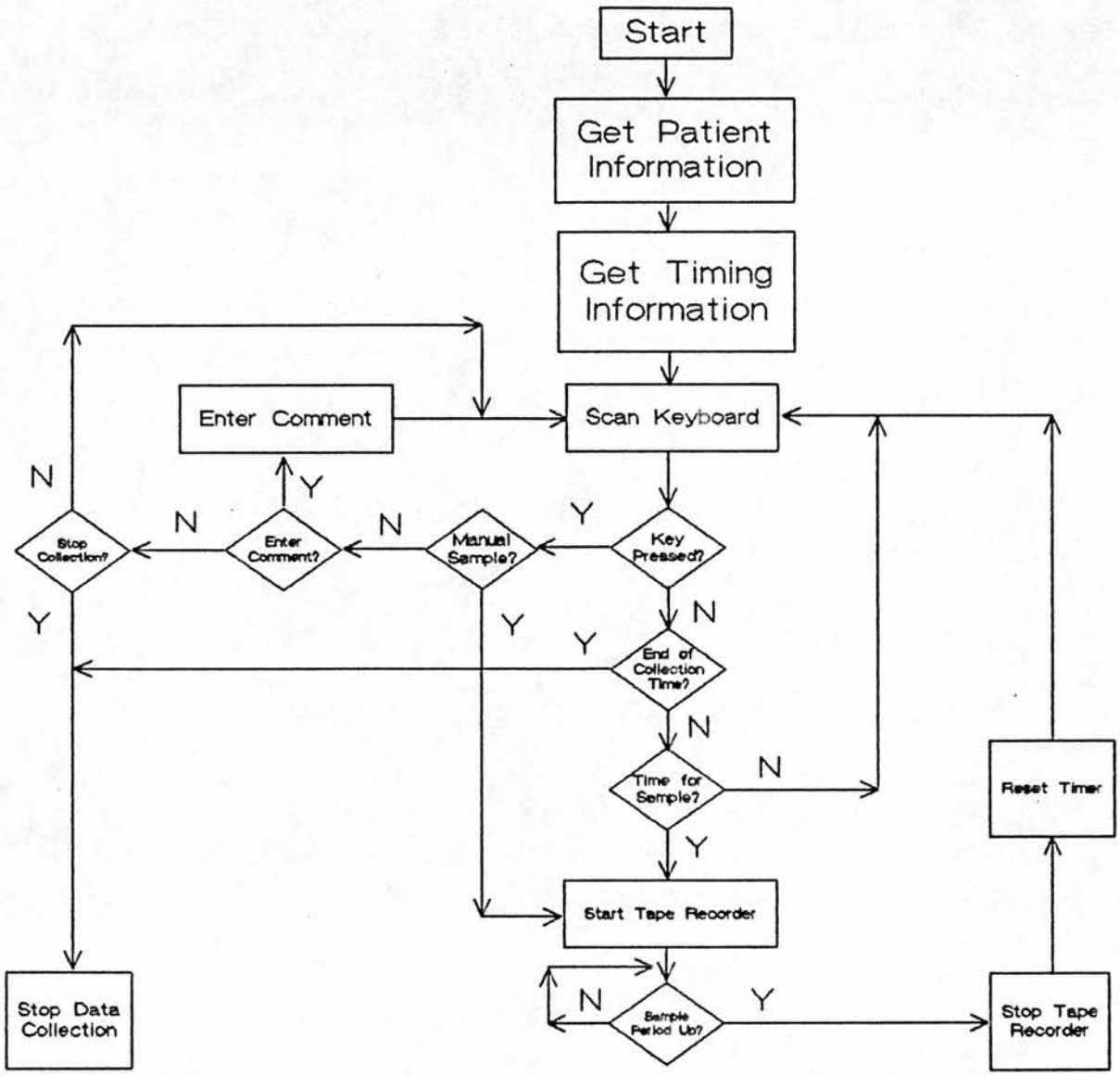

Appendix E: Schematic Diagram of the Waveform Conditioning Amplifier

All operational amplifiers used in this design are BIFET low noise amplifiers except the for LTC 1062[78] low pass filter chip which is a silicon gate CMOS device. All power is a regulated +- 8 volts DC and decoupled with 0.01 µF capacitors. The schematic diagram shown below is for a single channel conditioning amplifier.

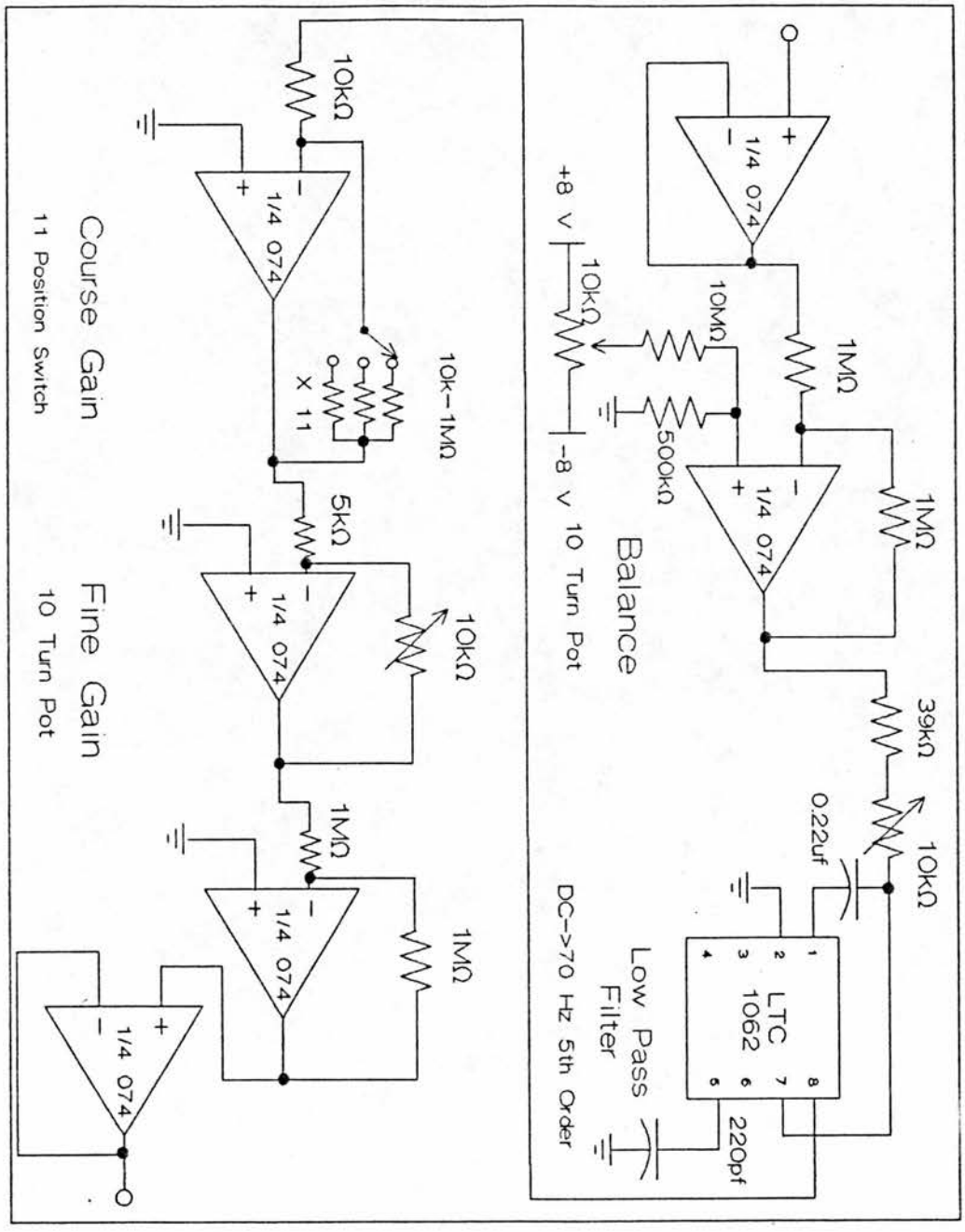

[78]Made by Linear Technologies, available from RS-Components Ltd., Corby, UK. This device is a 5th order all pole maximally flat lowpass filter with no DC error.

Appendix F: Frequency Analysis of the Waveform Recording System

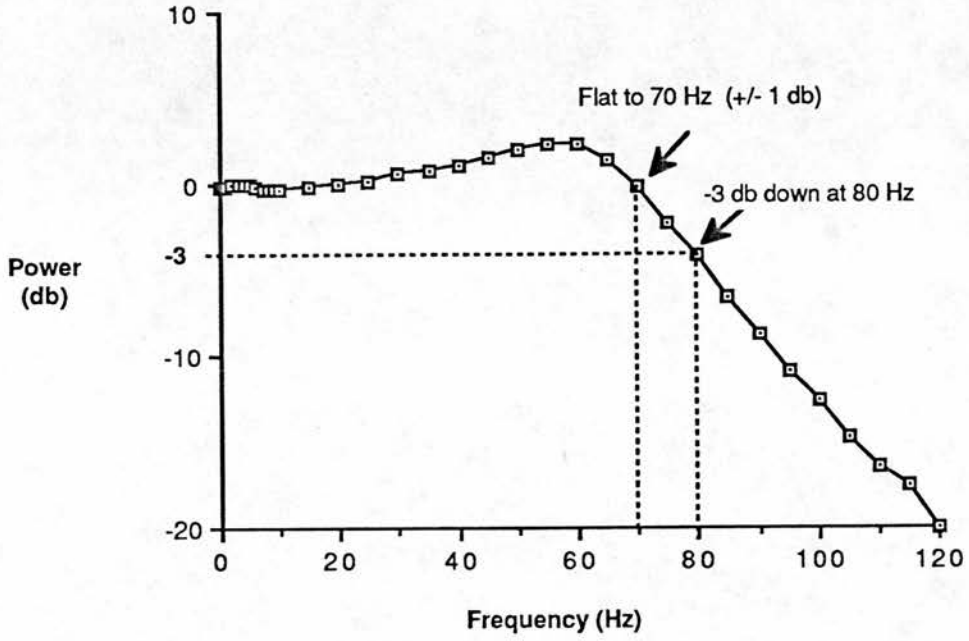

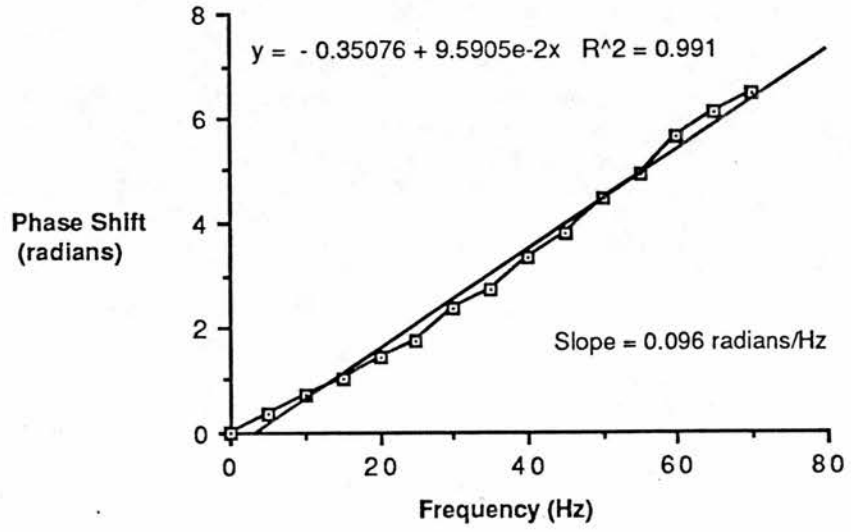

Appendix G: Flow Chart of the Data Analysis Program

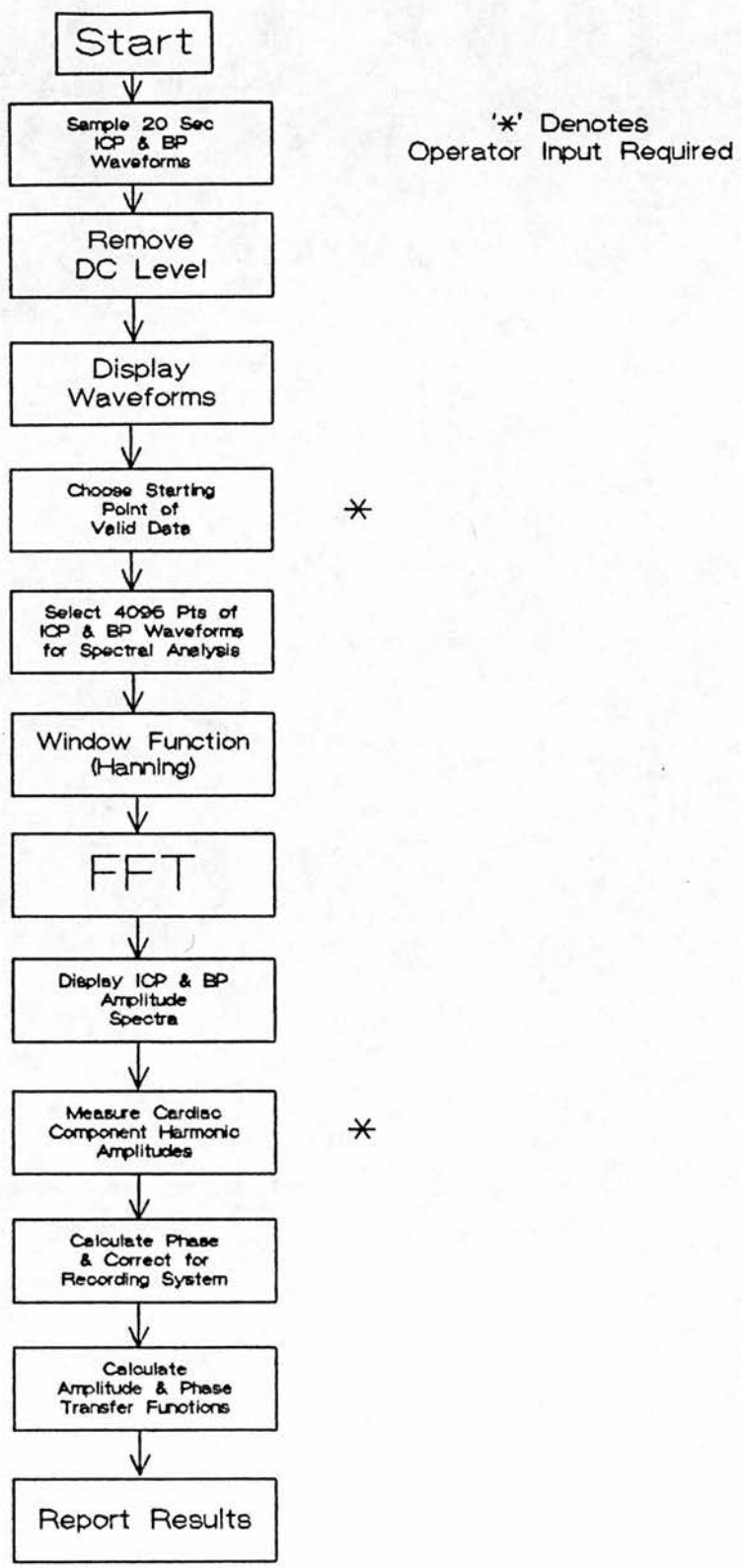

Appendix H: Sample Normal Probability and Box and Whisker Plots

In a normal probability plot each observed value is paired with the expected value from a normal distribution, where the expected value is calculated from the normal distribution equation based on the number of samples in the population and the rank order of the value from the population. If the distribution is normal then the points will fall approximately onto a straight line. The figure shown below is a probability plot of the natural log transformation of the fundamental of the curve type 4 amplitude transfer function group. The points fall on a straight line, indicating an approximately normal distribution.

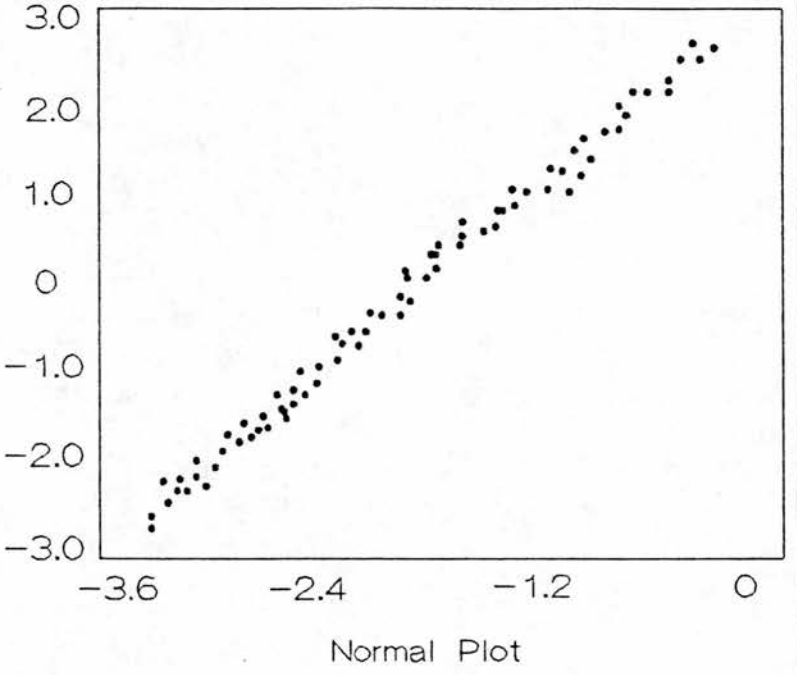

The Lillifors modification of the Kolmogorov-Smirnov (K-S) test was calculated as a measure of the goodness of fit of the data to a normal distribution. The K-S statistic for the data plotted above is 0.1342 with 201 degrees of freedom. This value of the statistic rejects the null hypothesis that the data is not significantly different from a normal population. However, with large data sets, it is virtually impossible to find data that is exactly normal and any goodness of fit test will reject the null hypothesis. In such instances it is sufficient that the data is approximately normally distributed (190). Lower values of the K-S statistic indicate the data is a better fit to the normal distribution. As can be seen from Table 3, with very few exceptions, the K-S statistic values fall below 0.1342 indicating that the natural log transformation of the data produces an approximately normal distribution.

A simple means of summarizing the distribution of the data is the box and whisker plot, shown below for the same data as the normal probability plot. The upper and lower box boundaries represent the 25th and 75th percentiles, with the median value represented by an asterisk. The "whiskers" plot the largest and smallest observed values that are not outliers, where an outlying value is one that is more than 1.5 box-lengths from the upper or lower quarter percentile.

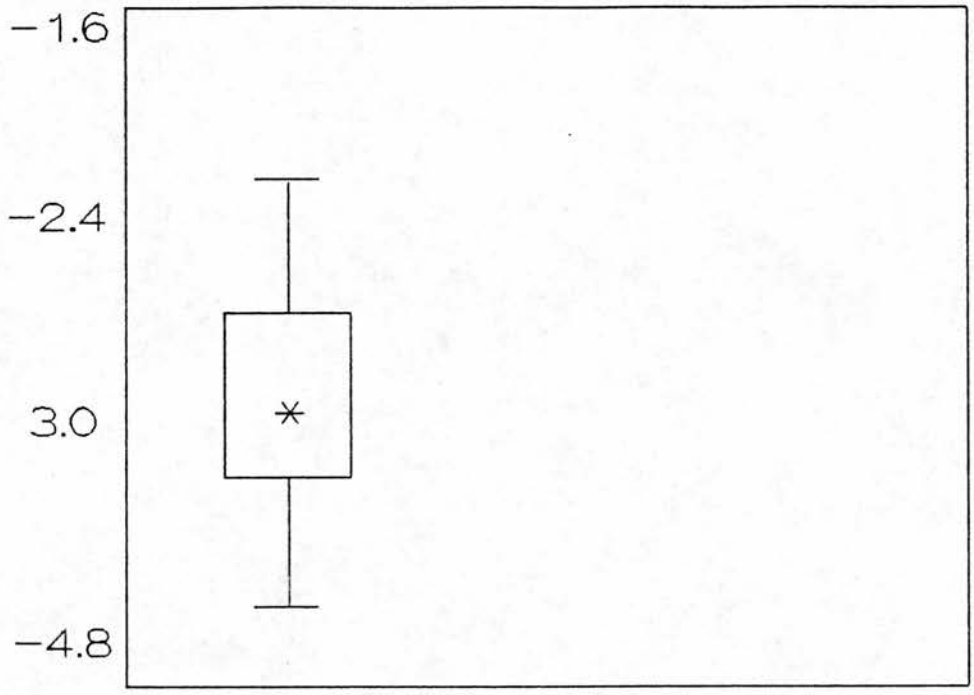

Box and Whisker Plot

Appendix I: Derivation of Improved Compliance Method Equation

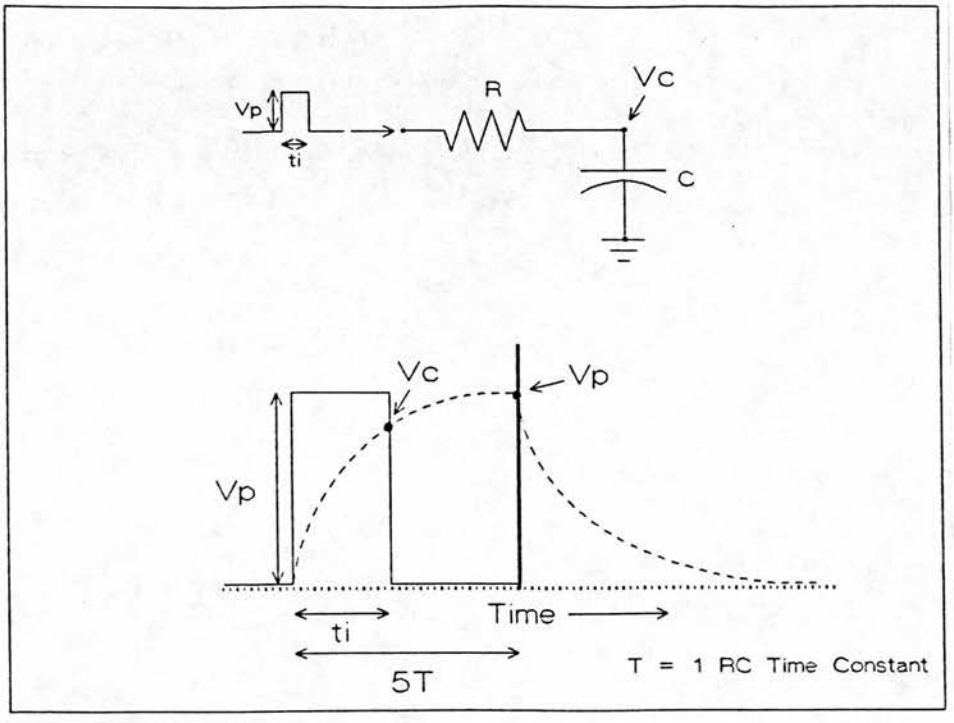

Capacitor charge equation:

$$V_c = V_p (1 - e^{-ti/RC}) \quad 1)$$

$$\Rightarrow \quad V_c = V_p - V_p e^{-ti/RC} \quad 2)$$

$$\Rightarrow \quad V_p - V_c = V_p e^{-ti/RC} \quad 3)$$

$$\Rightarrow \quad Ln(V_p - V_c) = Ln(V_p e^{-ti/RC}) \quad 4)$$

$$\Rightarrow \quad -Ln(V_p - V_c) = Ln(V_p e^{ti/RC}) \quad 5)$$

$$\Rightarrow \quad -Ln(V_p - V_c) - LnV_p = Ln\, e^{ti/RC} \quad 6)$$

$$\Rightarrow \quad Ln[V_p / (V_p - V_c)] = ti/RC \quad 7)$$

$$\Rightarrow \quad RC = ti / Ln[V_p / (V_p - V_c)] \quad 8)$$

$$\Rightarrow \quad C = \{ ti / Ln[V_p / (V_p - V_c)] \} / R \quad 9)$$

equation 9) is the improved compliance method equation

Appendix J: Schematic Diagram of the Pressure Signal and Timing Conditioning Unit

All power is a regulated +- 5 volts DC and decoupled with 0.01 µF capacitors. Potentiometer "P1" provides a variable input pulse trigger amplitude from zero to 2.0 Volts (producing 0 to 200 mm Hg pressure). Potentiometer "P2" provides a variable input pulse trigger duration from 20 to 1000 msec.

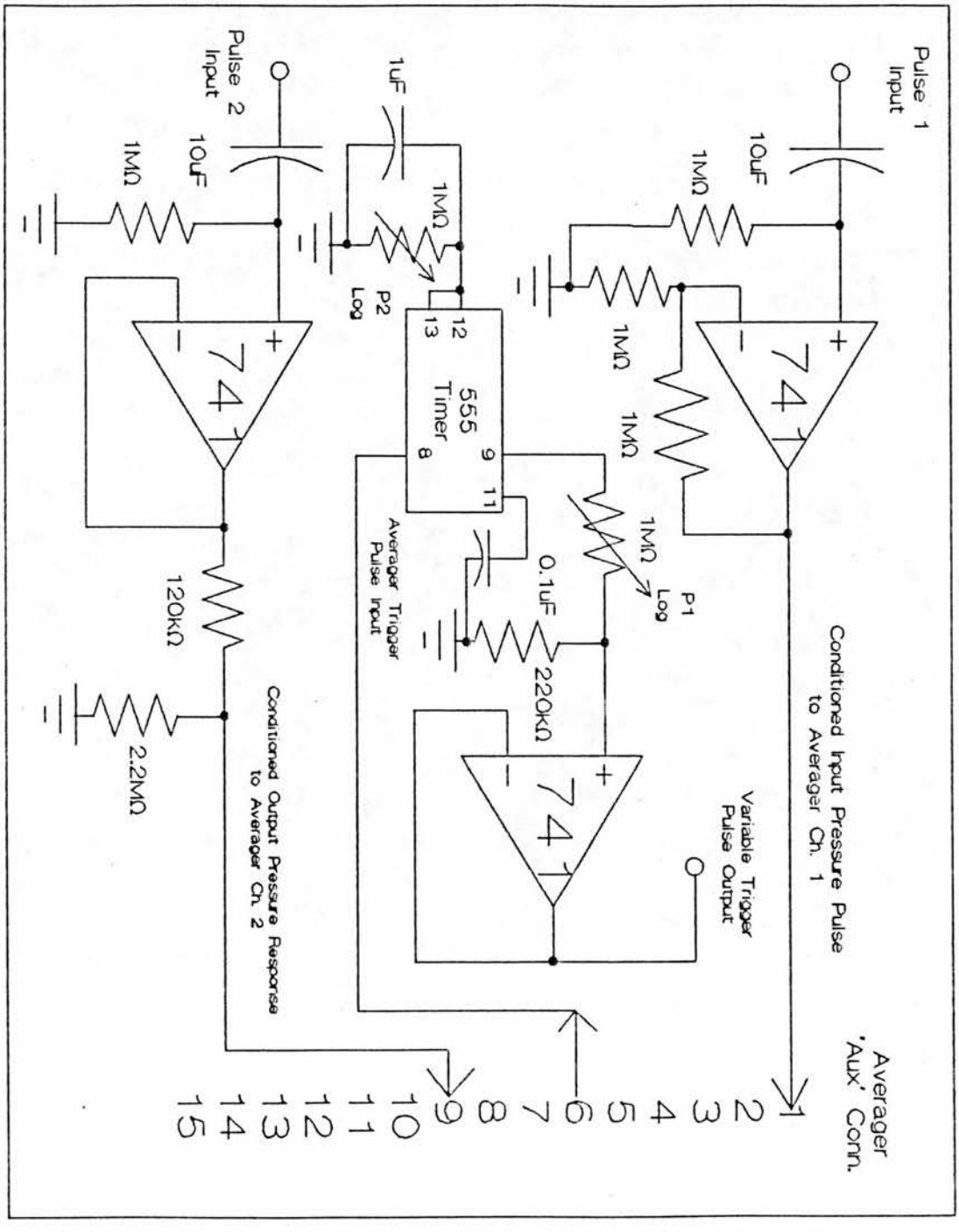

Appendix K: The Effect of the Pressure Generator Compliance on SPR Compliance

The speaker diaphragm compliance is in series with the system compliance and can be described by the following equivalent circuit:

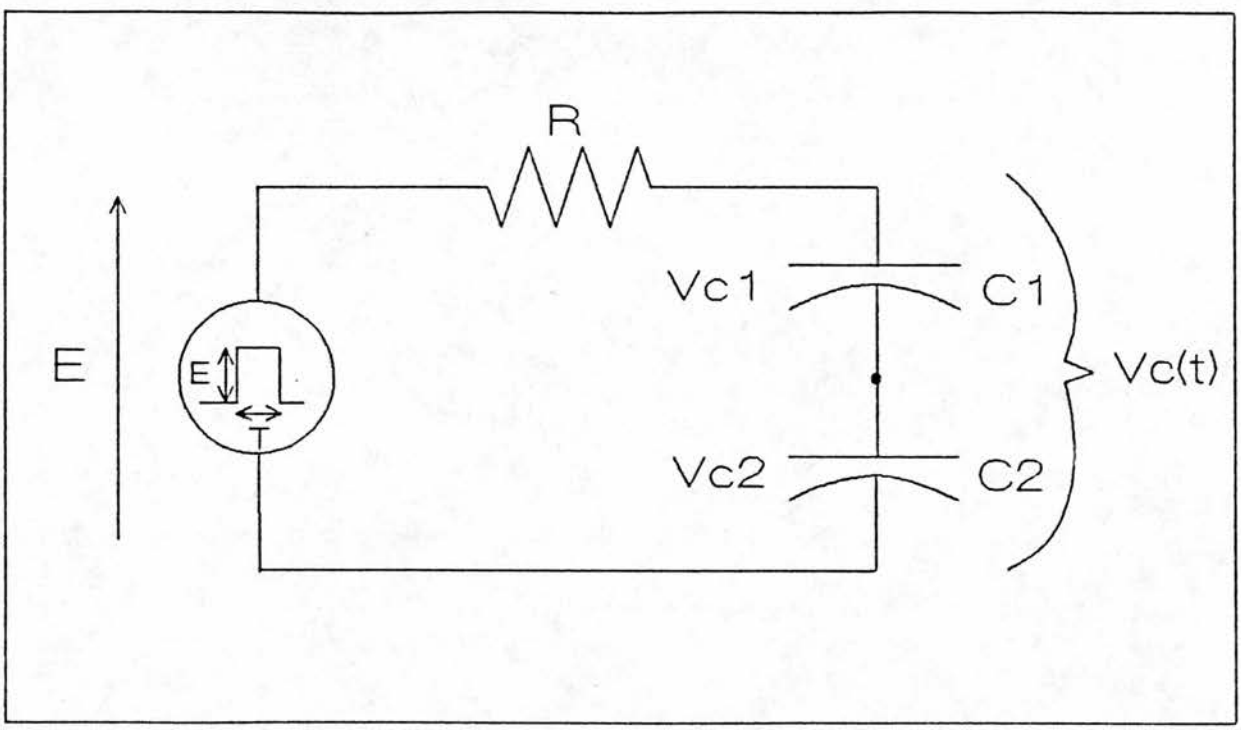

With reference to the above diagram:

let E = pressure generator input pressure

R = injection tubing resistance

T = pressure generator input pressure pulse period

C2 = lumped craniospinal compliance

C1 = pressure generator diaphragm compliance

Vc1 = pressure across C1

Vc2 = pressure across C2

Vc(t) = pressure across total compliance at time (t)

$$\text{Now } Vc2 = Vc(t)\ \frac{(C1)}{(C1+C2)} \qquad 1)$$

$$\text{and } Vc(t) = E(1 - e^{-t/R\{C1.C2/C1+C2\}}) \qquad 2)$$

$$\text{For } T << R\ \frac{(C1.C2)}{(C1+C2)} \qquad 3)$$

$$\text{then } Vc(t) \approx E \cdot \frac{t}{R\ \frac{(C1.C2)}{(C1+C2)}} \qquad 4)$$

$$\text{and when } t = T, \text{ then } Vc(T) = E \cdot \frac{T}{R\ \frac{(C1.C2)}{(C1+C2)}} \qquad 5)$$

$$\Rightarrow Vc(T) = \frac{ET(C1+C2)}{R.C1.C2} \qquad 6)$$

$$\Rightarrow Vc2(T) = \frac{C1}{C1+C2} \cdot Vc(T) \qquad 7)$$

substituting equation 6) for Vc(T)

$$\Rightarrow Vc2(T) = \frac{C1}{C1+C2} \cdot \frac{ET(C1+C2)}{R.C1.C2} \qquad 8)$$

$$\Rightarrow Vc2(T) = \frac{ET}{R.C2} \qquad 9)$$

So equation 9 shows that under the condition that:

$$T << R\ \frac{(C1.C2)}{(C1+C2)}$$

then Vc2 (and hence the compliance C2) at time (T) is independent of the pressure generator diaphragm compliance C1.

Appendix L: Flow Chart of the Infusion Method Data Collection Program

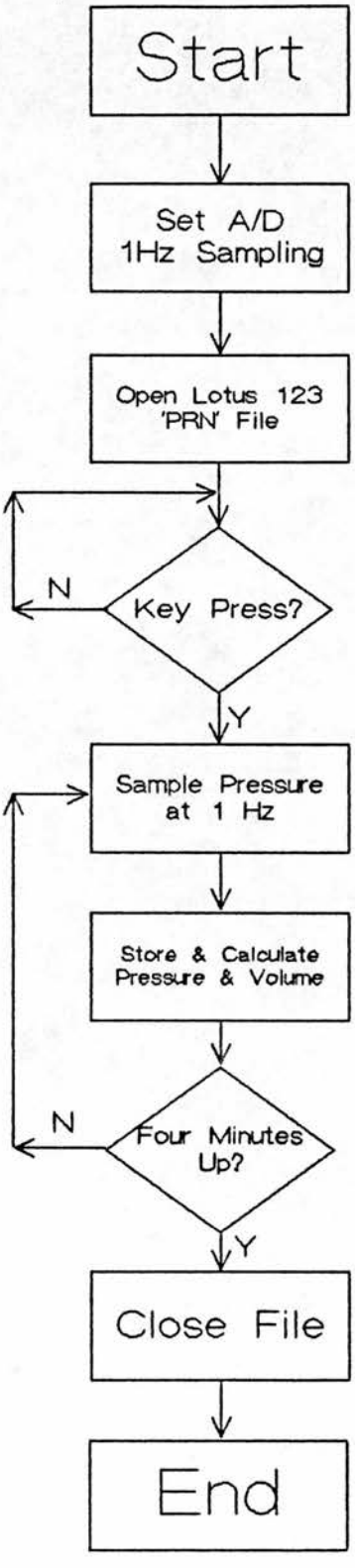

Appendix M: Calculation of CSF Outflow Resistance at Normal and Elevated ICP

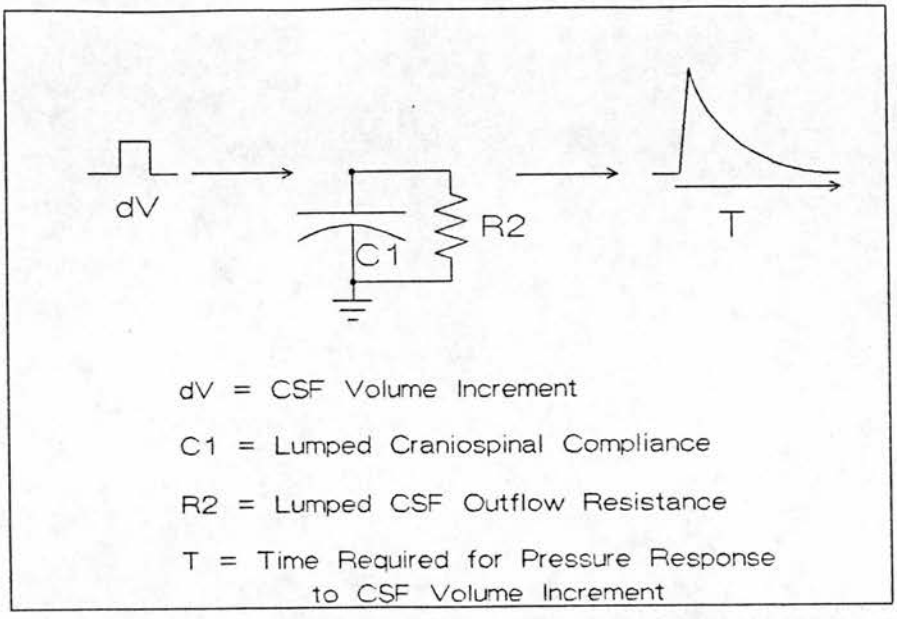

Method 1

The diagram shown above is a first approximation model of the craniospinal system consisting of a lumped craniospinal compliance (C1) and a CSF outflow resistance (R2). It can be seen that the pressure response to a volume injection (dV) takes time (T) to recover. The time to recover (T) is approximately equal to five time constants (τ), where the time constant (τ) is calculated as the product of C1 and R2[79].

Low ICP

As shown overleaf, the time to recover (T) after an intraventricular volume injection of 0.15 ml in a cat with low ICP (8 mm Hg) was 5 minutes or 300 seconds. This value (T) of 300 seconds represents 5 time constants (τ) which equals 5 x (R2C1). One time constant (τ) is therefore one-fifth of this value or 60 seconds. By substituting the measured value of craniospinal compliance (C1) into the equality: **R2C1 = 60 seconds,** the CSF outflow resistance (R2) can be calculated. The compliance values as measured by both SPR and VPR methods with low ICP are 0.010 and 0.021 ml/mm Hg respectively. The average compliance value from both methods gives C1 = 0.016 ml/mm Hg and substituting this value into the above equation yields a CSF outflow resistance (R2) with low ICP of

[79]In electrical terms, a capacitor (C) in series with a resistance (R) will charge up to 99.3% of its final value after 5 RC time constants.

65 mm Hg/ml/min[80]. This value of R2 is 18 times greater than the SPR method injection tubing resistance of 3.5 mm Hg/ml/min.

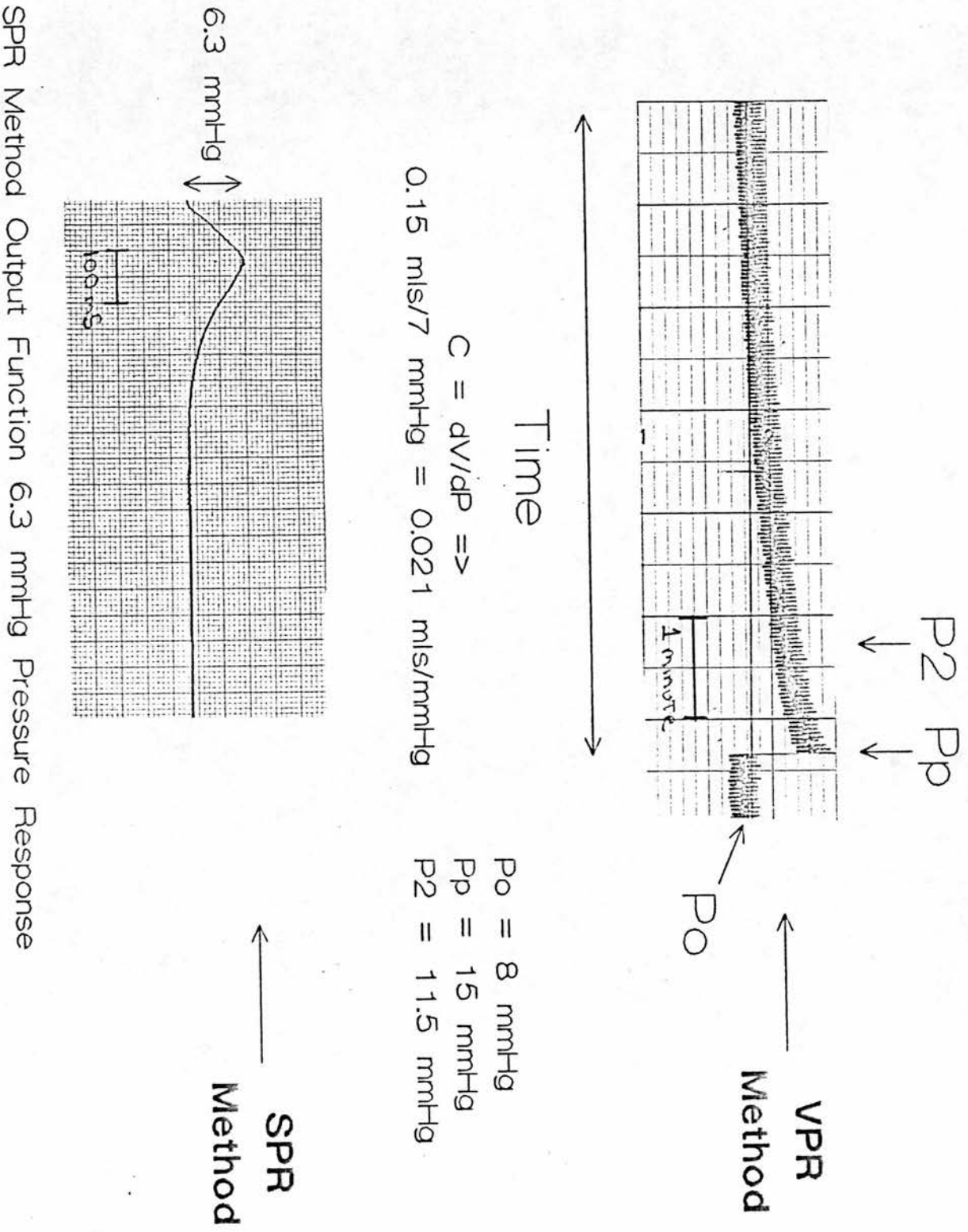

[80]One R2C1 time constant of 60 seconds with a C1 compliance of 0.016 ml/mm Hg gives an outflow resistance R2 of 60/0.016 = 3871 mm Hg/ml/sec. Dividing this value by 60 yields R2 in terms of minutes rather then seconds => 65 mm Hg/ml/min.

High ICP

As shown below, the time to recover (T) after an intraventricular volume injection of 0.15 ml in a cat with elevated ICP (90 mm Hg) was 3 minutes or 180 seconds. This value (T) of 180 seconds represents 5 time constants (τ) which equals 5 x (R2C1). One time constant (τ) is therefore one-fifth of this value or 36 seconds. By substituting the measured value of craniospinal compliance (C1) into the equality: **R2C1 = 36 seconds**, the CSF outflow resistance (R2) can be calculated. The compliance values as measured by both SPR and VPR methods with elevated ICP are 0.0020 and 0.0035 ml/mm Hg respectively. The average compliance value from both methods gives C1 = 0.0028 ml/mm Hg and substituting this value into the above equation yields a CSF outflow resistance (R2) with high ICP of 214 mm Hg/ml/min. This value of R2 is 61 times greater than the SPR method injection tubing resistance of 3.5 mm Hg/ml/min.

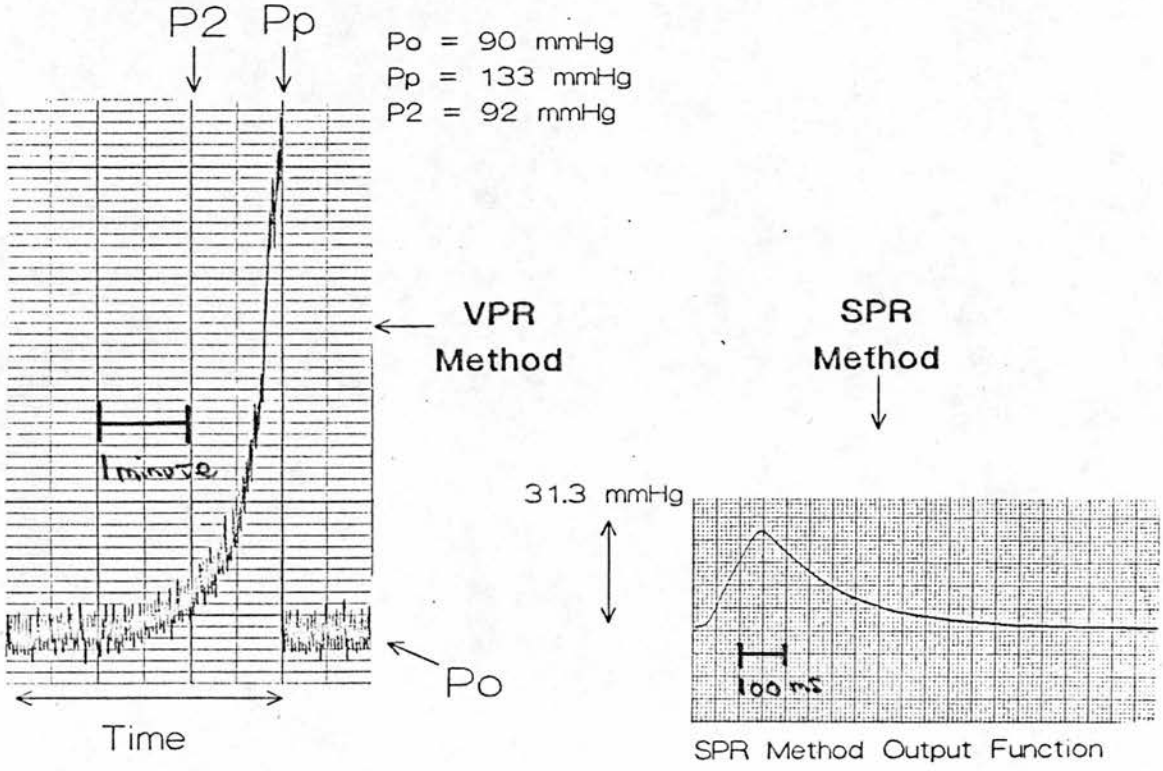

Method 2

Marmarou (41) derived an equation for calculation of the CSF outflow resistance based on the PVI volume-pressure test. This equation is shown below.

$$Ro = \frac{t2 \cdot Po}{PVI \cdot LOG\left[\frac{P2}{Pp} \cdot \frac{Pp - Po}{P2 - Po}\right]}$$

$$PVI = \frac{dV}{LOG\ \frac{Pp}{Po}}$$

Ro = CSF Outflow Resistance
PVI = Pressure Volume Index
t2 = time point on decay portion of response
Po = Initial ICP
Pp = Peak ICP
P2 = ICP at time t2 (usually 1 minute)

The table below substitutes the measured values of t2, Po, PVI, P2 and Pp from the volume-pressure responses at both low and elevated ICP in Marmarou's equation for calculation of CSF outflow resistance R2. This method yields outflow resistance values at low and elevated ICP of 79 and 104 mm Hg/ml/min respectively. These values are 22 and 30 times greater in value than the SPR method injection tubing resistance of 3.5 mm Hg/ml/min.

Parameter	Value	
	ICP = 8	ICP = 90
t2 (min)	1	1
Po (mmHg)	8	89
PVI (mls)	0.549	0.844
P2 (mmHg)	11.5	92
Pp (mmHg)	15	134
Ro (mmHg/ml/min)	78.6	104.1

Appendix N: Hydrogen Clearance Cerebral Blood Flow Method

Hydrogen gas meets most of the criteria for an ideal blood flow tracer:

a) metabolically inert;
b) not normally present in body tissues;
c) dissolves readily in lipids and diffuses rapidly in tissue (penetrates nervous tissue well);
d) low water:gas partition coefficient (0.018) (rapidly removed from arterial blood in pulmonary circulation).

Hydrogen can be readily measured through placement of platinum electrodes in brain tissue where the current produced by a platinum electrode when accepting the electrons generated by oxidation of hydrogen gas correlates to local tissue H2 gas concentration:

$$H2 \rightarrow 2H^{+} + 2e^{-} \qquad I = nFD\frac{(C)}{L}$$

where:

- I = current density per unit area per unit time
- n = number of electrons transferred by each molecule of hydrogen gas
- F = Faraday's number (6.02×10^{23})
- D = diffusion coefficient for hydrogen in the tissue
- L = distance between bulk hydrogen concentration and platinum electrode tip
- C = the hydrogen concentration in the bulk tissue

Polarizing the hydrogen electrode positive relative to a silver-silver chloride reference electrode makes the electrode more selective for hydrogen gas.

The Hydrogen Clearance technique, like other clearance techniques, is based on the principle of conservation of mass. As shown overleaf, if a tracer is injected into tissue then the tracer entering must either be taken up by the tissue or be converted to some other compound or leave the tissue.

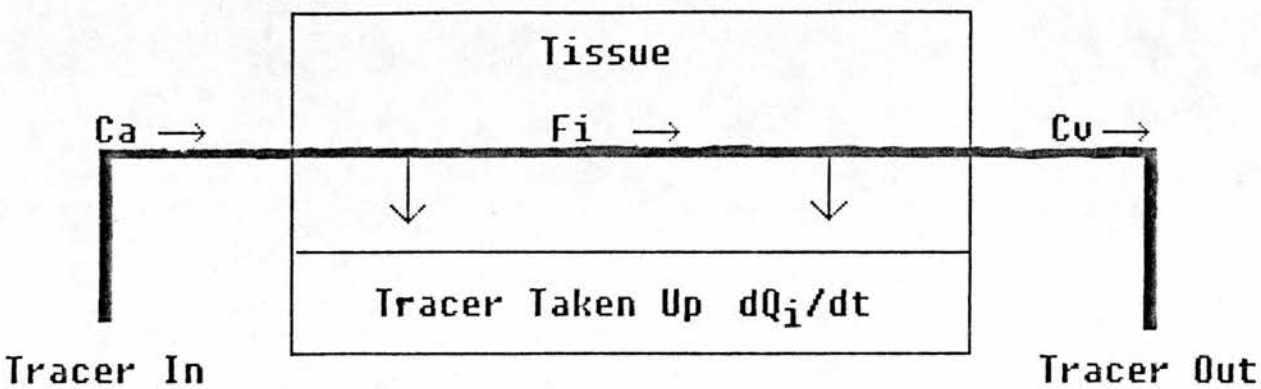

Fick was the first to use this principle to measure cardiac output based on oxygen consumption by the lungs which resulted in the well known Fick eqtn.:

$$F_i = \frac{dQ_i/dt}{(C_a - C_v)}$$

where:

F_i = tissue flow

C_v = Concentration of tracer leaving tissue

C_a = Concentration of tracer entering tissue

dQ_i/dt = Quantity of tracer removed by tissue per unit time (t)

The Hydrogen Clearance blood flow clearance equation can be derived directly from Fick's equation.

first define:

a) Concentration = Quantity/Volume $C = Q/V$ (grams/ml)

b) Flow = Volume/Time $F = V/T$ (ml/min)

c) Quantity/Time = Flow times Concentration since

$$\frac{V}{T} * \frac{Q}{V} = \frac{Q}{T}$$

d) let quantity per unit time = dQ/dt

e) define tissue volume (V_i) to include the vascular space and assume the tracer achieves instantaneous equilibrium between the vascular volume and tissue volume with a partition coefficient of y_i between blood and brain tissue

f) define:

F_i = tissue flow

F_a = arterial inflow to tissue

F_v = venous outflow from tissue

C_v = Concentration of tracer leaving tissue

C_a = Concentration of tracer entering tissue

dQ_i/dt = Quantity of tracer removed by tissue per unit time (t)

dQ_a/dt = Quantity of tracer present in the tissue arterial blood supply per unit time (t)

dQ_v/dt = Quantity of tracer present in the tissue venous blood supply per unit time (t)

y_i = Partition coefficient of tracer between blood and brain

$dQ_i/dt = F_i(C_a - C_v)$ Starting with Fick's eqtn. 1)

divide equation 1) throughout by the tissue volume V_i taking into account the partition coefficient of the tracer

ie. $Ci = y_iCa - y_iCv$

$$(dQ_i/V_i)/dt = \frac{F_i}{y_iVi}(C_a - C_v) \quad 2)$$

since concentration = quantity/volume

equation 2) becomes:

$$dC_i/dt = \frac{F_i}{y_iV_i}(C_a - C_v) \quad 3)$$

assume that, when the tissue is fully saturated with the tracer and has had time to equilibrate between the vascular and tissue compartments:

$C_i = y_i * C_v$ (Zuntz assumption) 4)

Zuntz assumption is that venous blood from a tissue is in equilibrium with the tissue itself with respect to inert gas

hence eqtn. 4) can be rearranged:

$C_v = C_i/y_i$ 5)

substituting eqtn. 5) for Cv in eqtn. 3):

$$dC_i/dt = \frac{F_i}{y_iV_i}\left(C_a - \frac{C_i}{y_i}\right) \quad 6)$$

this can be rearranged to give:

$$dC_i/dt = \frac{F_i}{y_iV_i}(y_iC_a - C_i) \quad 7)$$

and further rearranged to give:

$$dC_i/dt = \frac{-F_i}{y_iV_i}(C_i - y_iC_a) \quad 8)$$

further take the case where the tissue compartment is fully saturated with tracer and the arterial concentration of the tracer has fallen to zero

eqtn. 8) becomes:

$$dC_i/dt = \frac{-F_i}{y_i V_i} (C_i) \qquad 9)$$

let $k = \frac{F_i}{y_i V_i}$

eqtn. 9) can be rearranged to:

$$dC_i/dt = -k(C_i) \qquad 10)$$

eqtn. 10) can be integrated into:

$$C_{i(t)} = C_{i0} e^{-kt} \qquad 11)$$

eqtn. 11) is the hydrogen clearance eqtn:

where: $C_{i(t)}$ is the concentration of tracer in tissue at time (t)

C_{i0} is the initial concentration of tracer at time t = 0

k $k = \frac{F_i}{y_i V_i}$

where:

F_i = flow through tissue of tracer

y_i = partition coefficient of tracer between blood and brain tissue

V_i = tissue volume which includes vascular volume

since y_i for hydrogen gas is thought to be approximately 1.0 for brain tissue then k approximates tissue blood flow expressed as ml/100 grams/min, volume is expressed as grams on the assumption that the density of brain tissue is approximately 1.0

$$C_{i(t)} = C_{io} e^{-kt} \qquad 11)$$

Taking the natural logarithm of both sides of eqtn. 11) yields:

$$\ln C_{i(t)} = \ln C_{io} - kt \qquad 12)$$
$$\Rightarrow \quad Y = b + mX$$

eqtn. 12) is a linear eqtn. of form y = b + mx

By plotting the natural logarithm of the tissue hydrogen concentration against time, the slope of the line (k) is equal to the tissue blood flow. To calculate the blood flow it is necessary only to measure the tissue concentration of tracer at the start and during clearance of the tracer from the tissue.

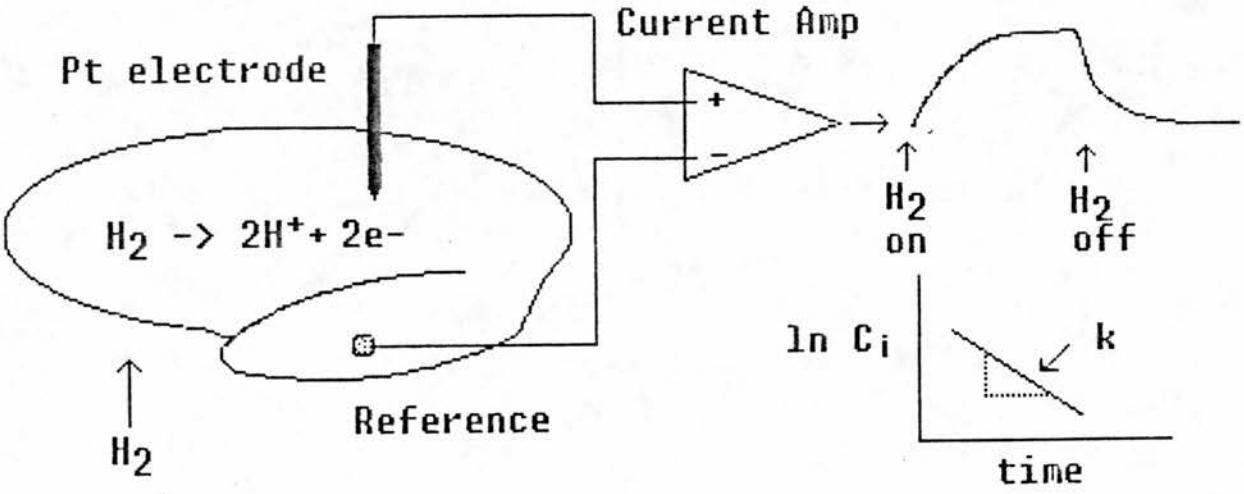

Most experimental hydrogen clearance curves are biexponential rather than monoexponential which indicates that two tissue compartments with different flow rates are present (assumed to be grey and white matter flow). The flow and the relative weight of both compartments can be calculated as shown below.

- $C(t) = W_g\, C_g\,(t) + W_w\, C_w\,(t)$

  where:

  $C(t)$ = total concentration of hydrogen in tissue at time (t)

  C_g and C_w = grey and white matter tissue hydrogen concentration at time (t)

  W_g and W_w = relative amounts of grey and white matter tissue compartments sensed by hydrogen electrode

- $W_g = I_g / (I_g + (I_w * R))$

  where:

  I_g and I_w = initial concentrations of hydrogen in grey and white matter tissue at onset of desaturation

  R = correction factor for differences in rate of saturation of the two compartments

  R = 1 for fully saturated tissue

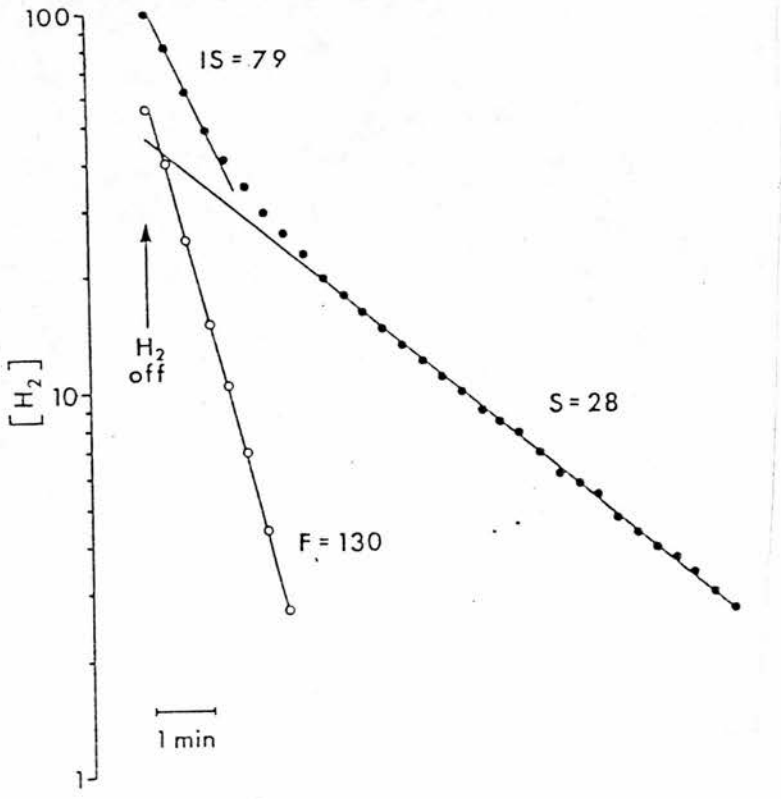

Advantages of Hydrogen Clearance Method:

a) Flow can be determined in any tissue where a small platinum electrode can be inserted.

b) Multiple flow determinations from the same tissue over long periods of time can be obtained:
   - flows every 15 minutes
   - ideal for testing CO2 reactivity or autoregulation.

c) It is one of the most inexpensive blood flow techniques to maintain.

Limitations of the Hydrogen Clearance Method

a) Despite the small size of electrodes some local tissue damage and compression may occur, and decreased flow or hyperaemia may result. The electrolytic etching of platinum electrodes to a sharp point can minimize the amount of tissue damage and compression.

b) Bicompartmental analysis is not without difficulties, particularly concerning the assumptions made about the partition coefficients from blood to grey or white matter, especially during ischaemia. To overcome this, most investigators standardize on the initial slope technique whereby, regardless of the presence of a second exponential component, the slope of the initial 1 - 2 minutes of the clearance curve is chosen for analysis. The initial slope index shows a good correlation to the weighted mean flow as calculated from bicompartmental analysis.

c) The vascular and tissue compartments are not always fully saturated with the tracer prior to clearance. Sufficient time must elapse for tissue saturation especially at low flows.

d) The arterial concentration of hydrogen does not fall immediately to zero during the first pass through the lungs. To overcome this, most investigators ignore the first 20 - 30 seconds of hydrogen clearance on the grounds that it is contaminated by arterial recirculation of H2.

e) The animals must be anaesthetised during measurement of blood flow because of the invasive nature of this technique, so compounding effects of the anaesthetic agents on the blood flow physiology must be considered.

f) Controversy still exists concerning the size of the tissue volume being sampled during hydrogen clearance; conservative estimates put the sample volume at 1.5 mm^3.

g) The sample volume will be dependent on the electrode dimensions, which vary from laboratory to laboratory, making the comparison of flow values difficult.

Electrode Etching Technique (Adapted from Farrar (157))

As shown overleaf, one inch length segments of 200 micron platinum wire are cut and held at an angle of 15 degrees to the vertical by small clips attached to a circular copper disc. The disc is rotated using a DC motor at a constant rate of 1 revolution per 5 seconds in a solution of 15% NaCN and 15% NaOH. The platinum wires are positioned in the clips so that each wire penetrates the etching solution by an equal amount (approximately 2 mm). The wires are rotated in the solution for 5 to 6 minutes while a 25 volt AC current is applied (peak current 1 Amp) between the platinum wire and a carbon rod reference electrode[81] placed in the etching solution. This process produces platinum wire tip diameters of between 10 and 20 microns tapering back over 1.5 mm to a base diameter of 100 microns.

The day before an experiment, electrodes are washed (15 minutes) in a solution containing 10% nitric acid and 30% hydrochloric acid which increases the active sites on the platinum surface, and then washed in distilled water. Insulation to the bared tip (1.5 mm) is provided by a set of telescoping polyethylene tubes[82]. To provide electrical contact with the

---

[81]Taken from a battery.

[82]Portex Ltd., Hythe, UK. Polyethylene tubing nos: 800/100/240/100, 800/100/160/100, 800/100/100/100.

platinum, a 5 cm tinned copper wire[83] is pushed between the etched platinum wire and the PE tubing. The insulating tubing is attached using fast drying epoxy under a dissecting microscope. This also allows measurement of the length of the tip exposed for cortical penetration.

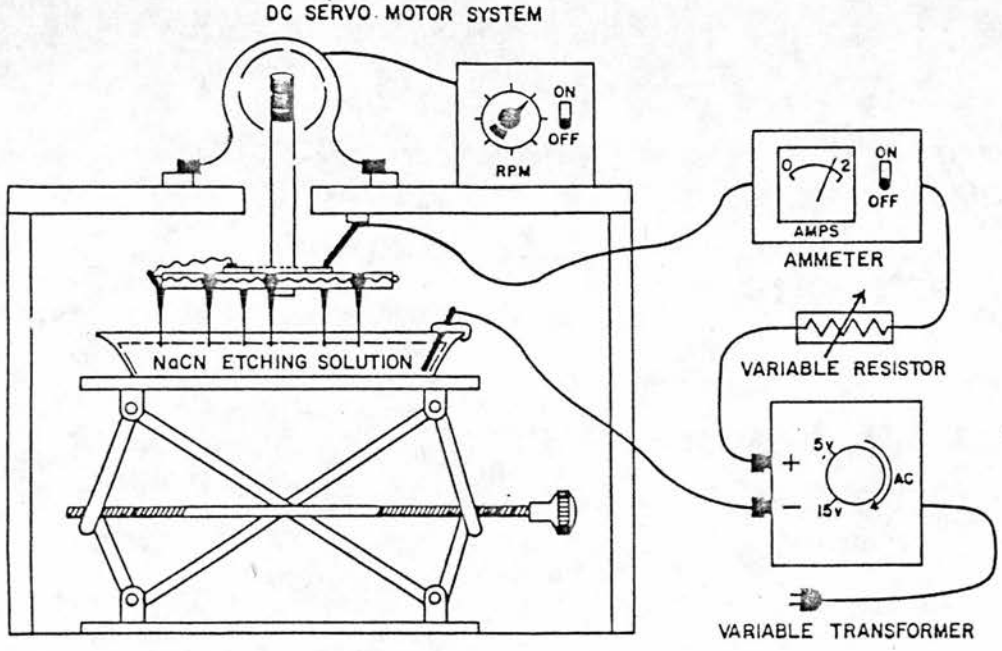

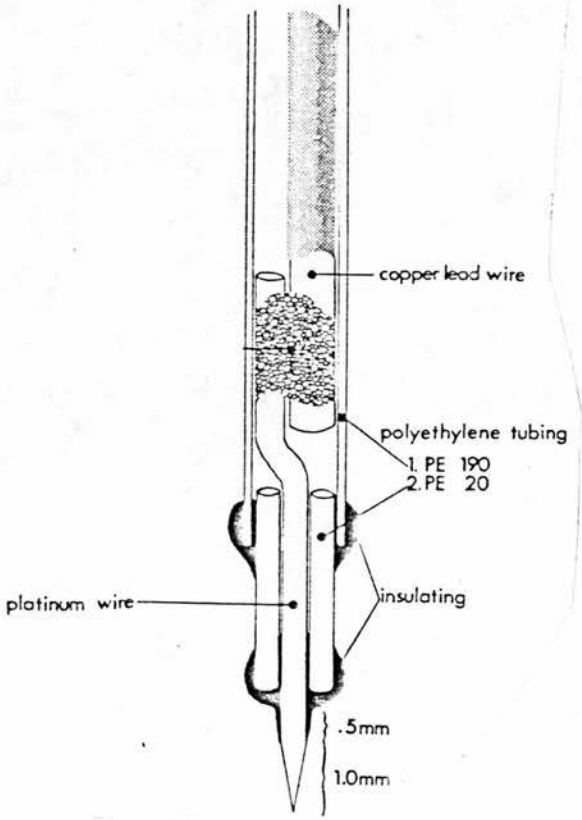

[83] 24 SWG tinned copper wire. Stock no. 355-085, RS-Components Ltd., Corby, UK.

Appendix O: Flow Chart of H2 Clearance CBF Program